PB82-115130

Remote Sensing of Sulfur Dioxide Effects on Vegetation. Volume II. Data

(U.S.) Tennessee Valley Authority, Norris

Prepared for

Environmental Protection Agency
Washington, DC

Jul 81

U.S. Department of Commerce
National Technical Information Service
NTIS

TVA

Tennessee
Valley
Authority

Office of Natural
Resources
Norris TN 37828

TVA/ONR/ARP-81/6

PB82-115130

EPA

United States
Environmental Protection
Agency

Office of Environmental
Engineering and Technology
Washington DC 20460

EPA-600/7-81-114
July 1981

Research and Development

Remote Sensing of Sulfur Dioxide Effects on Vegetation—Final Report

Volume II. Data

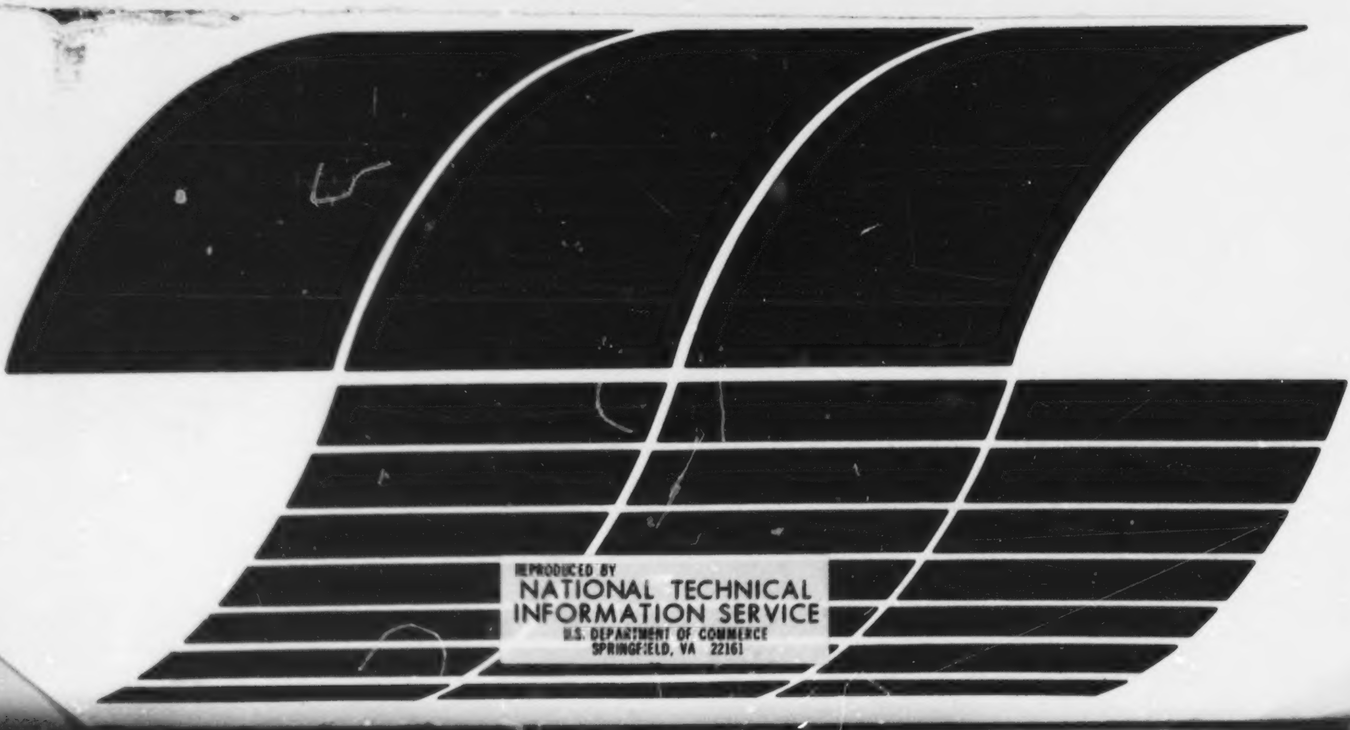

REPRODUCED BY
NATIONAL TECHNICAL
INFORMATION SERVICE
U.S. DEPARTMENT OF COMMERCE
SPRINGFIELD, VA 22161

RESEARCH REPORTING SERIES

Research reports of the Office of Research and Development, U.S. Environmental Protection Agency, have been grouped into nine series. These nine broad categories were established to facilitate further development and application of environmental technology. Elimination of traditional grouping was consciously planned to foster technology transfer and a maximum interface in related fields. The nine series are:

1. Environmental Health Effects Research
2. Environmental Protection Technology
3. Ecological Research
4. Environmental Monitoring
5. Socioeconomic Environmental Studies
6. Scientific and Technical Assessment Reports (STAR)
7. Interagency Energy-Environment Research and Development
8. "Special" Reports
9. Miscellaneous Reports

This report has been assigned to the INTERAGENCY ENERGY-ENVIRONMENT RESEARCH AND DEVELOPMENT series. Reports in this series result from the effort funded under the 17-agency Federal Energy/Environment Research and Development Program. These studies relate to EPA's mission to protect the public health and welfare from adverse effects of pollutants associated with energy systems. The goal of the Program is to assure the rapid development of domestic energy supplies in an environmentally-compatible manner by providing the necessary environmental data and control technology. Investigations include analyses of the transport of energy-related pollutants and their health and ecological effects; assessments of, and development of, control technologies for energy systems; and integrated assessments of a wide range of energy-related environmental issues.

This document is available to the public through the National Technical Information Service, Springfield, Virginia 22161.

TECHNICAL REPORT DATA

(Please read Instructions on the reverse before completing)

1. REPORT NO.
EPA-600/7-81-114

2.

3. RECIPIENT'S ACCESSION NO.
PB82 115130

4. TITLE AND SUBTITLE
Remote Sensing of Sulfur Dioxide Effects on Vegetation - Final Report - Volume II - Data

5. REPORT DATE
July 1981

6. PERFORMING ORGANIZATION CODE

7. AUTHOR(S)
C. Daniel Sapp

8. PERFORMING ORGANIZATION REPORT NO.
TVA/ONR/ARP-81/6

9. PERFORMING ORGANIZATION NAME AND ADDRESS
Office of Natural Resources
Tennessee Valley Authority
Norris, TN 37828

10. PROGRAM ELEMENT NO.
INE 625C

11. CONTRACT/GRANT NO.
80 BDJ

12. SPONSORING AGENCY NAME AND ADDRESS
U.S. Environmental Protection Agency
Office of Research and Development
Office of Energy, Minerals, and Industry
Washington, D.C. 20460

13. TYPE OF REPORT AND PERIOD COVERED
Final 1976-1980

14. SPONSORING AGENCY CODE

15. SUPPLEMENTARY NOTES
This project is part of the EPA-planned and -coordinated Federal Interagency Energy/Environmental R&D Program.

16. ABSTRACT

Three techniques for detecting and mapping sulfur dioxide (SO_2) effects on the foliage of sensitive crops and trees near large, coal-fired power plants were tested and evaluated. These techniques were spectroradiometry, photometric analysis of aerial photographs, and computer analysis of airborne multispectral scanner data.

Spectroradiometry is a useful, ground-based technique for measuring the changes in reflectance that accompany exposure of sensitive crops to SO_2. Photometric analysis of aerial color-infrared photographs has some practical advantages for measuring the reflectances of forest species or for synoptic point-sampling of extensive areas; these tasks cannot be done effectively by field crews. The relationships among reflectance, foliar injury, and yield of crops are complex and are affected by many extraneous variables such as canopy density. The SO_2 effects are easier to detect on winter wheat than on soybeans, but in either case they cannot be consistently detected by airborne remote sensors except under near-ideal conditions when the injury is moderate to severe. Airborne multispectral scanner data covering affected soybean fields were analyzed using three computer-assisted procedures: unsupervised, supervised, and pseudosupervised; the last method provided the best results. Landsat imagery was also investigated, but the foliar effects of SO_2 were too subtle to detect from orbit.

17. KEY WORDS AND DOCUMENT ANALYSIS

a. DESCRIPTORS		b. IDENTIFIERS/OPEN ENDED TERMS	c. COSATI Field/Group
Air pollution *	Infrared photography	Transport processes	
Electric power plants	Photometry	Char., meas. & monit.	
Photointerpretation	Reflectance	Crop & forest species	
Remote sensing *	Sulfur dioxide *	Digital image analysis	
Environmental surveys *	Plant pathology	Multispectral scanning	
		Microdensitometry	
		Tennessee Valley	

18. DISTRIBUTION STATEMENT
Release to public

19. SECURITY CLASS *(This Report)*
Unclassified

20. SECURITY CLASS *(This page)*
Unclassified

21. NO. OF PAGES
284

22. PRICE

EPA Form 2220-1 (Rev. 4-77) PREVIOUS EDITION IS OBSOLETE

TVA/ONR/ARP-81/6
EPA-600/7-81-114
July 1981

REMOTE SENSING OF SULFUR DIOXIDE EFFECTS ON VEGETATION

FINAL REPORT

VOLUME II - DATA

by

C. Daniel Sapp
Office of Natural Resources
Tennessee Valley Authority
Chattanooga, Tennessee 37401

Interagency Agreement EPA-IAG-D8-E721-DJ
Project No. E-AP 80 BDJ
Program Element No. INE 625C

Project Officer

James Stemmle
U.S. Environmental Protection Agency
401 M Street, SW.
Washington, DC 20460

Prepared for

OFFICE OF ENERGY, MINERALS, AND INDUSTRY
OFFICE OF RESEARCH AND DEVELOPMENT
U.S. ENVIRONMENTAL PROTECTION AGENCY
WASHINGTON, DC 20460

DISCLAIMER

This report was prepared by the Tennessee Valley Authority and has been reviewed by the Office of Energy, Minerals, and Industry, U.S. Environmental Protection Agency, and approved for publication. Approval does not signify that the contents necessarily reflect the views and policies of the Tennessee Valley Authority or the U.S. Environmental Protection Agency, nor does mention of trade names or commercial products constitute endorsement or recommendation for use.

ABSTRACT

Three techniques for detecting and mapping sulfur-dioxide (SO_2) effects on the foliage of sensitive crops and trees near large, coal-fired power plants were tested and evaluated. These techniques were spectroradiometry, photometric analysis of aerial photographs, and computer classification of airborne multispectral scanner data.

Spectroradiometry is a useful, ground-based technique for measuring the changes in reflectance that accompany exposure of sensitive crops to SO_2. Photometric analysis of aerial color-infrared photographs has some practical advantages for measuring the reflectances of forest species or for synoptic point-sampling of extensive areas; these tasks cannot be done effectively by field crews. The relationships among reflectance, foliar injury, and yield of crops are complex and are affected by many extraneous variables such as canopy density. The SO_2 effects are easier to detect on winter wheat than on soybeans, but in either case they cannot be consistently detected by airborne remote sensors except under near-ideal conditions when the injury is moderate to severe. Airborne multispectral scanner data covering affected soybean fields were analyzed using three computer-assisted classification procedures: unsupervised, supervised, and pseudosupervised; the last method provided the best results. Landsat imagery was also investigated, but the foliar effects of SO_2 were too subtle to detect from orbit.

This report was submitted by the Tennessee Valley Authority, Office of Natural Resources, in fulfillment of Energy Accomplishment Plan 80 BDJ under terms of Interagency Agreement EPA-IAG-D8-E721-DJ with the Environmental Protection Agency. Work was completed as of December 1980.

Partial

CONTENTS

Page

Abstract iii
Figures vii
Tables x
Acknowledgment xii

1. Introduction 1
    Background 1
    Reflectance Properties and Physiological Aspects of Vegetation 3
    Reflectance and Vegetative Stress 6
    Spatial Considerations 7
    Literature Review 7
    Purpose and Objectives 12
    Scope 12
    Hypothesis 14
2. Conclusions and Recommendations 15
    Conclusions 15
    Recommendations 17
3. Laboratory Spectroradiometry 18
    General 18
    Instruments 18
    Concepts of Radiance and Reflectance 21
    Curve Normalization 21
    Experimental Design 23
        Plants 23
        Scanning Procedure 24
        Analysis of Soybeans 24
        Analysis of Winter Wheat 25
    Results and Discussion 26
        Soybeans 26
        Winter Wheat 31
        Summary of Results 33
4. Field Spectroradiometry 37
    General 37
    Experimental Design 37
        Plot Preparation and Planting 37
        Exposure of Plots to SO_2 38
        Observations of Foliar Injury 41
        Scanning Procedure 42
        Normalization of Spectral Curves 45
    Results and Discussion 46
        Soybeans 46
        Winter Wheat 55
        Summary of Results 66

CONTENTS
(Continued)

Page

5. Interpretation and Analysis of Aerial Photographs 70
  - General 70
  - Methods and Instruments 70
    - Overflights 70
    - Photometric Analysis 75
  - Results and Discussion 79
    - General 79
    - Colbert Test 79
      - Field Conditions 79
      - Measurement and Comparison of Reflectance 83
    - Johnsonville Test 84
      - Field Conditions 84
      - Measurement and Comparison of Reflectance 88
    - Summary of Results 94

6. Analysis of Multispectral Scanner Data 96
  - General 96
  - Flight Lines and Sensor Characteristics 96
  - Ground Truth 102
    - Colbert Area 102
    - Shawnee Area 104
  - Data Reduction and Processing Procedures 104
    - Preprocessing Procedures 104
    - Processing Procedures 107
      - Pattern Recognition 107
      - Optimal Channel Selection 111
      - Conventional Analysis Procedures 113
    - Procedures for Evaluating Classification Accuracy . . 113
  - Results and Discussion 114
    - Optimal Altitudes 114
    - Colbert Test 115
      - Optimal MSS Channels 115
      - Unsupervised Classification 116
      - Supervised Classification 119
    - Shawnee Test 119
      - Optimal MSS Channels 119
      - Unsupervised Classification 121
      - Pseudosupervised Classification 124
    - Summary of Classification Results 135
    - Enhancement of Patterns of SO_2 Effects Within Soybean Fields 135

CONTENTS
(Continued)

Page

References 140

Appendices

A Specifications of Optical Multichannel Analyzer TSR System 144
B Spectral Curves, Laboratory Experiment 148
C Analysis of Variance, Laboratory Experiment 190
D Observations of Foliar Injury 195
E Spectral Curves, Experimental Plots 212
F Analysis of Variance, Experimental Plot 221
G Photometric Calibration 241
H NASA/ERL Letter Report 255
I Supervised Classification Procedure 257
J Pseudosupervised Classification Procedure 261
K Unsupervised Classification Procedure 264

FIGURES

Number Page

1 Reflectance of a typical leaf 4
2 Optical properties of a typical leaf 5
3 Effects of different spectroradiometer fields of view on data characteristics 8
4 Western part of Tennessee Valley showing four steam plants 13
5 TSR system configuration 19
6 TSR system components in laboratory 20
7 Procedure for normalizing spectral curves of radiance for laboratory experiments 22
8 Mean spectral curves for classes of chlorosis in soybeans exposed to SO_2 28
9 Mean spectral curves for classes of necrosis in soybeans exposed to SO_2 29
10 Mean spectral curves for classes of unaffected and SO_2-affected winter wheat 34
11 Map of experimental plot of soybeans 39
12 Map of experimental plot of wheat 39
13 Aerial view of experimental plot of wheat 41
14 Mobile platform for spectroradiometry 43
15 Geometric configuration for scanning subplots 44
16 Procedure for normalizing spectral curves of radiance for experimental field plots 46
17 Linear regression of yield on necrosis for soybeans exposed to SO_2 47
18 Mean spectral curves for soybeans exposed to SO_2 . . 49
19 Mean spectral curves for SO_2-affected soybeans . . . 52
20 Linear regressions of reflectance on necrosis for SO_2-affected soybeans 54
21 Linear regression of reflectance curve area on necrosis for winter wheat exposed to SO_2 56
22 Mean spectral curves for winter wheat exposed to SO_2 58
23 Mean spectral curves for SO_2-affected winter wheat 63
24 Linear regressions of reflectance on necrosis for winter wheat 65
25 Linear regression of yield on necrosis for SO_2-affected winter wheat 67
26 Linear regressions of reflectance on yield of SO_2-affected winter wheat 68
27 Colbert Steam Plant area in northwestern Alabama . . 71
28 Johnsonville Steam Plant area in western Tennessee . 72
29 Shawnee Steam Plant area in western Kentucky 73
30 Widows Creek Steam Plant area in northeastern Alabama 74
31 Grid for intensive sampling of soybean field near Colbert Steam Plant 78

FIGURES
(Continued)

Number		Page
32	Flight lines and SO_2-affected areas near Colbert Steam Plant in 1977	80
33	Aerial CIR photograph showing Colbert area in 1977 .	81
34	Regression of IR/red ratio and foliar injury levels for Colbert soybean fields photographed in 1977	84
35	Thematic maps showing patterns in a soybean field near Colbert Steam Plant in 1978	85
36	Computer-generated perspective views of a soybean field near Colbert Steam Plant in 1978	86
37	Flight lines and SO_2-affected areas near Johnsonville Steam Plant	89
38	Aerial CIR photograph of area near Johnsonville Steam Plant	90
39	Statistical regressions of reflectance, injury levels, and yield for Johnsonville soybean fields	93
40	Selected SO_2-affected areas and flight lines near Colbert Steam Plant in northwestern Alabama in 1977	98
41	Selected SO_2-affected areas and flight lines near Shawnee Steam Plant in western Kentucky in 1978 . .	99
42	Basic components of a digital multispectral scanner system	100
43	Configuration for airborne MSS data acquisition . . .	101
44	Distribution of SO_2-affected soybean fields near Colbert Steam Plant in 1977	103
45	Distribution of SO_2-affected soybean fields near Shawnee Steam Plant in 1978	105
46	Eight MSS channels depicting a scene near Colbert Steam Plant	106
47	Data Analysis System at EMSL-LV	108
48	Functional tasks for processing MSS data on Data Analysis System at EMSL-LV	109
49	Hypothetical two-dimensional plot of naturally clustered spectral measurements of soybeans	111
50	Unsupervised classification of MSS data for Colbert area	117
51	Distribution of SO_2 effects within soybean fields near Colbert Steam Plant	118
52	Unsupervised classification of MSS line 2 data near Shawnee Steam Plant	122
53	Distribution of SO_2 effects within soybean fields near Shawnee Steam Plant (MSS line 2, unsupervised)	123
54	Pseudosupervised classification of MSS line 2 data near Shawnee Steam Plant	127

FIGURES

(Continued)

Number		Page
55	Distribution of SO_2 effects within soybean fields near Shawnee Steam Plant (MSS line 2, pseudosupervised)	128
56	Pseudosupervised classification of MSS line 3 data near Shawnee Steam Plant	132
57	Distribution of SO_2 effects within soybean fields near Shawnee Steam Plant (MSS line 3)	133
58	Enhanced MSS image (line 2) of area near Shawnee Steam Plant showing SO_2-affected soybean fields . .	137

TABLES

Number Page

1 Data Classes and Foliar Effects of SO_2 on Soybeans . 27
2 Simple Correlation Coefficients (r) for Single-Band Reflectance and Foliar Injury to Soybeans 31
3 Data Classes and Foliar Effects of SO_2 on Winter Wheat 32
4 Simple Correlation Coefficients (r) for Single-Band Reflectance and Foliar Injury to Winter Wheat . . . 33
5 Reflectance Statistics for Classes of SO_2-Affected Winter Wheat 35
6 SO_2 Dose, Injury, and Yield of Soybeans 47
7 Significant Differences in Reflectance between SO_2-Exposed and Control Soybeans 51
8 Simple Correlation Coefficients (r) for Single-Band Reflectance, Foliar Injury, and Yield of Soybeans . 53
9 Significant Differences in Reflectance and Yield between SO_2-Affected and Unaffected Soybeans . . . 55
10 Total Reflectance, SO_2 Dose, Foliar Injury, and Yield of Winter Wheat 56
11 Significant Differences in Reflectance among Four Classes of SO_2-Exposed Winter Wheat and Control 57
12 Reflectance, Necrosis, SO_2 Concentrations, and Yield for Winter Wheat by Dose Class 61
13 Reflectance, Necrosis, and Yield for Winter Wheat by Injury Class 62
14 Simple Correlation Coefficients (r) between Reflectance and Two Other Variables (Necrosis and Yield) for Wheat 64
15 Significant Differences in Reflectance and Yield among Four Necrosis Classes of SO_2-Affected Winter Wheat 66
16 Reflectance and Foliar Injury for Colbert Soybean Fields Photographed in 1977 83
17 Reflectance, Foliar Injury, and Yield for Soybean Fields near Johnsonville 91
18 Coefficients of Determination (r^2) for Reflectance, SO_2 Injury, and Yield of Soybean Fields near Johnsonville 92
19 Multispectral Scanner Channels 112
20 Optimal MSS Channels for Detecting and Classifying SO_2-Affected Soybean Fields near Colbert Steam Plant in 1977 115
21 Comparison of Field Observations of SO_2 Effects on Soybeans and Results of MSS Unsupervised Classification for Colbert Scene 2 120
22 Optimal MSS Channels for Detecting and Classifying SO_2-Affected Soybean Fields near Shawnee Steam Plant in 1978 121

TABLES
(Continued)

Number Page

23 Comparison of Field Observations of SO_2 Effects on Soybeans and Results of MSS Unsupervised Classification for Shawnee Flight Line 2 125

24 Comparison of Field Observations of SO_2 Effects on Soybeans and Results of MSS Pseudosupervised Classification for Shawnee Flight Line 2 130

25 Comparison of Field Observations of SO_2 Effects on Soybeans and Results of MSS Pseudosupervised Classification for Shawnee Flight Line 3 134

26 Summary of Errors Using Three Procedures for Detecting and Classifying SO_2 Effects on Soybeans 136

27 Within-Field SO_2 Effects on Soybeans near Shawnee Steam Plant in 1978 138

ACKNOWLEDGMENT

The EPA Project Officer for this research project is James Stemmle, 401 M Street, SW., Washington, DC. His contribution to the direction of the research and his constructive review of the reported results are appreciated. The TVA Project Director is Herbert C. Jones, Supervisor, Air Quality Research Section, Air Resources Program, River Oaks Building, Muscle Shoals, Alabama.

SECTION 1

INTRODUCTION

BACKGROUND

The effects on vegetation of sulfur dioxide (SO_2) emissions from large, coal-fired power plants have been recognized as a potential problem for several decades. For measuring the intensity, geographical distribution, and areal extent of foliar injury, remote sensing offers numerous advantages over traditional field-based surveillance. The traditional method for gathering such information is to observe and record injury to SO_2-sensitive indicator species such as ragweed and blackberry. Fixed SO_2 monitoring stations are used to determine the spatial characteristics of plume contact with the ground. Information from field observations and monitors is often used to prepare maps illustrating the foliar injury from SO_2 episodes.

Some problems exist with the traditional approach to surveying and identifying SO_2 effects. The network of fixed SO_2 monitors around most coal-fired power plants is often inadequate for mapping the exact limits of the plume's contact with the ground. Field botanical surveillance is usually restricted to readily accessible areas because of the requirement to reconnoiter extensive areas quickly. The complex process of identifying and recording symptoms of foliar injury requires highly trained personnel who must distinguish between SO_2 effects and similar effects produced by herbicides, lack of essential plant nutrients, and senescence.

Remote sensing can assist those engaged in field surveillance of SO_2 effects on crops and trees. The technique provides a permanent record on film or magnetic tape. An airborne instrument platform can continuously cover extensive areas, some of which may be inaccessible to field teams.

The coverage can be essentially synoptic rather than spread over a period of several days or more. Perhaps the greatest advantage of remote sensing over field observations has to do with its greater objectivity and consistency of measurements over time and space.

The state of the art of remote sensing requires that ground truth--field observations--be gathered to support the analysis of the remotely sensed data. Preliminary but detailed information must be gathered concerning differences in spectral reflectance between the objects of interest (affected foliage) and the background (unaffected foliage). Spectral measurements may be made in the laboratory, in the field, or in both. If a sufficient number of the resulting spectral curves is analyzed statistically, the investigator can develop some sound generalizations about the changes in spectral reflectance that occur after vegetation is stressed by SO_2. Such information would allow the selection of appropriate sensor configurations, films, filters, scanner channels and bandwidths, and other options.

Although the traditional procedure for acquiring radiant energy data in the field involves making measurements at discrete points with a portable spectroradiometer, comparable data may also be obtained indirectly by making point measurements of the optical density of aerial photographs covering the area. With appropriate calibrations, calculations, and corrections of the data, either technique yields spectral reflectances that may indicate SO_2-induced stress. Whereas spectroradiometry is primarily a research method, aerial photographic radiometry--or photometry--can be used operationally to determine the reflectance of agricultural crops and forest species. Moreover, aerial photographs are permanent records of an air pollution episode that may be reexamined later if necessary. No terrain is inaccessible to remote sensors. Vast areas may be reconnoitered in hours rather than in weeks or months.

REFLECTANCE PROPERTIES AND PHYSIOLOGICAL ASPECTS OF VEGETATION

The first consideration of this effort was selection of an appropriate region of the electromagnetic spectrum. For detecting the effects of air pollution on vegetation, we selected the visible region, from 400 to 700 nanometers (nm) wavelength; the near-infrared region, from 700 to 1300 nm; and the thermal (far) infrared region from 8 to 14 micrometers (μm). This selection was based partly on the inherent properties of the spectrum and partly on the capabilities and availabilities of remote sensors.

Consider a typical reflectance spectrum of a leaf (Figure 1). Only part of the incident energy is reflected; the remainder is absorbed or transmitted (Figure 2). Beyond 1200 nm there is a zone of high absorption by water.[1] The visible region also shows high absorption of incoming radiation; in this case it is caused by leaf pigments including chlorophylls, carotenes, xanthophylls, and anthocyanins.[2] Although chlorophylls govern the reflectance in the visible spectrum, these pigments have no effect in the infrared; they are completely transparent to infrared radiation.[3]

It is generally accepted that the high infrared reflectivity of leaves is caused by their internal cellular structure. Some of the incoming radiation is diffused and scattered through the cuticle and epidermis to the mesophyll cells and air cavities inside the leaf. The radiation is reflected and refracted many times within the leaf. When chlorophyll and water are present in the leaf, the air cavities are filled and absorptance of radiation predominates. This accounts for spectral bands of low reflectance and transmittance by leaves.[4]

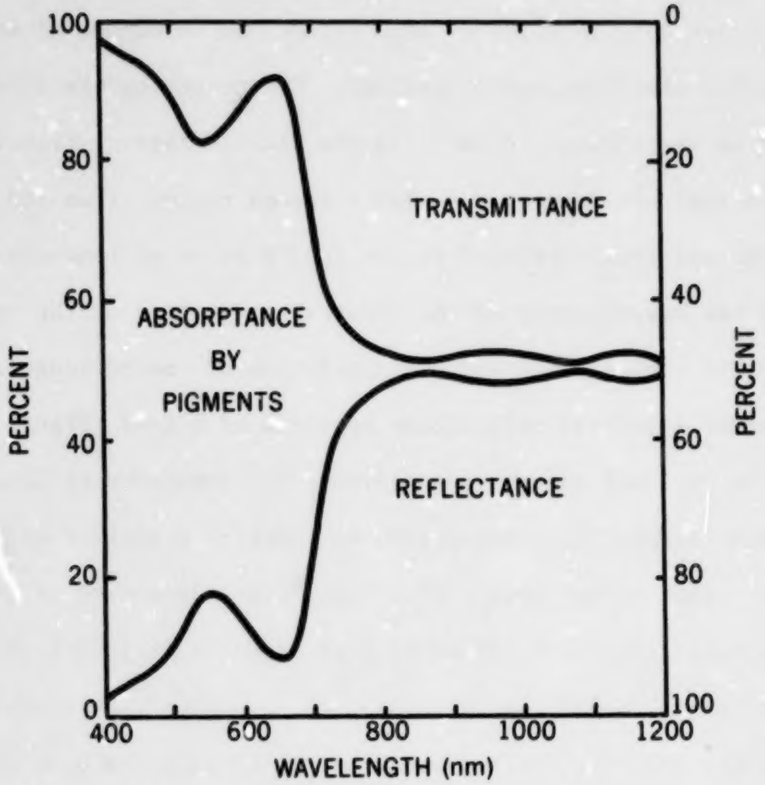

Figure 1. Reflectance of a typical leaf in the visible and near infrared.

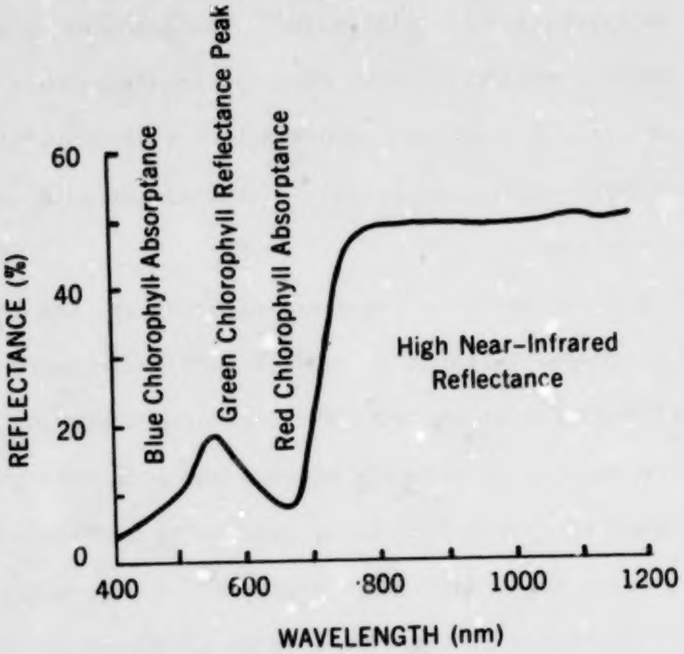

Figure 2. **Optical properties of a typical leaf in the visible and near infrared.**

REFLECTANCE AND VEGETATIVE STRESS

When leaves are affected by disease and physiological stress, the greatest change in reflectance occurs in the visible region rather than the infrared because of the sensitivity of chlorophyll to physiological disturbances.[4] Moreover, changes in infrared reflectance are not very reliable for indicating stress in plants.[5] In advanced stages of senescence, the infrared reflectance always decreases, most likely because of the breakdown or deterioration of cell walls.[6] What happens to visible reflectance as a leaf is stressed? Wert measured ponderosa pine foliage affected by oxidant air pollution and reported that visible reflectance increased as chlorophyll content decreased.[7] This agrees with empirical data gathered for this report.

Our approach used the visible, the near-infrared, and the far-infrared spectra. The ratio of near-infrared to red (IR/red) reflectance has received considerable attention by many investigators, beginning with Jordan[8] in 1969, who used it to estimate biomass and leaf area index. Colwell[9,10] also found the ratio useful for estimating biomass. Others[11,12,13] applied the IR/red ratio to Landsat image analysis for determining range grassland biomass. The ratio is considered to be a measure of relative "greenness" of vegetation.[14] Thus, the implication is that the ratio is associated with vegetative vigor or stress as well as canopy density (leaf area index) and, roughly, photosynthetically active biomass. Because the ratio is associated with so many other variables, it cannot be a perfect indicator of stress; however, it appears to be the best available measure.

The actual reflectance curve of a species or variety of plant under stress is not easily predicted. Visible reflectance generally increases with stress, but the response of reflectance in the near-infrared is variable, although it eventually decreases in advanced senescence. In remote sensing studies, the stress-causing agent cannot usually be identified without ground truth. Foliar markings, which indicate the identity of the agent, cannot be resolved from the distances or altitudes at which the sensor is operated. However, clusters of stressed plants can often be distinguished from a background of normal plants.

SPATIAL CONSIDERATIONS

This study relates spectral measurements of reflectance from individual leaves to the reflectance from entire canopies such as might be imaged by remote sensors. The effects of the background (soil surface, other vegetation, and shadows) must be considered. These normally reduce the reflectance of a canopy below that of a single leaf.

The remote sensor field of view is another consideration. Figure 3 illustrates the effects of field of view on data characteristics. The three inner concentric circles represent receptor apertures (angles) of 6 minutes, 20 minutes, and 1 degree, and the sensor would read a correct spectral signature for the crop (soybeans). The outer circle (3-degree aperture) would read a meaningless mixture of trees, cultural features, and soybeans.

LITERATURE REVIEW

Although considerable data have been published to describe remote sensing applications in plant disease and the detection of moisture stress, very little information exists on the use of this tool for the detection and study of air pollution effects on vegetation. Most of the reported studies deal only with the use of aerial color-infrared photography. There is some continuing work at the Environmental Protection Agency (EPA)

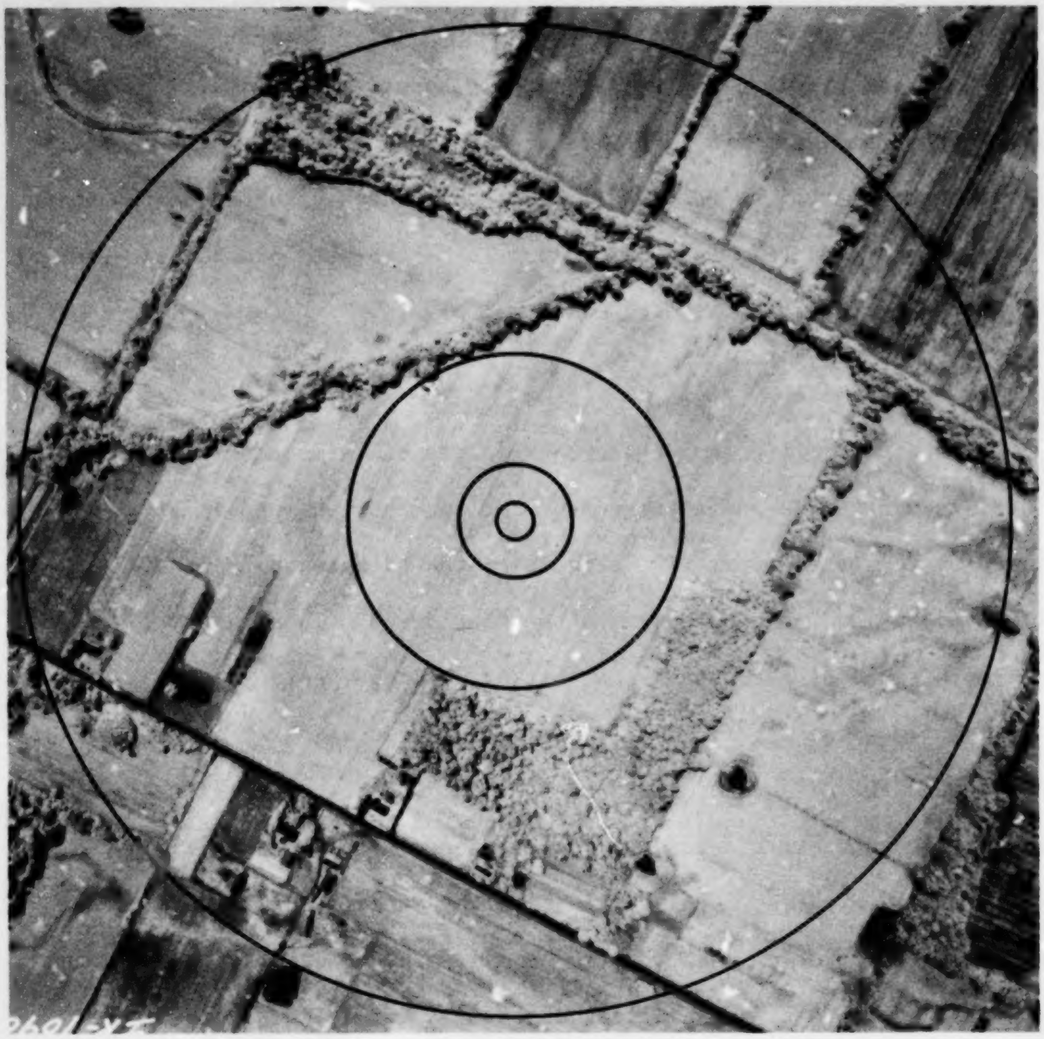

Figure 3. Effects of different spectroradiometer fields of view on data characteristics. The three inner concentric circles (representing apertures 6', 20', and 1°) would indicate a correct spectral signature for the crop (soybeans), but the outer circle (3°) would produce an integrated, meaningless mixture of reflectance from trees, cultural features, and soybeans. (Infrared photo by Tennessee Valley Authority, scale approximately 1:6000.)

at Las Vegas and Corvallis, using Landsat and airborne multispectral scanner data for the detection of air pollution effects on vegetation.

Volume II of the Manual of Remote Sensing[15] outlines some of the remote sensing work dealing with air pollution effects on forest lands. The works of Miller, et al,[16] Heller,[17] and Wert[18] in 1969 are quoted. These investigators studied the effects of oxidant air pollution on ponderosa pine foliage in the area of Los Angeles, California, using color films. The best combination of film and scale for detecting the air pollution effects was reported as Anscochrome D/200 color film with a didymium rare-earth filter, taken at large scale (1:1,600).

Zealer, Heller, Norick, and Wilkes[19] published a report in 1971 covering the feasibility of using aerial color photography to detect and evaluate SO_2 injury to timber stands in the vicinity of the Widows Creek Steam Plant in northeast Alabama. These investigators reported that normal color film, exposed through a didymium filter at very large scales (1:800 to 1:1,584), was the most accurate system, thus confirming the results of the 1969 report by Heller.[20] EPA asked the Tennessee Valley Authority (TVA) to participate with the U.S. Forest Service in the 1971 study because TVA had identified visible SO_2 effects on the foliage of trees in the vicinity of the Widows Creek Steam Plant and was conducting intensive ground surveys to determine the extent and severity of the injury.

Some published findings describe attempts to use satellite data for detecting zinc smelter air pollution damage and alteration to vegetation. Fritz and Pennypacker[21] were unable to distinguish an affected eastern white pine stand from a healthy stand because of insufficient spatial resolution of the Landsat MSS system. An earlier report by Wiegand[22] describes successful application of similar satellite data to differentiate chlorotic (iron deficient) and normal grain sorghum plants. Affected areas as small as 1.1 hectares (ha) could be detected using digital techniques including the ratio of channel 5 (red) to channel 7 (near-infrared). Fritz and Pennypacker's negative results seem to contradict the earlier findings of Wiegand, indicating that more work needs to be done using satellite platforms for detection of SO_2 effects. NASA concludes that the successful use of Landsat imagery to detect SO_2 effects depends on the severity of the air pollution effects (Dr. Cartmill, personal communication, 1976). Regardless, the limits of detection need to be determined and defined.

A few publications describe the use of aerial color-infrared photography from aircraft to detect and study SO_2 effects on vegetation. Murtha[23] describes a method whereby SO_2 damage to forest lands can be evaluated from flying heights up to 12,200 meters (m) and at image scales as small as 1:160,000. It was not possible, however, to delineate zones of "light injury" using such techniques.

German scientists have used aerial photography for detecting air pollution injury to trees. Color-infrared film at large scale (1:5,000) is favored for the task. East German investigators have used spectrozonal (multispectral) aerial photography at scales ranging from 1:5,000 to 1:8,000).[24]

Walker and Dahm[25] developed a method for measuring environmental stress. Aerial color-infrared film was used to detect moisture stress, air pollution-induced stress, and disease-induced injury or damage to vegetation. A patented "photometric" calibration technique accounts for the variables affecting the image scene.

Schott, et al.,[26] recently published a report (not dated) that described an aerial photographic technique for measuring vegetative stress from SO_2.

The authors correlated infrared reflectance, measured from the photograph, with stress. They recommend that photographs be obtained during the maximum vigor period. The final report describes several problems that prevented the acquisition of definitive results. These problems included lack of photography during the appropriate part of the growth cycle, lack of sensitometric data, and presence of senescent plants.

Some studies have focused upon laboratory use of photography for the detection of air pollution effects on vegetation. Pell and Brock recently completed a fumigation chamber study of hybrid poplar response to ozone.[27] Special filters and a densitometer were used for the photographic experiment. The investigators state that the infrared photographs showed areas of injury that were not otherwise visible to the observer. Other laboratory work involving photographing diseased plants using color-infrared, black-and-white infrared, and other photographic films has been published. These papers are too varied to summarize, but many excellent papers dealing with the topic are published in the Journal of the Biological Photographic Association, such as one authored by Jackson, entitled "Detection of Plant Disease Symptoms by Infrared."[28] The Eastman Kodak publication M-28 on infrared photography also has technical merit.[29]

A basis for interpretation of thermal infrared imagery for detection of moisture stress in vegetation is given by Rohde and Olson.[30] Their results could perhaps be extended to detecting vegetative stress induced by air pollution. Their idea is that stressed vegetation should be several degrees warmer than adjacent healthy vegetation in early afternoon when transpiration rates are at maximum, and that thermal infrared scanning can detect this difference.

Finally, another publication should be mentioned although its intent is not to deal with the photographic technique at all. This is a pictorial atlas by Jacobson and Hill which is helpful in recognizing air pollution injury to vegetation. The book contains pictures of affected leaves and descriptions of the characteristics of injury and damage. The color shifts described have a direct application to remote sensing.[31]

PURPOSE AND OBJECTIVES

The purpose of this five-year study was to analyze and evaluate remote sensing techniques to detect and map the effects of SO_2 emissions from large, coal-burning power plants on the foliage of sensitive crops and trees. The objectives were to test, refine, and develop remote sensing instrumentation and techniques for this purpose. Ground-based, airborne, and satellite platforms were used for gathering data.

SCOPE

The scope of the project included four coal-fired power plant sites, several experimental plots, and several species of vegetation. These sites were: the Shawnee Steam Plant in western Kentucky; the Widows Creek Steam Plant in northeastern Alabama; the Colbert Steam Plant in northwestern Alabama; and the Johnsonville Steam Plant in western Tennessee (Figure 4). The experimental plots were located in Muscle Shoals, Alabama, and near Widows Creek Steam Plant. Laboratory-based spectroradiometric experiments were performed on soybeans, wheat, and cotton at a TVA facility in Muscle Shoals. The digital image analysis was done at EPA's Environmental Monitoring Systems Laboratory in Las Vegas, Nevada (EMSL-LV), and at TVA's Mapping Services Branch in Chattanooga, Tennessee. Photometric analysis of aerial photographs showing SO_2-affected soybean fields was performed at Calspan's Advanced Technology Center in Buffalo, New York.

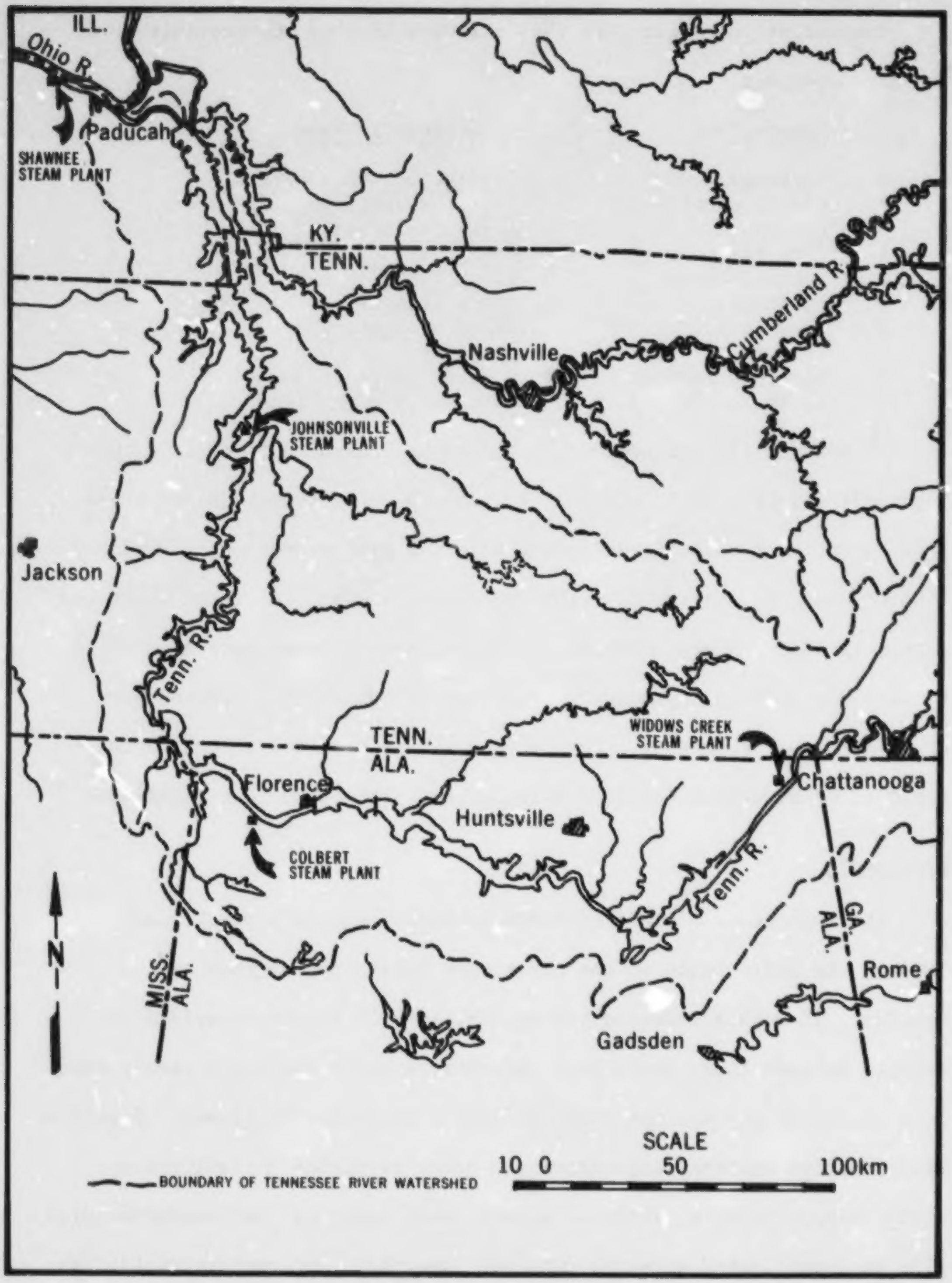
ILL.
Ohio R.
Paducah
SHAWNEE STEAM PLANT
KY.
TENN.
Nashville
Cumberland R.
JOHNSONVILLE STEAM PLANT
Jackson
Tenn. R.
TENN.
ALA.
WIDOWS CREEK STEAM PLANT
Chattanooga
Florence
Huntsville
COLBERT STEAM PLANT
N
MISS.
ALA.
Tenn. R.
GA.
ALA.
Rome
Gadsden
BOUNDARY OF TENNESSEE RIVER WATERSHED
SCALE
10 0
50
100km

Figure 4. Western part of Tennessee Valley showing four steam plants.

Investigations began with the following list of SO_2-sensitive crop and tree species:

	Common Name	Scientific Name
1.	Soybeans	*Glycine max* (L.) Merr.
2.	Winter wheat	*Triticum aestivum*
3.	Cotton	*Gossypium hirsatim*
4.	Virginia pine	*Pinus virginiana*
5.	Loblolly pine	*Pinus taeda*
6.	White pine	*Pinus strobus*
7.	Shortleaf pine	*Pinus echinata*
8.	Hickory	*Carya* sp.
9.	Northern red oak	*Quercus rubra* (L.)
10.	Southern red oak	*Quercus falcata* Michx

As the project progressed, its scope was narrowed to exclude the hardwoods (numbers 8, 9, and 10), because SO_2-affected stands of these trees were never encountered. Some affected pine stands were found and studied, but the injury was light and discontinuous. Affected wheat and cotton fields were never found, so SO_2 injury to plots containing these species was induced experimentally for study. Affected soybeans were studied in the laboratory, in experimental plots outdoors, and in the field under natural conditions using several remote-sensing techniques.

HYPOTHESIS

The hypothesis of this research is that there is a relationship between the reflectance of the plants and foliar injury from sulfur dioxide. If such a relationship exists, it will be characterized in detail, because there would be a theoretical basis for using remote sensors to detect and map the distribution of SO_2-affected plants. Possible relationships between reflectance and other variables including crop yield, canopy density, stage of growth, soil moisture, and weediness will also be investigated whenever data are adequate. Appropriate statistical tests will be used to measure the strength of associations between and among variables.

SECTION 2

CONCLUSIONS AND RECOMMENDATIONS

CONCLUSIONS

Spectroradiometry is a useful technique for measuring the changes in visible and near-infrared (IR) reflectance that may accompany SO_2-induced injury to the foliage of sensitive row crops. The technique has proven impractical for measuring reflectances of mature trees because of the difficulty in scanning such large objects systematically from specific angles. Spectroradiometry is practical for providing data before performing remote-sensor overflights so that the instrument systems can be designed and calibrated to detect the stress.

Complex relationships exist between reflectance and foliar injury to soybeans and winter wheat. Laboratory-based scanning experiments indicate that the total (visible plus IR) spectrum is associated with the necrosis symptom but not chlorosis in soybean foliage. The IR spectrum alone shows no association with either symptom, but the IR/red ratio does correlate significantly (α=.05) with necrosis in soybeans. In scans of wheat, the total visible spectrum, as well as the green and red bands, shows close relationships with chlorosis and necrosis. IR scans of wheat were not made for the laboratory experiment.

Analysis of data from scans of experimental field plots shows no relationship between reflectance and the observed symptoms of injury to the soybeans. The natural range of variation in reflectance of the foliage is evidently greater than the effects induced by SO_2. For wheat, however, there is an association between reflectance and observed necrosis and chlorosis in wheat. The relationship includes the total (visible and IR) spectrum, as well as the individual green, red, and IR bands.

The crop yield variable is related to the reflectance of wheat but not of soybeans. The red band and the IR/red reflectance ratio of wheat is closely associated with yield.

Aerial overflights of SO_2-affected soybean fields near three coal-fired power plants produced color-infrared photographs from which reflectances were obtained photometrically. When the reflectance measurements were compared with field observations of foliar injury, the results showed that single-band reflectance (green, red, and IR bands) was not statistically related to foliar injury. Comparison of the IR/red ratio and injury showed conflicting results. The green, red, and IR bands were each highly related to yield, but the IR/red ratio was not.

Analysis of multispectral scanner data indicates it is possible to differentiate SO_2-affected soybean fields from unaffected fields when the canopies are continuous (uniform and dense) and the foliar effects are at least moderate to severe. A "pseudosupervised" classification procedure provides greater accuracy than two other procedures, "unsupervised" and "supervised," and it can distinguish moderately to severely affected soybeans from unaffected soybeans with errors ranging from 11 to 24 percent.

Experience with three aircraft altitudes for acquiring scanner data indicates that 1800 m flying height is superior to 500 and 3660 m for detecting and mapping moderate to severe chlorosis symptoms on the foliage of row crops. Light chlorosis may be below the threshold of detection of an aerial multispectral scanner or camera system regardless of platform altitude, and is certainly too subtle to be detected by these sensors in orbital vehicles such as Landsat. The results also indicate that unless the SO_2 effects on foliage are severe enough to result in necrosis, they will not be detectable from any operational altitude (>150 m above ground level) by remote sensors. Even when necrosis is present, detection may be possible only under ideal conditions when the influence of masking variables (weediness, non-SO_2-related stress, etc.) is absent.

RECOMMENDATIONS

Spectroradiometry should be an integral part of flight planning for remote sensor data acquisition whenever the goal is to detect and map stressed crops. The scanning technique is useful for measuring the spectral differences between target and background so that success in detecting stressed vegetation can be predicted. It also has value as a laboratory instrument for quantifying levels of foliar injury.

Photometric analysis of aerial photographs is a potential alternative to field-based scanning with a spectroradiometer. It could be useful if reflectances need to be sampled at many points or over an extensive area. Our negative findings were probably a result of extraneous variables controlling reflectance. The color-infrared film type should normally be used instead of conventional color film, because infrared film shows the patterns of stress better and provides superior penetration of atmospheric haze.

Multispectral scanning from aircraft should be used, if appropriate, to detect and map SO_2-related injury to row crops whenever the foliar symptoms are at least moderate and consist primarily of necrosis, and the canopy is continuous, dense, and weed-free. These conditions are quite restrictive because SO_2 effects in the field are usually subtle and consist mainly of chlorosis. These effects cannot be detected consistently with currently available airborne or spaceborne remote sensors.

SECTION 3

LABORATORY SPECTRORADIOMETRY

GENERAL

Spectroradiometry provides information on the spectral reflectance characteristics of objects. This section describes the results of a series of laboratory experiments in which spectroradiometry was used to obtain spectral curves of visible and near-infrared reflectance of SO_2-affected soybean and wheat plants. Some SO_2-affected cotton plants were scanned, but technical problems with instruments invalidated the data and the experiment could not be repeated because of scheduling conflicts.

The following section describes attempts to verify the findings using data from experimental field plots. The laboratory research included growing uniform groups of plants in a greenhouse; exposing them in a controlled fashion to SO_2 in a laboratory exposure chamber; systematically observing the foliar effects of SO_2; scanning the plants with a spectroradiometer while controlling as many of the variables as possible; and finally, statistically analyzing the results to make some sound generalizations about the spectral changes that plants undergo when they are affected by SO_2.

INSTRUMENTS

Two different types of spectroradiometers were used to scan the plants. The project began with a conventional instrument and later acquired a new, state-of-the-art multichannel telespectroradiometer (TSR). Both TSR's provided spectral curves of reflectance versus wavelength.

The conventional TSR was used to scan the wheat plants. Its slow ($\geq$20-second) scan speed was not a problem in the laboratory. Spectral coverage ranged from 400 to 700 nanometers (nm) in the visible channel.

A separate, cooled optical head is used to scan the red and infrared spectrum from 600 to 1000 nm. Unfortunately, the two heads cannot be used simultaneously. Output is in radiance units and the system has a 4-nm spectral resolution. The telescope field of view (FOV) was either 1 or 3 degrees. The same telescope and FOV's were used with the other TSR described below.

The TSR used to scan the soybeans has an optical multichannel detector. It is a microprocessor-controlled optical system that TVA adapted to remote sensing in the laboratory and field. Application of optical multichannel TSR's to the natural sciences has been very rare.[32] The TVA system is called an Optical Multichannel Analyzer (OMA-2) manufactured by Princeton Applied Research Corporation.[33] Figure 5 illustrates the configuration of the system; Appendix A provides details and specifications of the components. Scanning is essentially instantaneous (total scan time = 0.7 milliseconds), and data storage is on flexible disc. Figure 6 shows the components of the OMA-2 system.

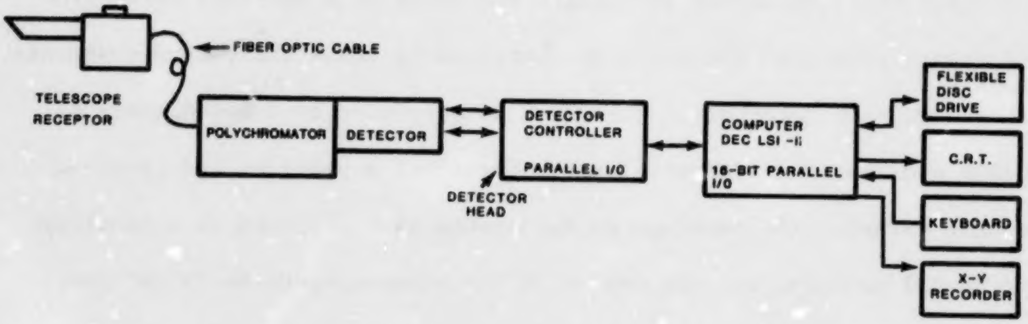
FIBER OPTIC CABLE
TELESCOPE RECEPTOR
POLYCHROMATOR
DETECTOR
DETECTOR CONTROLLER
PARALLEL I/O
DETECTOR HEAD
COMPUTER DEC LSI -II
16-BIT PARALLEL I/O
FLEXIBLE DISC DRIVE
C.R.T.
KEYBOARD
X-Y RECORDER

Figure 5. TSR system configuration.

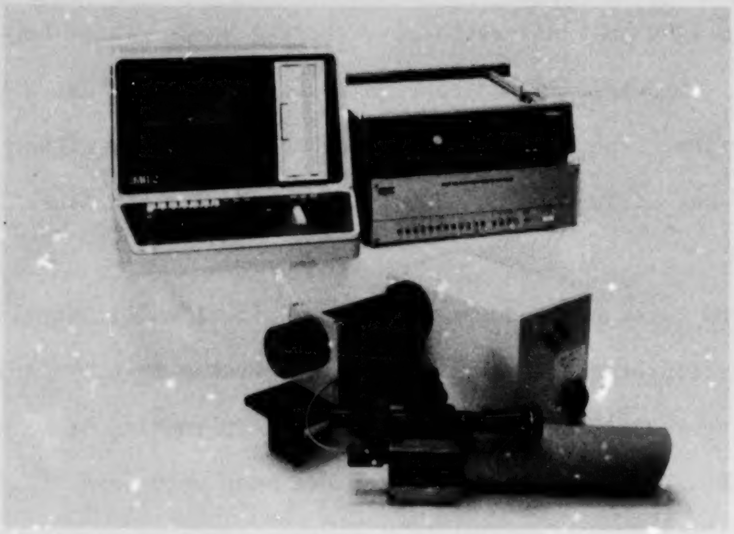

Figure 6. TSR system components in laboratory. The telescope is normally mounted on a tripod.

The OMA-2 operation is unique because it accumulates scans, integrating them over a preselected time frame or number of scans. Such accumulation improves the signal-to-noise ratio and averages out short-term variations caused by movement of foliage or inadvertent movements of the instrument platform during scanning. The shape of a spectral curve from an ordinary slow-scan TSR would be distorted by these short-term movements.

The vidicon detector of the OMA-2 is sensitive to a broad range of visible and near-infrared wavelengths (Appendix A provides the spectral response curve). The coverage of our system is restricted to a spectrum that is 337 nm wide, but the center of the scanned spectrum can be positioned anywhere within the range of detector sensitivity. For the soybeans, we selected a range of 430 to 767 nm, which included the green chlorophyll peak, the red chlorophyll absorptance region, and part of the near-infrared reflectance plateau. The spectral resolution of the system is about 2-4 nm, being limited in our case by the size of the input slit to the spectrometer, the diameter of the fiber optics bundles, and our success in aligning the optical components before each set of measurements.

The intensity scale (y-axis) of the OMA-2 cathode-ray tube display reads in counts per channel. For each sample, a total of 500 discrete channels was scanned at the 140-μs/channel rate. The y-axis was calibrated by scanning a lamp having a known spectrum. Background subtraction, statistical grouping, and averaging of curves were performed on the console keyboard, after which the curves were stored on flexible discs.

CONCEPTS OF RADIANCE AND REFLECTANCE

The term "reflectance" describes the ratio of radiant energy reflected from a surface to that incident upon it. Reflectance cannot be measured directly, but can be computed from measurements of radiant energy. The shape of the radiance curve obtained is a function of three wavelength-dependent parameters: (1) variation of the intensity of illumination; (2) variation of the reflected energy; and (3) variation in sensitivity of the detector. If parameter (2) is to be isolated from parameters (1) and (3), a standard surface with an established reflectance curve should be used. This curve may then provide the basis for normalizing radiance curves (Figure 7).

CURVE NORMALIZATION

Spectral curves were normalized to convert them from radiant energy units to reflectance units. The instrument used to scan the soybeans had an integral LSI-11 minicomputer, which is used to store, process, and manipulate the curves. The TSR used to scan the wheat has an analog output. These curves were digitized separately on the graphics tablet of a

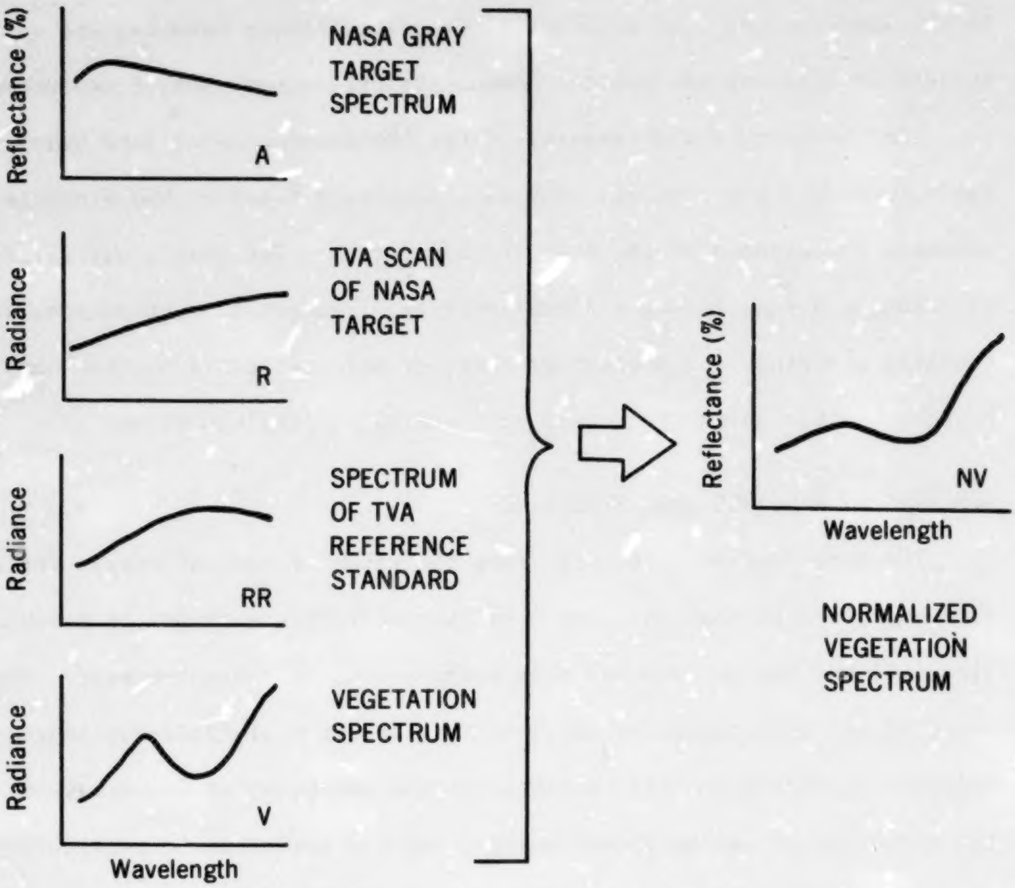
Reflectance (%)
A
NASA GRAY TARGET SPECTRUM
Radiance
R
TVA SCAN OF NASA TARGET
Radiance
RR
SPECTRUM OF TVA REFERENCE STANDARD
Radiance
V
VEGETATION SPECTRUM
Wavelength
Reflectance (%)
NV
Wavelength
NORMALIZED VEGETATION SPECTRUM

(1) One-time procedure to generate absolute curve (C):

$$C = (RR \cdot A) / R$$

(2) Subsequent procedure to produce normalized curves of vegetation (NV):

$$NV = (V \cdot C) / RR$$

Figure 7. Procedure for normalizing spectral curves of radiance for laboratory experiments.

Tektronix 4014 graphics terminal; they were then normalized, averaged, and otherwise manipulated and stored using an IBM 370 computer.

As Figure 7 illustrates, the scanning procedure incorporated a standard 18-percent gray reflecting surface, which was one of a set of panels borrowed from NASA. This NASA gray target has a reflectance curve supplied with it. For convenience, a small (20- by 25-cm), 18-percent gray card was calibrated against the NASA gray target for day-to-day use in the laboratory and field. The gray card--the TVA reference standard--was scanned along with the vegetation to provide a basis for curve normalization. Reference standards and calibration curves are illustrated in Appendix B.

EXPERIMENTAL DESIGN

Plants

Soybean and winter wheat plants were grown to maturity in a greenhouse. Each step in the procedure was carefully controlled to assure uniform groups of plants. Registered seed guaranteed varietal purity. The soil mixture consisted of specific proportions of Decatur loam, sand, and peat, with nitrogen, phosphorus, and potassium nutrients added and the pH adjusted to 6.5. The photoperiod was maintained at 14 h of light by timers on the greenhouse lights. Watering was carefully controlled on a pot-by-pot basis.

Groups of plants were exposed to SO_2 in a controlled exposure chamber for specific doses to create the foliar effects. After exposure, the plants were returned to the greenhouse, and the effects gradually appeared. Observations of chlorosis and necrosis were made a week after exposure to assure that all the effects had developed.

Scanning Procedure

All scanning was done in the laboratory under carefully controlled illumination. Individual soybean leaflets and wheat canopies were scanned. The lamps were carefully oriented to minimize the specular (glare) component of light into the telescope. This was done for wheat and soybeans by maintaining a 45-degree angle between the telescope axis and the tungsten-halogen (3200 kelvins) lamps. The range (distance between telescope and plant) was determined by selecting a telescope FOV of 1 or 3 degrees and filling the FOV with foliage to minimize the contribution of the background. Overhead views of the wheat canopies were obtained by orienting the top of the plant container so that it was perpendicular to the telescope axis. When individual soybean leaflets were scanned, their surfaces were mounted flat on a board that was perpendicular to the telescope axis. Soybean leaflets were detached and scanned immediately after the observations were recorded. The wheat plants were scanned, pot-by-pot, after observation was completed. The experiments are discussed below in greater detail.

Analysis of Soybeans

Groups of soybeans were exposed to one of several SO_2 doses that were chosen to create a wide range of foliar effects. The peak concentrations and durations of exposure were (1) 15720 $\mu g/m^3$ for 0.50 and 0.67 h and (2) 10480 $\mu g/m^3$ for 0.75 and 1.25 h. A total of 153 leaflets was scanned. The selection was made by determining which nodes were affected on the most severely affected plants and then including the leaflets growing on these nodes on all plants. The unaffected leaflets on those nodes were also included. The spectral reflectance curves were grouped in broad classes by level of injury. A mean curve was computed for each class or combination of classes to show trends in the relationship between foliar effects and reflectance. Analysis of variance was used to determine whether differences among classes were statistically significant. This analysis was done for specific wavelengths: blue (450 nm), green (550 nm), red (650 nm), and infrared (750 nm). The statistical analysis included the two components of foliar injury, chlorosis and necrosis. F-tests were used to determine significance of differences in reflectance between injury classes at significance levels of $\alpha=.05$ and $\alpha=.10$.[34]

Analysis of Winter Wheat

Winter wheat plants (Coker variety) were grown in containers in the greenhouse using the same closely controlled procedures as described for soybeans. The mature plants were exposed to five levels of SO_2 in the controlled exposure chamber to create a wide range of foliar effects. The SO_2 concentrations (all 3-h averages) used were 3930, 5240, 6550, 7860, and 9170 $\mu g/m^3$. After exposure, the plants were returned to the greenhouse to allow the effects to develop. A week later, the plants were observed systematically, pot-by-pot, to obtain data on the chlorosis and necrosis components. Effects ranged from none for the control group to "very severe" for the groups receiving 6550, 7860, and 9170 $\mu g/m^3$ SO_2.

When observations were complete, spectral scanning began. For this task, the Gamma Scientific TSR was used. The analog curves of visible radiance were digitized, normalized, averaged, and plotted on a Tektronix 4014 computer terminal with digitizer graphics tablet. The near-infrared (IR) curves had to be obtained with a separate optical head. No useful IR scans of wheat were obtained because of problems in calibration. These problems were solved later by substituting the OMA-2 TSR for the Gamma

Scientific model. The IR curves obtained for this study were not statistically analyzed because apparent variation was slight--typically less than 2 percent (Appendix B).

Correlation-regression analysis and one-way analysis of variance (ANOVA) were performed on the wheat. The latter procedure focused on differences among injury classes. F-tests were used to determine significance ($\alpha=.05$).[35] This analysis was done for three specific wavelengths--450 nm, 550 nm, and 650 nm.

RESULTS AND DISCUSSION

Soybeans

Descriptive statistics for foliar injury (chlorosis and necrosis) were obtained for soybeans (Table 1). The class boundaries were selected to conform to traditional breakpoints used in field surveillance of SO_2 effects. These chlorosis classes were "unaffected (0%)," "light (1-10%)," "moderate (11-25%)," "severe (26-50%)," and "very severe (>50%)." For necrosis the "severe" and "very severe" classes were combined and represented all levels above 25 percent.

The individual reflectance curves for soybeans were arithmetically averaged to produce a mean curve for each class of chlorosis and necrosis (Figures 8 and 9).

Some of the averaged reflectance curves for chlorosis (Figure 8) show more separation than others. Chlorosis class 4 (very severe injury) has the highest visible and lowest IR reflectance of all. However, the other classes are not separable at any wavelength.

The averaged reflectance curves for necrosis show more differences among classes than those for chlorosis (Figure 9). The greatest separation is in the red wavelengths (chlorophyll absorption band), at about

TABLE 1. DATA CLASSES AND FOLIAR EFFECTS OF SO_2 ON SOYBEANS

Chlorosis					Necrosis				
Qualitative level of injury	Class	Range (%)	Mean injury (%)	No. of leaflets	Qualitative level of injury	Class	Range (%)	Mean injury (%)	No. of leaflets
None	0	0	0	7	None	0	0	0	7
Light	1	1-10	6.5	52	Light	1	1-10	6.9	15
Moderate	2	11-25	15.6	20	Moderate	2	11-25	21.7	3
Severe	3	26-50	39.3	29	Severe and very severe	3	>25	50.0	3
Very severe	4	>50	69.3	26					28
				134					

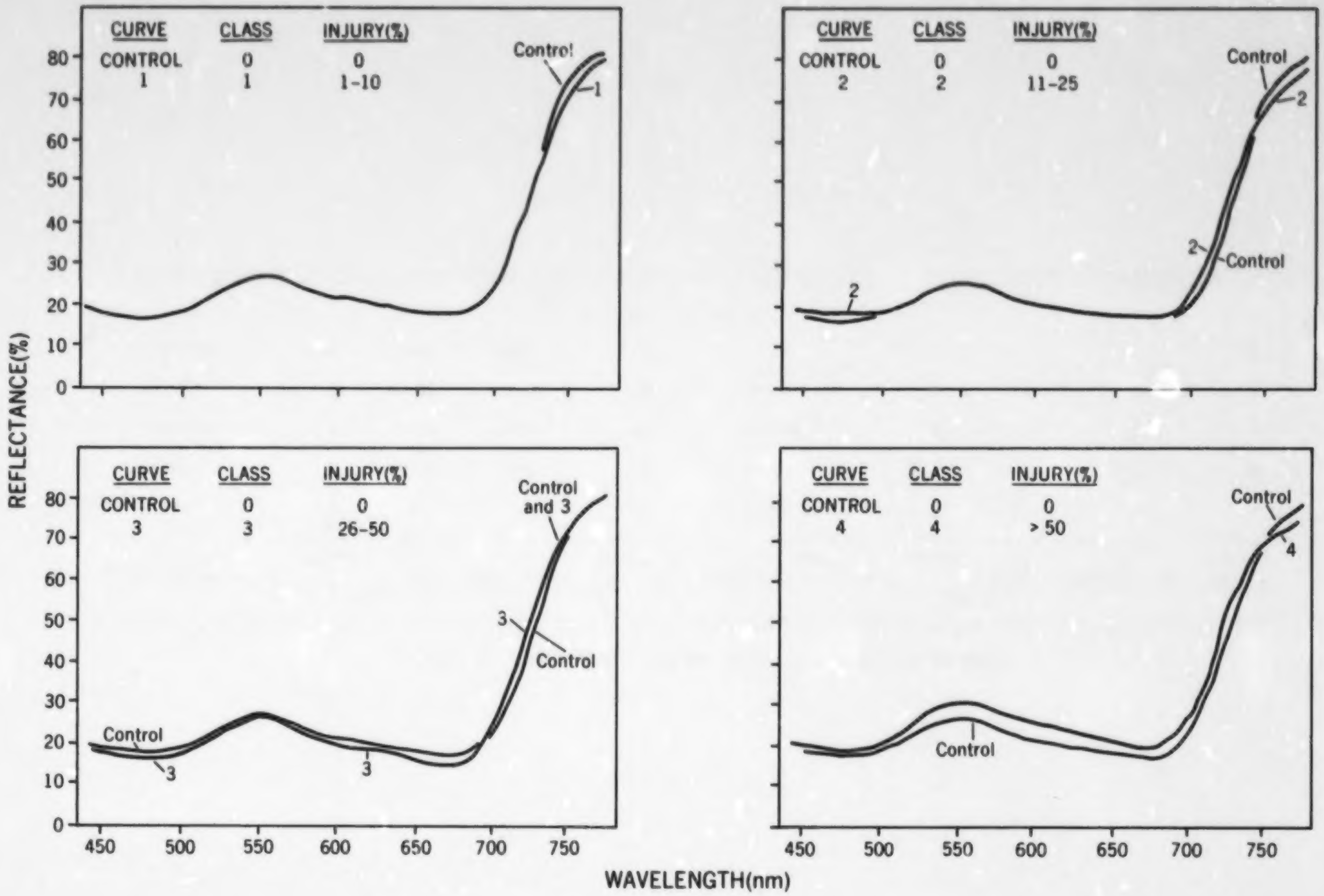

Figure 8. Mean spectral curves for classes of chlorosis in soybeans exposed to SO_2.

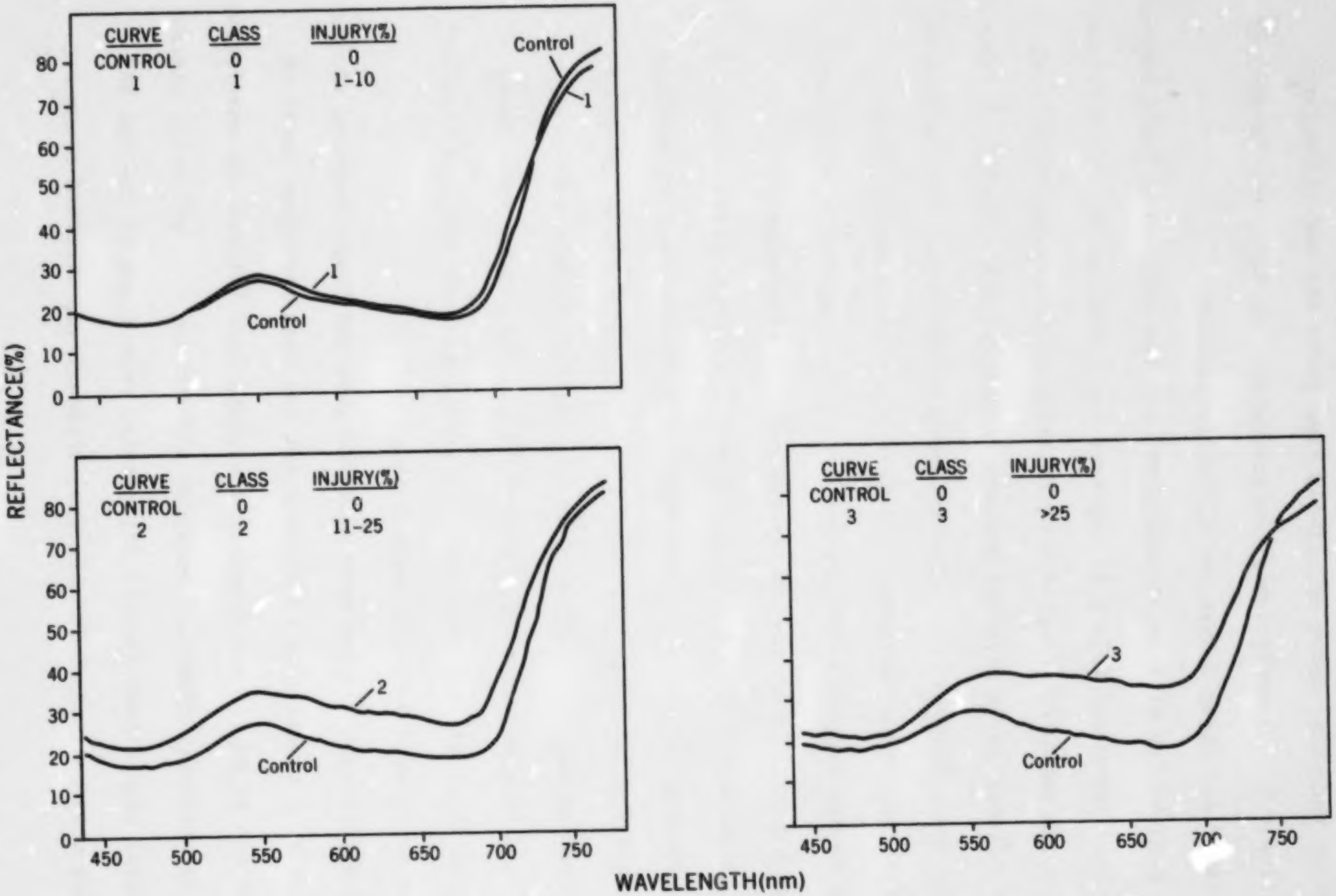

Figure 9. Mean spectral curves for classes of necrosis in soybeans exposed to SO_2.

650 nm. An ordered sequence is apparent in the curves, with curve 0 (control) having the lowest reflectance at all wavelengths. Class 3 (>25 percent necrosis) shows relatively high green and red reflectance and relatively low IR reflectance, as predicted. In fact, the IR reflectance is lower for class 3 than for all other classes.

The possibility of a relationship between the total area (cm^2) beneath each spectral curve and injury to soybeans was investigated. Correlation and regression analysis revealed a coefficient of determination (r^2) of only 0.22 between curve area and percent chlorosis, but a higher r^2 value (0.83) was found between curve area and percent necrosis. The regression showed that curve area increased with necrosis. Since the shape of a curve can change without affecting its total area, shifts in reflectance at various wavelengths or regions of the curve were examined.

The relative utility of four spectral bands (blue, green, red, and IR) for detecting foliar injury was examined by an analysis of variance using the reflectance data. The objective of the statistical procedure was to determine whether statistically significant differences in reflectance existed between pairs of injury classes. The classes were based on ranges of chlorosis and necrosis. In addition, each spectral band and the IR/red ratio were analyzed separately.

Some significant results were obtained from the comparisons of classes. For chlorosis, a significant difference (at the less stringent level of $\alpha=.10$, but not at $\alpha=.05$) was found in the green band between the unaffected and lightly chlorotic classes (combined) and the severely chlorotic class. For necrosis, significant ($\alpha=.05$) differences were found in the red and green bands between class 0 (unaffected) soybeans and affected classes 2 and 3 combined (necrosis >10 percent). A significant (α=.05) difference was also found in the IR/red ratio between the unaffected and affected soybeans.

The strength of the relationships between reflectance and foliar injury is indicated by the correlation coefficients listed in Table 2.

TABLE 2. SIMPLE CORRELATION COEFFICIENTS (r) FOR SINGLE-BAND REFLECTANCE AND FOLIAR INJURY TO SOYBEANS

Symptom	Blue	Green	Red	IR	IR/Red
Chlorosis	+0.20	+0.72	+0.36	-0.10	-0.32
Necrosis	+0.89	+0.92	+0.98	0.00	-0.94

Underlined coefficients are significant, α=.05

The table shows that the correlation coefficients for chlorosis, except for green reflectance, are below 0.50; for necrosis the visible reflectance bands, especially red, correlate much higher. IR reflectance showed no significant relationship to either chlorosis or necrosis.

The IR/red reflectance ratios listed in Table 2 should be an indirect indicator of stress in foliage, as explained previously. The low r (-0.32) between chlorosis and IR/red indicates essentially no relationship between these variables. However, there is a strong relationship (r=-0.94) between necrosis and the ratio. With increasing necrosis, the IR component of the ratio decreases and the red component increases, thus bringing the ratio value down, closer to unity.

Winter Wheat

The wheat was divided into six groups, five of which were exposed to different concentrations of SO_2 for 3 h in the chamber. One group was used for control. The range of foliar symptoms was broad, consisting primarily of necrosis (Table 3).

TABLE 3. DATA CLASSES AND FOLIAR EFFECTS OF SO_2 ON WINTER WHEAT

Qualitative level of effects[a]	Dose Class	No. of pots	Foliar Injury Mean chlorosis (%)	Foliar Injury Mean necrosis (%)	SO_2 concentration 3-h avg. ($\mu g/m^3$)
None	0	6	0	0	0 (control)
Light	1	4	1	2	3930
Moderate	2	2	1	22	5240
Very severe	3	4	4	50	6550
Very severe	4	3	5	56	7860
Very severe	5	2	5	76	9170

[a] Where light injury is $\leq$10 percent; moderate, 11-25 percent; severe, 26-50 percent; and very severe, >50 percent.

The scanning procedure yielded normalized curves which showed an increase in overall reflectance that corresponded to increasing foliar injury (Figure 9). The possibility of a relationship between the total area (cm^2) beneath each spectral curve and injury as well as SO_2 dose was investigated. Correlation and regression analysis revealed an r^2 of 0.72 between curve area and percent chlorosis in wheat. A closer association (r^2=0.85) emerged between curve area and percent necrosis. All relationships were positive; curve area increased with injury level. Next, curve area and SO_2 concentration ($\mu g/m^3$) were compared, yielding an r^2 of 0.85. This relationship was also positive.

The change in reflectance in particular wavelength regions was also studied. The red (650 ±4 nm) reflectance increased with increasing stress; this rise was particularly evident at moderate and severe levels of stress. Green (550 ±4 nm) peak reflectance also increased, but was more evident at light levels of stress (Figure 10).

Statistical analysis of the blue, green, and red reflectance curves for winter wheat yielded correlation coefficients ranging between +0.73 and +0.90 (Table 4). IR reflectances of wheat were not measured because of problems in instrument calibration.

TABLE 4. SIMPLE CORRELATION COEFFICIENTS (r) FOR SINGLE-BAND REFLECTANCE AND FOLIAR INJURY TO WINTER WHEAT

	Reflectance		
Symptom	Blue	Green	Red
Chlorosis	+0.83	+0.90	+0.81
Necrosis	+0.73	+0.83	+0.85

Underlined coefficients are significant, $\alpha=.05$

One-way analysis of variance was performed on the reflectance and injury data for wheat. The chlorosis component was divided into three classes, and the necrosis component was divided into four classes, based on the level of severity of injury (Table 5). The results showed that significant (F-test, $\alpha=.05$) differences existed among all classes for chlorosis and necrosis. The trends are readily apparent in means for the blue, green, and red reflectances listed in the table. Appendix C lists the results of the analysis of variance.

Summary of Results for Soybeans and Winter Wheat

The relationship between spectral reflectance and foliar injury from SO_2 is complex. It was analyzed by separating injury into its components--

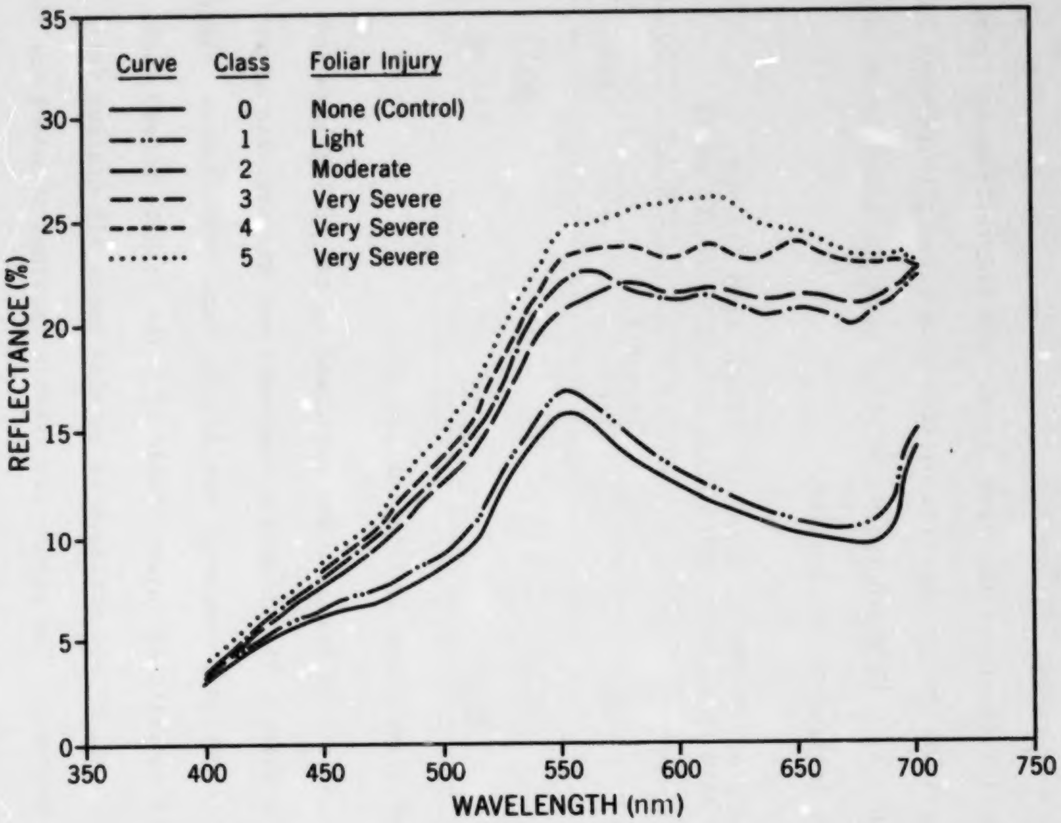

Figure 10. Mean spectral curves for classes of unaffected and SO_2-affected winter wheat. See Table 3 for SO_2 doses and levels of foliar injury.

TABLE 5. REFLECTANCE STATISTICS FOR CLASSES OF SO_2-AFFECTED WINTER WHEAT

Necrosis class[a]	Reflectance						Chlorosis class[b]	Reflectance					
	Mean (%)			Standard Deviation				Mean (%)			Standard Deviation		
	Blue	Green	Red	Blue	Green	Red		Blue	Green	Red	Blue	Green	Red
1 (0% injury)	6.4	16.2	10.3	.44	4.14	3.86	1 (0% injury)	6.4	16.2	10.3	.44	4.14	3.86
2 (1-25%)	7.3	17.6	12.4	.17	2.89	9.62	2 (0.1-1%)	7.7	20.2	19.0	.36	10.22	33.57
3 (26-50%)	7.9	21.1	21.6	.37	6.78	9.68	3 (>1%)	8.4	21.9	20.3	.78	7.20	32.76
4 (>50%)	8.7	23.7	24.3	.32	.25	1.84							

[a] For necrosis, 1-25% represents light/moderate injury; 26-50%, severe; and >50%, very severe.

[b] For chlorosis, all three classes represent very light injury.

chlorosis and necorsis--and reflectance into bands within the visible and near-infrared spectra. Results indicate that, for soybeans, only green-band reflectance could differentiate between severely chlorotic plants and unaffected or lightly chlorotic plants. Red-band reflectance could differentiate between necrotic and unaffected soybeans. The IR/red ratio was highly correlated (r=-0.94) with necrosis, but was not related to chlorosis in soybeans.

Scans of winter wheat yielded more uniformly positive results. Total visible reflectance as well as individual wavelength bands could be used to distinguish the SO_2 effects. Three classes of chlorosis and four classes of necrosis, based on severity, could be distinguished by their visible reflectance characteristics.

SECTION 4

FIELD SPECTRORADIOMETRY

GENERAL

This section of the report describes an extension of research to the field. Experimental plots of soybeans and winter wheat were grown to the seed-filling stage of development, exposed to several controlled doses of SO_2, and observed systematically to determine foliar effects. Then the plots were scanned row by row with the OMA-2 TSR. The resulting spectral curves were statistically analyzed to arrive at some soundly based generalizations on the changes in spectral reflectance that occur when these plants are stressed by SO_2. Results indicate the potential of reflectance-measuring remote sensors for detecting and mapping the effects of SO_2 emissions on these crops.

EXPERIMENTAL DESIGN

Plot Preparation and Planting

Soybeans (*Glycine Max* [L.] Merr. var Essex) and winter wheat (*Triticum aestivum* [L.] var Coker 68-15) were planted in separate 0.40-ha experimental plots. Care was taken to ensure uniformity of growth throughout the plot. Registered seed guaranteed varietal purity, fertilizer was spread, and herbicide was applied uniformly at time of planting. The soil had a high clay content but was uniform within each plot. The slope of the plot was slight but was adequate to provide good drainage.

Wheat was planted during early October 1978. The rows were drilled in pairs 18 cm apart, each pair being separated by 76 cm (center-to-center). At the time of SO_2 exposure, late April and early May 1979, coinciding with the beginning of head-filling, no variations in foliage density, color, or plant height were apparent.

Soybeans were planted during early May 1979 in rows spaced 76 cm apart. As with the wheat, no variations in foliage density, color, or height were apparent on any plants used for SO_2 fumigation. The SO_2 exposures were done during August at the pod-filling stage of development.

Exposure of Plots to Sulfur Dioxide

The wheat and soybeans were exposed to SO_2 at the stage of growth when the effects of the pollutant would theoretically have the greatest effect on yield of the crop. For the wheat, the critical time is the heading stage; for the soybeans, it is the pod-filling stage.

The exposures were effected in situ by dividing the plots into arrays of subplots, the wheat having five rows 6 m long, and the soybeans having three rows 6 m long. The two outer rows of the five in the wheat subplots served as buffers. A similar buffer function was served by plants on either end of each row beyond the 6-m segments to be exposed to the pollutant. Figures 11 and 12 illustrate the layout of the two experimental plots. The exposed subplots were paired with unexposed (control) subplots; this pairing was done to minimize locational influences on the results.

Treated plots were exposed to either 2620, 5240, 7860, or 10480 $\mu g/m^3$ of anhydrous SO_2 for two hours. The pollutant was introduced at the intake of a large blower which mixed and dispensed the desired SO_2 concentration through four 30-cm-diameter perforated, inflatable plastic tubes laid under the foliage, between the rows. In each case, the dose was changed by adjusting the concentration. The method was developed by TVA for another project which required a charcoal filter air pollution exclusion system to remove or exclude SO_2-polluted air from test plots located downwind of coal-fired power plants.[36] For the present experiments, the filters were removed from the electric blowers and SO_2 was injected into the airstream

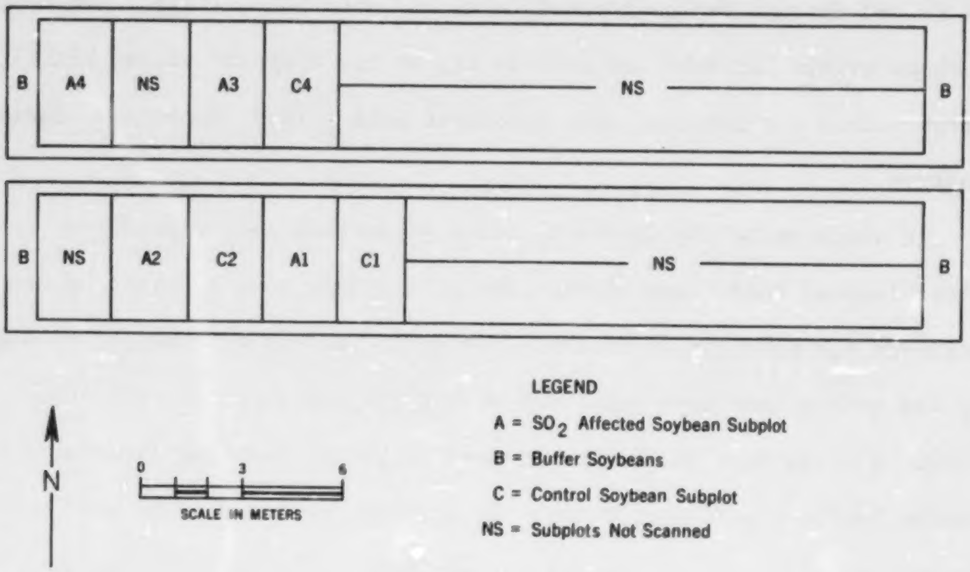
B
A4
NS
A3
C4
NS
B
B
NS
A2
C2
A1
C1
NS
B
LEGEND
A = SO_2 Affected Soybean Subplot
B = Buffer Soybeans
C = Control Soybean Subplot
NS = Subplots Not Scanned
N
0
3
6
SCALE IN METERS

Figure 11. Map of experimental plot of soybeans showing division into subplots.

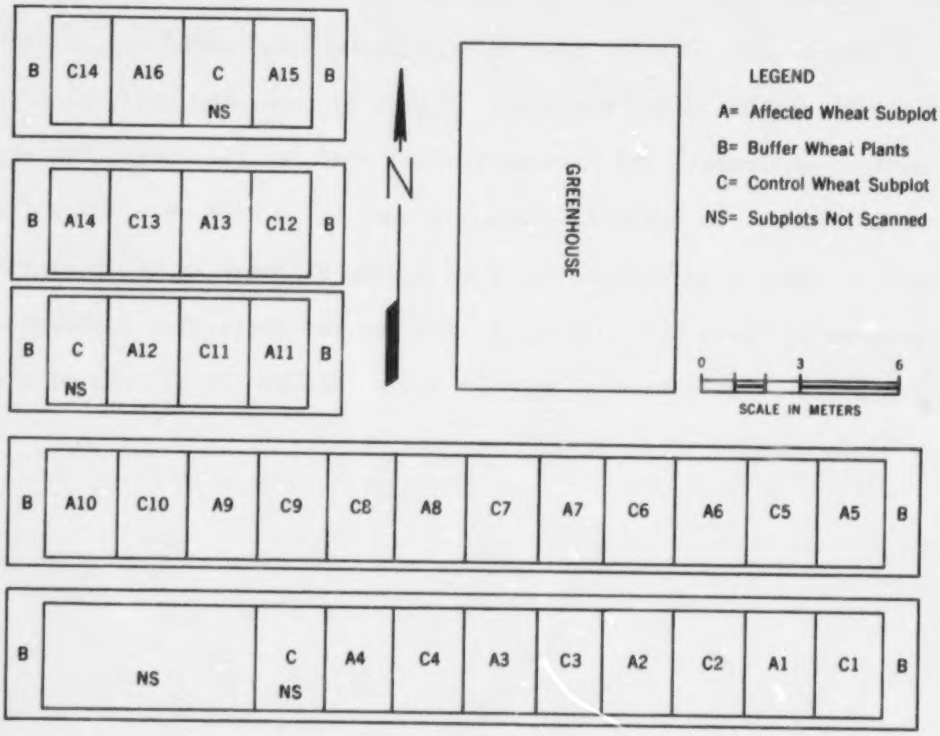
B
C14
A16
C
NS
A15
B
B
A14
C13
A13
C12
B
B
C
NS
A12
C11
A11
B
N
GREENHOUSE
LEGEND
A= Affected Wheat Subplot
B= Buffer Wheat Plants
C= Control Wheat Subplot
NS= Subplots Not Scanned
0
3
6
SCALE IN METERS
B
A10
C10
A9
C9
C8
A8
C7
A7
C6
A6
C5
A5
B
B
NS
C
NS
A4
C4
A3
C3
A2
C2
A1
C1
B

Figure 12. Map of experimental plot of wheat showing division into subplots.

and forced through the perforated tubes and onto the foliage. The concentrations within the tube and outside it, at the midpoint of the plant canopy within the subplot, were monitored with a Teco SO_2 monitor during exposure.

In addition to SO_2 exposure, other parameters were considered. Meteorological conditions at the time of exposure to air pollution can influence the severity of foliar effects.[37] Therefore, atmospheric humidity and temperature were monitored during the experiments. A Li-Cor diffusion-resistance porometer was used to verify that the stomata of the soybean leaflets were open before the gas was dispensed. The plot was watered the afternoon before every experiment. The applications usually began at approximately 10 a.m. and ended about 4 p.m., so that four subplots, representing one replication, were exposed each day.

Access to the subplots for the experimental equipment was provided by straight swaths across the plot. Figure 13 shows the wheat plot and the swaths, equipment, and instrumentation used for the controlled exposure experiment. Portable fiberglass fences 1.2 m high were moved from subplot to subplot to enclose the rows during exposure to the pollutant. The purpose of these barriers was to prevent the horizontal dispersion of the gas beyond the particular subplot and to reduce the effects of wind below 1.2 m height.

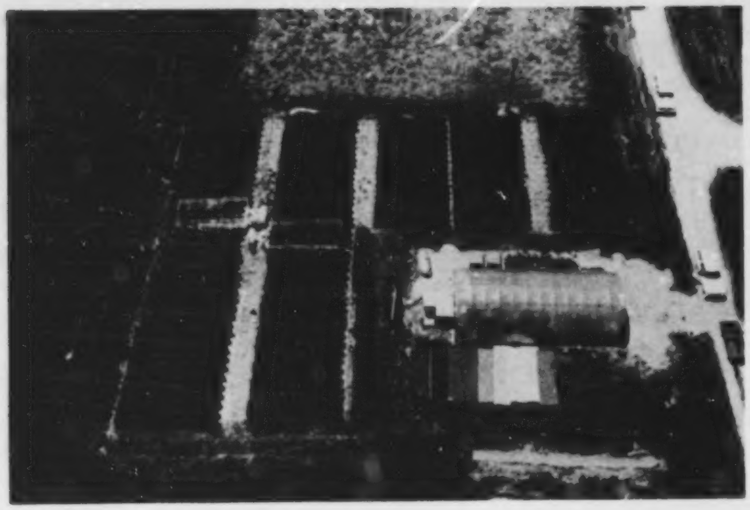

Figure 13. Aerial view of experimental plot of wheat showing equipment and instrumentation for controlled SO_2 exposure.

Observations of Foliar Injury

The foliar effects (symptoms) of SO_2 on vegetation typically emerge slowly, taking from several hours to several days to develop completely. The total time required for development depends on the level of dose, temporal characteristics of the concentration, and several other factors that vary from species to species.[38] Therefore, a week was permitted to elapse after exposure before the observations of foliar injury were made and recorded. Injury estimates using the L x A method (Appendix D) were made on ten randomly selected plants on each 6-m row. For winter wheat, the upper three of six leaves on each tiller were always selected for observation. (Senescence of the lower leaves was present on the soybeans and wheat.) The measurements for the ten plants were averaged, providing mean values for chlorosis and necrosis for each of the three rows within a particular subplot. For comparative purposes, the three row figures were averaged to yield a mean percentage of chlorosis or necrosis for the subplot. This procedure of observation was followed for soybeans and wheat.

Scanning Procedure

The plots were scanned as soon as practical before or after observations of foliar injury were made. Scanning required sunny weather, a condition that in summer was most likely to occur during mornings, so the scans were acquired during the 10:00 a.m. to 12:00 a.m. period. Several days were required to complete the scanning.

A van with an aluminum platform on top provided a convenient place for the operator and TSR (Figure 14). A helicopter was tested as a scanning platform but was judged unsatisfactory and inconvenient, so the van was used. Power for the instrument was provided by a portable, 1700-watt alternator which was shock-mounted on the platform. The voltage generated by the unit was controlled with a regulated transformer and solid-state surge eliminator. Vibrational effects on the optics were minimized with shock mounts.

The angle of view from the telescope to the target is an important factor in any spectral scanning experiment.[39] These angles were held constant during scanning by controlling the orientation of the van. Figure 15 shows the angular configuration and distances used. After each scan set was completed, the van was advanced one row for the next scan set. The NASA gray target was also scanned at the same angle and distance each time. A scan set consisted of 50 scans of a row of plants and 50 scans of the NASA gray target. The telescope was swiveled horizontally through 72 degrees after scanning the target, and then the vegetation was scanned. Minor adjustments in the vertical angle had to be made to compensate for topography.

Another important factor in any spectral scanning experiment is the angle of illumination.[40] Solar effects must be known and minimized or

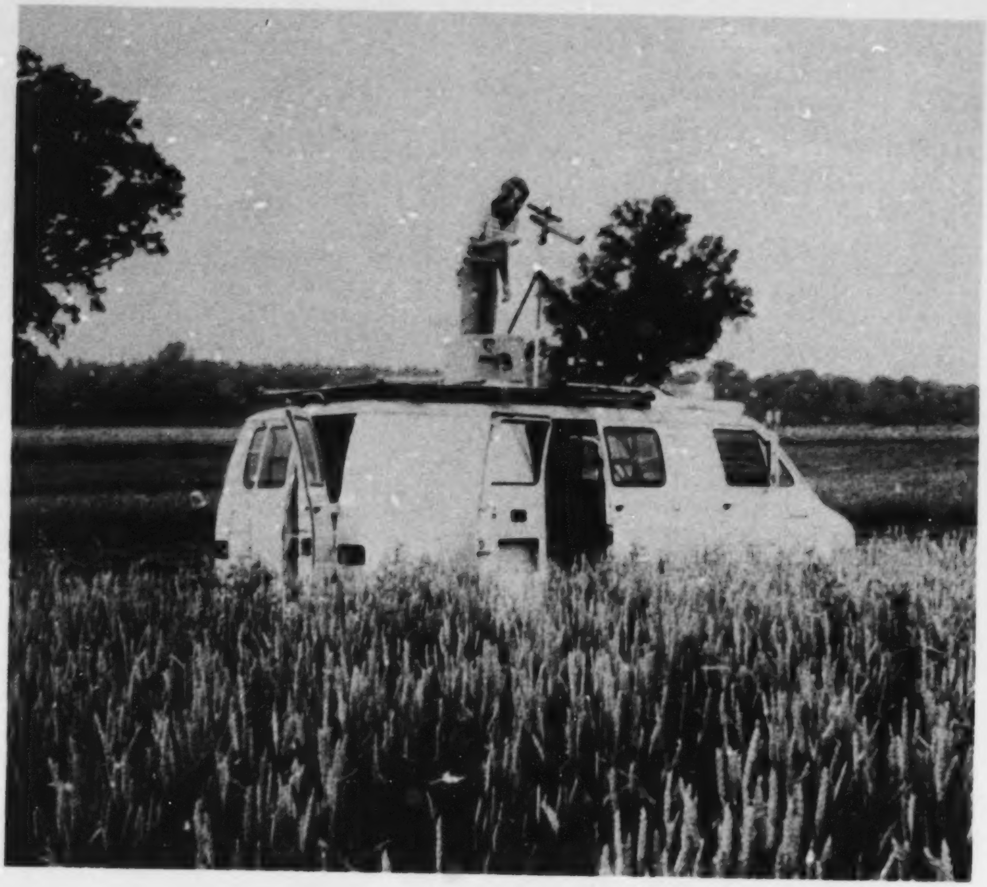

Figure 14. Mobile platform for spectroradiometry. Telescope, grating spectrometer, and power supply are on top and the OMA-2 console is inside the van.

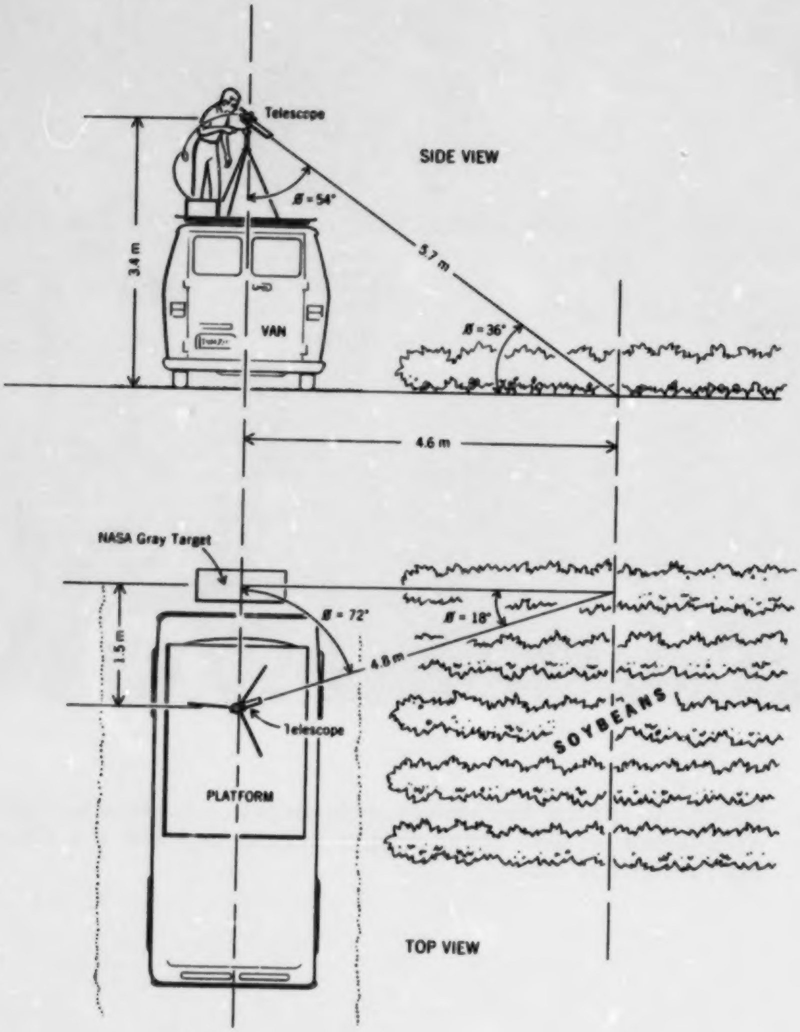
Telescope
SIDE VIEW
θ = 54°
5.7 m
3.4 m
VAN
θ = 36°
4.6 m
NASA Gray Target
θ = 72°
θ = 18°
1.5 m
4.8 m
Telescope
SOYBEANS
PLATFORM
TOP VIEW

Figure 15. Geometric configuration for scanning subplots.

compensated for. The van was oriented so that the sun was behind it and the plant canopy was fully illuminated on the side that was being scanned. Variations in illumination that occurred during scanning were compensated for by scanning the NASA gray target immediately before scanning the vegetation and normalizing each scan set according to the following procedure.

Normalization of Spectral Curves

As in the laboratory-based experiments, the spectral curves were normalized to convert from radiant energy units (counts per photon) to percent reflectance. This conversion was necessary to ensure comparability among curves that had been acquired under different conditions of illumination.

The conversion to percent reflectance involved scanning the NASA gray target and then immediately scanning the vegetation. No delay between the two scans was allowed because a change in illumination during the interval would introduce error. Normalization consisted of dividing the vegetation curve by the previous measurement of the NASA gray target and multiplying the resultant curve by the "true" reflectance curve for the target (Figure 16). Note that the actual NASA gray target was scanned instead of a TVA reference standard (gray card).

Normalization, background subtraction, statistical grouping, and averaging of curves were done from the console keyboard after scanning was complete. Then the curves were stored on flexible discs for output later to the x-y plotter.

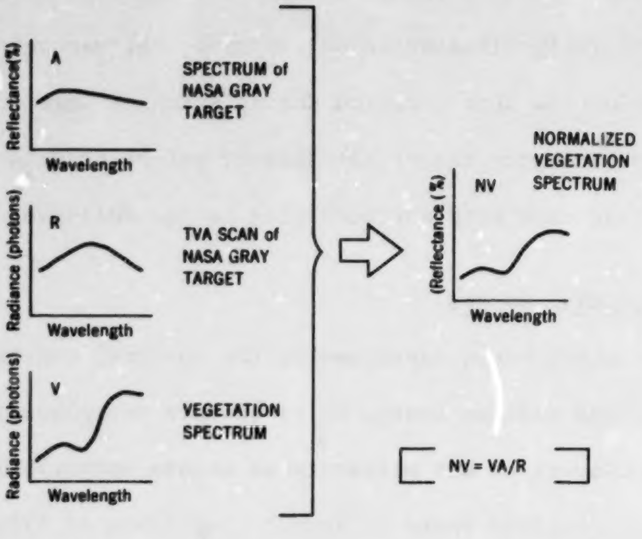
Reflectance(%)
A
Wavelength
SPECTRUM of NASA GRAY TARGET
Radiance (photons)
R
Wavelength
TVA SCAN of NASA GRAY TARGET
Radiance (photons)
V
Wavelength
VEGETATION SPECTRUM
NORMALIZED VEGETATION SPECTRUM
NV
(Reflectance (%)
Wavelength
NV = VA/R

Figure 16. Procedure for normalizing spectral curves of radiance for experimental field plots.

RESULTS AND DISCUSSION

Soybeans

Data from seven subplots of soybeans were analyzed statistically to determine relationships among reflectance, SO_2 dose (concentration x time), and foliar injury (chlorosis and necrosis). Reflectance was the dependent variable. First, the relationship between dose and injury was examined; then the relationship between dose and reflectance was studied; finally, the relationships between reflectance and injury, and between reflectance and yield were determined and characterized. The subplot measurements are listed in Appendix D.

The relationship between SO_2 dose and observed levels of foliar injury to soybeans is complex, as the preceding laboratory studies have shown. Plots of dose versus chlorosis and dose versus necrosis revealed no relationships (Table 6). No relationship was evident between either dose and

TABLE 6. SO_2 DOSE, INJURY, AND YIELD OF SOYBEANS

Dose Class	SO_2 Concentration (2-h avg)	No. of Subplots	No. of Rows	Mean Chlorosis (%)[a]	Mean Necrosis (%)[a]	Mean Yield (kg/ha)
1 (control)	0 μg/m³	3	8	0	0	2730
2	2620	1	3	25.0	0	2596
3	5240	1	3	14.3	45.0	2234
4	7860	1	3	41.0	0	2759
5	10480	1	2	11.5	30.0	2352

[a] Where light effects are classified as <10 percent; moderate effects, 11-25 percent; and severe effects, >25 percent. See Appendix D for method of computation.

either dose and yield or chlorosis and yield, but a significant (α=.05) negative correlation (r=-0.97) between necrosis and yield was indicated (Figure 17).

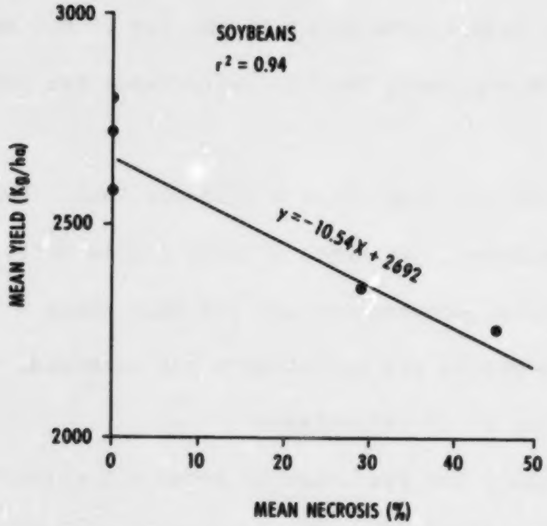

Figure 17. Linear regression of yield on necrosis for soybeans exposed to SO_2.

Next, the individual reflectance curves (shown in Appendix E) for the rows within subplots were sorted and grouped by SO_2 dose, then averaged to provide one mean curve for each of the four classes (Figures 18a, b, c, and d).

Correlation coefficients were calculated between total reflectance (the total area under the mean reflectance curve) and dose, injury, and yield. These statistics revealed no significant (α=.05) relationships. Since the shape of a curve can change without affecting its total area, shifts in reflectance at various wavelengths or regions of the curve were examined.

Consider the control and dose class 2 (Figure 18a). There is an obvious difference in visible reflectance around 500 to 550 nm, but otherwise the curves are similar. Now compare control with dose class 3 (Figure 18b): Prominent differences exist in the red (~ 650 nm) and IR (~ 750 nm) regions. With exposure, the red reflectance has increased and the IR has decreased.

Next, compare control and dose class 4 (Figures 18c). Some decrease in IR reflectance has occurred, but there is very little difference in the visible bands. Finally, compare control and dose class 5 (Figure 18d): Some increase in red reflectance has occurred, but the major change is a decrease in IR reflectance.

An analysis of variance was performed to compare control to the four dose classes combined (Table 7). Three spectral regions were sampled at their central wavelengths to provide representative data for analysis. Accordingly, green reflectance was measured at 550 nm; red, at 650 nm; and IR, at 750 nm. The measurements are listed in Appendix E.

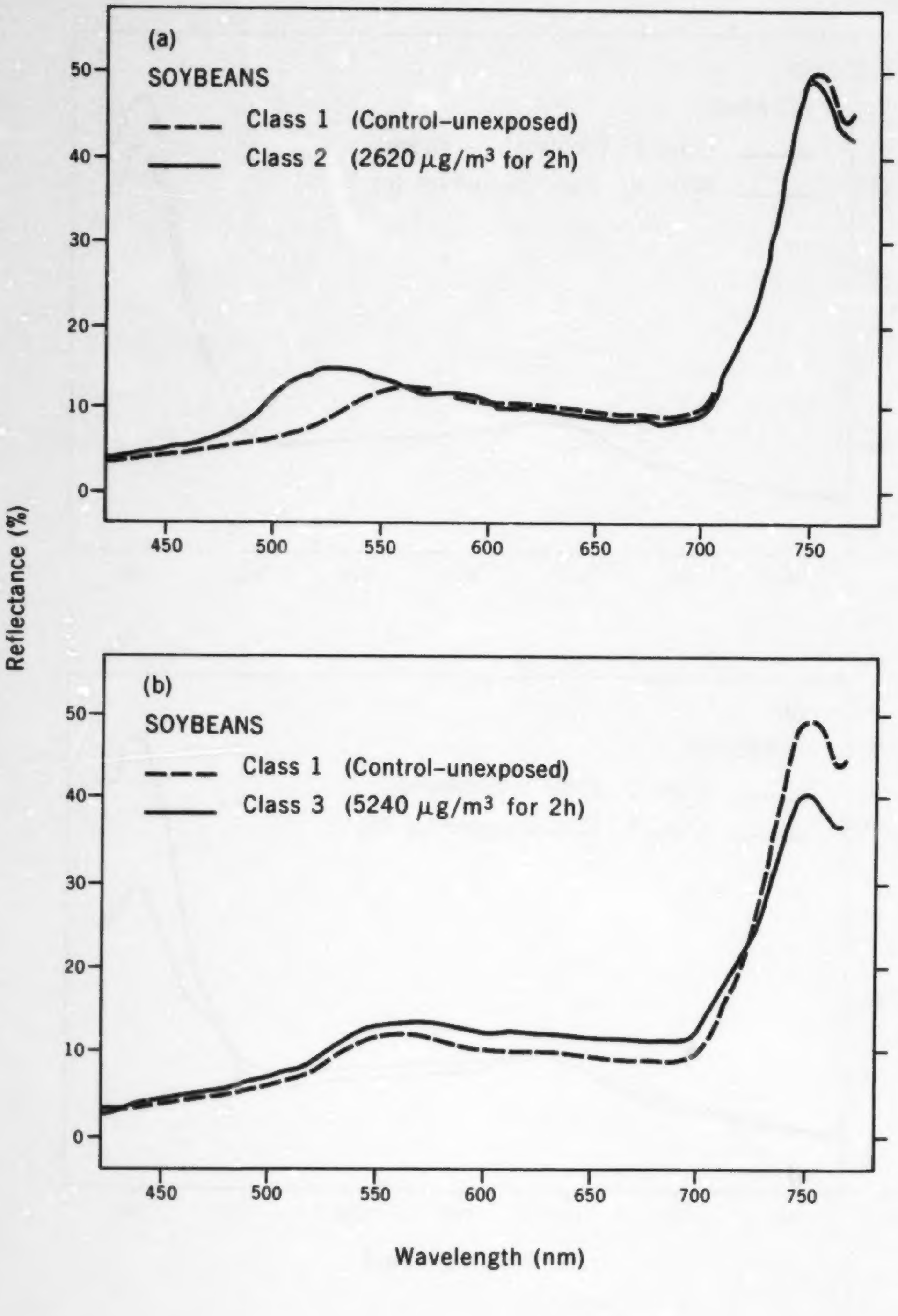

Figures 18a and b. Mean spectral curves for soybeans exposed to SO_2. Control also shown for comparison.

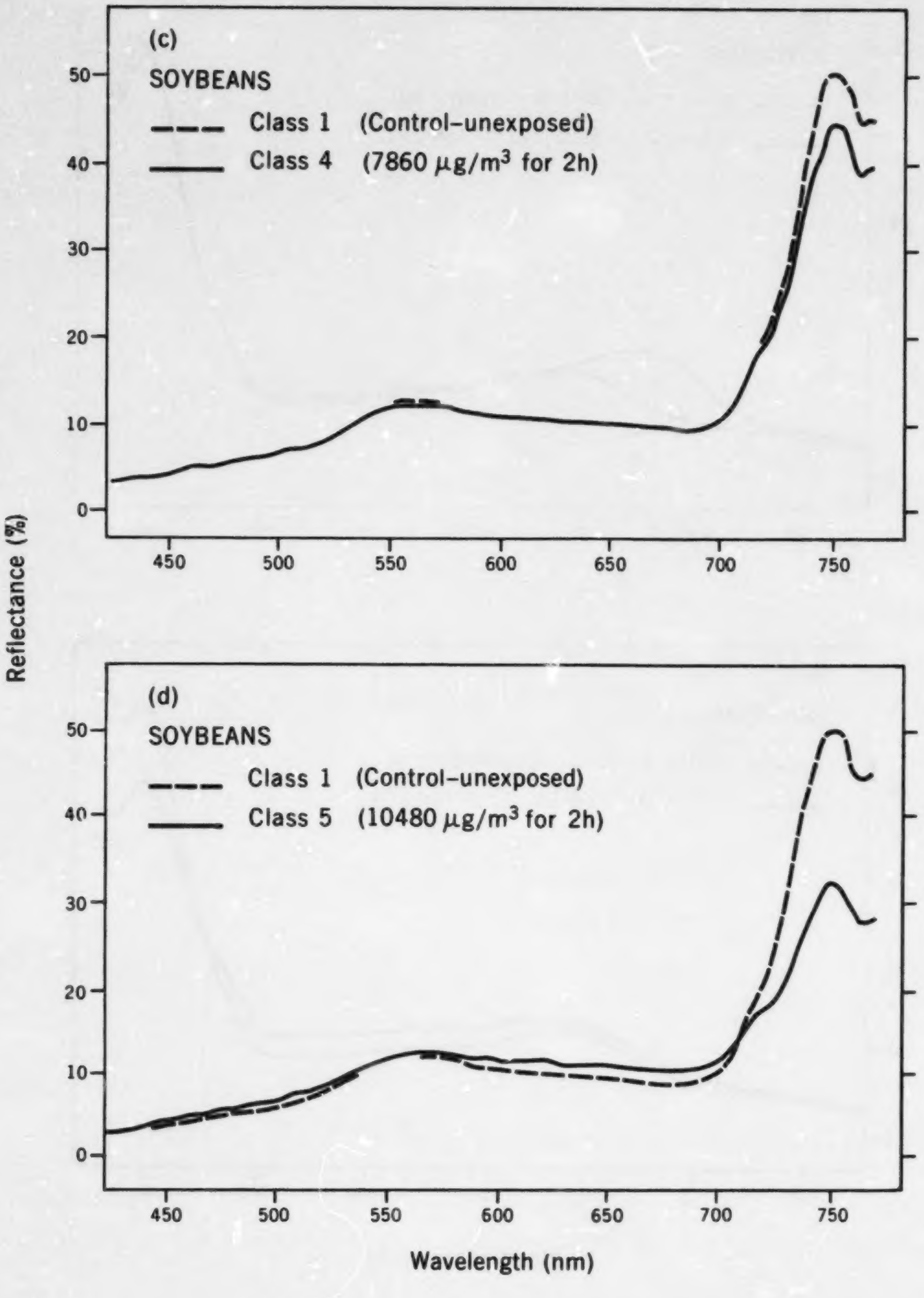

Figures 18c and d. Mean spectral curves for soybeans exposed to SO_2. Control also shown for comparison.

TABLE 7. SIGNIFICANT DIFFERENCES IN REFLECTANCE BETWEEN SO_2-EXPOSED AND CONTROL SOYBEANS

Dose Classes	Reflectance			
	Green	Red	IR	IR/Red
Control (unexposed) versus SO_2-exposed soybeans	0.87	3.07	4.58	6.95

Underlined values are significant, F-test, α=.05.

Table 7 indicates that the differences in green- and red-band reflectance for the dose classes are not statistically significant (F-test, α=.05). However, the differences in IR and IR/red reflectance are significant at this level.

Perhaps the most important comparison in this study is reflectance versus foliar injury. Appendix D shows that the affected subplots have higher reflectance in the green, higher in the red, lower in the IR, and a lower IR/red ratio. The yield of the affected subplots is also lower. These comparisons reveal general trends only. The mean curves in Figures 19a and b were obtained by grouping the reflectance measurements into three classes: control (unaffected soybeans), chlorotic soybeans, and necrotic soybeans. The mean curve for chlorotic soybeans (Figure 19a) shows lower IR reflectance than that for the control. The curve for necrotic soybeans (Figure 19b) shows greater differences: the IR reflectance is lower and the green and red reflectances are higher than that for the control.

Table 8 reveals that the visible reflectance variations correlate significantly (α=.05) with necrosis, but not with chlorosis. No significant correlation between reflectance and yield is indicated.

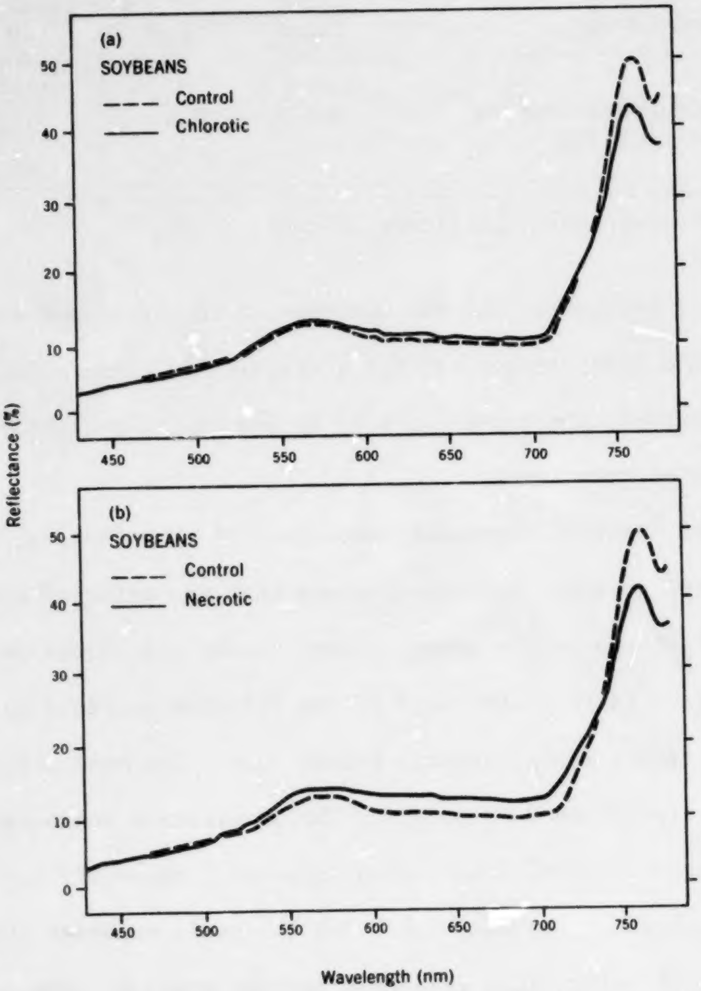

Figures 19a and b. Mean spectral curves for SO_2-affected soybeans. Control also shown for comparison.

TABLE 8. SIMPLE CORRELATION COEFFICIENTS (r) FOR SINGLE-BAND REFLECTANCE, FOLIAR INJURY, AND YIELD OF SOYBEANS

	Reflectance			
Symptom	Green	Red	IR	IR/Red
Chlorosis	+.47	+.57	-.62	-.68
Necrosis	+.83	+.97	-.65	-.84
Yield	+.00	+.33	+.55	+.51

Underlined coefficients are significant (α=.05).

Regressions of reflectance and foliar injury further characterize the significant relationships between these variables (Figures 20a, b, and c). The regression of necrosis and green reflectance shows a positive association (Figure 20a). The same is true for necrosis and red reflectance (Figure 20b). On the other hand, the correlation between necrosis and the IR/red ratio is negative (Figure 20c). The IR regression was not significant and is not shown.

To determine whether the differences in reflectance between SO_2-affected soybeans and control soybeans were significant, an analysis of variance was performed. Table 9 summarizes the results and Appendix F provides the details. There was a significant (α=.05) difference in IR and IR/red reflectance between the chlorotic soybeans and unaffected (control soybeans. There were also significant differences in red reflectance, IR reflectance, and the IR/red ratio between necrotic and unaffected soybeans.

There were no significant differences in yield between any of the classes of affected and unaffected soybeans. These findings agree with the insignificance of the r coefficients for yield versus reflectance (Table 8).

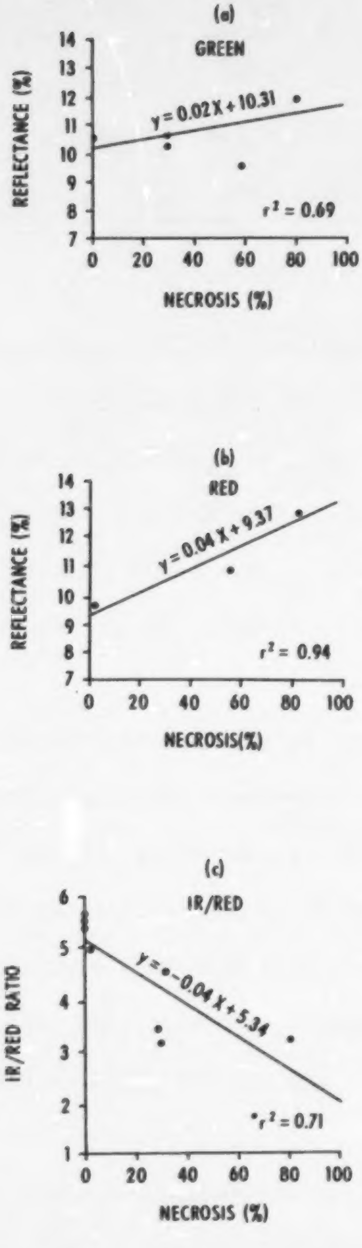

Figures 20a, b, and c. Linear regressions of reflectance on necrosis for SO_2-affected soybeans.

TABLE 9. SIGNIFICANT DIFFERENCES IN REFLECTANCE AND YIELD BETWEEN SO_2-AFFECTED AND UNAFFECTED SOYBEANS

Class	Test Statistic	Reflectance				Yield
		Green	Red	IR	IR/Red	
Chlorotic versus unaffected soybeans	F	0.87	2.28	6.94	6.93	2.80
Necrotic versus unaffected soybeans (neither necrotic nor chlorotic)	F	3.42	13.12	19.73	33.02	3.69

Underlined values are significant, F-test, $\alpha=.05$.

Winter Wheat

The 30 subplots of winter wheat were grouped by SO_2 dose class and foliar injury class to relate changes in spectral reflectance to the classes. Appendix D lists the subplot measurements. A comparison of the subplots shows that the exposed ones have higher red reflectance, lower IR reflectance, a lower IR/red ratio, lower yield, and, of course, a higher percentage of necrosis. Correlation and regression analyses were done to compare total reflectance (area under spectral curve) with dose, necrosis, and yield (Table 10). The only significant ($\alpha=.05$) relationship between percent area under the curve and any of these three variables was with necrosis ($r^2=0.66$); as necrosis increased, so did curve area (Figure 21). Next, the dose classes were examined with respect to the three individual spectral bands (green, red, and IR) and the IR/red ratio. Four 2-h concentrations of the pollutant and the control formed five dose classes.

TABLE 10. TOTAL REFLECTANCE, SO_2 DOSE, FOLIAR INJURY, AND YIELD OF WINTER WHEAT

Dose Class	Concentration (2-h avg)	Reflectance Curve Area (%)[a]	Yield (kg/ha)
1 (control)	0 μg/m^3	31.29	3094
2	2620	29.02	3325
3	5240	26.95	2479
4	7860	28.49	2241
5	10480	31.02	1894

Necrosis Class	Mean Necrosis (%)	Range of Necrosis (%)	Reflectance Curve Area (%)[a]	Yield (kg/ha)
1	7.7	≤10	21.05	3044
2	13.8	11-25	24.70	3128
3	33.8	26-50	25.79	3135
4	68.5	>50	26.82	2229

[a] Percentage of rectangular plotted area filled by the curve.

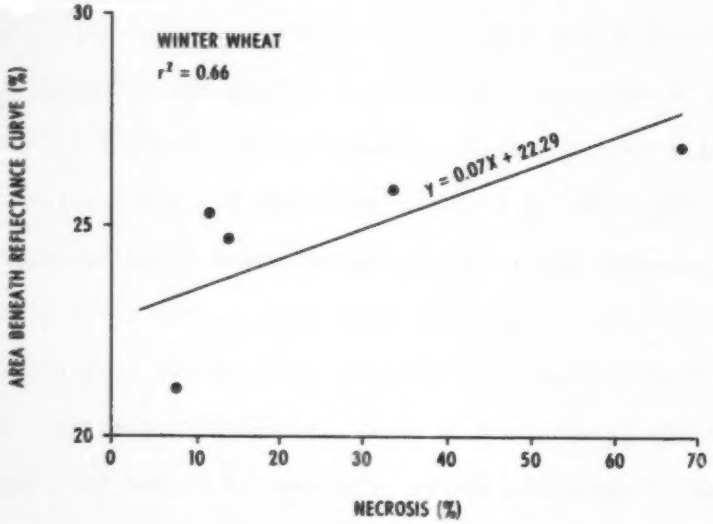

Figure 21. Linear regression of reflectance curve area on necrosis for winter wheat exposed to SO_2

The individual reflectance curves for each subplot were sorted and grouped by dose, then averaged to provide one mean curve for each of the five classes (Figures 22a, b, c, and d). The curves are plotted with the control (dose class 1) to display the relative differences. In Figure 22a (control and dose class 2) only minor differences are apparent; the exposed wheat has lower overall reflectance than the control. Figure 22b (control and dose class 3) shows that the green and IR reflectances of the exposed wheat are considerably lower, and the red reflectance is slightly higher than the control. Figure 22c (control and class 4) shows a response that is not markedly different than that of class 3. However, Figure 22d (control and class 5) shows a remarkable difference in the visible and IR wavelengths. The visible reflectance of the exposed wheat has increased markedly and the IR reflectance has decreased slightly when compared with control. An overall flattening of the spectral curve is evident. This flattening is a typical response for the reflectance of stressed vegetation.[41]

The five dose classes were compared using analysis of variance (Table 11). The table indicates that the differences among each of the five means of red, IR, and IR/red reflectance are statistically significant (α=.05). However, differences among the five means of green reflectance are not significant.

TABLE 11. SIGNIFICANT DIFFERENCES IN REFLECTANCE AMONG FOUR CLASSES OF SO_2-EXPOSED WINTER WHEAT AND CONTROL

Test Statistic	Reflectance			
	Green	Red	IR	IR/Red
F	1.37	3.82	9.25	14.71

Underlined values are significant, F-test, α=.05.

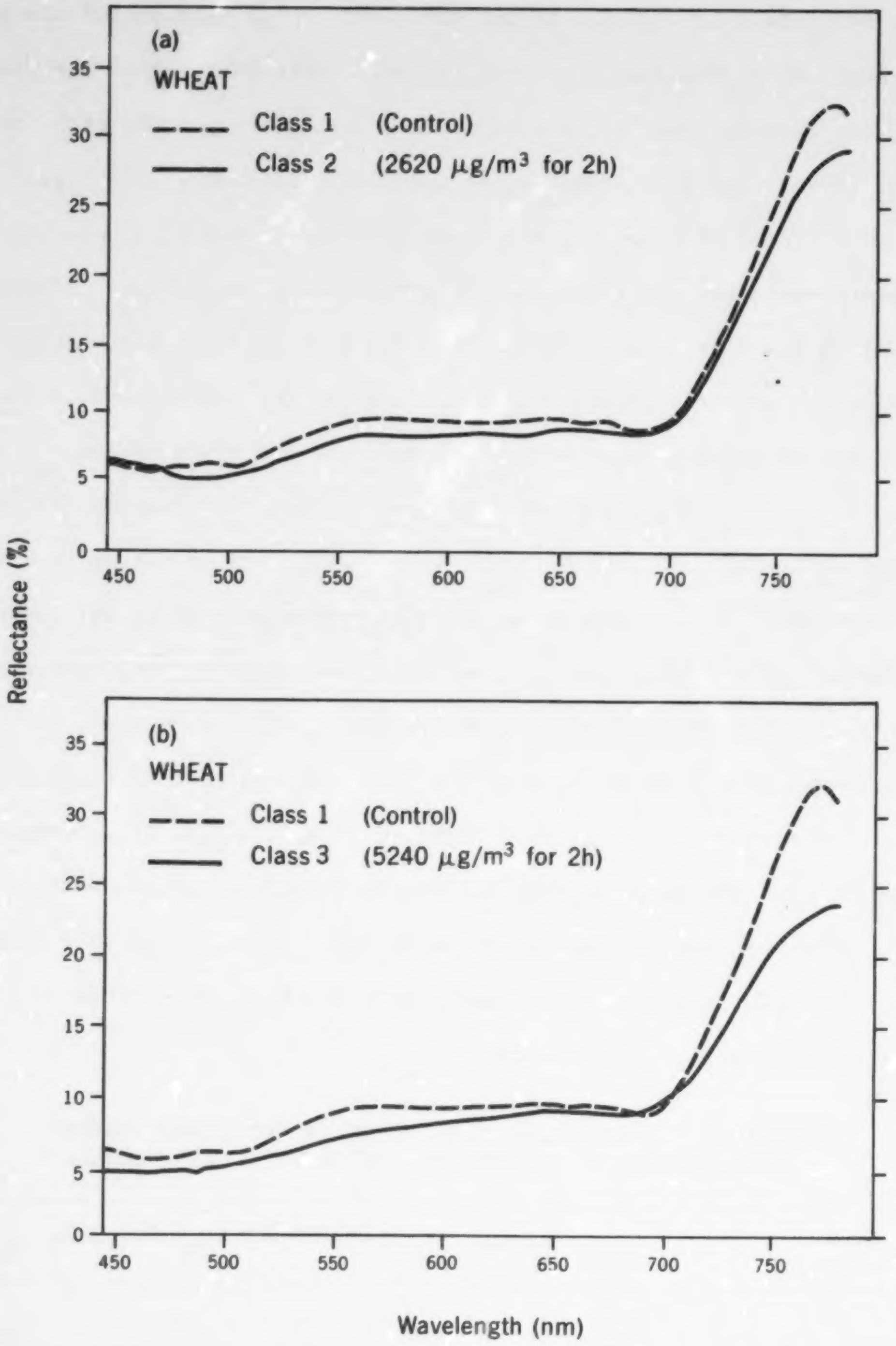

Figures 16a and b. Mean spectral curves for winter wheat exposed to SO_2. Control also shown for comparison.

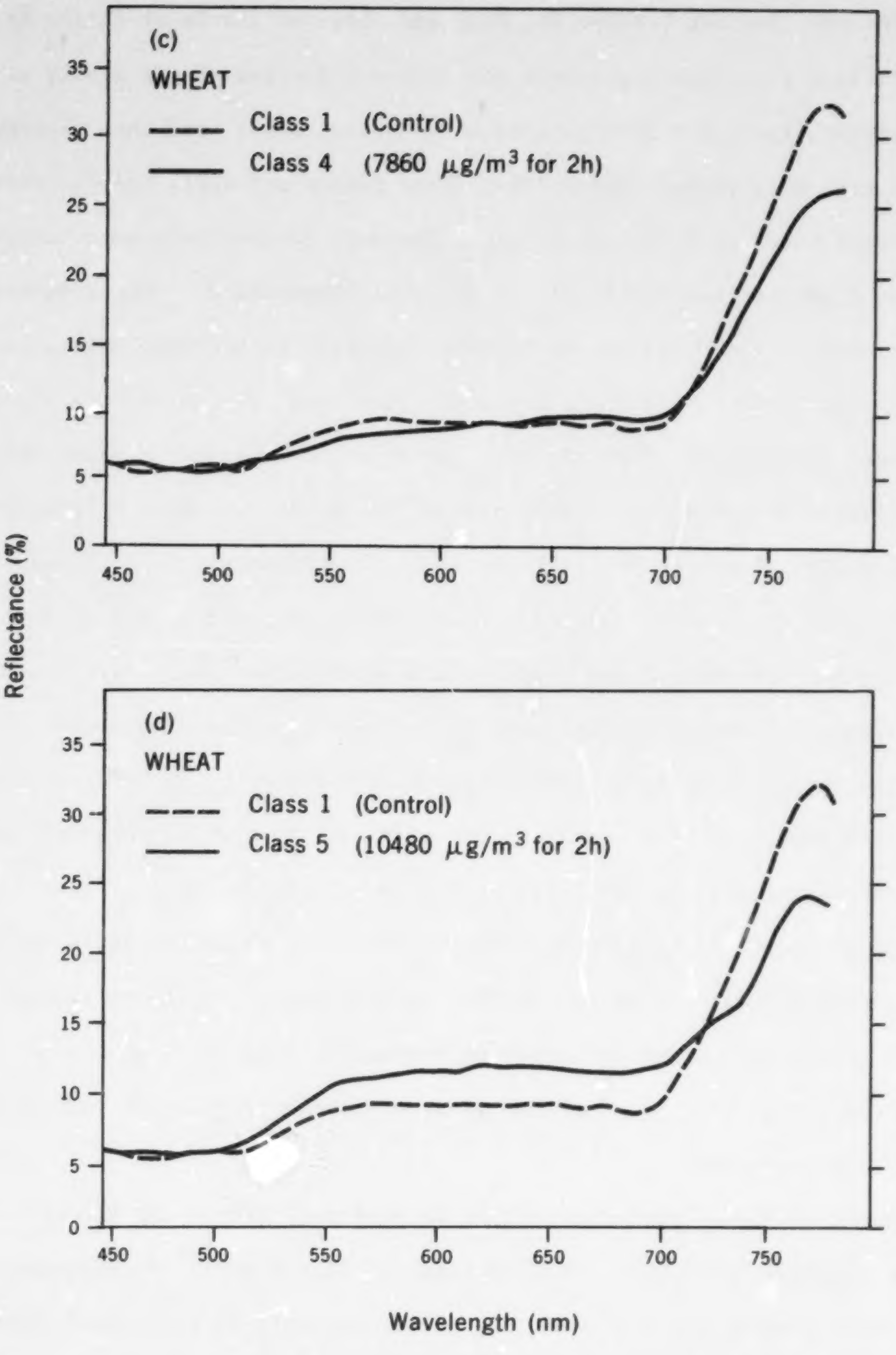

Figures 16c and d. Mean spectral curves for winter wheat exposed to SO_2. Control also shown for comparison.

The relationship between SO_2 dose and observed levels of foliar injury is not linear; in this experiment the necrosis symptoms began slowly at low dose levels, increased more rapidly at moderate levels, and then tapered off at high dose levels (Table 12). These trends may apply only to this particular data set. This statistical analysis focuses only upon necrosis because chlorosis was negligible in the plot (Appendix D). Characteristically, wheat responds to SO_2 by becoming necrotic rather than chlorotic.

In the study of foliar injury and reflectance, the necrosis percentages were grouped into four classes (Table 13). The injury classes and dose classes do not correspond because of the great variability in response of individual plants to the pollutant. The breakpoints for the classes of necrosis are the traditional boundaries used by field biologists. Four mean reflectance curves, each representing a necrosis class, were produced by grouping and averaging the individual curves (Figures 23a, b, and c).

The potential of reflectance measurements for detecting foliar injury was determined by statistical analysis of necrosis data and three reflectance bands (green, red, and IR), as well as the IR/red ratio. The objective of the statistical procedure was to determine whether statistically significant differences in reflectance existed among the injury classes. These classes were based on ranges of necrosis. Finally, statistical tests concerning the relationships among reflectance, necrosis, and crop yield were conducted.

Table 14 lists the relationships between reflectance and the two variables, necrosis and yield. The red band and IR/red ratio of reflectance seem to be most useful for detecting either necrosis or yield reduction.

TABLE 12. REFLECTANCE, NECROSIS, SO_2 CONCENTRATIONS, AND YIELD FOR WINTER WHEAT BY DOSE CLASS

Dose Class	SO_2 Concentration (2-h avg)	Mean Necrosis (%) ±S.D.	Mean Reflectance (%) ±S.D.			Mean IR/Red ±S.D.	Mean Yield (kg/ha)±S.D.
			Green	Red	IR		
1	0 μg/m^3	8.5±1.9[a]	10.83±1.31	10.39±1.26	32.16±5.83	3.13±0.36	3094±436
2	2620	19.4±6.7	10.55±1.15	10.58±1.79	29.19±4.80	2.86±0.73	3325±396
3	5240	58.1±17.5	9.76±0.60	11.27±0.58	25.16±3.82	2.23±0.30	2479±79
4	7860	67.0±16.0	10.60±0.68	11.60±1.43	32.07±9.10	2.84±0.99	2241±570
5	10480	76.6±15.5	10.81±1.61	12.15±1.71	24.03±5.37	1.96±0.16	1894±763

[a] Necrosis in Class 1 (control) is associated with natural senescence that occurred after scanning but before observations were made.

TABLE 13. REFLECTANCE, NECROSIS, AND YIELD FOR WINTER WHEAT BY INJURY CLASS

Injury Class[a]	Mean Necrosis ±S.D.	Mean Reflectance (%) ±S.D.			Mean IR/Red ±S.D.	Mean Yield (kg/ha) ±S.D.
		Green	Red	IR		
1	7.7±1.2	10.74±1.48	10.35±1.47	30.03±5.50	2.93±0.54	3109±511
2	13.8±3.8	10.86±0.96	10.71±1.32	33.37±5.68	3.19±0.76	3128±228
3	33.8±4.8	10.50±0.09	10.40±0.76	32.24±4.22	3.15±0.64	3007±642
4	68.5±16.6	10.39±1.21	11.72±1.43	27.00±7.72	2.32±0.74	2190±627

[a] Class 1 - ≤10% necrosis
2 - 11-25 %
3 - 26-50 %
4 - >50 %

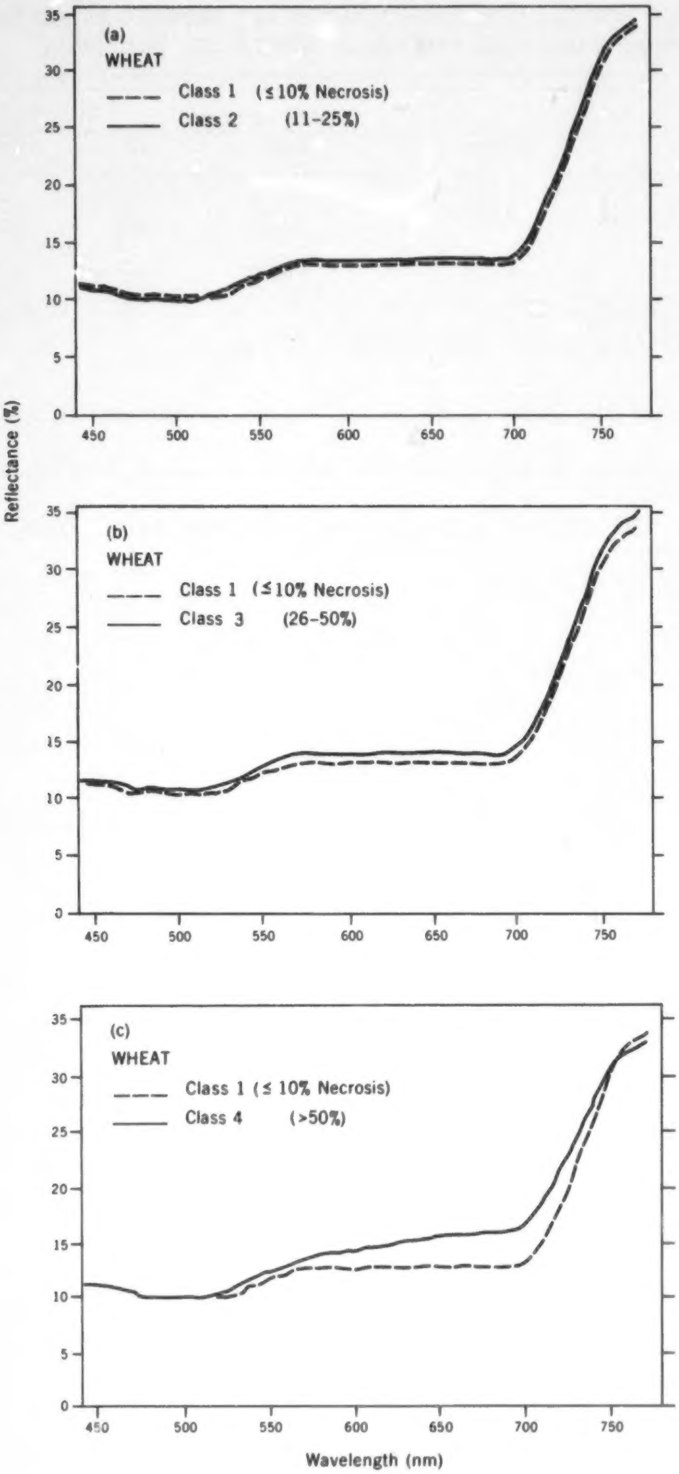

Figures 23a, b, and c. Mean spectral curves for SO_2-affected winter wheat.

TABLE 14. SIMPLE CORRELATION COEFFICIENTS (r) BETWEEN REFLECTANCE AND TWO OTHER VARIABLES (NECROSIS AND YIELD) FOR WHEAT

Symptom	Reflectance			
	Green	Red	IR	IR/Red
Necrosis	-.06	+.59	-.53	-.71
Yield	+.52	-.63	+.45	+.67

Underlined coefficients are significant, $\alpha=.05$.

The trends of the relationships are also noteworthy (Figures 24a, b, and c). Red reflectance increases and IR reflectance decreases as percent necrosis rises. The IR/red ratio decreases as necrosis rises. These findings conform to theory.[42]

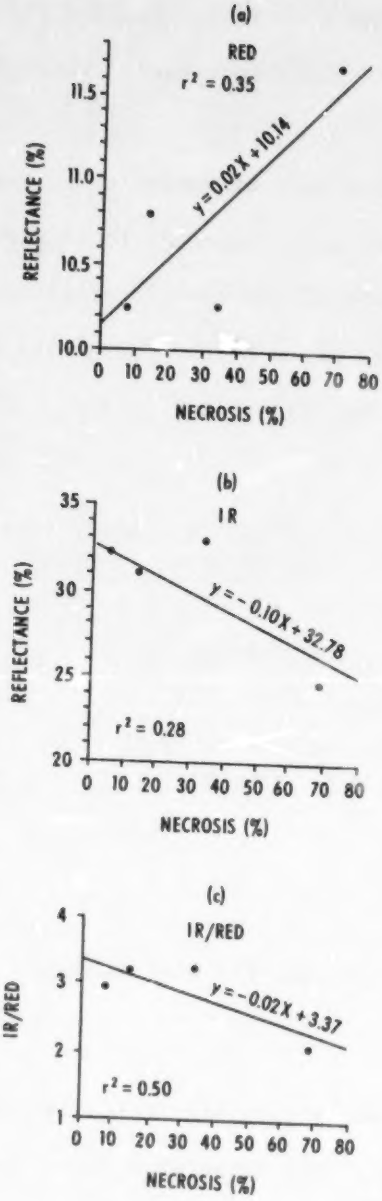

Figures 24a, b, and c. Linear regressions of reflectance on necrosis for winter wheat.

Yield of wheat is related to necrosis and reflectance. Yield and necrosis are inversely related (Figure 25). Green and IR reflectances and the IR/red ratio increase with yield (Figures 26a, b, and c), but red reflectance decreases as yield increases. These findings also conform to theory.[43]

Results of a one-way analysis of variance are summarized in Table 15. When the four injury classes were compared, there were significant (α=.05) differences between the means of red and IR reflectance, as well as the IR/red ratio and yield. The means of the green band reflectance for the necrosis classes were not significantly different. Details are presented in Appendix F.

TABLE 15. SIGNIFICANT DIFFERENCES IN REFLECTANCE AND YIELD AMONG FOUR NECROSIS CLASSES[a] OF SO_2-AFFECTED WINTER WHEAT

Test Statistic	Reflectance				Yield
	Green	Red	IR	IR/Red	
F	0.80	4.58	6.37	15.92	18.09

[a] Class 1 ≤10% necrosis
2 11-25%
3 26-50%
4 >50%

Underlined values are significant (F-test, α=.05).

Summary of Results

An analysis of variance showed statistically significant differences in IR reflectance and the IR/red ratio when chlorotic soybeans were compared with unaffected soybeans. Significant differences in red and IR reflectance as well as the ratio were found when necrotic soybeans were compared with unaffected soybeans. The affected soybeans had higher green and red but lower IR reflectance and a lower IR/red ratio than the

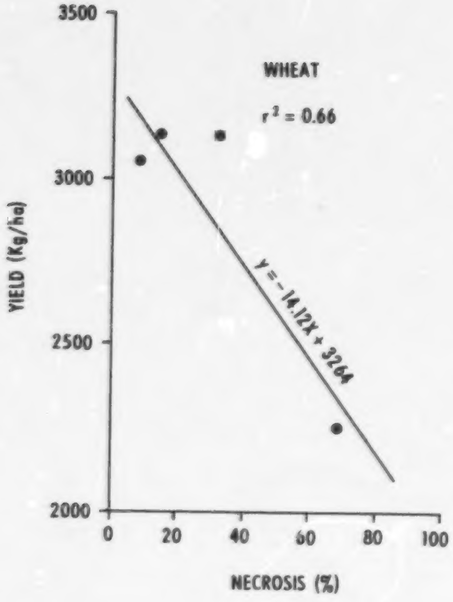

Figure 25. Linear regression of yield on necrosis for SO_2-affected winter wheat.

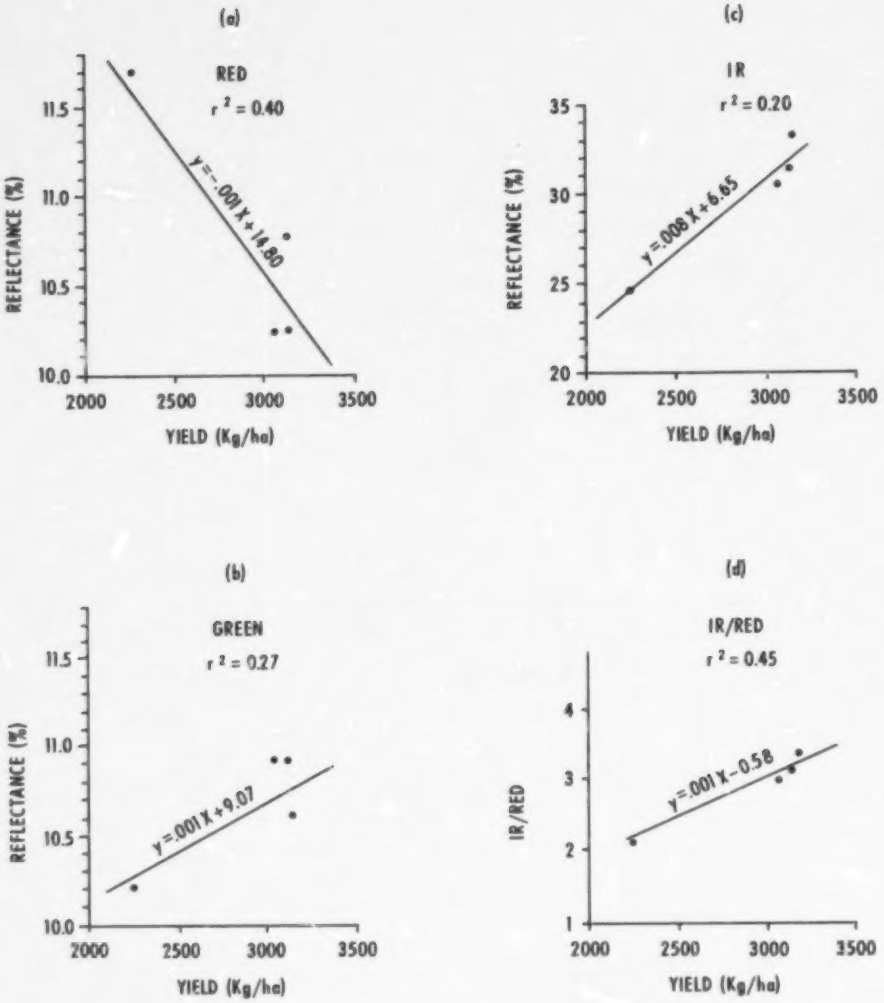

Figures 26a, b, c, and d. Linear regressions of reflectance on yield of SO_2-affected winter wheat.

unaffected soybeans. No relationship was found between reflectance and yield. The statistical tests were conducted at the 95 percent confidence level.

Statistical analysis of the reflectance data from the wheat plot gave more positive results than those obtained from the soybean plot. An analysis of variance revealed statistically significant differences in red and IR reflectance and the IR/red ratio, but not green, when four necrosis classes were compared. No chlorosis was observed. The necrotic wheat had higher red reflectance, lower IR, and a lower IR/red ratio than the unaffected wheat. Yield decreased as necrosis increased. The statistical tests were conducted at the 95 percent confidence level.

SECTION 5

INTERPRETATION AND ANALYSIS OF AERIAL PHOTOGRAPHS

GENERAL

During the first year of this project, the foliar effects of SO_2 on crop and tree species were detected, mapped, and studied qualitatively by conventional stereoscopic interpretation of aerial photographs. These results were not consistent because many physical variables other than foliar effects controlled the variations in exposure. Therefore, a method of photometric analysis was used to measure and calculate the reflectances of vegetation and other objects in aerial color-infrared (CIR) photographs. The calibration technique was especially valuable when photographs of a different flight line, altitude, or date were compared.

METHODS AND INSTRUMENTS

Overflights

Overflights of areas near four of TVA's 12 coal-fired power plants were performed during the 1977 and 1978 growing seasons when the foliar effects of SO_2 were still visible to ground observers. The overflights covered soybeans growing near Colbert Steam Plant in northwestern Alabama, Johnsonville Steam Plant in western Tennessee, Shawnee Steam Plant in western Kentucky; and soybeans, winter wheat, and pines growing near Widows Creek Steam Plant in northeastern Alabama (Figures 27, 28, 29, and 30). Altitudes for the overflights ranged from 500 to 1800 m above ground level (AGL). Large-format aerial mapping cameras equipped with 152-mm focal-length lenses were used to expose Kodak Aerochrome Infrared 2443 (CIR) false-color reversal film and Kodak Ektachrome MS Aerographic 2448

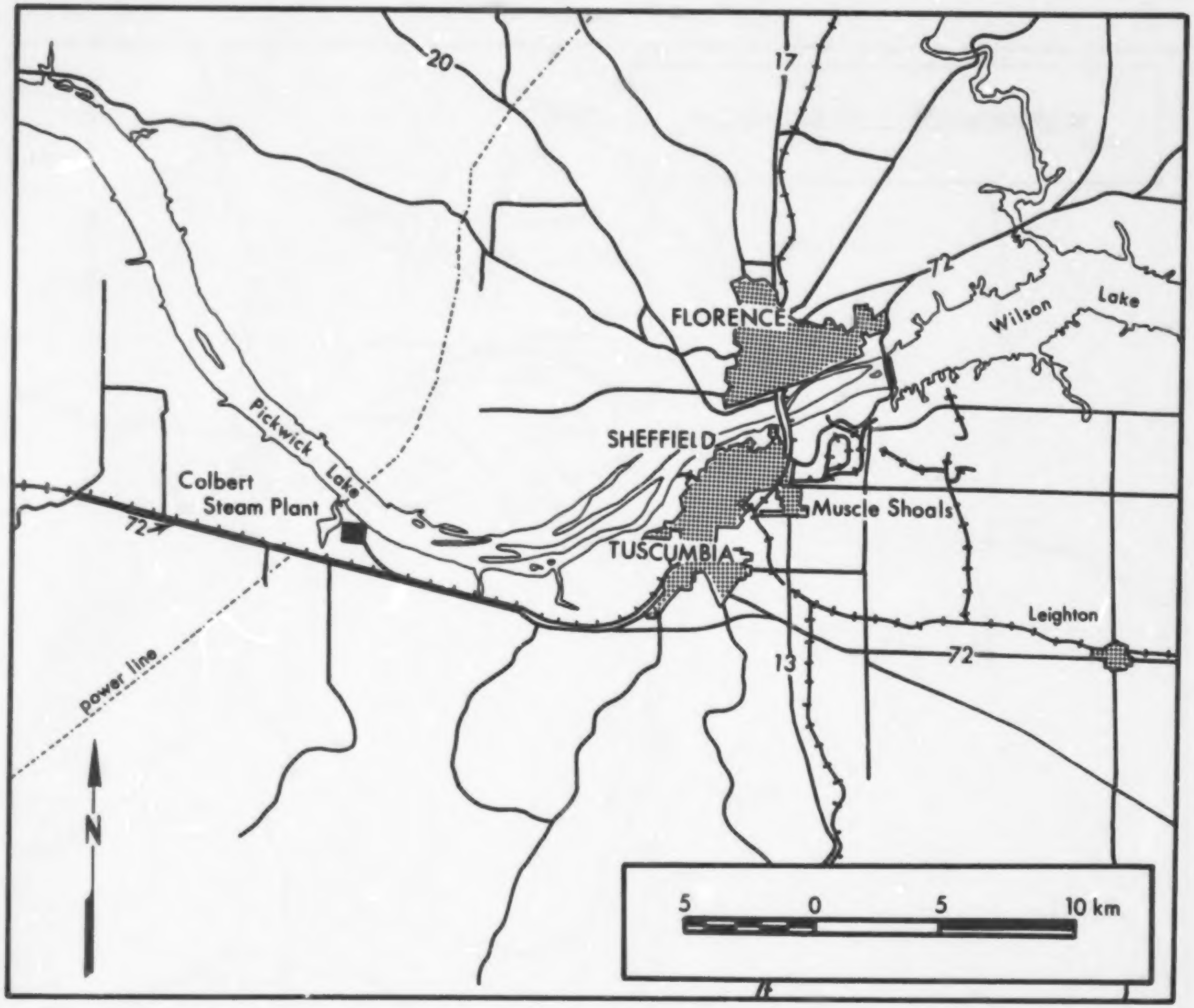
20
17
FLORENCE
72
Wilson
Lake
SHEFFIELD
Pickwick
Lake
Colbert
Steam Plant
72
Muscle Shoals
TUSCUMBIA
Leighton
72
13
power line
N
5
0
5
10 km

Figure 27. Colbert Steam Plant area in northwestern Alabama.

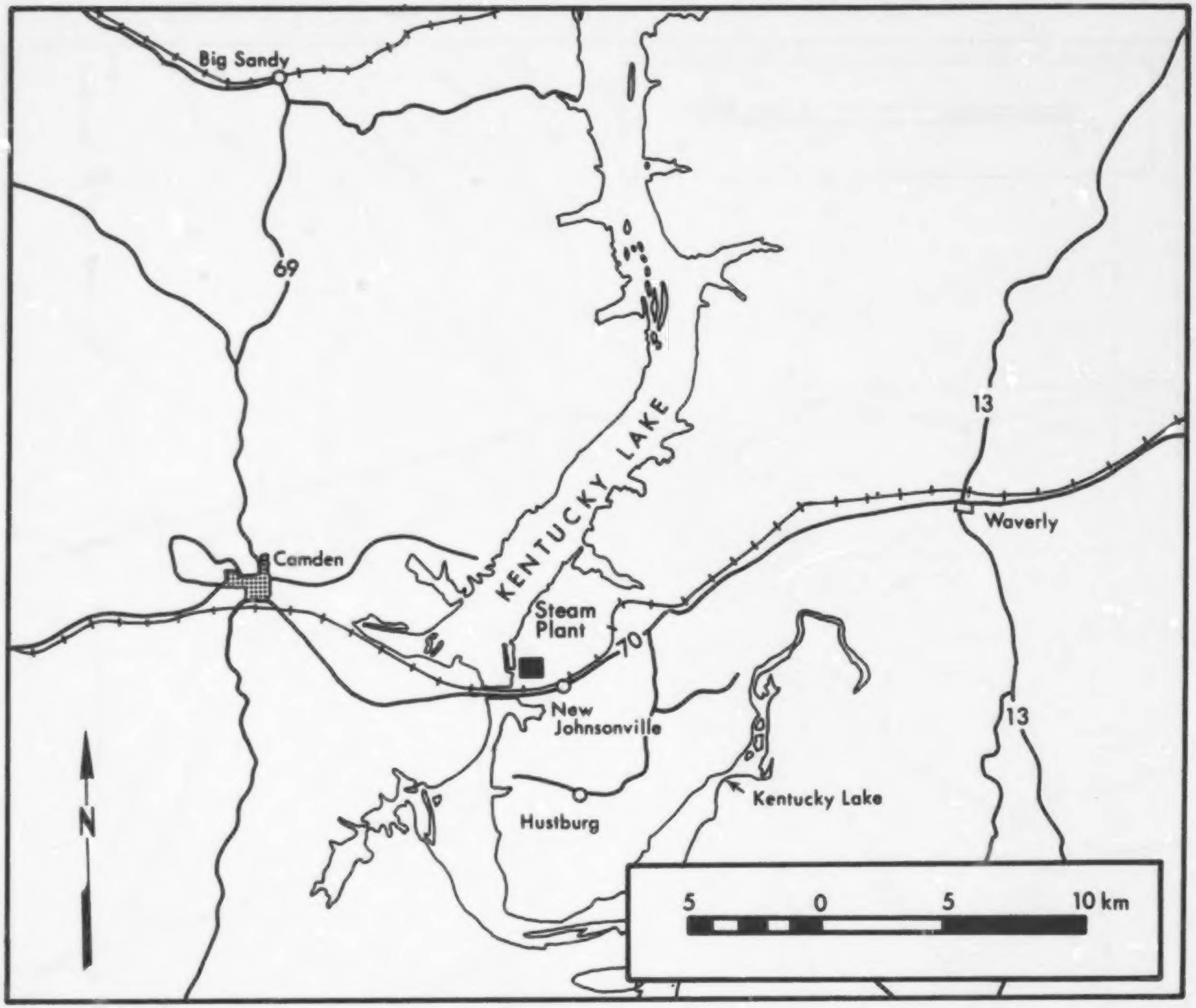
Big Sandy
69
Camden
KENTUCKY LAKE
Steam Plant
70
New Johnsonville
Hustburg
Kentucky Lake
13
Waverly
13
N
5
0
5
10 km

Figure 28. Johnsonville Steam Plant area in western Tennessee.

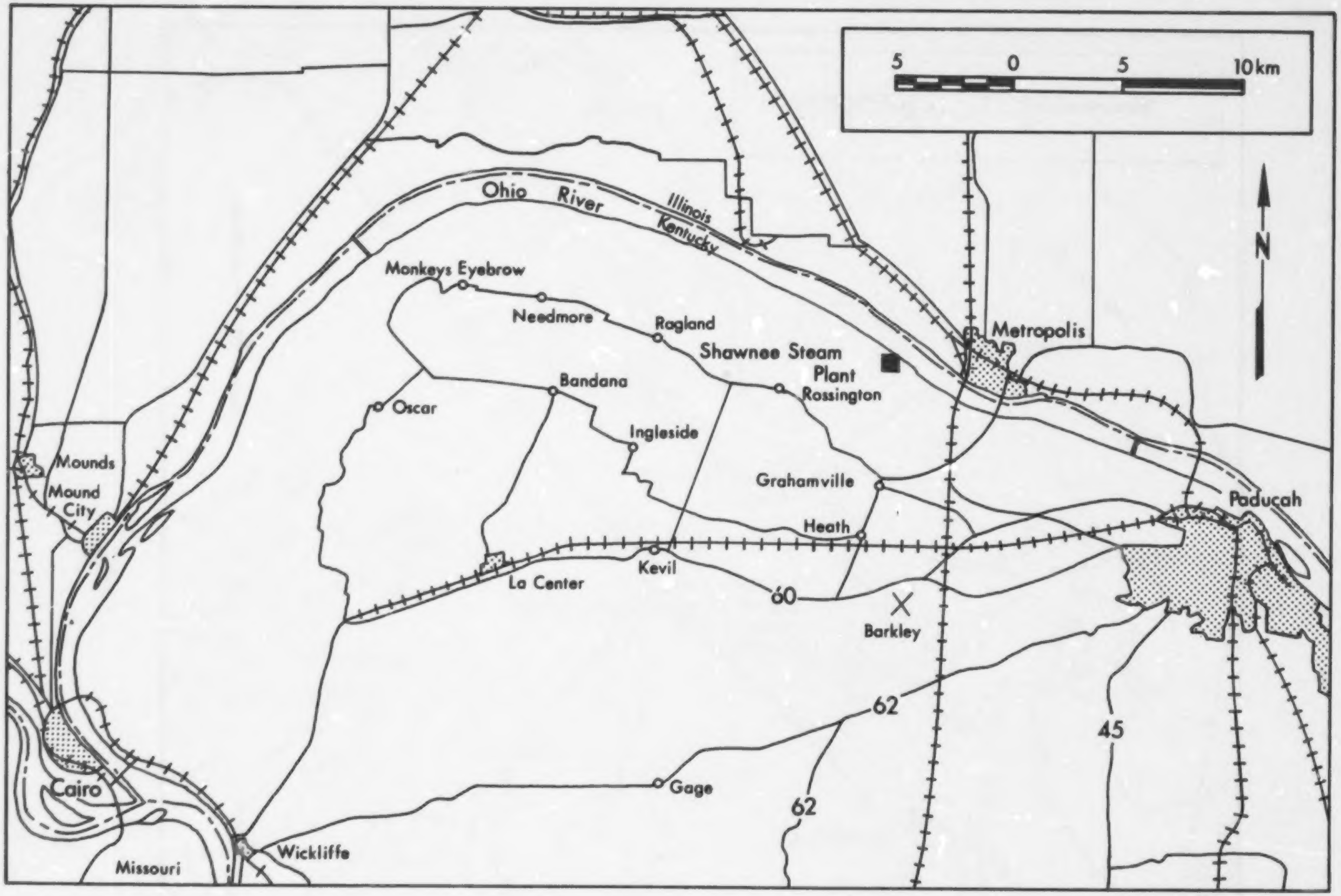
5
0
5
10km
N
Ohio River
Illinois
Kentucky
Monkeys Eyebrow
Needmore
Ragland
Shawnee Steam Plant
Rossington
Metropolis
Bandana
Oscar
Ingleside
Grahamville
Heath
Kevil
La Center
60
Barkley
Paducah
62
45
62
Gage
Mounds
Mound City
Cairo
Wickliffe
Missouri

Figure 29. Shawnee Steam Plant area in western Kentucky.

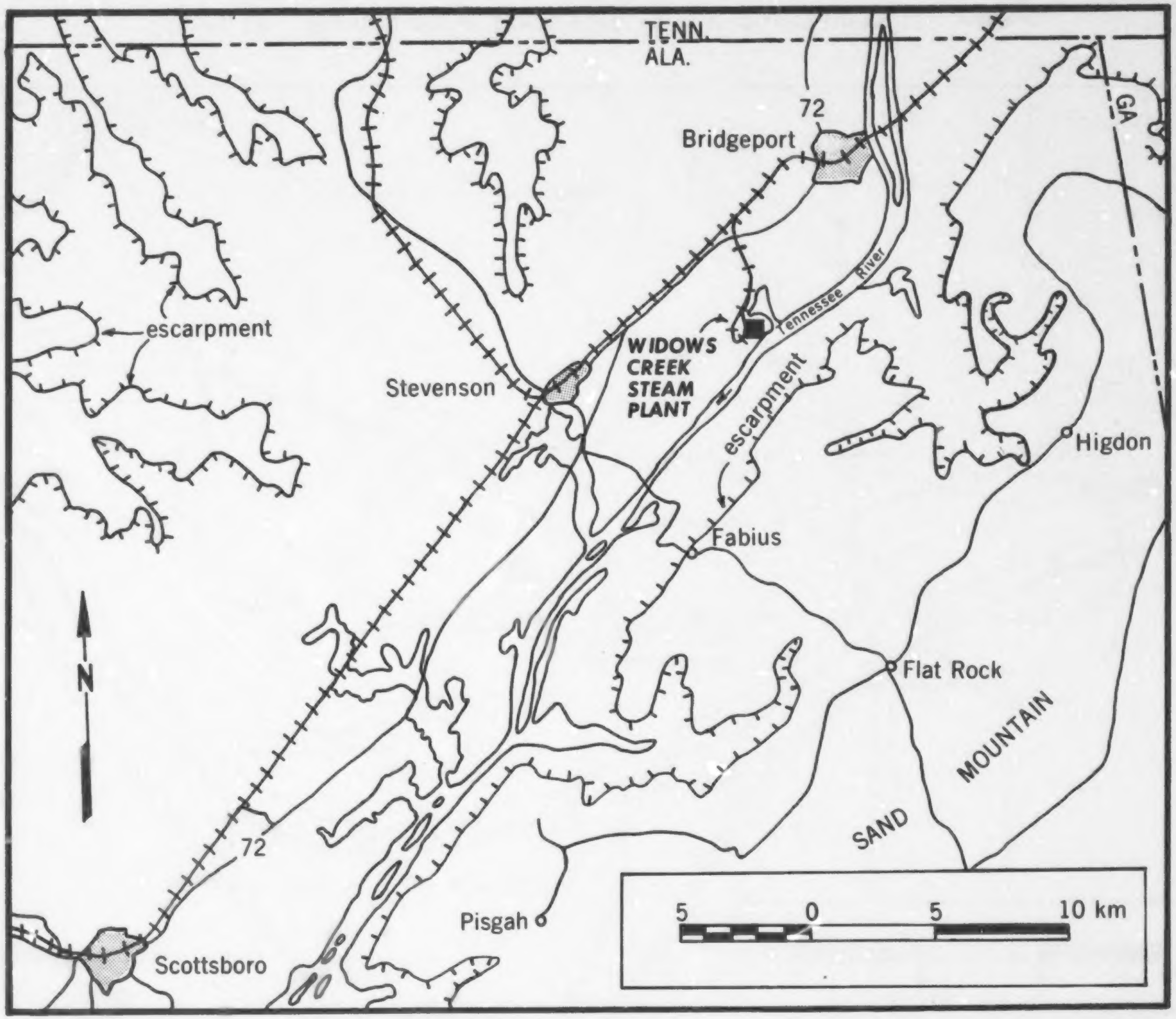
TENN.
ALA.
GA
72
Bridgeport
Tennessee River
WIDOWS CREEK STEAM PLANT
escarpment
escarpment
Stevenson
Higdon
Fabius
N
Flat Rock
MOUNTAIN
SAND
72
Pisgah
Scottsboro
5
0
5
10 km

Figure 30. Widows Creek Steam Plant area in northeastern Alabama.

true-color reversal film. The resulting range of image scales varied from about 1:3000 for the low-altitude runs to 1:12,000 for the high-altitude runs.

TVA used a Wild RC-8 camera over Johnsonville and Widows Creek, and EPA used Wild RC-10's over Johnsonville, Colbert, Shawnee, and Widows Creek. EPA also flew a Daedelus DS-1260 multispectral scanner over Colbert Steam Plant in 1977 and Shawnee Steam Plant in western Kentucky in 1978.

In July 1978 two soybean fields near Colbert were photographed for an intensive study. One field was SO_2-affected and one was not. TVA's Wild RC-8 mapping camera was used for basic CIR coverage and a cluster of three Hasselblad 70-mm cameras was used for black-and-white multiband photography. The Hasselblads had normal 80-mm focal-length lenses. The 70-mm multiband coverage covered the visible and near-IR spectral regions, and the cameras were fitted with narrow-band interference filters: a green (550 ±23 nm) filter, a red (650 ±23 nm) filter, and a visibly opaque (720 ±13 nm) filter.

Photometric Analysis

The primary objective of photometric analysis was to detect SO_2 effects in soybean fields by measuring differences in spectral reflectance. A secondary objective was to relate the reflectance measurements to yield of soybeans. To do this, systematic errors in the photographs were measured and eliminated through an image calibration process. The errors resulted from film processing, atmospheric effects, and variation in illumination. The reflectance patterns and trends were then compared with ground-truth data on SO_2 effects to ascertain whether any relationships existed.

Photometric analysis involved use of the Scene Color Standard (SCS) technique. Specific details of the SCS technique have been published.[44]

The basics of photometric analysis have been described by Lillesand in an introductory text.[45] Lillesand calls the technique photographic radiometry. The SCS procedure permits determination of the atmospheric and illumination variables directly from the photograph. One advantage is that no *a priori* knowledge of the reflectances of ground objects is necessary, because all the information for calculating reflectances is available from the photograph itself. Reflectances of specific objects, such as individual soybean plants on large-scale images or integrated spot canopy measurements on small-scale images, may be calculated from spot density measurements. For the analysis of 1977 photography, two densitometer apertures, 1.0 mm and 150 µm, were used. The 1-mm densitometer aperture was adequate for canopy sampling on the 1:12,000-scale photographs, where the spot covered a ground area 12 m in diameter. The 150-µm aperture was used to make density measurements in shadow areas. For the analysis of the 1978 Colbert photographs, a 150-µm aperture was used for density measurements of the canopy from the 1:12,000-scale CIR transparencies. The ground spot for sampling was thus 1.8 m in diameter. Also measured in the calibration process were images of asphalt surfaces (roofs and roads) and bare soil. Reflectances from these surfaces are relatively constant temporally and can be used to subtract the effects of atmosphere and illumination. Reflectances of other objects can be measured to an accuracy of about 5 percent of their true values.[46] This performance is comparable with that expected from a field radiometer.

The image calibration procedure required rigorous control of variables. A density step wedge was processed with the film so that processing effects could be measured. This procedure used sensitometric curves (D-log E) that plot density against relative log exposure values (Appendix G).

Tri-band (analytical) densities were then measured directly from the film and converted to changes in relative exposure.

Reflectances can be obtained from each of the three spectral bands comprising color film, whether the emulsion is true color or CIR. The spectral coverage of a particular band is determined by the sensitivity of that component of the film emulsion. For CIR, the emulsions are sensitive to either green, red, or near-infrared wavelengths.[47] Both densitometers were equipped with selectable filters (nos. 92, 93, 94, and 106), enabling the operator to measure density in any one or all three emulsion layers.

Reflectance values from one band may be divided by reflectance values from other bands to provide a ratio that may be a sensitive indicator of stress. Three simple ratios were calculated in this study: IR to red; IR to green; and red to green. The IR/red ratio approaches unity as the curve flattens with stress from SO_2 or some other agent.

For the 1978 Colbert test, a 21-ha affected field was sampled systematically with a 30-m spacing between points (Figure 31). The 196 points were then identified on the CIR photographs so that optical densities of the points could be measured with a microdensitometer and converted to reflectance. Statistical correlations were done on the IBM 370 computer using a SAS 76 program, and graphics displays were made on a Tektronix 4014 graphics terminal. The sampled parameters for this intensive study were red, green, IR, and IR/red reflectance; plant height, percent chlorosis (both L and A components of index); and field elevation. A Kelsh stereo plotter was used to construct a detailed topographic map of the field.

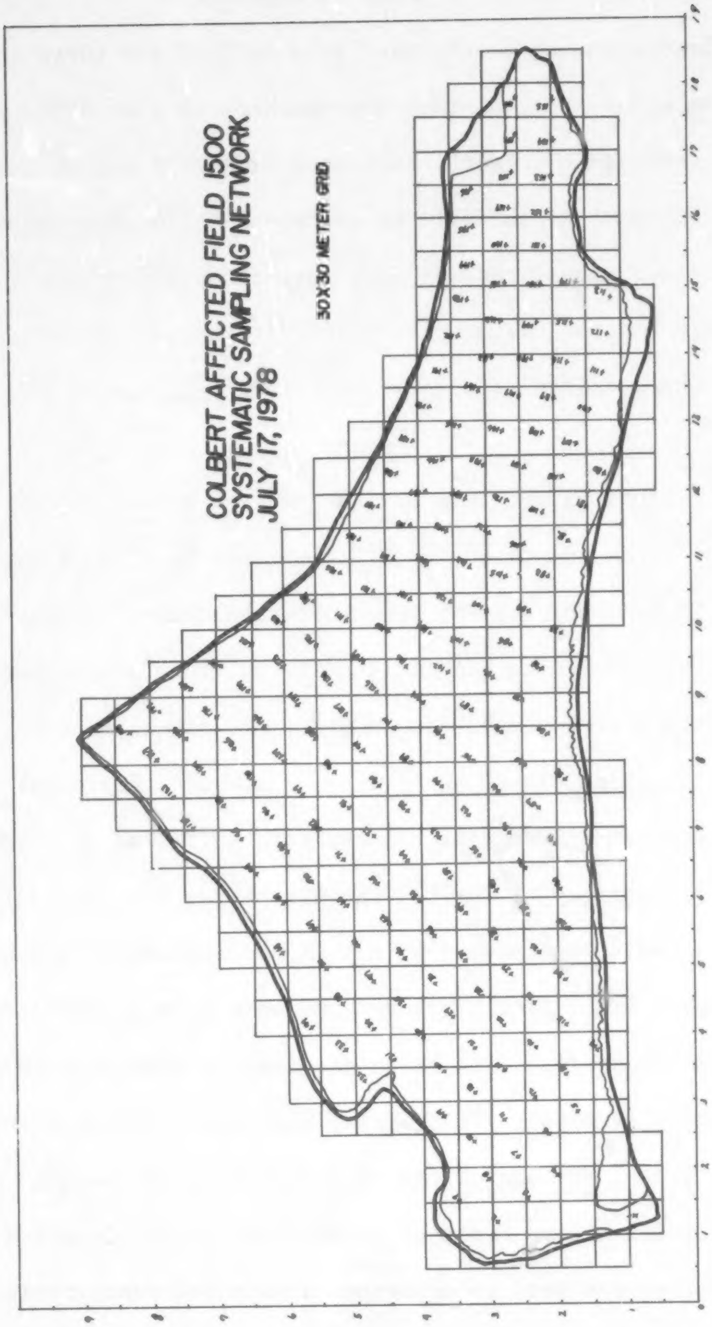
COLBERT AFFECTED FIELD 1500
SYSTEMATIC SAMPLING NETWORK
JULY 17, 1978
30X30 METER GRID
0
1
2
3
4
5
6
7
8
9
10
11
12
13
14
15
16
17
18
19

Figure 31. Grid for intensive sampling of soybean field near Colbert Steam Plant.

RESULTS AND DISCUSSION

General

The photometric analysis technique was tested with data from Colbert, Johnsonville, and Shawnee steam plants determine whether it could be used to derive spectral reflectances at sample points within selected SO_2-affected soybean fields. Ground-truth data describing the effects were available from all sites, including a field near Colbert that was intensively sampled.

Colbert Test

Field Conditions--

Exposures to SO_2 caused visible foliar injury to soybeans in the Colbert project area on August 3 and August 26, 1977 (Figure 32). EPA was asked to perform an overflight after the first exposure; but because of concurrent requests, the aircraft did not arrive until August 29. Drought-induced senescence and growth of the soybean canopy and weeds in areas of adequate moisture tended to dilute the SO_2 effects. Effects from the August 26 injury were still fresh. An attempt was made to distinguish and separate SO_2-related stress from these natural effects through photometric analysis of the aerial photographs.

Analysis of the Colbert photographs taken in 1977 focused on five soybean fields that fell within a single frame (Figure 33). Four of the fields were affected by SO_2 and one was unaffected. The photographs also show a set of six test panels (arrow) for calibrating reflectance in the photometric analysis procedure. The soybeans were mature (generally 7 to 10 nodes high) and had stopped showing new growth but were not yet senescent. Some areas were infested with cockleburs [Xanthium strumarium (L.)]. The soybean canopies were generally continuous, with only a few areas of

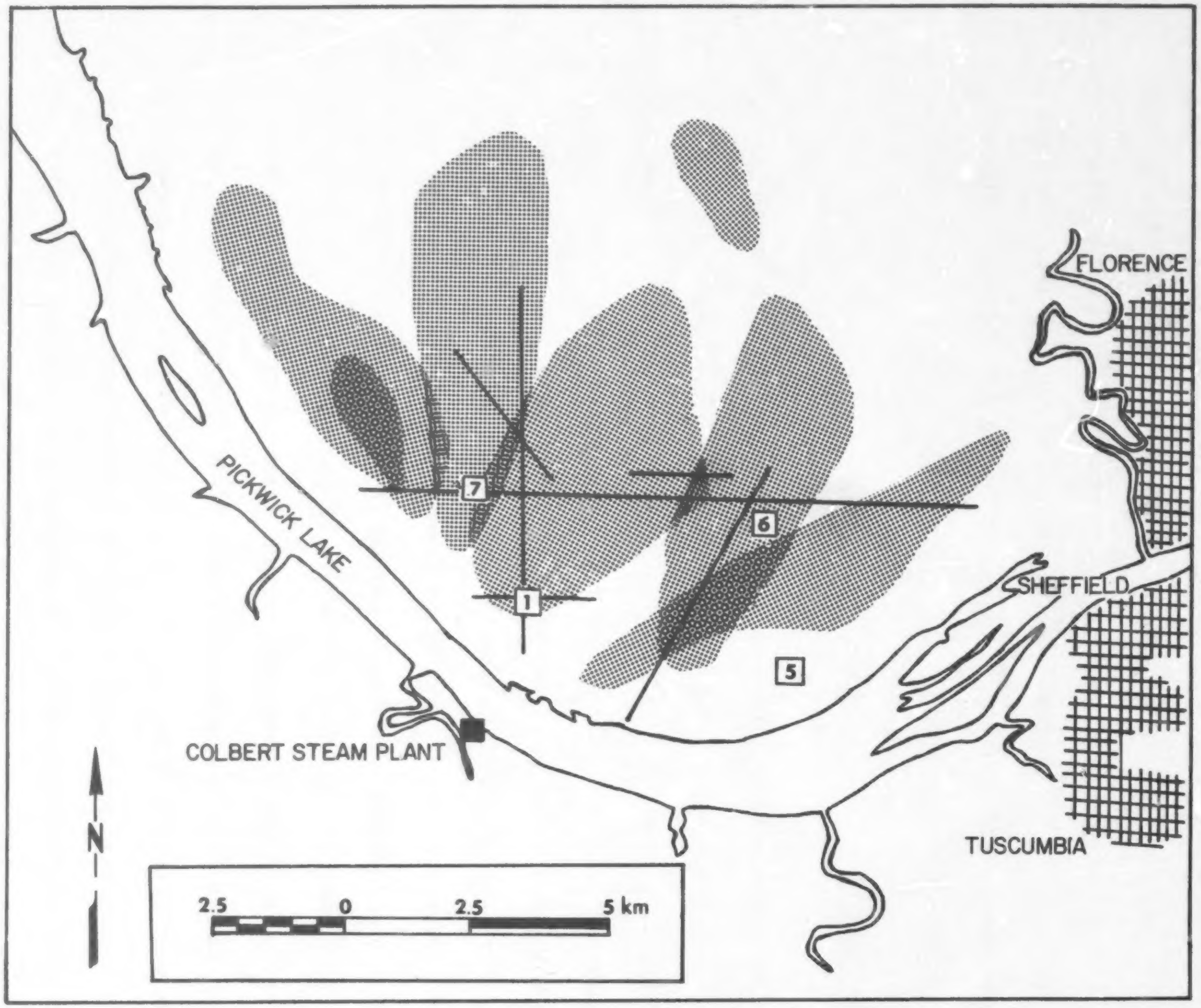
FLORENCE
SHEFFIELD
TUSCUMBIA
PICKWICK LAKE
COLBERT STEAM PLANT
7
1
6
5
N
2.5
0
2.5
5 km

Figure 32. Flight lines and SO_2-affected areas near Colbert Steam Plant in 1977. Boxed numbers locate fixed SO_2 monitoring stations. Overlapped patterns indicate areas of multiple exposures of plants to SO_2.

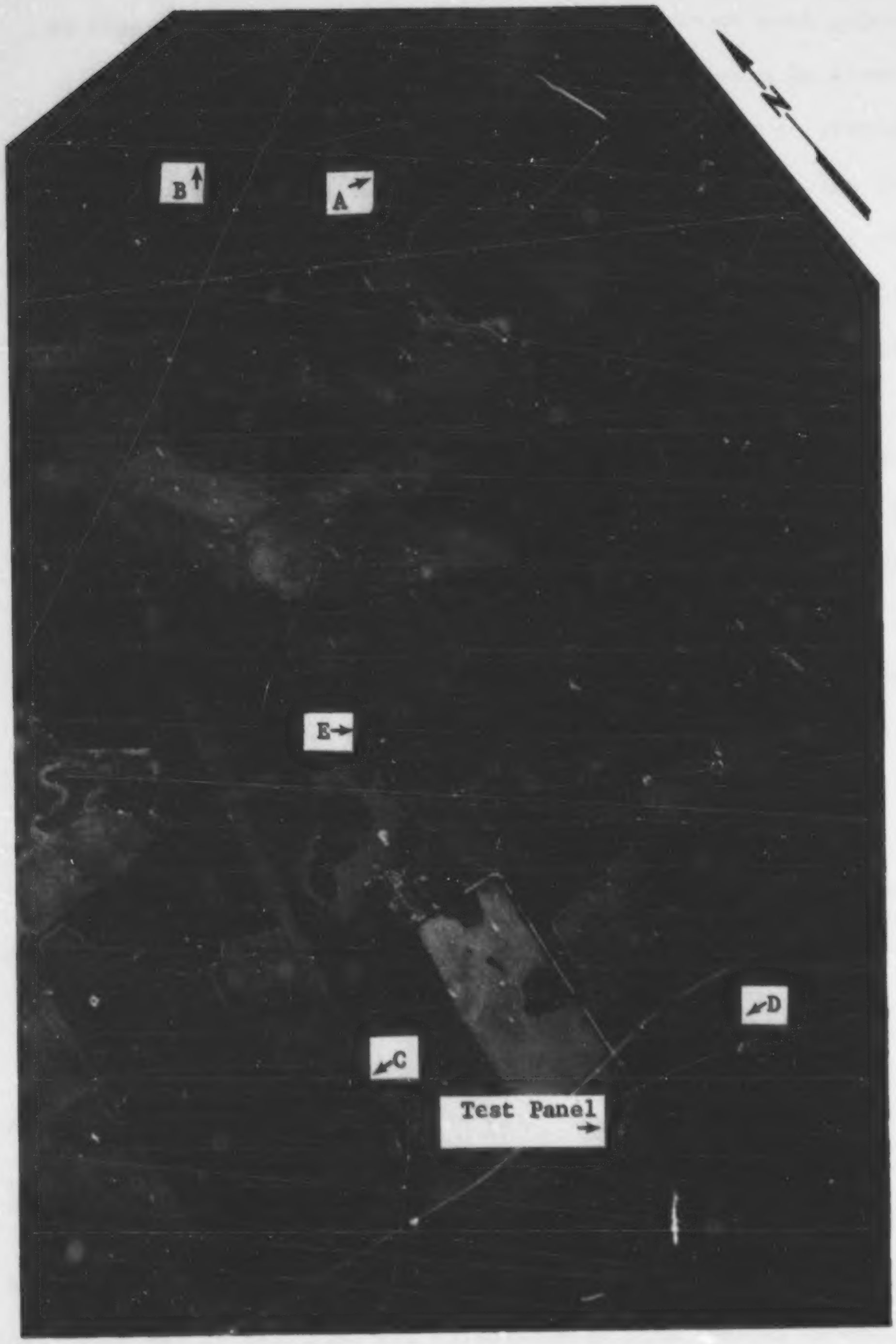
N
B
A
E
D
C
Test Panel

Figure 33. Aerial CIR photograph showing Colbert area in 1977. Letters identify selected soybean fields discussed in report. Scale 1:12,000.

soil showing from overhead. The effects of SO_2 exposure consisted of light levels of chlorosis, but no necrosis.

Analysis of the Colbert photographs taken in 1978 focused on two fields of mature Essex soybeans, one of which was affected by SO_2. The chlorosis was about a week old and ranged from very light to moderate in intensity. There was no necrosis. The affected field covered 21 ha, and had a uniform canopy and no weed infestations (Appendix D). The soil in some of the low areas was damp.

Measurement and Comparison of Reflectance--

For the 1977 test, the sample points were systematically selected within the fields and the optical density of the film at each point was measured with the microdensitometer. The densities were then converted to reflectance. Exceptions to uniform sampling were made when required by irregular field boundaries. No relationships between the reflectance statistics and foliar injury levels were indicated. The SO_2-affected soybeans showed lower IR and higher red reflectance; this finding was in accordance with theory.[48]

A comparison of the injury levels with the reflectance ratios for the five fields showed that the field with the highest mean ratio (A) was unaffected by SO_2; field B, with 2 percent injury, had the next highest mean ratio; and field C, with the highest level of injury, had the lowest mean ratio (Table 16). It appears then, that the lower the IR/red ratio, the greater the SO_2 effects. Figure 34 further illustrates the relationship between injury and IR/red. Field D was infested with weeds and had a discontinuous canopy; this heterogeneity was reflected in the high standard deviation (1.11) for its reflectance ratio. A low standard deviation would indicate a homogeneous canopy and few weeds.

TABLE 16. REFLECTANCE AND FOLIAR INJURY FOR COLBERT SOYBEAN FIELDS PHOTOGRAPHED IN 1977

Field designation[a]	Green(%)		Red(%)		IR(%)		IR/Red		Observed injury (%)
	Mean	S.D.	Mean	S.D.	Mean	S.D.	Mean	S.D.	
A	4.68	0.27	4.67	0.11	26.93	1.51	5.77	0.34	0
B	6.02	0.25	5.43	0.37	28.98	1.04	5.34	0.68	2
C	7.53	0.63	9.05	1.54	27.23	1.93	3.01	0.49	4[c]
D	5.70	0.03	5.62	0.08	25.57	3.78	4.55	1.11	2
E	4.57	1.69	5.27	0.91	25.90	2.39	4.91	0.57	2

[a] Keyed to Figure 31.

[b] LxA method (Appendix D).

[c] Estimated because of conflicting data.

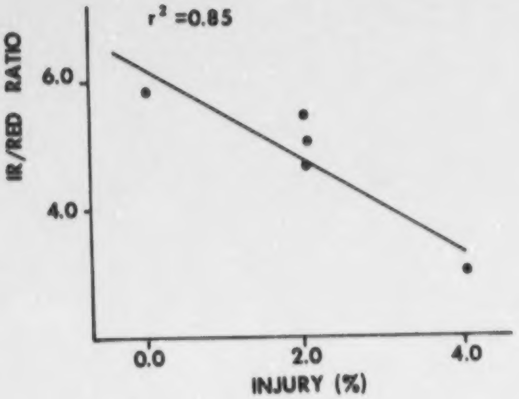

Figure 34. Regression of IR/red ratio and foliar injury levels for Colbert soybean fields photographed in 1977.

For the 1978 Colbert intensive study, data from 196 sample points within an affected field were compared to determine the relationships between reflectance and three other parameters: chlorosis, plant height, and elevation of the field. These data were mapped to discern correspondence in patterns (Figures 35a through c). Statistical regressions of reflectance versus chlorosis, and chlorosis versus elevation were calculated. None of these relationships was significant (α=.05), and the r^2 coefficients were all below 0.25 (Appendix D). When all data points with soybean plant heights less than eight nodes and chlorosis ≤ 1 percent were excluded, the change in r^2 was minimal. A comparison of three-dimensional plots of the data shows little similarity between or among the variations in reflectance, chlorosis, and plant height (Figures 36a through e).

Johnsonville Test

Field Conditions--

Two incidents of SO_2 injury to vegetation occurred in the photographed Johnsonville area during July 1977. The effects were classified generally

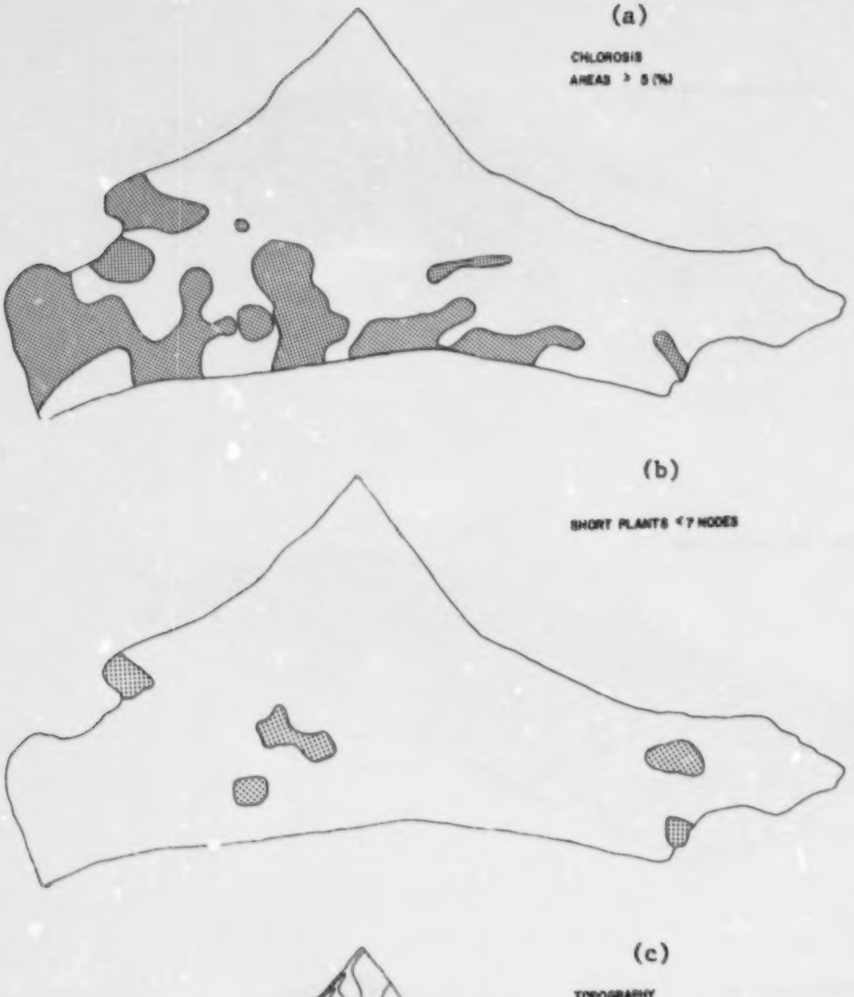
(a)
CHLOROSIS
AREAS > 5 (%)
(b)
SHORT PLANTS <7 NODES
(c)
TOPOGRAPHY
2 FOOT (0.6m) CONTOURS

Figures 35a-c. Thematic maps showing patterns in a soybean field near Colbert Steam Plant in 1978.

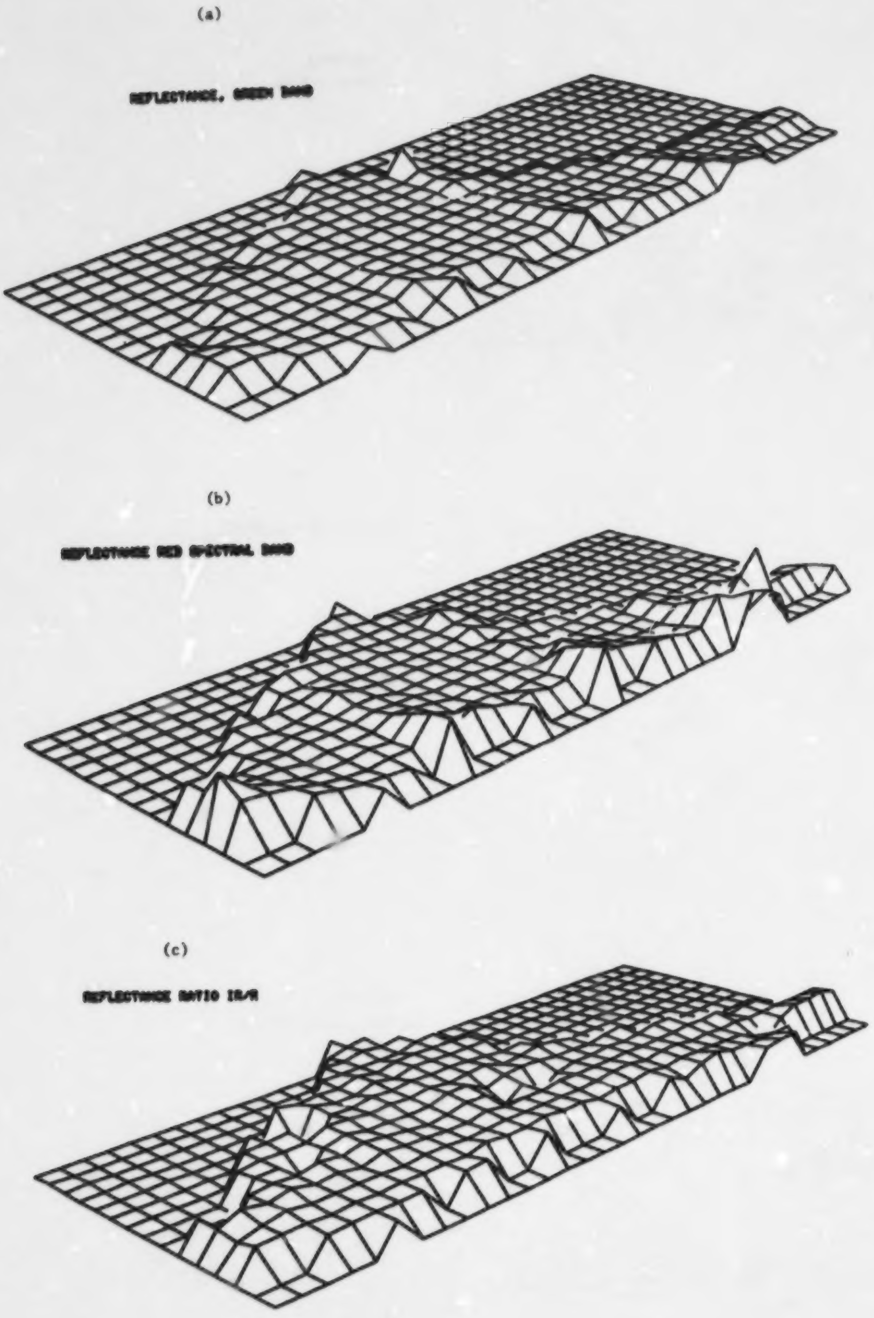

Figures 36a-c. Computer-generated perspective views of a soybean field near Colbert Steam Plant in 1978. The vertical axis represents reflectance, and the horizontal axes represent locations of sample points. (Compare with Figure 35.)

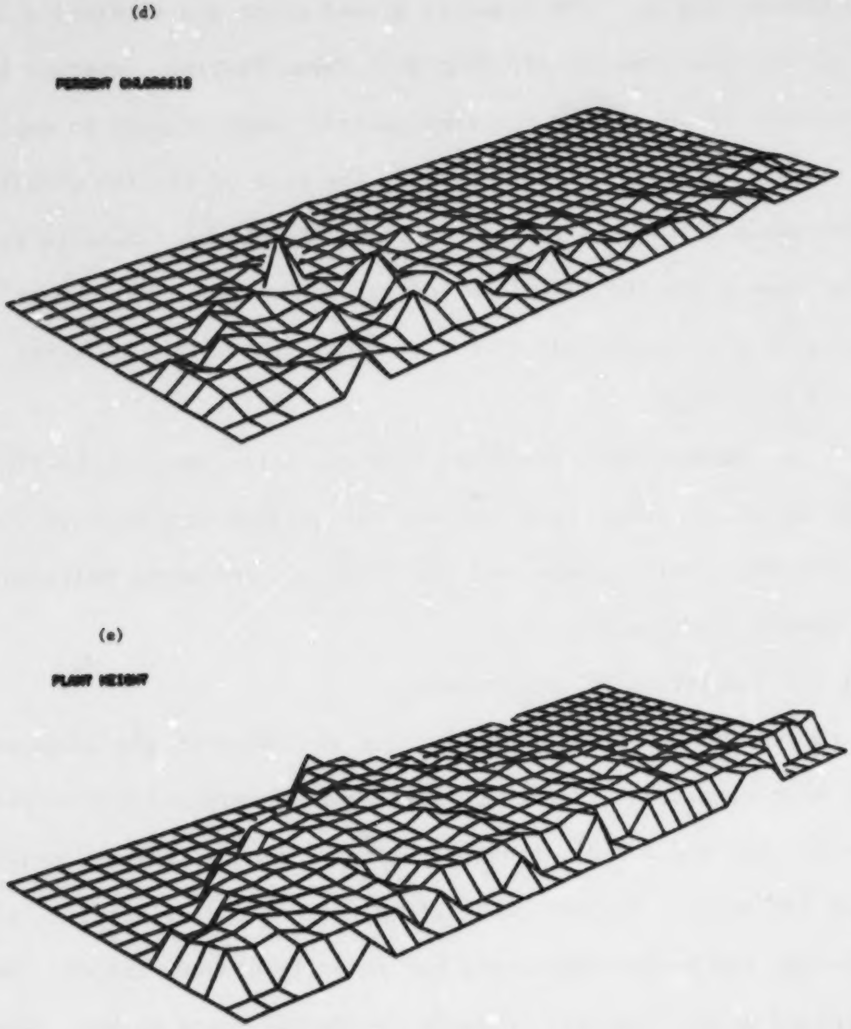

Figures 36d, e. Computer-generated perspective views of a soybean field near Colbert Steam Plant in 1978. In these graphs the vertical axis represents observed chlorosis (d) and plant height (e). The horizontal axes represent locations of sample points in the field. (Compare with Figures 35 and 36.)

as light to moderate. The earliest incident occurred on July 3 in an area northwest of the plant (Figure 37). The effects persisted and were photographed by EPA on July 21. TVA acquired ground truth and obtained a duplicate copy of the film from the EPA Vint Hill Farms Station. Another SO_2 incident occurred on July 23 in the same general area. Injury to soybeans was still visible in the field on August 2, the date of the TVA overflight.

The photometric analysis focused first on 15 soybean fields in the Johnsonville area where the SO_2 plume contacted the crop. The number was later reduced to nine to exclude fields of immature soybeans. Figure 38 shows some of the fields.

As with the Colbert data analysis, this analysis involved the field-to-field variations in reflectance ratios; the relationship between the ratios and the SO_2 injury levels; and the relationships among reflectance, SO_2 injury levels, and yield.

Measurement and Comparison of Reflectance--

Reflectances from soybean fields located northwest of the Johnsonville Steam Plant were compared to determine whether they were related to foliar injury levels. The SO_2 effects ranged from very light to severe, providing a full scale for study. The affected area contained no-till fields, tilled (plowed) fields, and barren (unplanted but recently plowed) fields. Some fields contained mature soybeans, whereas others had young plants. Some fields had been planted twice. Weeds, mainly cockleburs, were prevalent in some of the no-till fields. Some no-till fields contained wheat stubble between the rows of bean plants.

The image densities were measured, and the values were converted to percentage reflectance. Means, standard deviations, and ratios were computed (Table 17 and Appendix G). Coefficients of determination were

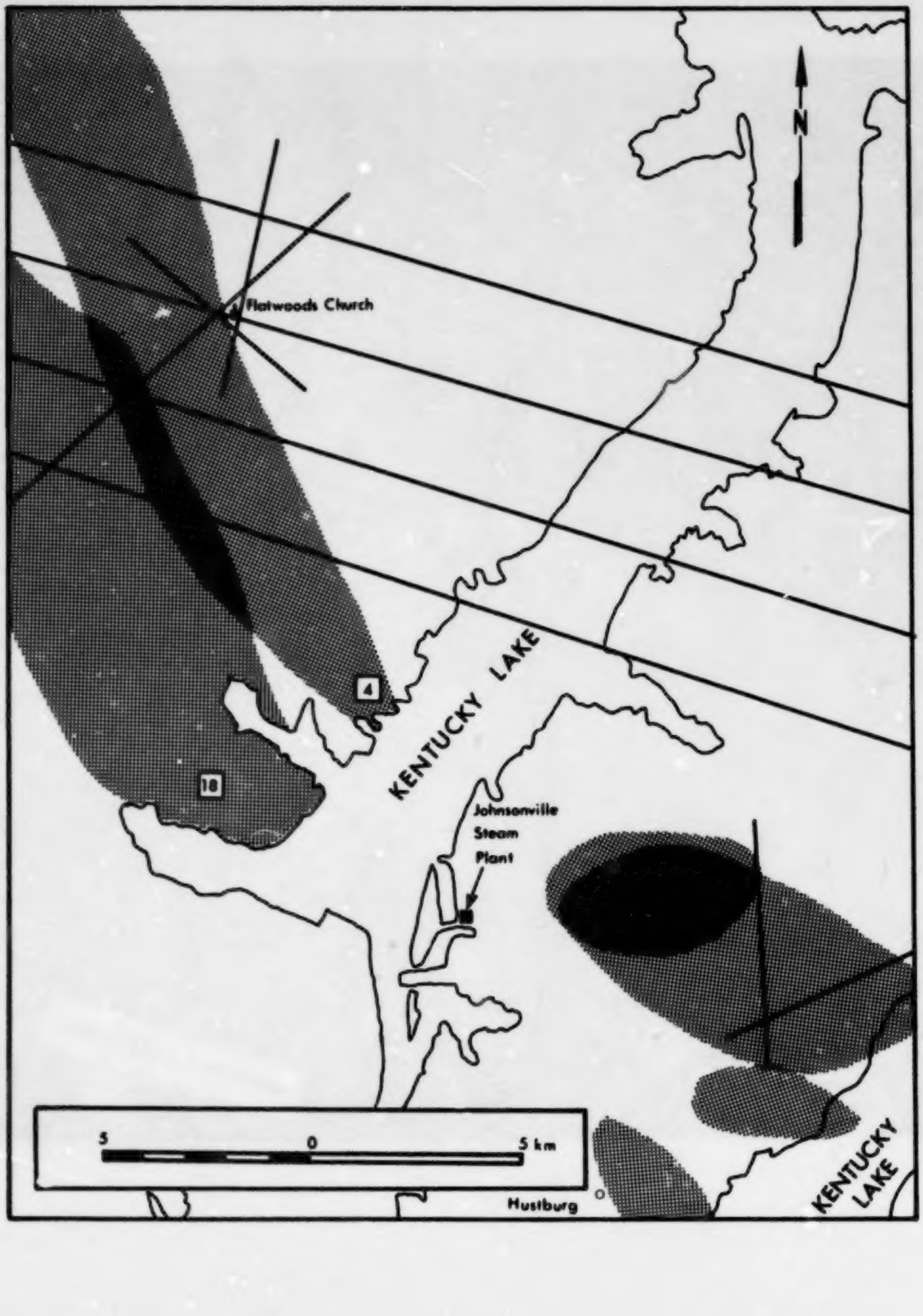
N
Flatwoods Church
4
18
KENTUCKY LAKE
Johnsonville
Steam
Plant
5
0
5 km
Hustburg
KENTUCKY
LAKE

Figure 37. Flight lines and SO_2-affected areas near Johnsonville Steam Plant. Overlapped patterns indicate areas of multiple exposures of plants to SO_2.

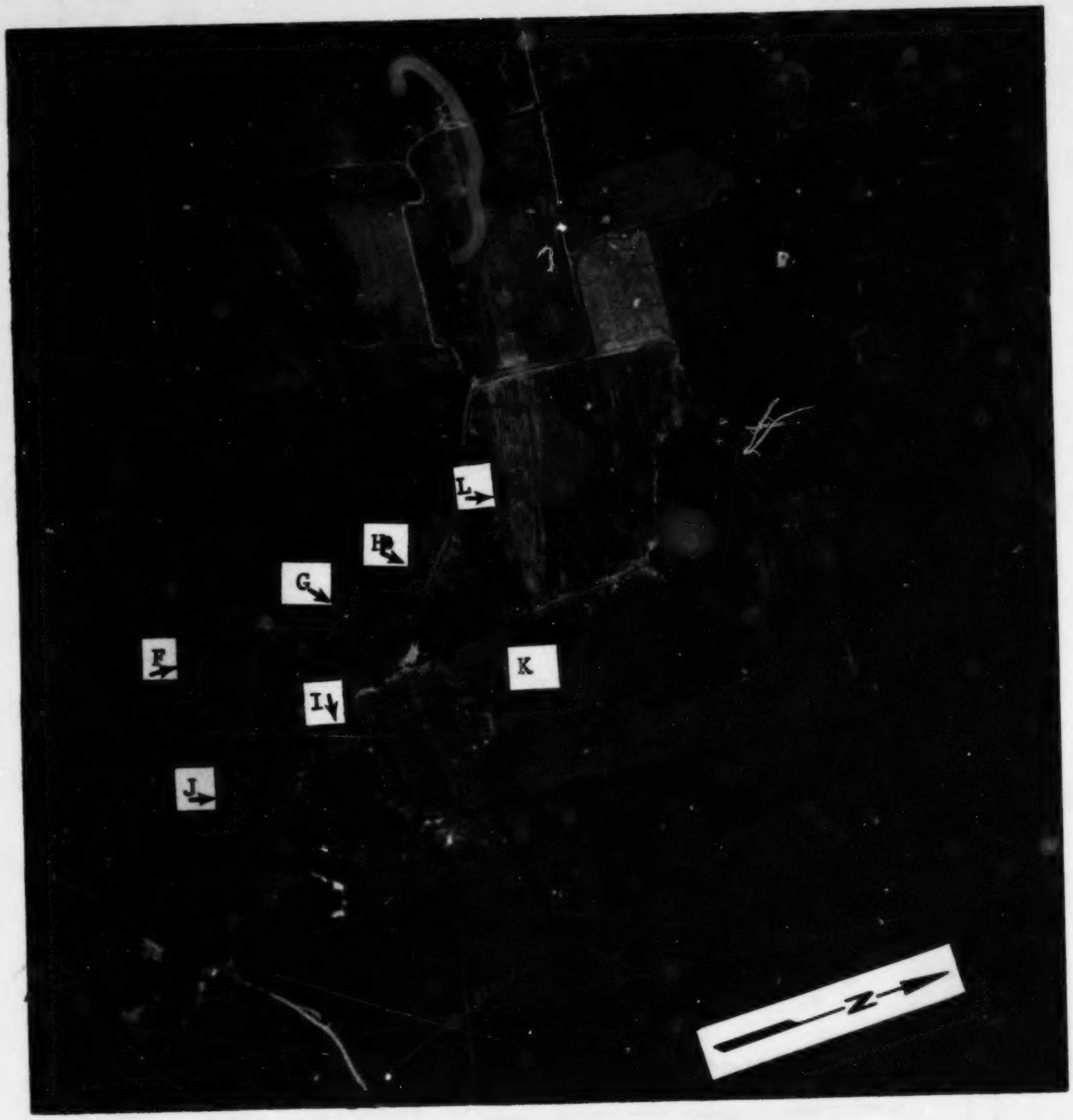

Figure 38. Aerial CIR photograph of area near Johnsonville Steam Plant. Letters identify selected fields discussed in report. Photo taken by EPA in 1977.

TABLE 17. REFLECTANCE, FOLIAR INJURY, AND YIELD FOR SOYBEAN FIELDS NEAR JOHNSONVILLE

Field Designation	Reflectance								Observed level of injury[a] (%)	Yield		
	IR (%)		Red (%)		Green (%)		IR/Red					
	Mean	S.D.	Mean	S.D.	Mean	S.D.	Mean	S.D.		bu/acre	m^3/ha	kg/ha
F	21.1	3.7	6.4	1.0	7.2	0.8	3.3	0.66	34.8	22.5	0.300	3676[b]
G	23.2	4.5	6.5	0.9	7.5	1.3	3.6	0.73	44.6	23.4	0.312	3823[b]
H	24.8	2.8	7.3	0.8	7.9	0.6	3.4	0.55	20.2	28.0	0.373	4574
I	24.0	4.3	6.8	0.7	7.8	0.6	3.5	0.65	30.8	28.5	0.380	4656
J	17.9	1.7	6.6	0.6	7.0	0.7	2.7	0.35	20.0	22.4	0.299	3659
K	22.6	1.8	6.7	0.6	7.8	0.5	3.4	0.46	22.0	24.9	0.332	4068
L	25.7	1.0	4.6	0.8	4.7	0.6	5.6	0.95	14.5	31.0	0.413	5064[c]
Bare soil	20.6	1.9	17.1	2.0	13.7	1.0	1.2	0.10	-	-	0.000	0

[a] L x A method (Appendix D).

[b] Yield = 1/2 actual reported value due to double planting.

[c] Tilled field; all others are no-till.

calculated for reflectance versus SO_2 injury, and reflectance versus yield (Table 18). The IR/red ratio correlated significantly (α=.05) with injury, although the positive direction of the relationship was not what was expected (Figure 39a). None of the single-band reflectances had any relationship with injury.

TABLE 18. COEFFICIENTS OF DETERMINATION (r^2) FOR REFLECTANCE, SO_2 INJURY, AND YIELD OF SOYBEAN FIELDS NEAR JOHNSONVILLE[a]

Parameter	Green	Red	IR	IR/Red	Injury[b]
Injury	0.02	0.33	0.04	0.32	-
Yield	0.74	0.65	0.61	0.23	0.07

[a] Underlined coefficients are significant (α=.05).

[b] Percent injury for fields calculated by the L x A method (Appendix D). Yield data were collected in fields at harvest.

The best indicator of yield was green reflectance (Figure 39b), although the red and IR reflectances (Figures 39c and d) were also good. In fact, all relationships between single-band reflectance and yield were significant (α=.05). However, the IR/red ratio and yield did not correlate significantly at this level (Figure 39e). Yield also actually increased with injury (Figure 39f). A possible explanation for this relationship is related to canopy density. The density variable, as measured from overhead photographs, is associated with stage of growth, availability of soil moisture, soil fertility, and many other factors that affect plant conditions before, during, and after an incident of exposure to SO_2. The more dense canopy is probably associated with higher yield. Injury level was apparently not a sufficiently powerful factor to overcome the density (and, therefore, yield) factor.

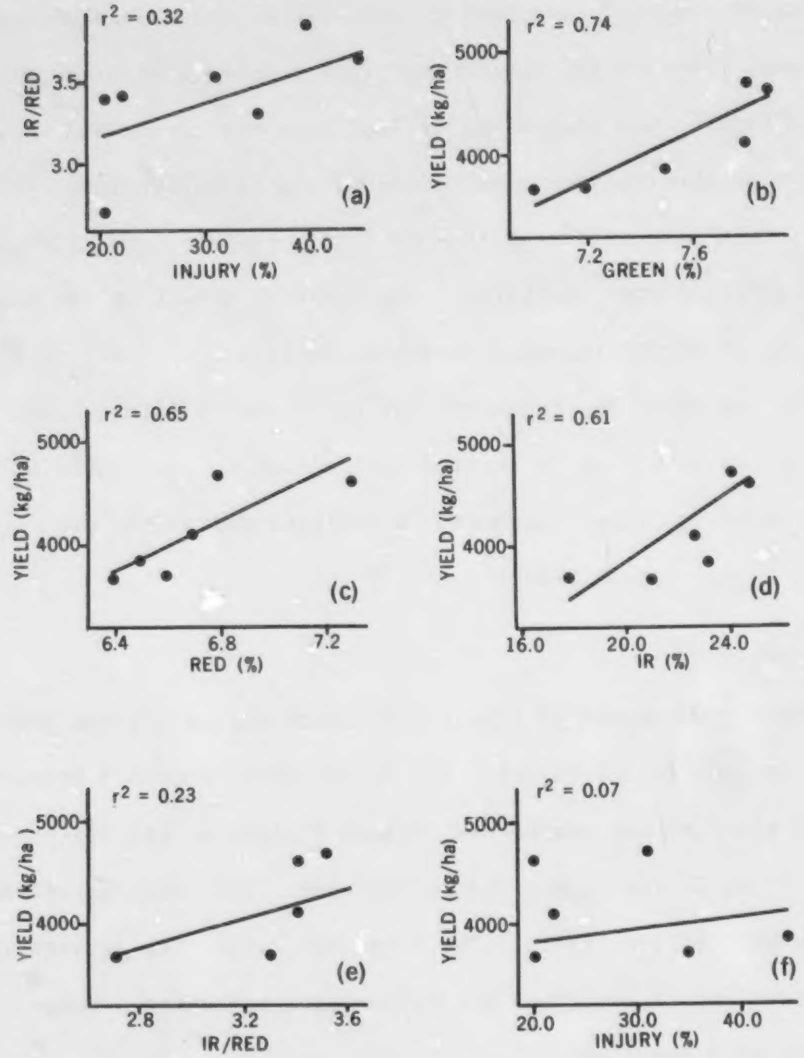

Figures 39a through f. Statistical regressions of reflectance, injury levels, and yield for Johnsonville soybean fields.

The relationship between the effects of power plant emissions and productivity of crops is not well known. In general, crop yields are not affected by SO_2 exposure unless visible foliar effects occur. Evidently, over 5 percent of the leaf area must be affected to measurably reduce yield.[48] Common practice for estimating yield reduction involves field sampling to determine the percentage of leaf area destroyed, and applying an empirically or theoretically derived factor to calculate loss. The difficulty is that many uncontrollable cultural, edaphic, and climatic factors also affect yield. Certainly, the stage of growth at the time of exposure to SO_2 is one of the more important factors. Significant reductions in yield caused by SO_2 exposures during the pod-filling stage of growth in soybeans have been documented and related to the amount of foliar chlorosis.[49] However, other exposures to soybeans during the prebloom stage did not significantly reduce yield.[50]

SUMMARY OF RESULTS

The Colbert data showed no significant correlations between single-band reflectance and foliar injury. The IR/red ratio provided better separation of affected and unaffected soybean fields, as the affected soybeans had lower IR and higher red reflectance. The ratio correlated significantly with injury levels. The lower the ratio, the greater the injury. A low standard deviation for reflectance indicated a homogeneous canopy with few weeds.

The Johnsonville data showed conflicting results. The IR/red ratio increased with injury, rather than decreased. The ratio did correlate significantly with injury in spite of the direction of the relationship being the reverse of what was theorized. All single-band reflectances correlated significantly with yield, although the ratio did not.

Extraneous variations in canopy density associated with stage of growth may have caused these inconsistencies and may also have reversed the direction of the relationship between IR/red and injury.

SECTION 6

ANALYSIS OF MULTISPECTRAL SCANNER DATA

GENERAL

Automated classification of digital data from airborne multispectral scanners plays an increasingly prominent role in remote sensing and supplements traditional techniques of photo interpretation. Three times since 1975 TVA has arranged MSS overflights of SO_2-affected soybean fields. The first overflight, which covered the Shawnee Steam Plant area near Paducah, Kentucky, was conducted in 1975 by NASA/Earth Resource Laboratory (ERL), Slidell, Louisiana, using their RS-18 scanner. Despite acquisition of comprehensive ground truth the results of the analysis were negative because of diverse farming practices and differing stages of crop growth (Appendix H). The second scanner overflight was conducted in 1977 by EMSL-LV with an eleven-channel scanner over the Colbert Steam Plant area in northwestern Alabama. The third overflight was conducted in 1978 by EMSL-LV with the same scanner over the Shawnee Steam Plant area. Analyses of the 1977 and 1978 data are covered in this report. For comparison, several data classification procedures were used to produce different classification images (maps) for comparison. There are many ways to classify MSS data and each problem seems to require a different procedure. Our objective was to determine which of the available classification procedures would provide the best map of the SO_2 effects. Ground truth would determine accuracy.

FLIGHT LINES AND SENSOR CHARACTERISTICS

The remote sensing overflights of the Colbert Steam Plant site and of the Shawnee Steam Plant site were conducted on August 29, 1977, and on

August 15, 1978, respectively. The same equipment and sensors were used at both locations. Timing of the overflights was critical. Optimal conditions were clear weather, a high sun angle, a full soybean canopy in most of the fields, and SO_2 effects that were visible to the field observer. These conditions were satisfied at both sites in late August when the crop had stopped putting on new growth, but was not yet senescent. Figures 40 and 41 show the flight lines for data acquisition and the areas of plume contact with the vegetation near the two sites.

The MSS system was a Daedelus DS-1260, 11-channel scanner (Figure 42). It had a visible band, 10-channel spectrometer and a thermal infrared detector. The scanner was roll-stabilized and its scan rate was synchronized with aircraft ground speed, which for these overflights was approximately 300 km/h (160 knots). A Wild-Heerbrugg RC-10 mapping camera with a 152-mm focal-length lens and Kodak Aerochrome Infrared type 2443 (CIR) film was used concurrently for aerial photography. The nominal width of photo coverage was about 20 percent narrower than the MSS coverage.

Nominal flying heights specified for the sites were 500 and 1800 m AGL. Unsatisfactory results had been obtained during analysis of MSS data of Shawnee acquired by NASA from 3600 m AGL in 1975, so lower altitudes were used in an attempt to improve the quality of the data.

Flying height and certain sensor characteristics determine the image resolution of a scanner. At 500 m, the Daedelus scanner yields a picture element (pixel) with a diameter of about 1 m on the ground. From 1800 m, the pixel diameter is about 4 m. These pixel dimensions are determined by the instantaneous field of view (IFOV) of the scanner; for the Daedelus system this figure is 2.5 milliradians.[51] Figure 43 shows the flight configuration and illustrates that the width of coverage along the flight

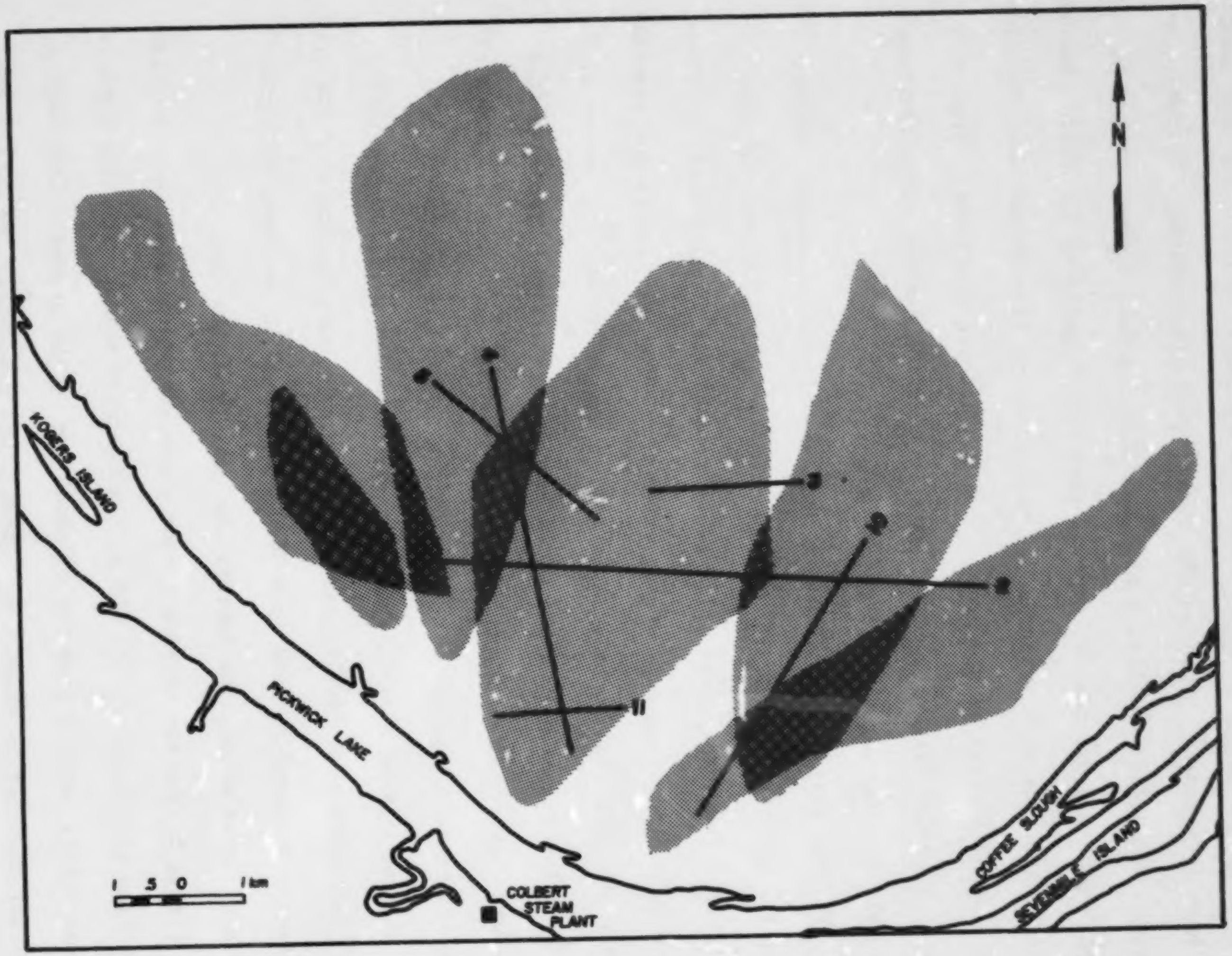
N
KOGERS ISLAND
PICKWICK LAKE
COLBERT
STEAM
PLANT
COFFEE SLOUGH
SEVENMILE ISLAND
11
1 .5 0 1 km

Figure 40. Selected SO_2-affected areas and flight lines near Colbert Steam Plant in northwestern Alabama in 1977. Overlapped patterns indicate areas of multiple exposures of plants to SO_2.

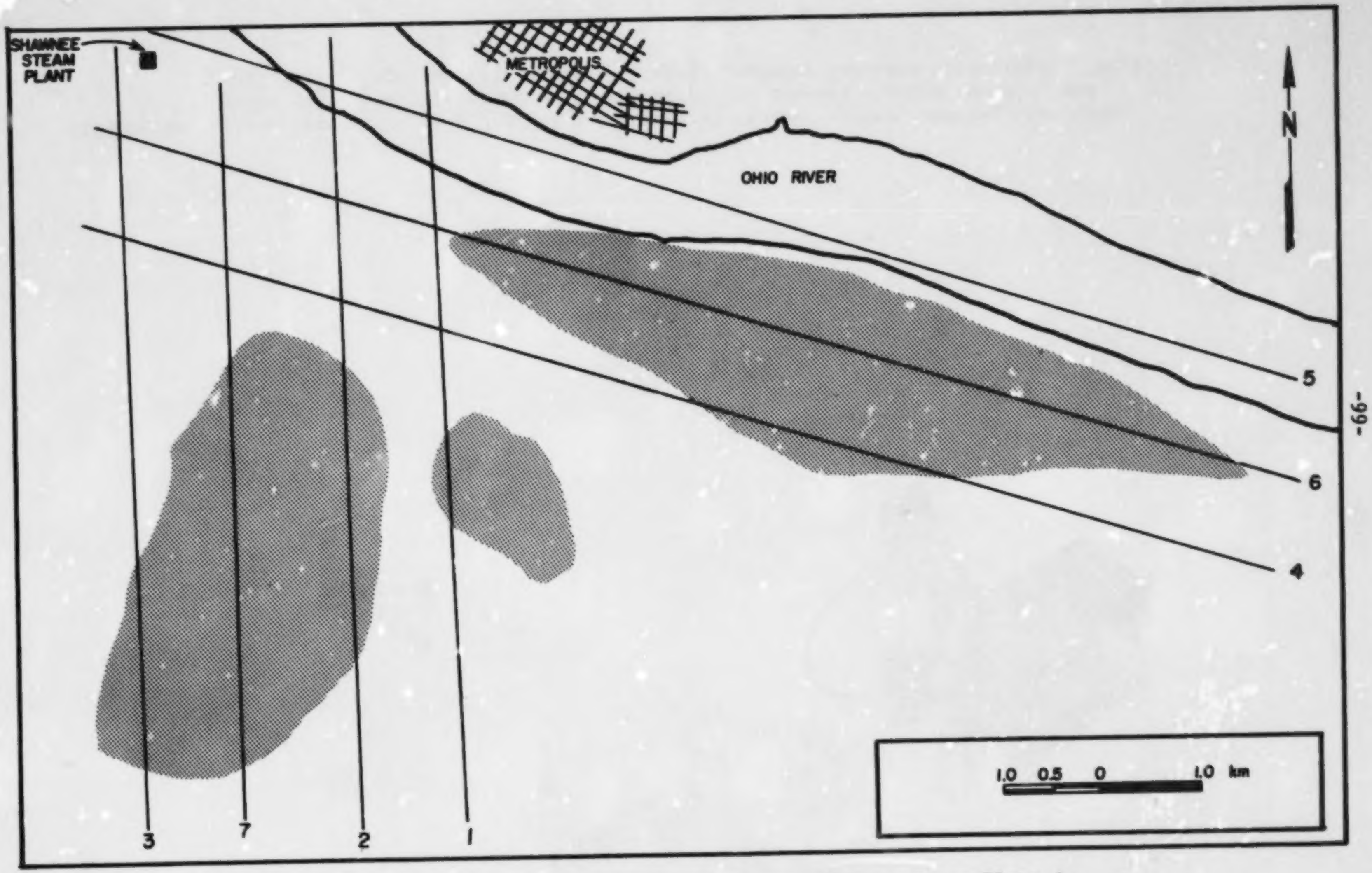
SHAWNEE STEAM PLANT
METROPOLIS
OHIO RIVER
N
5
6
4
3
7
2
1
1.0 0.5 0 1.0 km

Figure 41. Selected SO_2-affected areas and flight lines near Shawnee Steam Plant in western Kentucky in 1978.

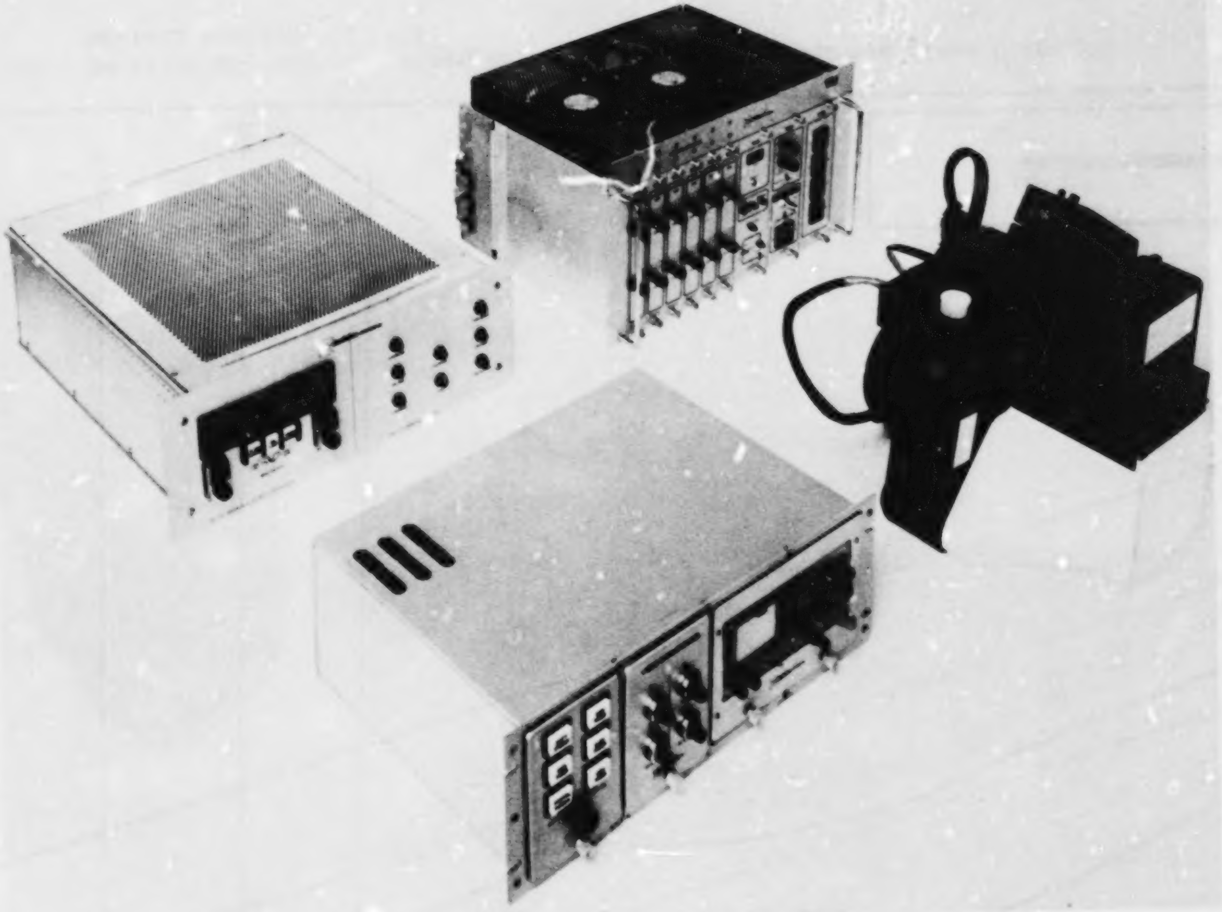

Figure 42. Basic components of a digital multispectral scanner system, showing scan head, power distributor/reference source controller, scanner control console, and digitizer. Tape recorder not shown (photo courtesy Daedelus Enterprises, Inc.).

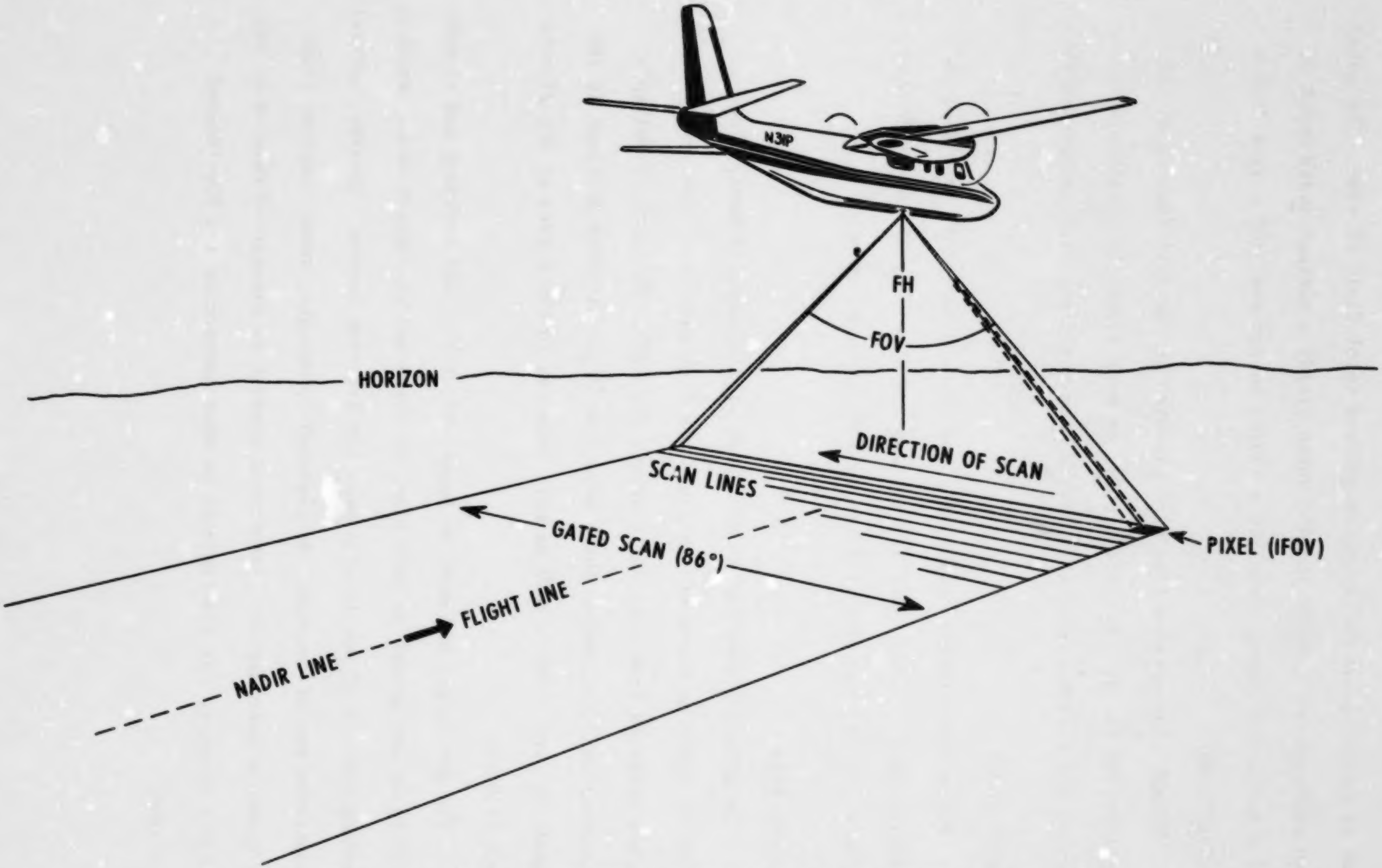
N31P
FH
FOV
HORIZON
DIRECTION OF SCAN
SCAN LINES
GATED SCAN (86°)
PIXEL (IFOV)
FLIGHT LINE
NADIR LINE

Figure 43. Configuration for airborne MSS data acquisition.

line is proportional to flying height and total field of view. The gated scan angle of the scanner is 86°, which yields a nominal swath width of 933 m (ground distance) from 500 m flying height and 3359 m from 1800 m flying height.

Flight line orientations were dictated by the distribution of the SO_2-affected fields. For efficiency, as many fields as possible were scanned per flight line. Each flight line was classified independently.

GROUND TRUTH

Field surveillance biologists from TVA and personnel from EMSL-LV gathered data on SO_2 injury to soybeans and other vegetation at Shawnee. Colbert ground truth was gathered by TVA personnel only.

Colbert Area

The affected area was located west of Florence, Alabama, about three to seven km north of the power plant (Figure 44). The vegetation injury occurred from July 20 to August 31, 1977. Evidence of multiple exposures was confirmed. There were four SO_2 monitoring stations in the immediate area. About 1620 ha were involved in the survey of SO_2 effects near Colbert.

The overflight was made on August 29, 1977. The soybeans had stopped putting on new growth by that time, so there was no concern about possible masking effects of new foliage over the affected leaves. However, natural senescence was of concern. Accelerated by drought, these symptoms began to occur in late August. Senescence appears as widespread chlorosis, but a field observer can discriminate between senescence and SO_2-induced chlorosis.

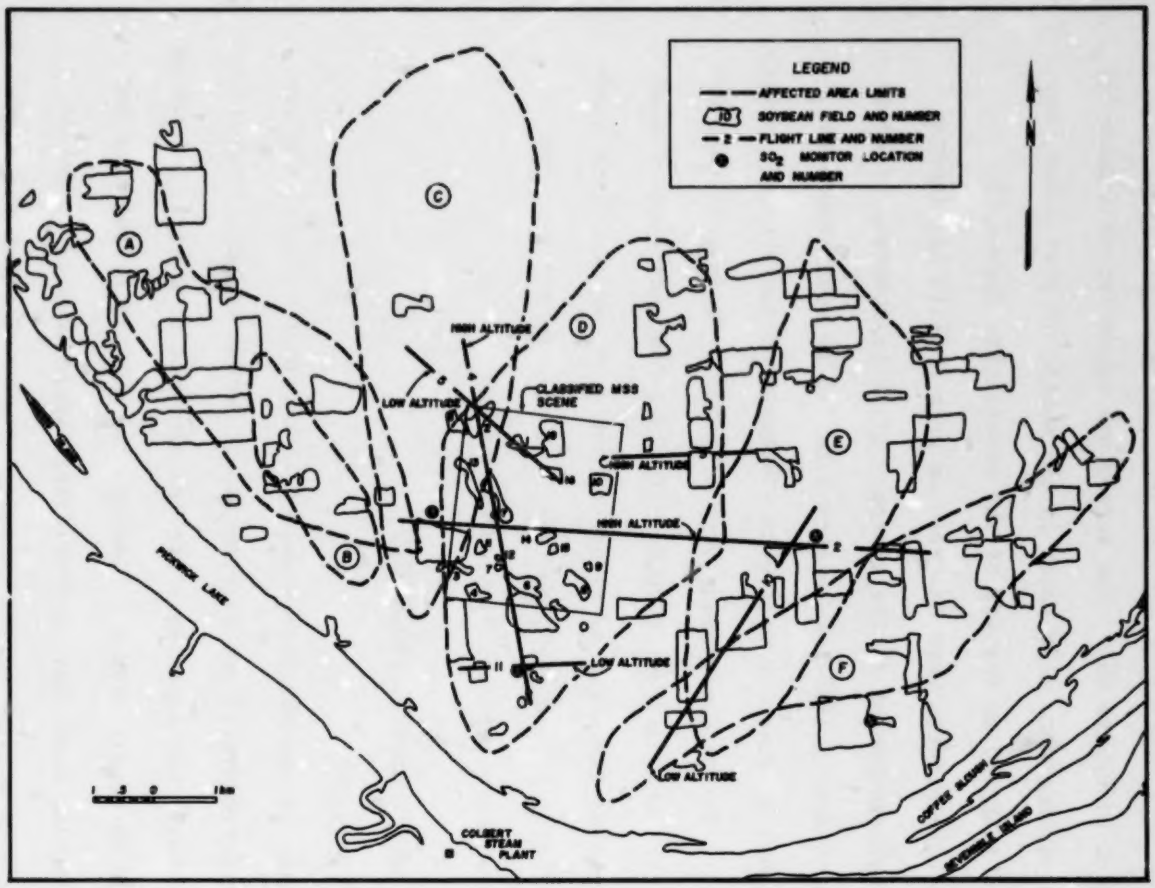
LEGEND
AFFECTED AREA LIMITS
10 SOYBEAN FIELD AND NUMBER
2 FLIGHT LINE AND NUMBER
SO_2 MONITOR LOCATION AND NUMBER
N
A
B
C
D
E
F
HIGH ALTITUDE
LOW ALTITUDE
CLASSIFIED MSS SCENE
PICKWICK LAKE
COLBERT STEAM PLANT
COFFEE SLOUGH
SEVENMILE ISLAND
km

Figure 44. Distribution of SO_2-affected, continuous-canopy soybean fields near Colbert Steam Plant in 1977.

Shawnee Area

For Shawnee, the SO_2 concentrations, winds, and apparent age of effects indicated that vegetation was affected on August 7, 1978, in three areas (A, B, and C on Figure 45). The survey was conducted on August 7-11. Additional observations were made later in the month; in particular, new ground truth was gathered on the day of the overflight, August 15.

The most severe effects were observed in area A (1113 ha) located 3.4 to 11.9 km east-southeast of the source. Light to moderate effects were noted in both area B (870 ha) located 3 to 7.5 km south-southeast, and area C (121 ha) located 5.0 to 7.0 km southeast of the source. Within these three areas, 857 ha of soybeans were affected. The map (Figure 45) shows both affected and unaffected soybean fields, the unaffected fields being located outside the areas of plume contact A, B, and C. Many unaffected soybean fields beyond the immediate area of interest were not surveyed and, therefore, are not plotted on the map.

DATA REDUCTION AND PROCESSING PROCEDURES

Preprocessing Procedures

Preprocessing of the MSS data involved three steps. First, the raw data tapes were decommutated and reformatted to become computer-compatible tapes (CCT's). Next, the tapes were checked for data anomalies, including missing data and recording errors. Finally, the quality of the data was checked by inspecting hard copy or displaying single-channel images on the color television monitor of the console. Figure 46 shows the eight decommutated channels for an agricultural scene near Colbert Steam Plant.

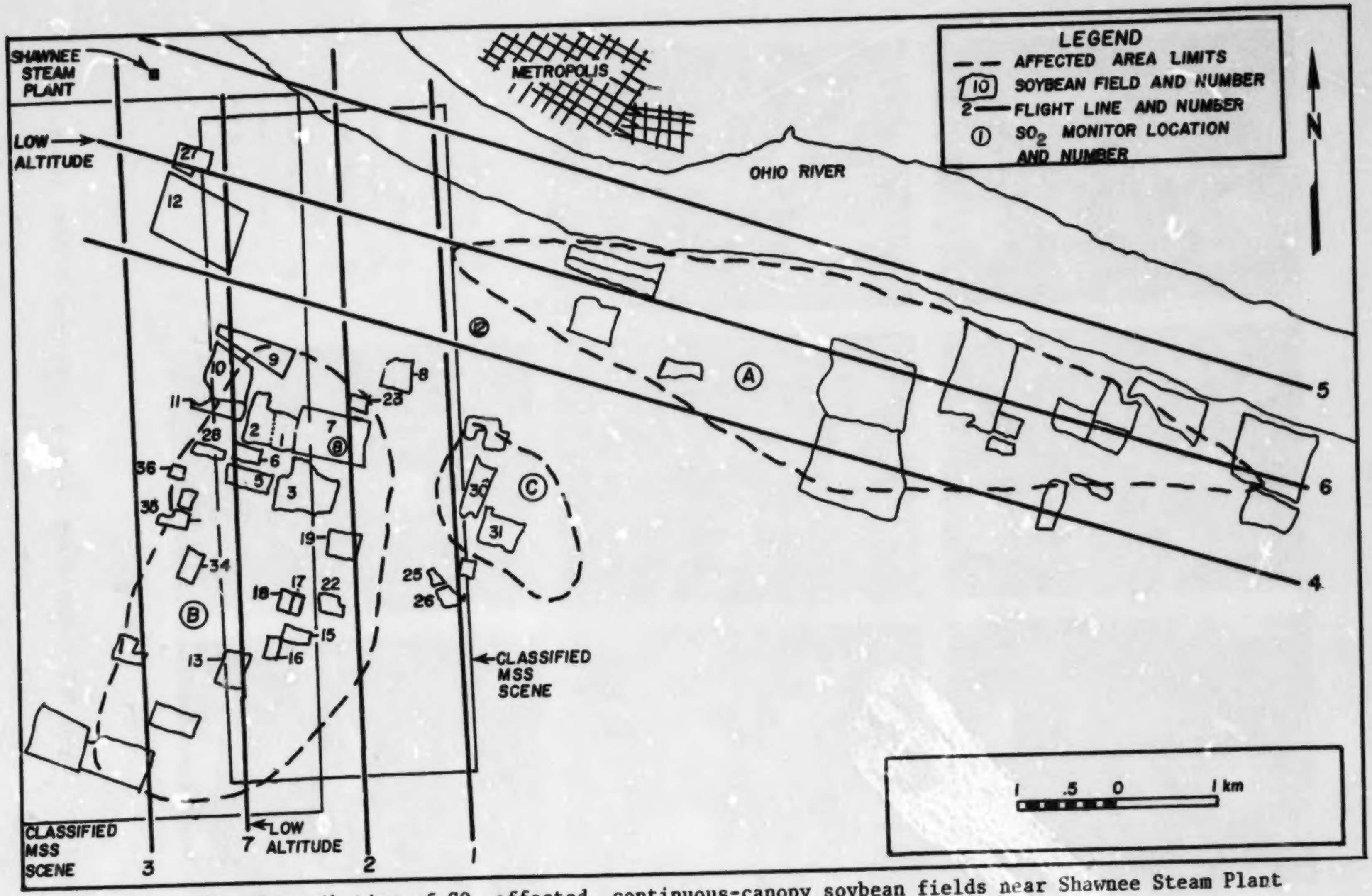
SHAWNEE STEAM PLANT
LOW ALTITUDE
METROPOLIS
OHIO RIVER
LEGEND
AFFECTED AREA LIMITS
10 SOYBEAN FIELD AND NUMBER
2 FLIGHT LINE AND NUMBER
① SO2 MONITOR LOCATION AND NUMBER
N
27
12
9
10
11
28
2
7
B
6
5
3
8
23
36
35
34
19
18
17
22
B
15
16
13
12
A
C
30
31
25
26
5
6
4
CLASSIFIED MSS SCENE
1 .5 0 1 km
CLASSIFIED MSS SCENE
3
7
LOW ALTITUDE
2
1

Figure 45. Distribution of SO_2-affected, continuous-canopy soybean fields near Shawnee Steam Plant in 1978. Fields without numbers had discontinuous canopies.

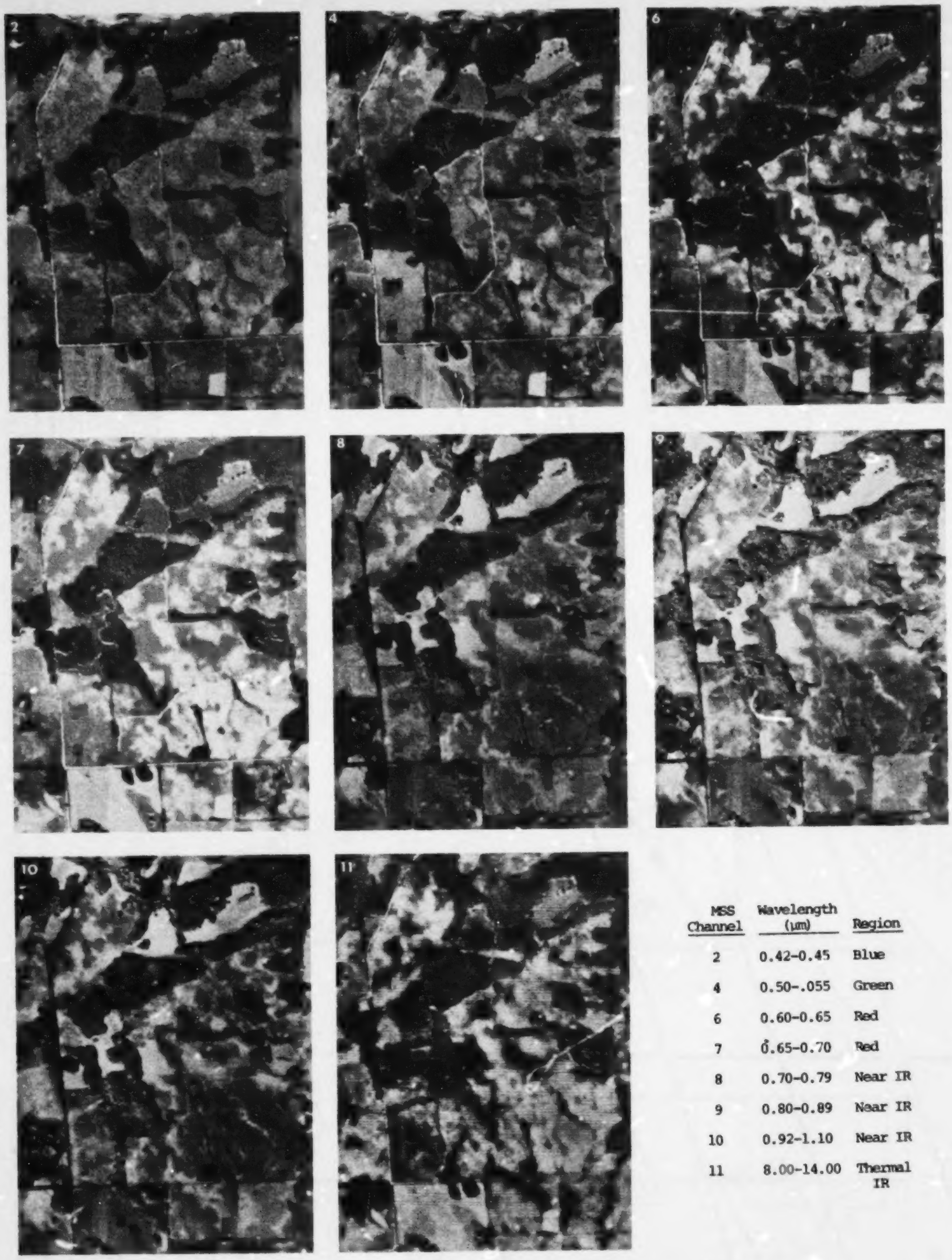

MSS Channel	Wavelength (μm)	Region
2	0.42-0.45	Blue
4	0.50-.055	Green
6	0.60-0.65	Red
7	0.65-0.70	Red
8	0.70-0.79	Near IR
9	0.80-0.89	Near IR
10	0.92-1.10	Near IR
11	8.00-14.00	Thermal IR

Figure 46. Eight MSS channels depicting a scene near Colbert Steam Plant.

Processing Procedures

Pattern Recognition--

The CCT's were processed on the EMSL-LV Data Analysis System (DAS) (Figure 47). The operation was organized as tasks, each being composed of one or more software programs (Figure 48). The heart of the processing operation is the pattern recognition block.[52] Spectral pattern recognition is a numerical process for simplifying the complex patterns inherent in MSS data. The process results in a limited number of spectrally separable, discrete classes of data. A decision strategy is used by the computer to assign pixels to classes.

In this project, the MSS data were classified independently using three procedures: supervised, pseudosupervised, and unsupervised (Appendices I, J, and K). The supervised procedure heavily used analyst and computer time, and it also required *a priori* knowledge of the scene that had to be gained through *in situ* measurements and interpretation of aerial photographs acquired along with the MSS data. Ground truth was used to program the computer to recognize SO_2-affected soybeans, unaffected soybeans, and background vegetative and nonvegetative cover.

The pseudosupervised classification procedure is a modification of the conventional supervised procedure. It was used to analyze the Shawnee data acquired in 1978, and is a modified maximum likelihood classifier for four MSS channels (MAXL4). It uses a very fast clustering program in combination with a minimal amount of information provided by the analyst to train the computer to recognize certain phenomena such as soybean fields. This information is provided for small ground areas and called training samples. These areas have relatively homogeneous spectral

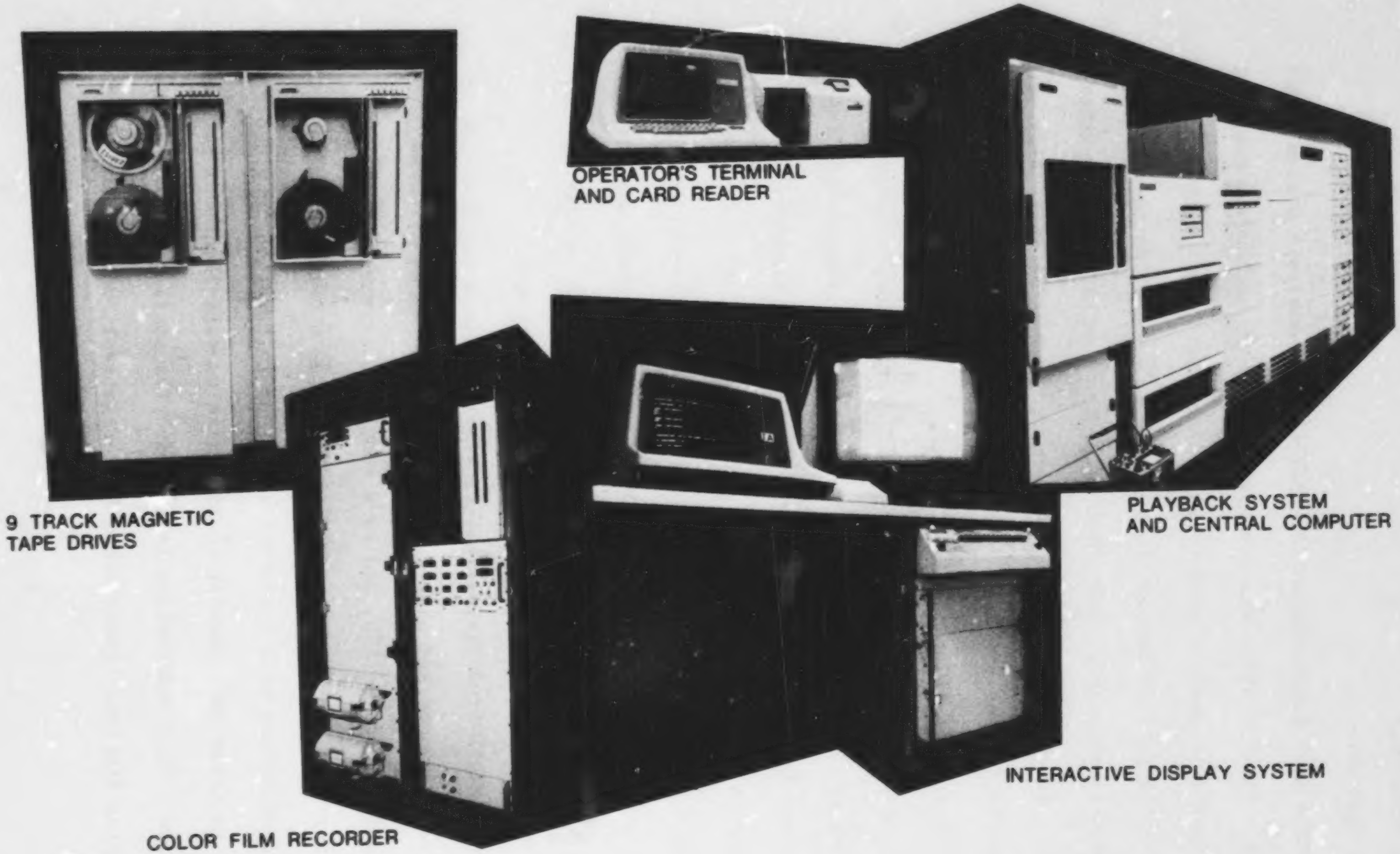
OPERATOR'S TERMINAL
AND CARD READER
9 TRACK MAGNETIC
TAPE DRIVES
PLAYBACK SYSTEM
AND CENTRAL COMPUTER
INTERACTIVE DISPLAY SYSTEM
COLOR FILM RECORDER

Figure 47. Data Analysis System at EMSL-LV (EPA photopraph).

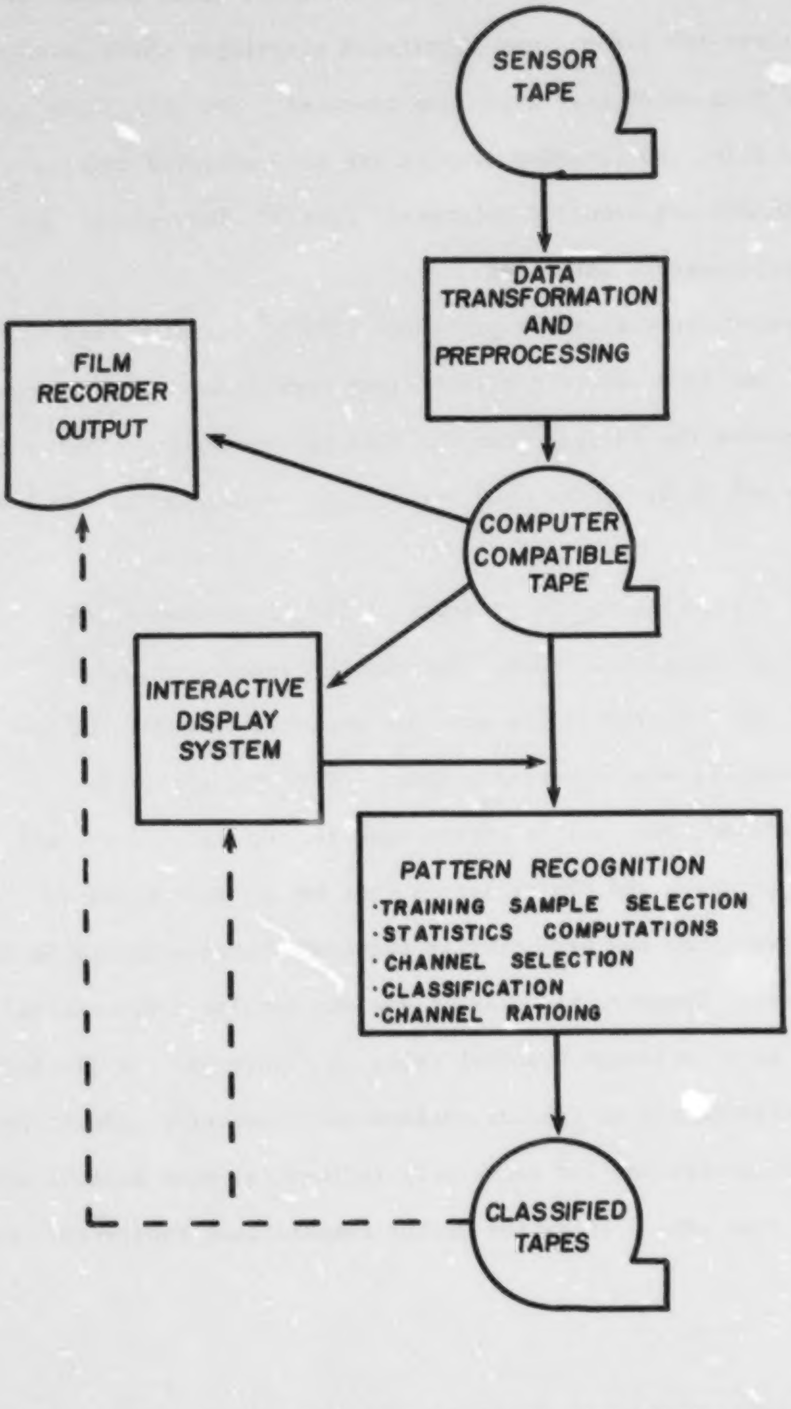
SENSOR TAPE
DATA TRANSFORMATION AND PREPROCESSING
FILM RECORDER OUTPUT
COMPUTER COMPATIBLE TAPE
INTERACTIVE DISPLAY SYSTEM
PATTERN RECOGNITION
·TRAINING SAMPLE SELECTION
·STATISTICS COMPUTATIONS
·CHANNEL SELECTION
·CLASSIFICATION
·CHANNEL RATIOING
CLASSIFIED TAPES

Figure 48. Functional tasks for processing MSS data on Data Analysis System at EMSL-LV.

characteristics. The CCT's were manipulated initially under SEARCH, an unsupervised trainer for the maximum likelihood classifier which generates up to 49 classes from which statistics are computed. The statistics are then stored in a file, and training samples are then selected using a combination of SEARCH and manually determined data.[53] The rest of the classification procedure is automated.

An unsupervised classification procedure (UNSUP) was also used to process digital data from selected flight lines over Shawnee and Colbert. The procedure removes the analyst from the data processing loop, since no training samples are used, so the need for a priori knowledge of the scene is not great.[54]

However, an evaluation of the accuracy of the final classified product always requires ground truth. Whereas the supervised and pseudosupervised (MAXL4) classifiers use informational classes, the unsupervised classifier uses spectral classes. Once the spectral classes are determined, the analyst checks them for utility. A typical problem with the unsupervised classifier is that two or more types of phenomena to be separated may have similar spectral characteristics (e.g., soybeans and weeds). Unsupervised classifiers may involve n-dimensional cluster analysis as illustrated hypothetically in Figure 49. In cluster analysis, the determination of cluster centers and boundaries affects the results; these determinations are especially influential when dealing with multidimensional data sets. Iterative vector computations facilitate these operations.[55]

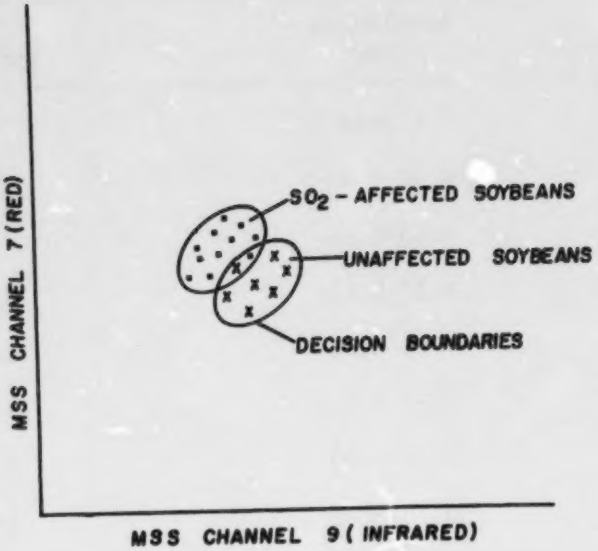
SO_2 - AFFECTED SOYBEANS
UNAFFECTED SOYBEANS
DECISION BOUNDARIES
MSS CHANNEL 7 (RED)
MSS CHANNEL 9 (INFRARED)

Figure 49. Hypothetical two-dimensional plot of naturally clustered spectral measurements of soybeans.

Optimal Channel Selection--

When the number of channels that can be processed simultaneously on the computer is less than the number of channels acquired during the overflight, a method for selecting the best channels for classifying the phenomena of interest is needed. For our analysis of Colbert and Shawnee data, the 10 original channels were reduced to 8 (Table 19), the maximum number the computer could accept. The thermal infrared channel from Shawnee was one of those eliminated because it had shown little utility during the previous analysis of Colbert. The unsupervised classifier used all eight preselected channels, but these were reduced to four for supervised and pseudosupervised classifications. Previous analyses of airborne MSS data have shown no advantage in processing more than four to six channels.[56]

TABLE 19. MULTISPECTRAL SCANNER CHANNELS[a]

Channel	Wavelength (μm)	Spectral region
1	Not used	
2[b]	0.42-0.45	Blue
3[c]	0.45-0.49	Blue
4[b,c]	0.50-0.55	Green
5[c]	0.55-0.60	Green
6[b,c]	0.60-0.65	Red
7[b,c]	0.65-0.70	Red
8[b,c]	0.70-0.79	Near-IR
9[b,c]	0,80-0.89	Near-IR
10[b,c]	0.92-1.10	Near-IR
11[b]	8.00-14.0	Thermal IR
12	Not used	

[a] Specifications from Daedelus Enterprises, Incorporated.

[b] Channels used for Colbert in 1977.

[c] Channels used for Shawnee in 1978.

The optimal channel selection procedure used a program entitled SEPARATION which calculated the interclass distance separation to derive the optimal four channels and displayed results in a matrix format.[57] This procedure was followed for each flight line of data.

Conventional Analysis Procedures--

The aerial CIR photographs were interpreted stereoscopically, and field identifications, field boundaries, and other information were identified on registered overlays. Soybean fields were examined for uniformity of canopy density, closure, weediness, and presence of visible effects from SO_2. The photointerpreted information supported field observations and selection of training samples.

Procedures for Evaluating Classification Accuracy

To evaluate the classifications, the color-coded patterns of the MSS scene were compared with ground truth. During interactive processing, a color table was set up so that certain colors represented specific land cover types, such as affected or unaffected soybeans. Our evaluation measured how closely the depicted pattern of colors corresponded to actual land cover patterns as determined by field observation.

In MSS data classification there are errors of omission and errors of commission. The first error results in underclassification and the second, in overclassification of the phenomena of interest.

The evaluation of accuracy of the MSS classifications began by measuring the areas of specific coded colors in the scene with a planimeter. Pixel counts were not used because they were not obtainable on a field-by-field basis. (The shapes of the fields were generally irregular.) The area figures were recorded and tabulated along with the percentage of area affected in each field. This percentage is the P factor of the LxAxP index

(Appendix D) used in the field to describe foliar injury. Then the areas of each field were multiplied by P, yielding measurements for the proportion of affected soybeans in each field. All area measurements were converted from image-based units to hectares. For example, an accurate classification of a particular soybean field known to be 50 percent affected by SO_2 would exist if half of the imaged area within the field appeared in the color selected to represent affected soybeans. The location, pattern, and clustering of the affected pixels within the delineated field boundaries were not considered in this evaluation.

After the measurements were tabulated on a field-by-field basis, they were summed. The measured (color-coded) areas and actual field-derived values were then compared to determine the accuracy of the classification. Accuracy was measured by computing the classification error E, a percentage representing the error of omission or commission. The formula used is

$$E(\%) = \frac{|a - m|}{a} \times 100$$

where $\underline{a}$ is the actual observed area of SO_2-affected soybeans expressed as a percentage of total field area, and $\underline{m}$ is the measured area of the appropriate coded color representing SO_2-affected soybeans within the field. Factor $\underline{m}$ is an image-derived area measurement.

RESULTS AND DISCUSSION

Optimal Altitudes

The MSS lines over Colbert and Shawnee were flown at 1800 m and 500 m AGL. Unsupervised classification of the lower altitude data from Colbert indicated that they provided no improved accuracy, so analysis of it was discontinued. A low-altitude line generates more data per kilometer flown and is therefore more costly and time-consuming to analyze.

Colbert Test

Optimal MSS Channels--

Computer algorithms were used to compute divergence matrices showing optimal separation of data classes and maximum divergence among individual areas (agricultural fields). The matrices provided a means for selecting the best four channels from eight (Table 20). The results of the two

TABLE 20. OPTIMAL MSS CHANNELS FOR DETECTING AND CLASSIFYING SO_2-AFFECTED SOYBEAN FIELDS NEAR COLBERT STEAM PLANT IN 1977

Procedure[a]	MSS channel designation[b]	Wavelength (μm)	Spectral region
1	4	0.50-0.55	Green
	7	0.65-0.70	Red
	8	0.70-0.79	Near-IR
	9	0.80-0.89	Near-IR
2	4	0.50-0.55	Green
	6	0.60-0.65	Red
	7	0.65-0.70	Red
	8	0.70-0.79	Near-IR

[a] Procedures discussed in text.

[b] See Table 19 for the 8 channels considered for Colbert.

procedures are similar, as the green, red, and near-IR channels were chosen each time. The blue and thermal IR channels were rejected; these two spectral regions have inherently low contrast with respect to vegetation.

Unsupervised Classification--

The UNSUP classification procedure was only partly successful in mapping SO_2 effects. The classification (Figure 50) was studied to determine how closely its patterns corresponded to ground truth. Specifically examined were the separation of soybean fields from all other land cover without consideration of SO_2 effects and the separation of SO_2-affected soybean fields from unaffected soybean fields.

The colors of the unsupervised classification were coded during interactive processing so that dark red represented affected soybeans and medium red represented unaffected soybeans.

The entire scene, including the soybean fields and areas outside the fields, was examined first. Since the dark and medium red areas outside the actual fields are not soybeans, they represent overclassification. The overclassification error is 7.2 percent, a figure obtained by dividing the area of total red color (78.4 ha) by the total scene area (1081.8 ha) and multiplying by 100. Field checking identified these erroneous red areas as patches of weeds in otherwise defoliated cotton fields. The 7.2-percent error was judged to be acceptable so we attempted to distinguish SO_2-affected soybeans from unaffected soybeans. Evaluation of the accuracy of this classification requires considering the patterns within the soybean fields. The MSS scene includes 18 soybean fields (Figure 51). All areas of dark and medium red color, representing affected and unaffected soybeans, respectively, were measured

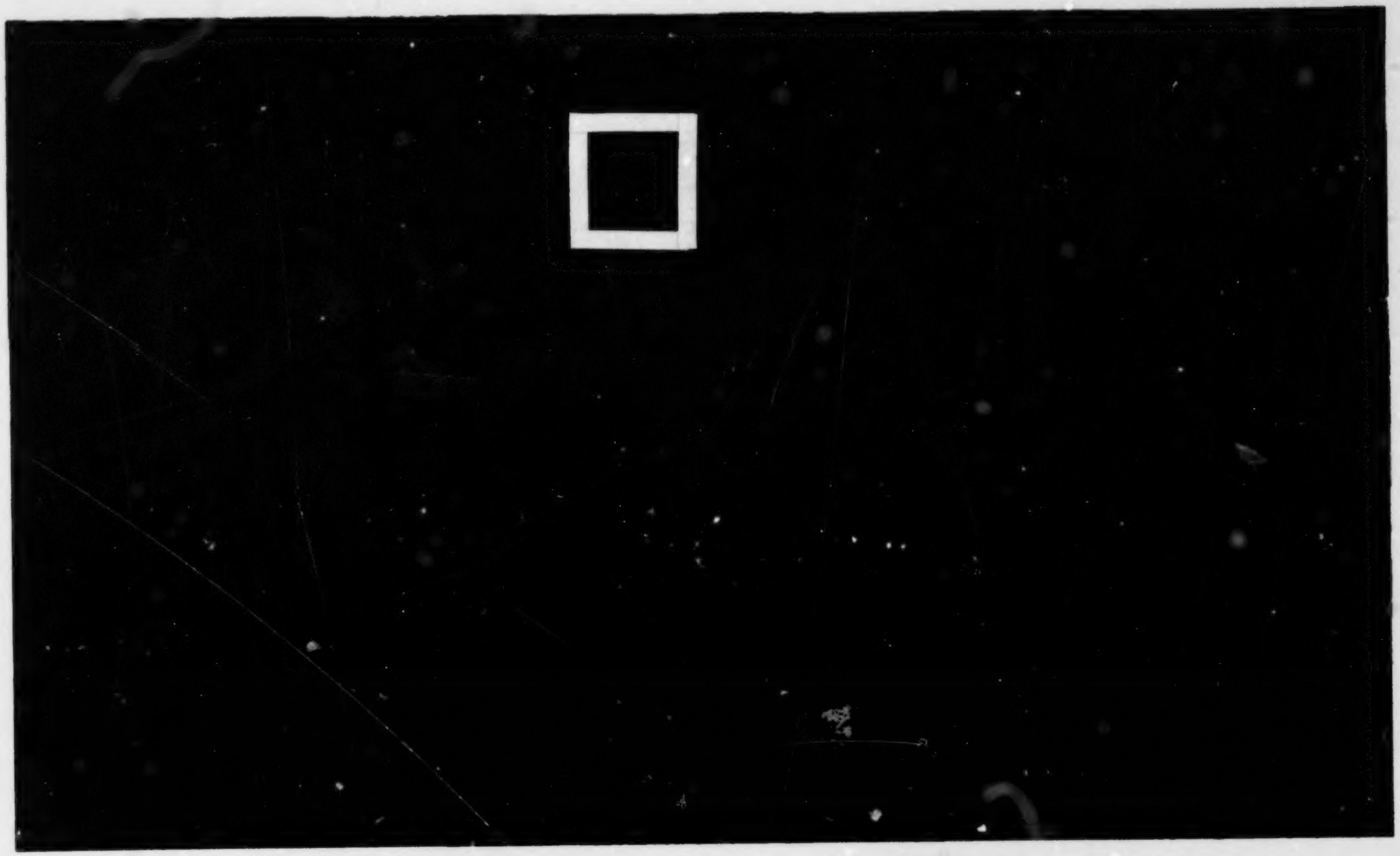

Unaffected Soybeans
SO_2-Affected Soybeans

Figure 50. Unsupervised classification of MSS data for Colbert area. See Figure 51 for distribution of soybean fields and SO_2 effects.

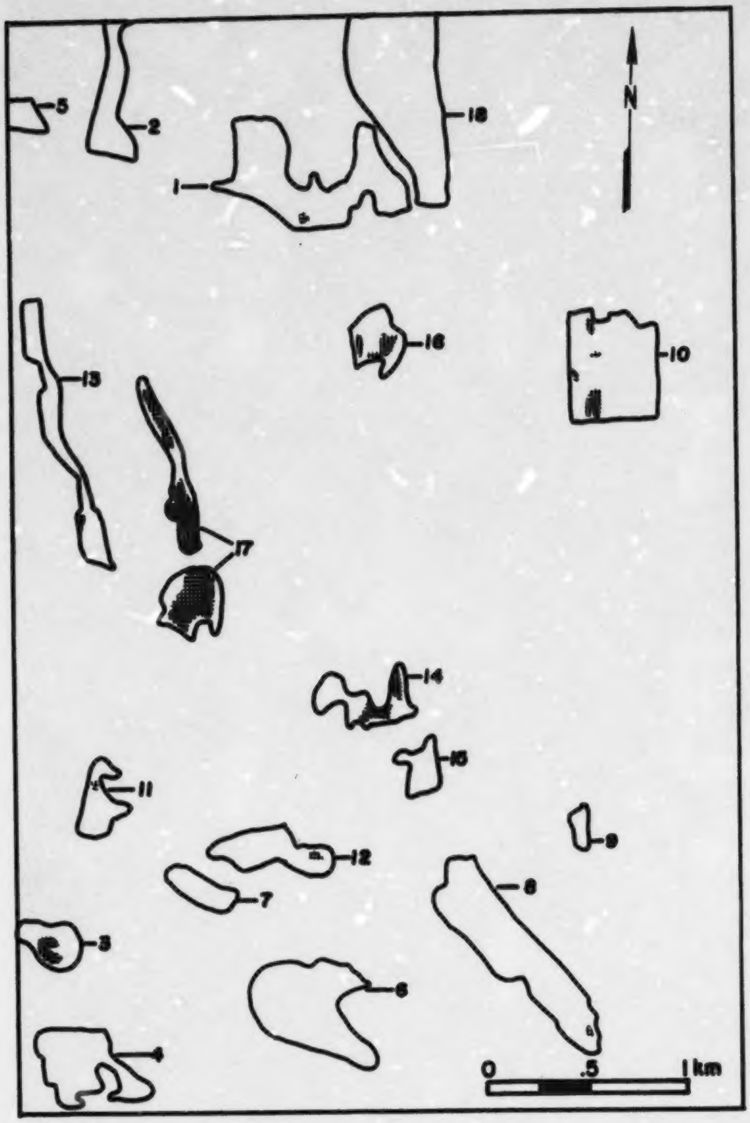
N
1
2
3
4
5
6
7
8
9
10
11
12
13
14
15
16
17
18
0
.5
1 km

Figure 51. Distribution of SO_2 effects (screened pattern) within dense-canopy soybean fields near Colbert Steam Plant. Keyed to unsupervised classification (Figure 50).

and the numbers were converted to equivalent ground area in hectares. The ground truth was obtained by multiplying the area of each field by an observation of the proportion of soybeans affected in the field, the result being a figure representing the area of affected soybeans for each field.

Comparison of the image colors and ground truth revealed an overclassification of 142 percent for the unsupervised procedure (Table 21).

In summary, the unsupervised classification procedure could separate soybeans from other land cover with an error of commission of 7.2 percent. It could not, however, distinguish SO_2-affected soybeans from unaffected soybeans. The difficulty is attributed to the low levels of foliar injury prevailing at Colbert during the 1977 overflight. The highest percentage of area affected in any dense-canopy soybean field was 12 percent (Table 21).

Supervised Classification--

The supervised procedure was unsuccessful in separating soybeans from other field crops because of spectral overlap of the classes. These results are considered inconclusive because they were not tested on a full range of foliar effects.

Shawnee Test

Optimal MSS Channels--

As stated previously, the best channels for classifying soybeans were selected with the SEARCH algorithm. The unsupervised classifier used all eight decommutated channels (numbers 3 through 10, Table 19), but the pseudosupervised classifier required reducing the number of channels to four.

TABLE 21. COMPARISON OF FIELD OBSERVATIONS OF SO_2 EFFECTS ON SOYBEANS AND RESULTS OF MSS UNSUPERVISED CLASSIFICATION FOR COLBERT SCENE 2

	Ground truth			MSS classification		
Field identification	Field area (ha)	Proportion of field affected (%)[a]	Actual affected area (ha)	Measured affected area (ha)	Measured unaffected area (ha)	Error (%)
1	15.26	1.6	0.24	0.21	15.05	12.5
2	5.64	2.7	0.15	0.00	5.64	100.0
3	2.09	4.8	0.10	0.63	1.46	530.0
4	6.27	4.8	0.30	0.00	6.27	100.0
5	1.25	4.0	0.05	0.00	1.25	100.0
6	10.66	0.6	0.06	0.00	10.66	100.0
7	1.88	0.6	0.01	0.00	1.88	100.0
8	14.63	12.0	1.76	0.21	14.42	88.1
9	1.05	2.0	0.02	0.00	1.05	100.0
10	12.54	4.0	0.50	0.84	11.70	68.0
11	2.72	2.7	0.07	0.21	2.51	200.0
12	4.18	0.4	0.02	0.21	3.97	950.0
13	6.48	2.4	0.16	0.21	6.27	31.3
14	3.76	0.2	0.01	1.05	2.71	10,400.0
15	3.14	0.0	0.00	0.00	3.14	0.0
16	4.39	0.6	0.03	0.84	3.55	2,700.0
17	9.82	1.6	0.16	4.81	5.01	2,906.3
18	16.72	1.0	0.17	0.00	16.72	100.0
TOTAL			a = 3.81	m = 9.22		

Classification error = $\frac{|a - m|}{a} \times 100 = \frac{|3.81 - 9.22|}{3.81} \times 100 = 142.0$ percent overclassified

---

[a] P factor of LxAxP index (Appendix D).

Table 22 lists the channels selected for the north-south and east-west flight lines. A blue channel was selected for the north-south lines instead of green. Earlier selections using Colbert data preferred green to blue. SEARCH is influenced by the spectral characteristics of the scanned terrain and features, and an abundance of water in the scene will alter the result from that obtained if the scene were all land. Part of the Ohio River was included in the Shawnee flight lines and this may have biased the selection.

TABLE 22. OPTIMAL MSS CHANNELS FOR DETECTING AND CLASSIFYING SO_2-AFFECTED SOYBEAN FIELDS NEAR SHAWNEE STEAM PLANT IN 1978

MSS channel designation[a]	Flight Line	Wavelength (μm)	Spectral region
3	2,3	0.45-0.49	Blue
7		0.65-0.70	Red
8		0.70-0.79	Near-IR
9		0.80-0.89	Near-IR
5	5	0.55-0.60	Green
7		0.65-0.70	Red
8		0.70-0.79	Near-IR
9		0.80-0.89	Near-IR

[a] MSS channels 3 through 10 considered. Procedure for channel selection accomplished by calculating interclass distance separation.

Unsupervised Classification--

The unsupervised classifier (UNSUP) was also applied to flight line 2 data. Only the dense-canopy fields were included in the evaluation. A total of 32 dense-canopy soybean fields, 25 of which were affected by SO_2, are depicted in the scene (Figures 52 and 53).

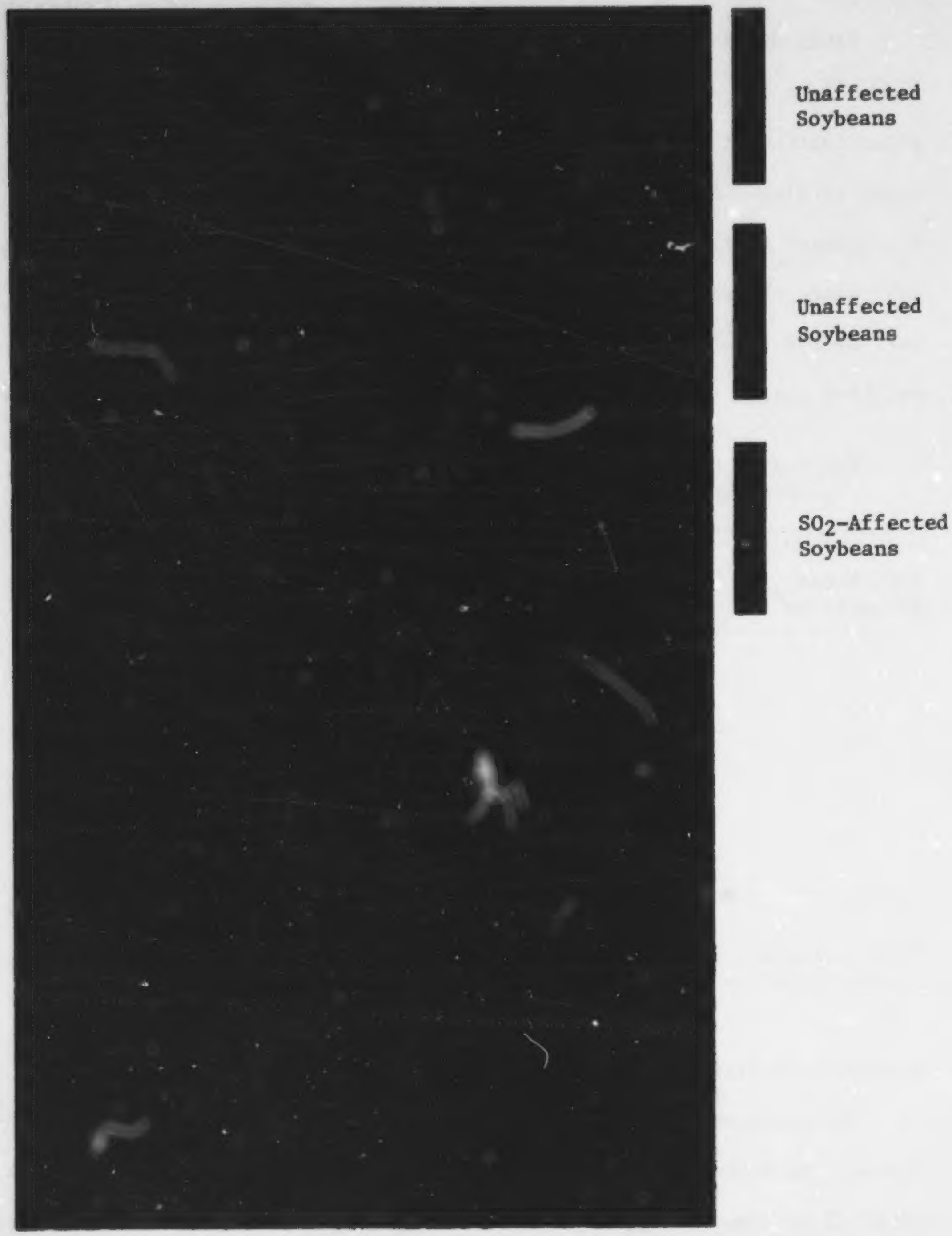
Unaffected Soybeans
Unaffected Soybeans
SO_2-Affected Soybeans

Figure 52. Unsupervised classification of MSS line 2 data near Shawnee Steam Plant. See Figure 53 for distribution of soybean fields and SO_2 effects.

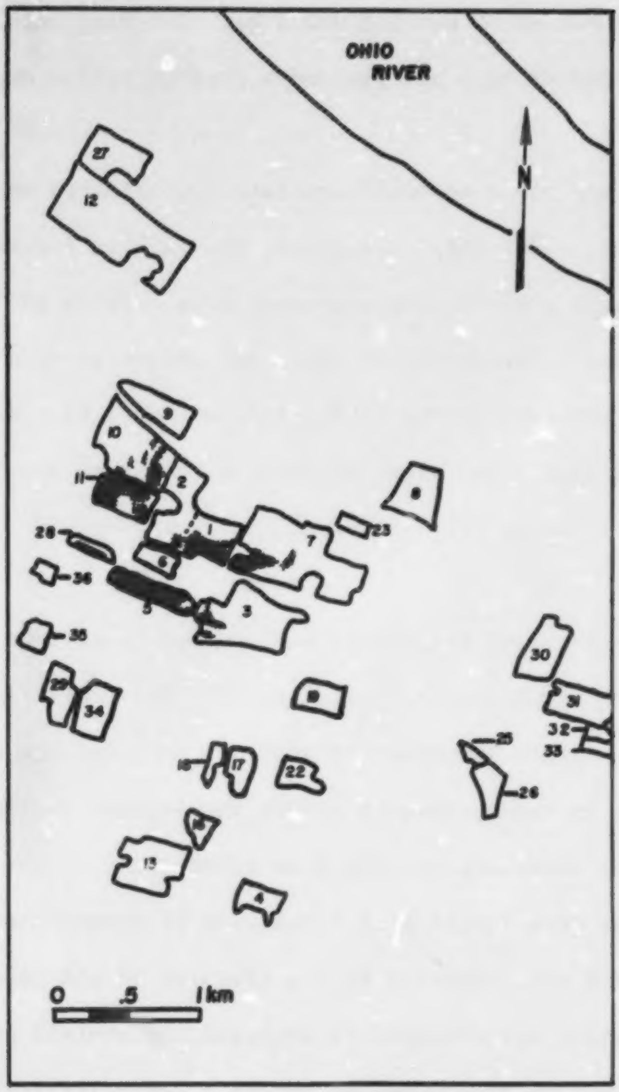
OHIO RIVER
N
27
12
9
10
11
2
1
7
8
23
28
6
36
5
3
35
30
31
32
33
29
34
25
26
16
17
22
18
13
4
0
.5
1 km

Figure 53. Distribution of SO_2 effects (screened pattern) within dense-canopy soybean fields near Shawnee Steam Plant. Keyed to MSS flight line 2, unsupervised classification (Figure 52).

The classification scheme was moderately successful in differentiating soybean fields from other land cover. The green-colored areas appearing where soybeans did not exist totaled 242.5 ha. Dividing this by the total scene area analyzed (3192.3 ha) yielded a classification error of 7.6 percent.

The UNSUP classifier could not differentiate SO_2-affected soybeans from unaffected soybeans. For this evaluation, the analyst focused only upon the patterns appearing within the soybean fields. Table 23 lists the fields and relevant data. The measured light- and medium-green areas, representing affected soybeans in the scene, totaled 223.1 ha. According to ground truth, the actual total affected area in the scene was 110.8 ha, so the classification error is 101.4 percent.

Pseudosupervised Classification--

The MAXL4 pseudosupervised classifier was applied to east-west flight line 5 and north-south flight lines 2 and 3. The classification of line 5 data was eventually abandoned because of complications associated with variations in canopy density within the soybean fields there. This discussion describes results from lines 2 and 3 only.

The classification from flight line 2 contains 26 dense-canopy soybean fields, 21 of which were affected by SO_2 (Figures 54 and 55). The area of each of the colors was measured to evaluate the overall performance of the classifier. To determine the extent of overclassification, if any, we measured the total area of the colors representing soybeans where the crop did not exist. For this scene, the classification error was 5.1 percent, a figure derived by dividing the total area of misidentified soybeans (109.1 ha) by the total scene area analyzed (2120.6 ha).

TABLE 23. COMPARISON OF FIELD OBSERVATIONS OF SO_2 EFFECTS ON SOYBEANS AND RESULTS OF MSS UNSUPERVISED CLASSIFICATION FOR SHAWNEE FLIGHT LINE 2

Field identification	Ground truth			MSS classification		Error (%)
	Field area (ha)	Proportion of field affected (%)[a]	Actual affected area (ha)	Measured affected area (ha)	Measured unaffected area (ha)	
1	11.7	20	2.3	11.7	0.0	408.7
2	17.6	0	0.0	17.6	0.0	-
3	24.3	40	9.7	21.8	2.5	124.7
4	6.9	40	2.8	5.9	1.0	110.7
5	8.5	40	3.4	8.5	0.0	150.0
6	5.3	60	3.2	5.3	0.0	65.6
7	32.4	50	16.2	32.4	0.0	100.0
8	14.2	0	0.0	2.5	11.7	-
9	8.1	50	4.1	6.8	1.3	65.9
10	25.1	50	12.6	10.9	14.2	13.5
11	8.9	40	3.6	7.5	1.4	108.3
12	40.5	0	0.0	21.8	18.7	-
13	16.2	50	8.1	6.8	9.4	16.0
16	4.5	50	2.3	3.4	1.1	47.8
17	4.9	40	2.0	4.9	0.0	145.0
18	2.8	30	0.8	2.8	0.0	250.0
19	6.5	70	4.6	5.9	0.6	216.7
22	5.3	90	4.8	5.1	0.2	6.3
23	1.6	20	0.3	1.6	0.0	433.3
25	2.0	0	0.0	0.8	1.2	-
26	4.0	0	0.0	2.5	1.5	-
27	8.1	0	0.0	8.1	0.0	-
28	4.1	40	1.6	4.1	0.0	156.3
29	5.3	80	4.2	5.3	0.0	26.2
30	13.0	30	3.9	5.1	7.9	30.8
31	12.1	50	6.1	0.0	12.1	100.0
32	1.6	70	1.1	0.0	1.6	100.0
33	3.2	60	1.9	0.0	3.2	100.0
34	7.3	90	6.6	7.3	0.0	10.6

TABLE 23 (Continued)

Field identification	Ground truth			MSS classification		Error (%)
	Field area (ha)	Proportion of field affected (%)[a]	Actual affected area (ha)	Measured affected area (ha)	Measured unaffected area (ha)	
35	6.5	40	2.6	5.9	0.6	126.9
36	2.8	70	2.0	0.8	2.0	60.0
TOTALS			a = 110.8	m = 223.1		

Classification error = $\frac{|a - m|}{a} \times 100 = \frac{|110.8 - 223.1|}{110.8} = 101.4$ percent overclassified

---

[a] Factor P of LxAxP index (Appendix D).

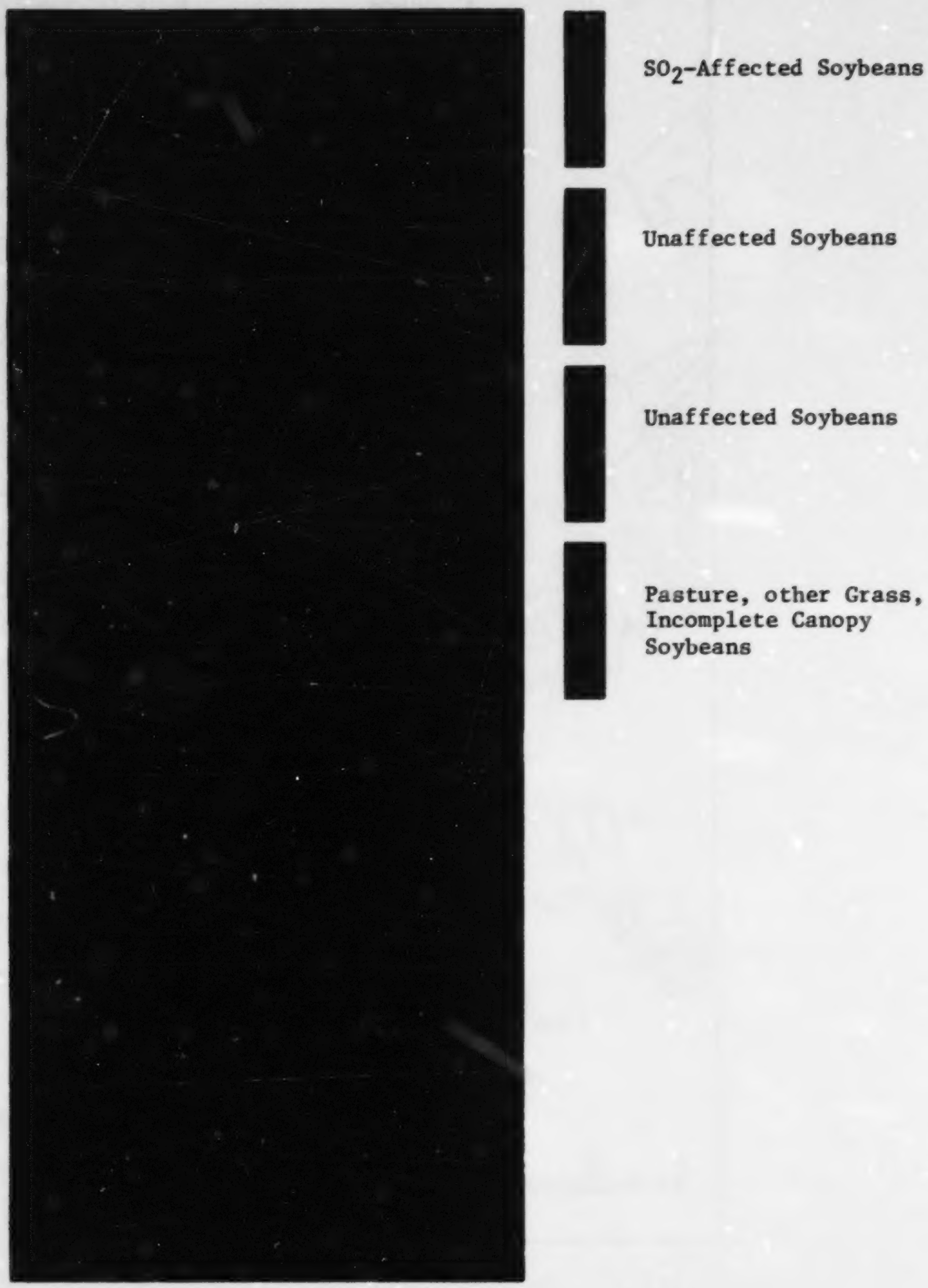
SO_2-Affected Soybeans
Unaffected Soybeans
Unaffected Soybeans
Pasture, other Grass, Incomplete Canopy Soybeans

Figure 54. Pseudosupervised classification of MSS line 2 data near Shawnee Steam Plant. For distribution of SO_2 effects within soybean fields, see Figure 55.

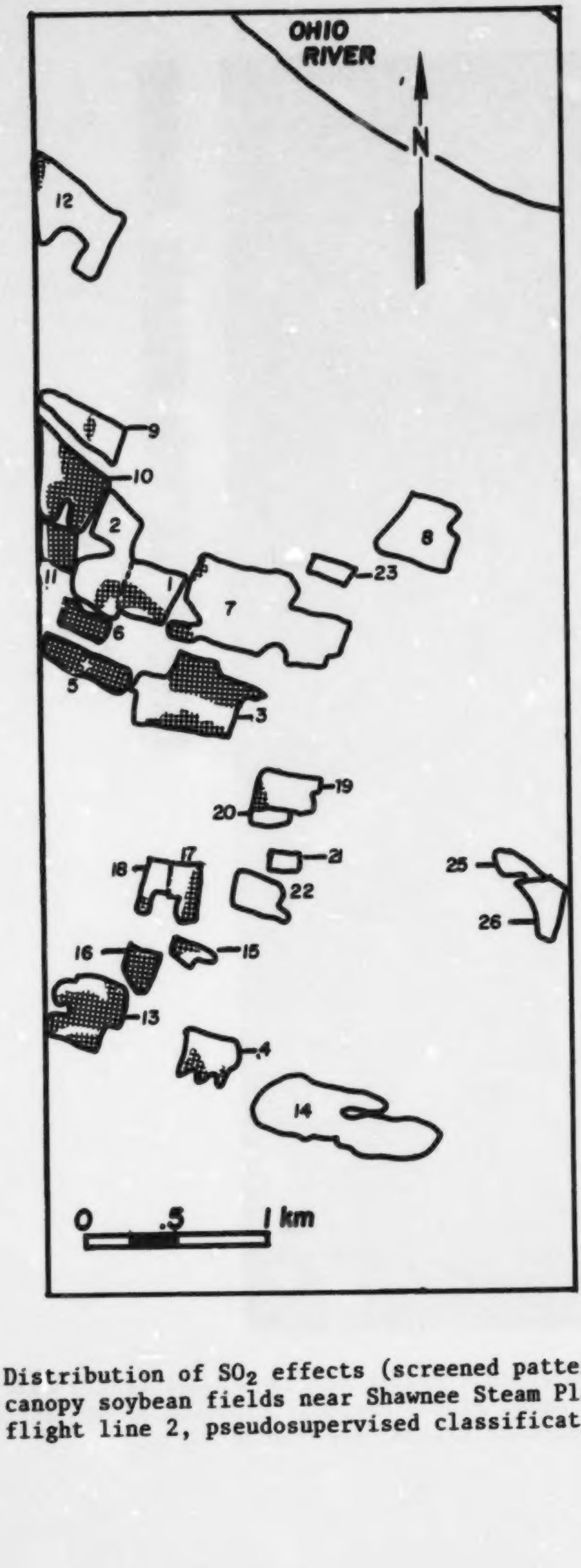
OHIO
RIVER
N
12
9
10
2
11
1
7
8
23
6
5
3
19
20
17
18
21
22
25
26
16
15
13
4
14
0
.5
1 km

Figure 55. Distribution of SO_2 effects (screened pattern) within dense-canopy soybean fields near Shawnee Steam Plant. Keyed to flight line 2, pseudosupervised classification (Figure 54).

The primary objective of this study was to determine how well the MAXL4 classifier could differentiate SO_2-affected soybeans from unaffected soybeans. For this determination, only the colors appearing within the delineated field boundaries were considered. Table 24 lists the fields, their actual affected proportions, the affected areas measured from the classified image, and the totals where appropriate. According to ground truth, the total area of SO_2-affected soybeans was 102.1 ha. The light green color representing SO_2-affected soybeans on the image covers 77.2 ha. The error is therefore 24.4 percent underclassified.

In summary, the pseudosupervised classification of line 2 data has resulted in an overclassification of soybeans, without regard to SO_2 effects, of about 5 percent. The attempt to differentiate SO_2-affected soybeans and unaffected soybeans resulted in an underclassification error of about 24 percent.

The pseudosupervised classification from flight line 3 depicts 22 dense-canopy soybean fields, 19 of which were affected by SO_2 (Figures 56 and 57, and Table 25). The correspondence of the color-coded patterns to the actual distribution of soybeans was excellent, the area of misidentification being only 20.2 ha and the total analyzed scene area being 3207.4 ha. The error of commission, 0.6 percent, represents a slight overclassification of soybeans without regard to SO_2 effects.

The separation of SO_2-affected soybeans and unaffected soybeans with the pseudosupervised classifier was good for line 3 data. The total area coded as soybeans (medium yellow) in the scene is 81.7 ha. The actual area determined by field observations was 73.4 ha, so the classification error is 11.3 percent.

TABLE 24. COMPARISON OF FIELD OBSERVATIONS OF SO_2 EFFECTS ON SOYBEANS AND RESULTS OF MSS PSEUDOSUPERVISED CLASSIFICATION FOR SHAWNEE FLIGHT LINE 2

	Ground truth			MSS classification		
Field identification	Field area (ha)	Proportion of field affected (%)[a]	Actual affected area (ha)	Measured affected area (ha)	Measured unaffected area (ha)	Error (%)
1	11.7	20	2.3	2.5	9.2	8.7
2	17.6	0	0.0	1.7	15.9	-
3	24.3	40	9.7	13.4	10.9	38.1
4	6.9	40	2.8	2.5	4.4	10.7
5	8.5	40	3.4	6.8	1.7	100.0
6	5.3	60	3.2	5.1	0.2	59.4
7	32.4	50	16.2	1.7	30.7	89.5
8	14.2	0	0.0	0.0	14.2	0.0
9	8.1	50	4.1	0.8	7.3	80.5
10	25.1	50	12.6	11.7	13.4	7.1
11	8.9	40	3.6	6.8	2.1	88.9
12	40.5	0	0.0	1.7	38.8	-
13	16.2	50	8.1	12.6	3.6	55.6
14	30.4	30	9.1	0.0	30.4	100.0
15	2.0	40	0.8	0.9	1.1	12.5
16	4.5	50	2.3	4.5	0.0	95.7
17	4.9	40	2.0	1.7	3.2	15.0
18	2.8	30	0.8	0.4	2.4	50.0
19	6.5	70	4.6	0.8	5.7	82.6
20	1.6	80	1.3	0.3	1.3	76.9
21	2.8	80	2.2	0.0	2.8	100.0
22	5.3	90	4.8	0.7	4.6	85.4
23	1.6	20	0.3	0.0	1.6	100.0

TABLE 24 (Continued)

Field identification	Ground truth			MSS classification		Error (%)
	Field area (ha)	Proportion of field affected (%)[a]	Actual affected area (ha)	Measured affected area (ha)	Measured unaffected area (ha)	
24	12.6	30	3.8	0.0	12.6	100.0
25	2.0	0	0.0	0.0	2.0	0.0
26	4.0	0	0.0	0.0	4.0	0.0
TOTALS			a = 102.1	m = 77.2		

$$\text{Classification error} = \frac{|a - m|}{a} \times 100 = \frac{|102.1 - 77.2|}{102.1} = 24.4 \text{ percent underclassified}$$

---

[a] Factor P of LxAxP index (Appendix D).

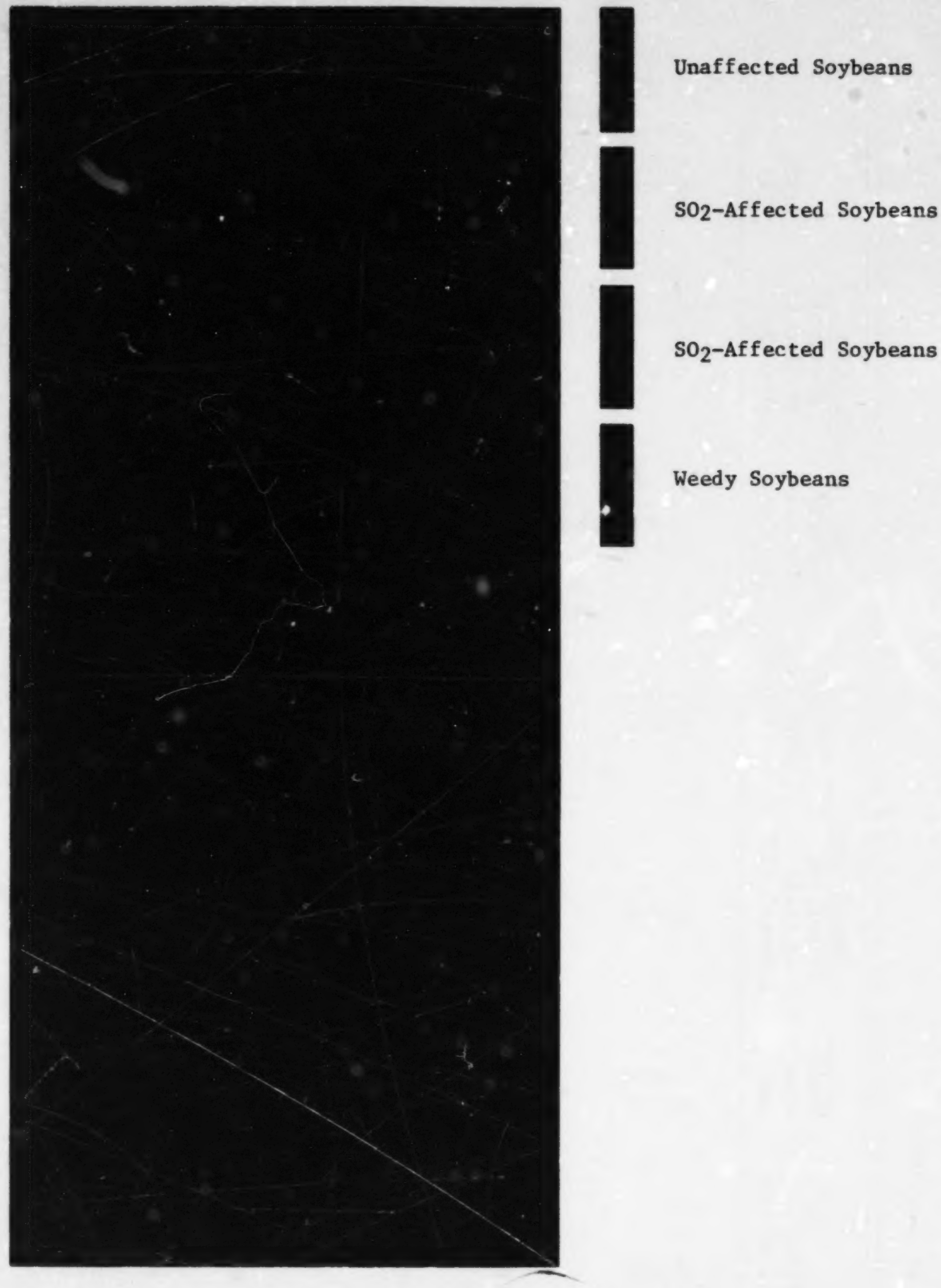
Unaffected Soybeans
SO_2-Affected Soybeans
SO_2-Affected Soybeans
Weedy Soybeans

Figure 56. Pseudosupervised classification of MSS line 3 data near Shawnee Steam Plant. For distribution of SO_2 effects within soybean fields, see Figure 57.

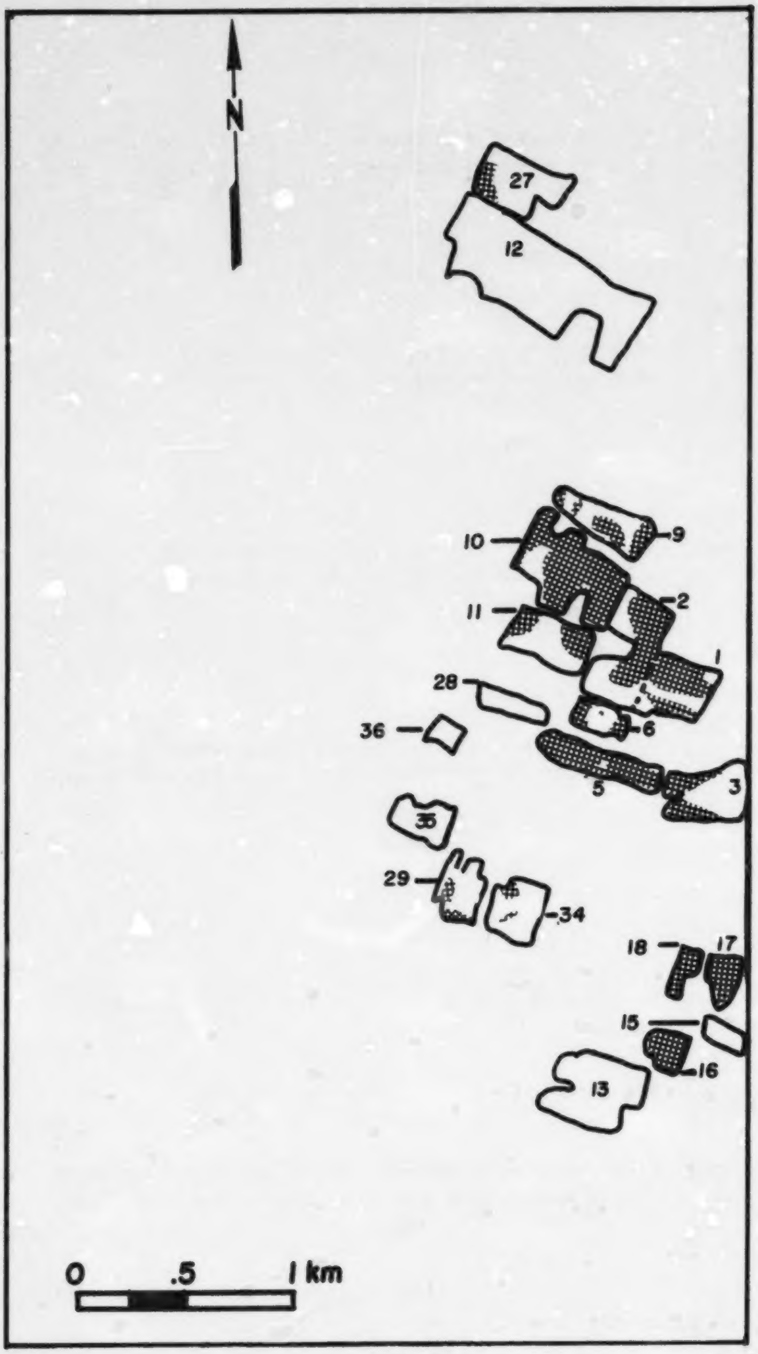
N
27
12
10
9
2
11
1
28
6
36
5
3
35
29
34
18
17
15
16
13
0
.5
1 km

Figure 57. Distribution of SO_2 effects (screened pattern) within dense-canopy soybean fields at Shawnee Steam Plant. Keyed to flight line 3, pseudosupervised classification (Figure 56).

TABLE 25. COMPARISON OF FIELD OBSERVATIONS OF SO_2 EFFECTS ON SOYBEANS AND RESULTS OF MSS PSEUDOSUPERVISED CLASSIFICATION FOR SHAWNEE FLIGHT LINE 3

	Ground truth			MSS classification		
Field identification	Field area (ha)	Proportion of field affected (%)[a]	Actual affected area (ha)	Measured affected area (ha)	Measured unaffected area (ha)	Error (%)
1	11.7	20	2.3	6.8	4.9	195.7
2	17.6	0	0.0	9.2	8.4	-
3	24.3	40	9.7	5.1	19.2	47.4
5	8.5	40	3.4	8.5	0.0	150.0
6	5.3	60	3.2	4.2	1.1	31.2
9	8.1	50	4.1	5.1	3.0	24.4
10	25.1	50	12.6	19.2	5.9	52.4
11	8.9	40	3.6	3.4	5.5	5.6
12	40.5	0	0.0	0.0	40.5	0.0
13	16.2	50	8.1	2.6	13.6	67.9
15	2.0	40	0.8	0.0	2.0	100.0
16	4.5	50	2.3	4.5	0.0	95.7
17	4.9	40	2.0	3.9	1.0	95.0
18	2.8	30	0.8	2.8	0.0	250.0
20	1.6	80	1.3	0.0	1.6	100.0
21	2.8	80	2.2	0.0	2.8	100.0
27	8.1	0	0.0	2.5	5.6	-
28	4.1	40	1.6	0.0	4.1	100.0
29	5.3	80	4.2	1.3	4.0	69.0
34	7.3	90	6.6	1.3	6.0	80.3
35	6.5	40	2.6	0.0	6.5	100.0
36	2.8	70	2.0	1.3	1.5	35.0
TOTALS			a = 73.4	m = 81.7		

$$\text{Classification error} = \frac{|a - m|}{a} \times 100 = \frac{|73.4 - 81.7|}{73.4} = 11.3 \text{ percent overclassified}$$

---

[a] Factor P of LxAxP index (Appendix D).

In summary, the pseudosupervised classification of line 3 data resulted in less than 1 percent overclassification of soybeans without regard to SO_2 effects. The attempt to differentiate SO_2-affected soybeans and unaffected soybeans resulted in an underclassification of about 11 percent.

Summary of Classification Results

The results of the evaluation of the three procedures for classification of the MSS data are summarized in Table 26. The pseudosupervised classifier is superior to the others, but it should be kept in mind that the Colbert test dealt with low-level SO_2 effects, whereas the Shawnee test dealt with a wide range of foliar injury. The supervised classifier may have yielded better results had it been available for analyzing moderately or severely injured soybeans.

Enhancement of Patterns of SO_2 Effects Within Soybean Fields

The classifications previously described dealt only with field-to-field differences in SO_2 effects. Within-field variations should also be considered, but verification of the patterns in the field was not possible because of time constraints on the ground observers at Shawnee. Still, sufficient field data was available to verify the patterns in a few areas.

The I^2S Image Processing System at TVA's Mapping Services Branch in Chattanooga was used to enhance and display selected scenes of MSS data covering the Shawnee area. A density level-slicing procedure was used to display the background in monochrome and the SO_2-effects in orange (Figure 58). The correspondence of patterns is fairly close in some fields (compare Figures 58 and 55). Only those soybean fields that were in the scene and had dense, mature canopies were considered. Table 27

TABLE 26. SUMMARY OF ERRORS USING THREE PROCEDURES FOR DETECTING AND CLASSIFYING SO_2 EFFECTS ON SOYBEANS

Task	Site with very light to light SO_2 effects		Site with moderate to severe SO_2 effects	
	Unsupervised	Supervised	Unsupervised	Pseudosupervised
Separation of soybeans from other land cover	+7.2%	*	+7.6%	+5.1% (line 2); +0.6% (line 3)
Separation of SO_2-affected from unaffected soybeans	+142.0%	*	+101.4%	-24.4% (line 2); +11.3% (line 3)

*Inconclusive results, error not determined.
+ indicates overclassification.
- indicates underclassification.
Zero percent would indicate no error.

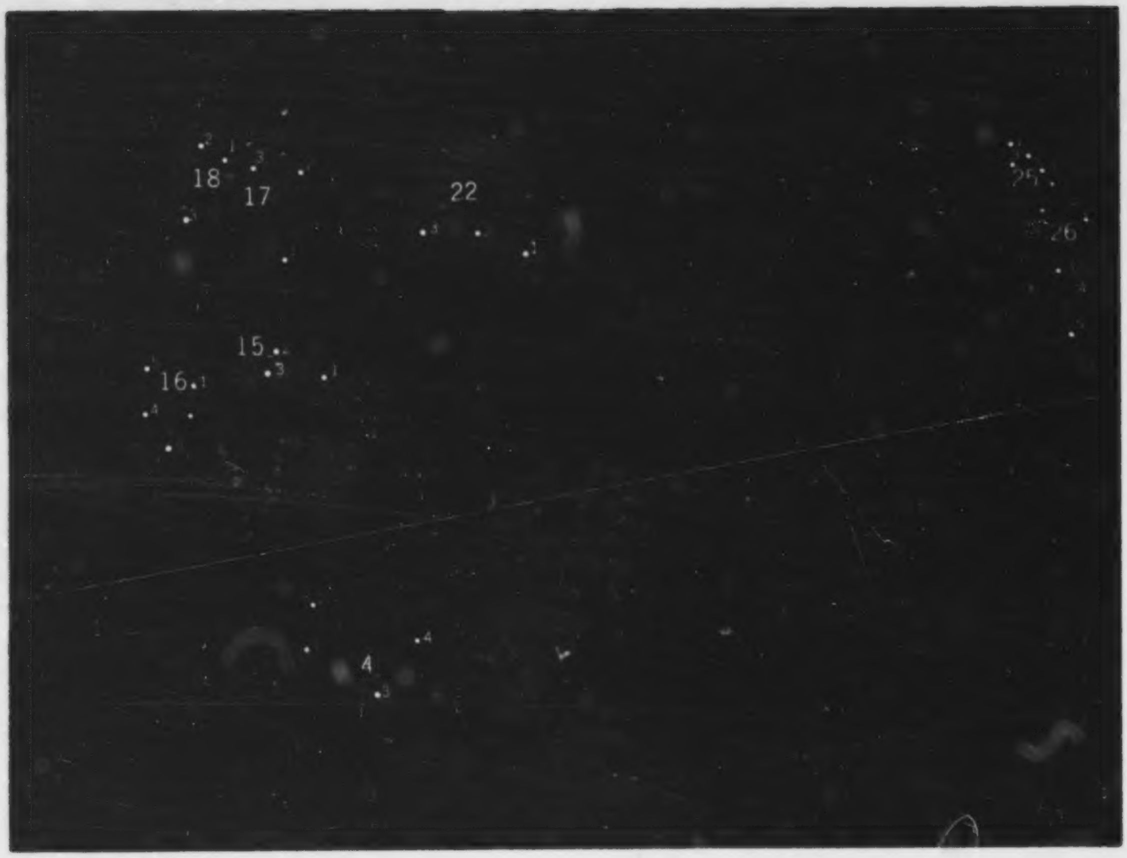

Figure 58. Enhanced MSS image (line 2) of area near Shawnee Steam Plant showing SO_2-affected soybean fields. Dense-canopy soybean fields are numbered, the designations corresponding to those in text and Table 28. Light toned pattern indicates chlorosis. Numbered points are sites of observations (Table 27).

TABLE 27. WITHIN-FIELD SO_2 EFFECTS ON SOYBEANS NEAR SHAWNEE STEAM PLANT IN 1978

Field Designation[a]	Data Point	Chlorosis[b] (%)	Mean Chlorosis (%)[a]	Overall Level of Chlorosis
4	1	3.0	1.8	Very Light
	2	1.2		
	3	1.4		
	4	1.6		
15	1	1.8	4.2	Very Light
	2	4.8		
	3	6.0		
16	1	3.2	6.1	Light
	2	4.0		
	3	6.0		
	4	7.2		
	5	10.0		
17	1	2.4	2.4	Very Light
	2	2.0		
	3	2.7		
18	1	1.2	1.6	Very Light
	2	1.8		
	3	1.8		
22	1	25.0	20.8	Severe
	2	24.0		
	3	13.5		
25	1	0.0	0.0	Unaffected
	2	0.0		
	3	0.0		
	4	0.0		
	5	0.0		
26	1	0.0	0.0	Unaffected
	2	0.0		
	3	0.0		
	4	0.0		
	5	0.0		

[a] Field number keyed to flight line 2 maps presented previously (Figure 55).

[b] LxAxP index (Appendix D).

lists the individual chlorosis observations for each point and a mean chlorosis value for each field. The data are interpreted as follows:

Field 4: Contradictory results. The field is affected and the image shows effects, but the patterns do not coincide.

Field 15: Good correspondence of image pattern with ground truth.

Field 16: Contradictory results. The field is apparently affected, but the image shows it to be unaffected.

Field 17: Fairly good correspondence. The data point showing the highest level of chlorosis falls within the orange area, and the points outside the orange area have lower levels of chlorosis. All of the field is apparently affected to some degree.

Field 18: General correspondence. All of the field was apparently chlorotic and the image shows it as orange.

Field 22: Correspondence uncertain. The image indicates presence of spotty effects, but the ground truth neither confirms nor denies it. Ground truth does indicate some severe effects.

Field 25: Corresponds. No effects in field or on image.

Field 26: Corresponds. No effects in field or on image.

These comparisons indicate that either the field observations need to be made differently or in more detail, or that the enhanced patterns do not represent the effects. It would not generally be practical to increase the density of observations within each field because of time constraints on field surveillance teams. The problem is probably that the scanner cannot detect very light and light chlorosis.

REFERENCES

1. Allen, W. A. and A. J. Richardson. Interaction of Light with a Plant Canopy. J. Opt. Soc. Amer., 58:1023-28, 1968.

2. Gates, D. M., H. J. Keegan, J. C. Schleter, and V. R. Weidner. Spectral Properties of Plants. Appl. Opt., 4(1):11-19, 1965.

3. Knipling, H. B. Physical and Physiological Basis for the Reflectance of Visible and Near-Infrared Radiation from Vegetation. Remote Sensing of Environ., 1:155-159, 1970.

4. Ibid.

5. Ibid.

6. Knipling, H. B. Leaf Reflectance and Image Formation on Color-Infrared Film, in Johnson, P. L., ed., Remote Sensing in Ecology. University of Georgia Press, Athens, p. 20, 1969.

7. Wert, S. L. A System for Using Remote Sensing Techniques to Detect and Evaluate Air Pollution Effects on Forest Stands. Proc., Sixth International Symposium on Remote Sensing of Environ., Ann Arbor, Michigan, p. 174, 1973.

8. Jordan, C. F. Derivation of Leaf Area Index from Quality of Light on the Forest Floor. Ecology 50 (4) 663-666, 1969.

9. Colwell, J. E. Bidirectional Spectral Reflectance of Grass Canopies for Determination of Above Ground Standing Biomass. Ph.D. Thesis, Univ. Michigan, 174 pp., 1973.

10. Colwell, J. E. Vegetation Canopy Reflectance. Remote Sensing of Environ., 3:175-183, 1974.

11. Rouse, J. W., R. H. Haas, J. A. Schell, and D. W. Deering. Monitoring Vegetation Systems in the Great Plains with ERTS. Third ERTS Symposium, NASA SP-351 I, 309-317, 1973.

12. Rouse, J. W., R. H. Haas, J. A. Schell, D. W. Deering, and J. C. Harlan. Monitoring the Vernal Advancement and Retrogradation (Greenwave Effect) of Natural Vegetation. NASA/GSFC Type III final report, Greenbelt, Maine, 371 pp, 1974.

13. Johnson, G. R. Remote Estimation of Herbaceous Biomass. M.S. Thesis, Colorado State Univ., Fort Collins, 120 pp., 1976.

14. Tucker, C. J. Red and Photographic Infrared Linear Combinations for Monitoring Vegetation. NASA/GSFC Tech Memo 79620, Greenbelt, Maryland, p. 26, 1978.

15. Reeves, R. G., A. Anson, and D. Landen, Manual of Remote Sensing, Vol. 2, Am. Soc. Photogramm., Falls Church, Virginia, 1975, p. 1407.

16. Miller, P. R., J. R. Parameter, Jr., B. H. Flick, and C. W. Martinez. Ozone Dosage Response of Ponderosa Pine Seedlings. Air Pollution Control Assoc. Jour., 19:435-438, 1969.

17. Heller, R. C. Large-Scale Color Photo Assessment of Smog-Damaged Pines. Proc., Am. Soc. Photogramm. and Soc. Photog. Sci. and Eng., New York: 85-98, 1969.

18. Wert, S. L. A System for Using Remote Sensing Techniques to Detect and Evaluate Air Pollution Effects on Forest Stands. Proc., Sixth Internat. Symposium on Remote Sensing of Environ., Ann Arbor, Michigan, 1169-78, 1969.

19. Zealer, K. A., R. C. Heller, N. X. Norwick, and M. Wilkes, The Feasibility of Using Color Aerial Photography to Detect and Evaluate Sulphur Dioxide Injury to Timber Stands. U.S. Forest Service, Berkeley, California, November 1971.

20. Heller, R. C., op. cit.

21. Fritz, E. L., and S. P. Pennypacker. Attempts to Use Satellite Data to Detect Vegetative Damage and Alteration Caused by Air and Soil Pollutants. Phytopathology, 65(10):1056-60, 1975.

22. Wiegand, C. L. Reflectance of Vegetation, Soil, and Water. U.S. Dept. Agr., Agr. Res. Serv., Progress Report Type II, E74-10265, Weslaco, Texas, 59 pp., 1974.

23 Murtha, P. A. SO_2 Forest Damage Delineation on High-Altitude Photographs. Canada Centre for Remote Sensing, Proc., First Canadian Symposium on Remote Sensing, Ottawa, Canada, 71-82, 1972.

24. Reeves, R. G., A. Anson, and D. Landen. op cit.

25. Walker, J. E., and D. B. Dahm. Measuring Environmental Stress. Environ. Sci. and Tech., 9(8):714-719, 1975.

26. Schott, J. R., D. W. Gaucher, and J. E. Walker. Aerial Photographic Technique for Measuring Vegetation Stress from Sulfur Dioxide. Calspan Corporation Report YB-5967-M-1. Buffalo, New York, No date, 17 pp.

27. Pell, E., and R. Brock. Spatial and Spectral Mapping of the Response of Vegetation to Air Pollutants (Summary), Center for Air Environment Studies, The Pennsylvania State University, Annual Report, 1974-75.

28. Jackson, R. Detection of Plant Disease Symptoms by Infrared, J. Biol. Phot. Assoc. 32(2):45-58, 1964.

29. Eastman Kodak Company. Applied Infrared Photography, Pub. No. M-28. Rochester, New York, 88 pp., 1972

30. Rohde, W. G. and C. E. Olson, Jr. Detecting Tree Moisture Stress. Photogramm. Eng. 36(6):561-566, 1970.

31. Jacobson, J. S. and A. C. Hill (eds.). Recognition of Air Pollution Injury to Vegetation: A Pictorial Atlas. Air Pollution Control Assoc. Inf. Report. 1, 1970.

32. Talmi, Y. Application of Optical Multichannel Spectrometric Detectors. American Laboratory, p. 79, March 1978.

33. Princeton Applied Research Corporation. OMA-2 Model 1215 Operations Manual. Princeton, New Jersey, 158 pp., 1978.

34. Barr, A. J., J. H. Goodnight, J. P. Soll, and J. T. Helwig. A User's Guide to SAS76. Sparks Press, Raleigh, North Carolina, p. 275, 1976.

35. Ibid.

36. Jones, H. C., N. L. Lacasse, W. S. Liggett, and F. P. Weatherford. Experimental Air Exclusion System for Field Studies of SO_2 Effects on Crop Productivity. EPA-600/7-77-122, 67 pp, 1977.

37. Ibid., p. 1-5.

38. Ibid.

39. Holmes, R. A. Field Spectroscopy, in Remote Sensing with Special Reference to Agriculture and Forestry. Washington, D.C.: National Academy of Sciences, p. 298-308, 1970.

40. Ibid.

41 Murtha, op cit., p. 1149.

42. Ibid.

43. Ibid.

44. Piech, K. R., and J. E.Walker. Interpretation of Soils. Photogramm. Eng., 38(1):87-94, 1974.

45. Lillesand, T. M. An Introduction to Photographic Radiometry and and Spectral Pattern Recognition. State University of New York, Syracuse, 1976, p. 1.

46. Walker, J. E., Personal Communication, 1977.

47. Eastman Kodak Company. Infrared and Ultraviolet Photography. Part 2, Applied Infrared Photography, Tech. Pub. M-27/28-H. Rochester, New York, 1972.

48. Barrett, T. W., and H. M. Benedict. Sulfur Dioxide, in Recognition of Air Pollution Injury to Vegetation. Air Pollution Control Association, Pittsburgh, Pennsylvania, pp. C1-C17, 1970.

49. Jones, H. C., F. P. Weatherford, W. S. Liggett, Jr., and J. R. Cunningham. Effect of Foliar Injury Caused by Exposure to Sulfur Dioxide on Yield of Soybeans - Results of a Large Scale Field Investigation. Division of Environmental Planning, Tennessee Valley Authority, Muscle Shoals, Alabama. Manuscript in preparation.

50. Jones, H. C., J. R. Cunningham, S. B. McLaughlin, N. T. Lee, and S. S. Ray. Investigation of Alleged Air Pollution Effects on Yield of Soybeans in the Vicinity of the Shawnee Steam Plant. E-EB-73-3, Division of Environmental Planning, Tennessee Valley Authority, Muscle Shoals, Alabama, 36 pp., 1973.

51. Daedelus Enterprises, Inc., Daedelus DS-1260 Multispectral Scanner, Ann Arbor, Michigan, undated brochure.

52. Anderson, J. E., and C. E. Tanner. Remote Monitoring of Coal Strip Mine Rehabilitation. U.S. Environmental Protection Agency, Report EPA-600/7-78-149, p. 8, 1978.

53. Tanner, C. E. Unpublished Documentation. Lockheed Electronics Company, Las Vegas, Nevada, 1979.

54. Pooley, J. Unpublished Program Documentation for Unsupervised Sequential Cluster Program (UNSUP), NASA/Earth Resource Laboratory, Slidell, Louisiana, 11 pp. including update, 1976.

55. Su, M. Y. The Composite Sequential Clustering Technique for Analysis of Multispectral Scanner Data. NASA Contractor Report CR-128999. Marshall Space Flight Center, Alabama, 1-1, 1972.

56. Bauer, M. E., J. E. Cipra, P. E. Anuta, and J. B. Etheridge. Identification and Area Estimation of Agricultural Crops by Computer Classification of Landsat MSS Data. Remote Sensing of Environ., 8(1), p. 90, 1979.

57. Pearson, R. Unpublished Program Documentation for Optimum Channel Selection, NASA/Earth Resources Laboratory, Slidell, Louisiana, date unknown.

58. Tanner, C. E., op cit.

59. Pooley, J., op cit.

APPENDIX A

SPECIFICATIONS OF OPTICAL MULTICHANNEL ANALYZER TSR SYSTEM

SPECIFICATIONS OF OPTICAL MULTICHANNEL TSR SYSTEM

SYSTEM DESCRIPTION

The OMA-2 Optical Multichannel Analyzer is a microprocessor-controlled multichannel optical detector and visual display system consisting of the 1215 console, 1216 detector controller, 1252E detector, and components adapted by TVA including a telescope, a fiber-optic cable and faceplate, and an x-y recorder.

Component	Specifications
Console, Model 1215	
Front Panel	84-key keyboard, 41-cm diagonal display, flexible disc drive (IBM compatible format).
Rear panel	Analog recorder output.
Memory system	Monostore XI/Planar LSI-11 16K x 16 memory assembly by Monolithic Systems Corporation; signal interface through DEC LSI-11 I/O bus.
RAM data storage	4K single precision, 2K double precision.
Disc storage	Operating system plus 100 spectral curves of 500 double precision points each.
Arithmetic functions	+, -, ÷, natural log, and decimal log; constants, powers, and roots on full curves; arithmetic functions are formatted in algebraic notation with parenthesis capability for seven reference curves and recursive operation up to disc capacity.
Power input	115/230 V ± 10 percent, 50/60 Hz, 450 watts.
Dimensions	44.86 cm W x 72.72 cm D x 39.27 cm H.
Unit weight	50 kg
Spectrometer, Model 1225 (Jobin Yvon M25 grating monochromator)	Focal length 0.25 m, aperture f/3, holographic grating, 152.65 grooves/mm, blazed at 2 μm, input slits, 2 available, 0.25 mm or 0.90 mm wide.

Component	Specifications
Detector, Model 1252E (IR-enhanced)	Silicon-vidicon target, sensitivity 2400 photons/count at 600 nm, background noise 1.5 counts rms max., full-scale 16,383 counts/channel/frame, dynamic range 1 x 10^4 min., linearity as a function of intensity ± 1 percent, scanned area 12.5 x 12.5 mm, useful spectral range 350 to 1100 nm (scan width restricted to 337 nm band)
Detector controller, Model 1216	16-bit computer peripheral, frame scan time 10 to 70 ms, channel time 20 to 140 μs, number of channels scanned 2 to 512/track, number of tracks 1 to 256, power input 115/230 V ± 10 percent, 50/60 Hz, 14 watts, dimensions 44.2 cm W x 46.7 cm D x 13 cm H, unit weight 15.5 kg.
Fiber optic interface, Model 1225Q	152.4 cm L x 0.1 mm D (input slit, output circle), quartz fiber optics bundles, adaptor faceplate connects cable to polychromator.
X-Y recorder	Hewlett-Packard Model 2D-2
Telescope	Gamma Scientific, Inc., Model 2020-31 f/2.8, focal length 190 mm, selectable angles of view 3°, 1°, 20', 6'.
Calibration lamps	Pen-Ray Krypton 760-nm line; Pen-Ray low-pressure mercury vapor 436-, 546-, 579-nm lines.

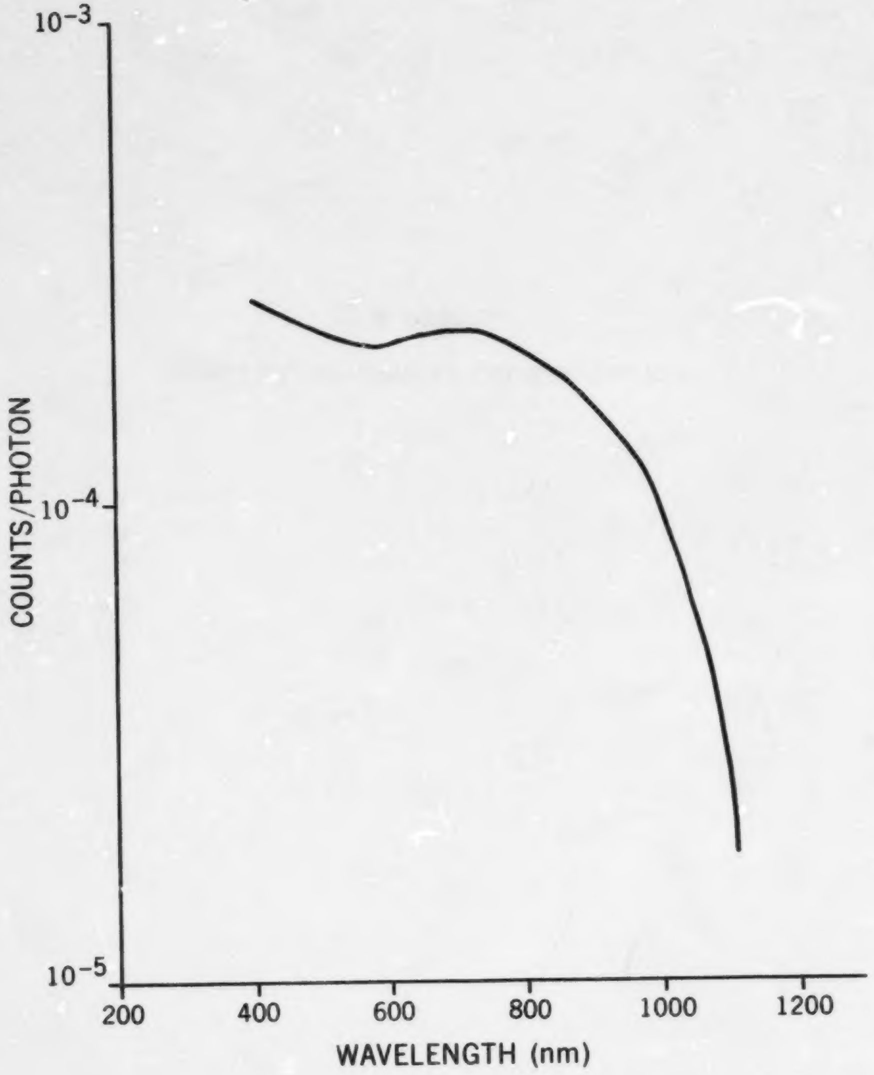

Figure A-1. Typical spectral response of Model 1252E infrared-enhanced silicon-vidicon detector (data from Princeton Applied Research Corporation).

APPENDIX B

SPECTRAL CURVES, LABORATORY EXPERIMENT

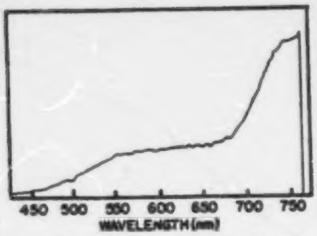

SPECTRUM Soybeans
RECORD 14/1
SO_2 CONC 15720
μg/m^3 .50 h
FOLIAR INJURY:
TOTAL 30 %
CHLOROSIS 10 %
NECROSIS 20 %
Y-AXIS COUNTS AT 767nm 7611

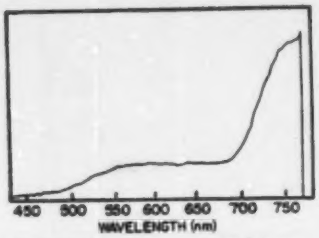

SPECTRUM Soybeans
RECORD 14/2
SO_2 CONC 15720
μg/m^3 .50 h
FOLIAR INJURY:
TOTAL 15 %
CHLOROSIS 10 %
NECROSIS 5 %
Y-AXIS COUNTS AT 767nm 5405

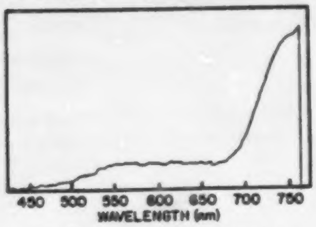

SPECTRUM Soybeans
RECORD 14/3
SO_2 CONC 15720
μg/m^3 .50 h
FOLIAR INJURY:
TOTAL 5 %
CHLOROSIS 5 %
NECROSIS %
Y-AXIS COUNTS AT 767nm 4700

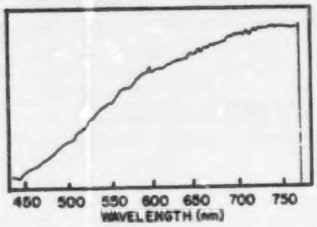

SPECTRUM Gray Panel
RECORD 14/4
SO_2 CONC
μg/m^3 h
FOLIAR INJURY:
TOTAL %
CHLOROSIS %
NECROSIS %
Y-AXIS COUNTS AT 767nm 63676

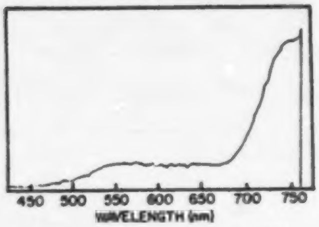

SPECTRUM Soybeans
RECORD 14/5
SO_2 CONC 15720
μg/m^3 .50 h
FOLIAR INJURY:
TOTAL 0 %
CHLOROSIS %
NECROSIS %
Y-AXIS COUNTS AT 767nm 282133

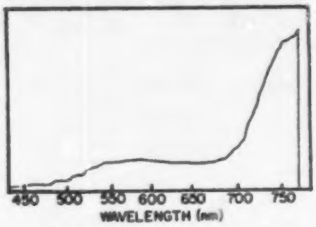

SPECTRUM Soybeans
RECORD 14/6
SO_2 CONC 15720
μg/m^3 .50 h
FOLIAR INJURY:
TOTAL 0 %
CHLOROSIS %
NECROSIS %
Y-AXIS COUNTS AT 767nm 285230

Figure B-1. Individual Spectral Curves - Soybeans

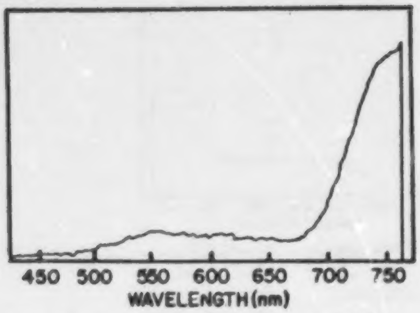

SPECTRUM Soybeans RECORD 14/7
SO_2 CONC 15720 μg/m^3 .50 h
FOLIAR INJURY: TOTAL 15 %
CHLOROSIS 10 %
NECROSIS 5 %
Y-AXIS COUNTS AT 767nm 260787

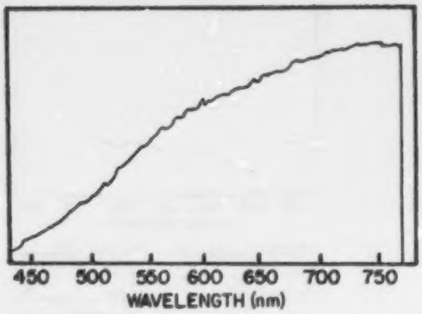

SPECTRUM Gray panel RECORD 14/8
SO_2 CONC μg/m^3 h
FOLIAR INJURY: TOTAL %
CHLOROSIS %
NECROSIS %
Y-AXIS COUNTS AT 767nm 64229

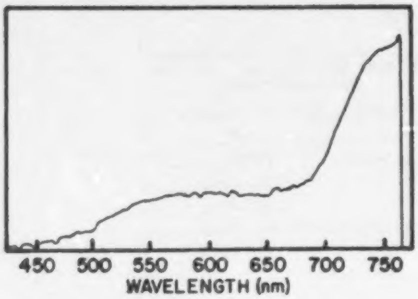

SPECTRUM Soybeans RECORD 14/9
SO_2 CONC 15720 μg/m^3 .50 h
FOLIAR INJURY: TOTAL 5 %
CHLOROSIS 5 %
NECROSIS %
Y-AXIS COUNTS AT 767nm 307699

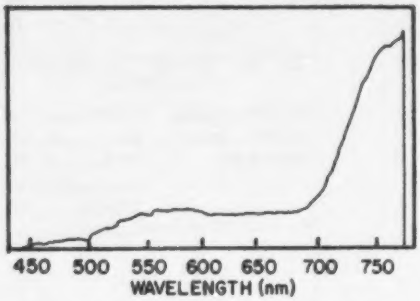

SPECTRUM Soybeans RECORD 14/10
SO_2 CONC 15720 μg/m^3 .50 h
FOLIAR INJURY: TOTAL 0 %
CHLOROSIS %
NECROSIS %
Y-AXIS COUNTS AT 767nm 290475

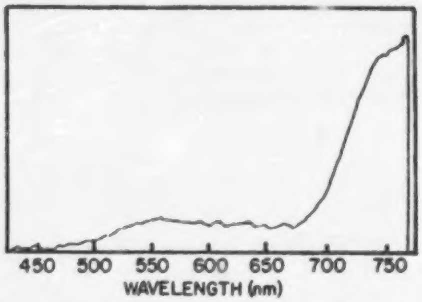

SPECTRUM Soybeans RECORD 14/11
SO_2 CONC 15720 μg/m^3 .50 h
FOLIAR INJURY: TOTAL 0 %
CHLOROSIS %
NECROSIS %
Y-AXIS COUNTS AT 767nm 272187

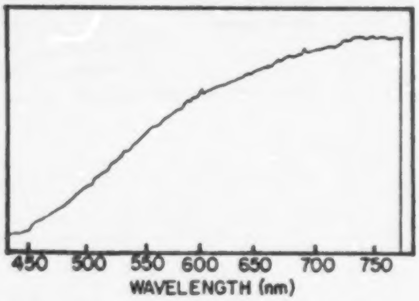

SPECTRUM Gray Panel RECORD 14/12
SO_2 CONC μg/m^3 h
FOLIAR INJURY: TOTAL %
CHLOROSIS %
NECROSIS %
Y-AXIS COUNTS AT 767nm 63786

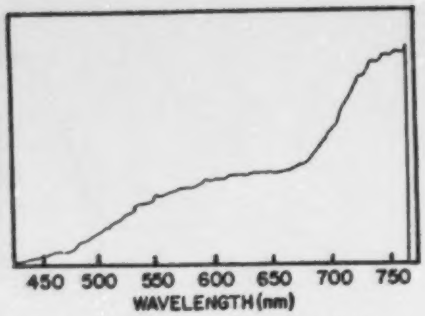

SPECTRUM Soybeans
RECORD 14/13
SO_2 CONC 15720
μg/m^3 .50 h
FOLIAR INJURY:
TOTAL 30 %
CHLOROSIS 30 %
NECROSIS 10 %
Y-AXIS COUNTS AT 767nm 262284

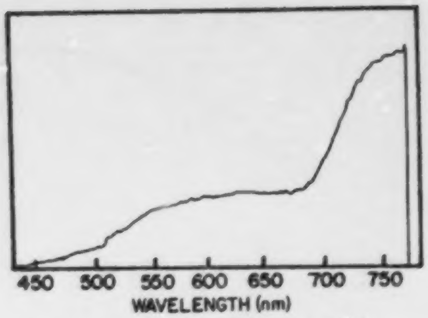

SPECTRUM Soybeans
RECORD 14/14
SO_2 CONC 15720
μg/m^3 .50 h
FOLIAR INJURY:
TOTAL 50 %
CHLOROSIS 40 %
NECROSIS 10 %
Y-AXIS COUNTS AT 767nm 227891

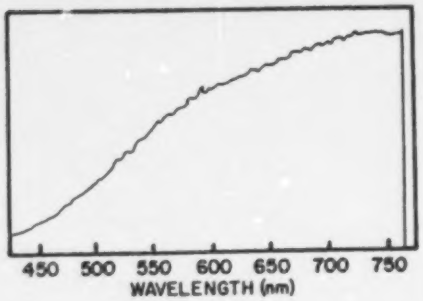

SPECTRUM Grey Panel
RECORD 14/16
SO_2 CONC
μg/m^3 h
FOLIAR INJURY:
TOTAL %
CHLOROSIS %
NECROSIS %
Y-AXIS COUNTS AT 767nm 64035

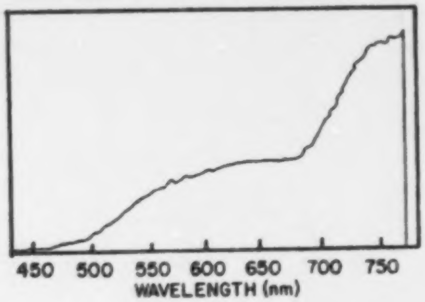

SPECTRUM Soybeans
RECORD 14/17
SO_2 CONC 15720
μg/m^3 .50 h
FOLIAR INJURY:
TOTAL 90 %
CHLOROSIS 60 %
NECROSIS 30 %
Y-AXIS COUNTS AT 767nm 273650

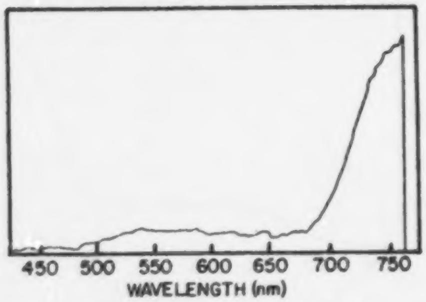

SPECTRUM Soybeans
RECORD 14/18
SO_2 CONC 15720
μg/m^3 .50 h
FOLIAR INJURY:
TOTAL 40 %
CHLOROSIS 40 %
NECROSIS %
Y-AXIS COUNTS AT 767nm 281540

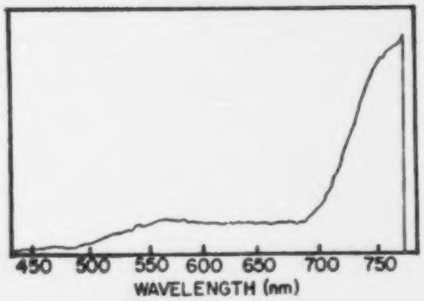

SPECTRUM Soybeans
RECORD 14/19
SO_2 CONC 15720
μg/m^3 .50 h
FOLIAR INJURY:
TOTAL 5 %
CHLOROSIS 5 %
NECROSIS %
Y-AXIS COUNTS AT 767nm 260811

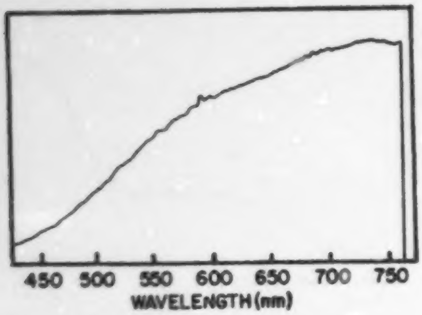

SPECTRUM Gray panel
RECORD 14/20
SO$_2$ CONC ____
μg/m^3 ____ h
FOLIAR INJURY:
TOTAL ____ %
CHLOROSIS ____ %
NECROSIS ____ %
Y-AXIS COUNTS AT 767nm 63929

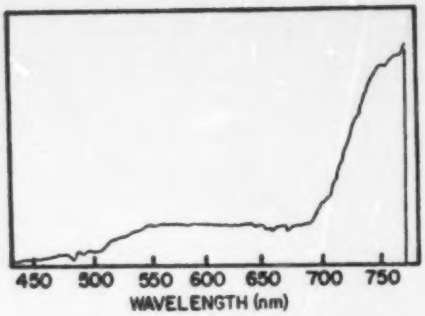

SPECTRUM Soybeans
RECORD 14/21
SO$_2$ CONC 15720
μg/m^3 .50 h
FOLIAR INJURY:
TOTAL 10 %
CHLOROSIS 10 %
NECROSIS ____ %
Y-AXIS COUNTS AT 767nm 280671

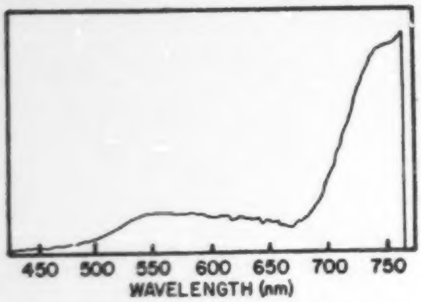

SPECTRUM Soybeans
RECORD 14/22
SO$_2$ CONC 15720
μg/m^3 .50 h
FOLIAR INJURY
TOTAL 90 %
CHLOROSIS 80 %
NECROSIS 10 %
Y-AXIS COUNTS AT 767nm 273364

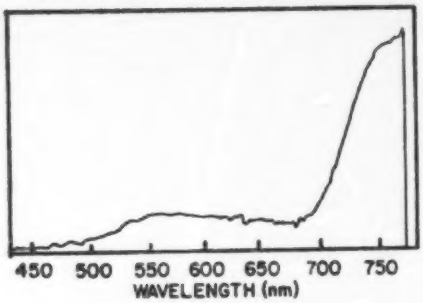

SPECTRUM Soybeans
RECORD 14/23
SO$_2$ CONC 15720
μg/m^3 .50 h
FOLIAR INJURY:
TOTAL 60 %
CHLOROSIS 50 %
NECROSIS 10 %
Y-AXIS COUNTS AT 767nm 265504

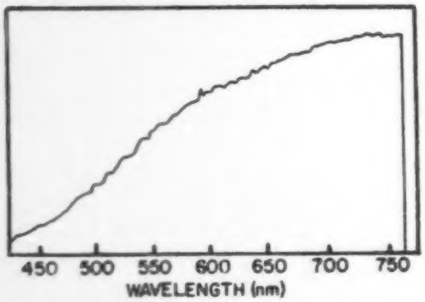

SPECTRUM Grey Panel
RECORD 14/24
SO$_2$ CONC ____
μg/m^3 ____ h
FOLIAR INJURY:
TOTAL ____ %
CHLOROSIS ____ %
NECROSIS ____ %
Y-AXIS COUNTS AT 767nm 64474

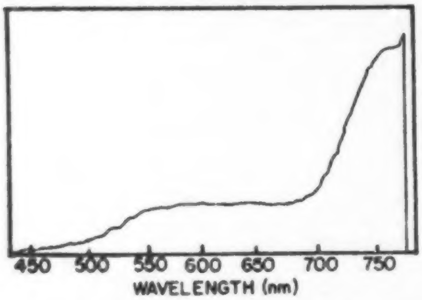

SPECTRUM Soybeans
RECORD 14/25
SO$_2$ CONC 15720
μg/m^3 .50 h
FOLIAR INJURY:
TOTAL 10 %
CHLOROSIS 10 %
NECROSIS ____ %
Y-AXIS COUNTS AT 767nm 286048

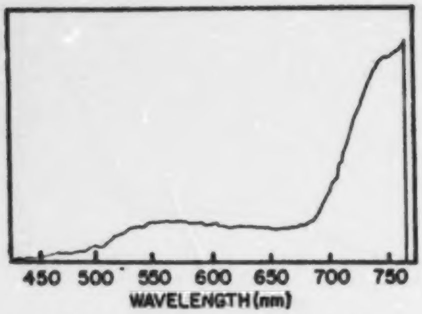

SPECTRUM Soybeans RECORD 14/26
SO_2 CONC 15720 $\mu g/m^3$ .50 h
FOLIAR INJURY: TOTAL 5 %
CHLOROSIS 5 %
NECROSIS ___ %
Y-AXIS COUNTS AT 767nm 278203

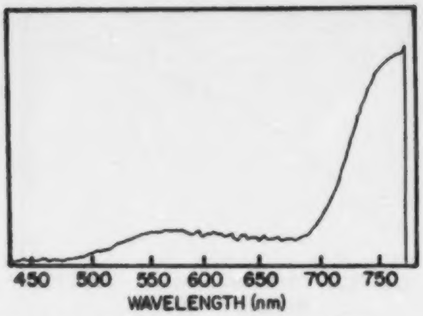

SPECTRUM Soybeans RECORD 14/27
SO_2 CONC 15720 $\mu g/m^3$ .50 h
FOLIAR INJURY: TOTAL 10 %
CHLOROSIS 10 %
NECROSIS ___ %
Y-AXIS COUNTS AT 767nm 264688

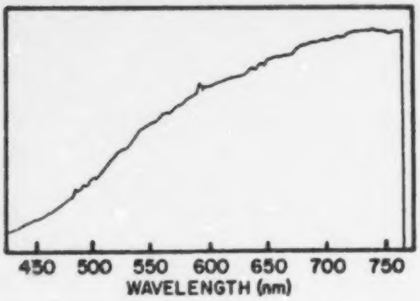

SPECTRUM Gray Panel RECORD 14/28
SO_2 CONC ___ $\mu g/m^3$ ___ h
FOLIAR INJURY: TOTAL ___ %
CHLOROSIS ___ %
NECROSIS ___ %
Y-AXIS COUNTS AT 767nm 64321

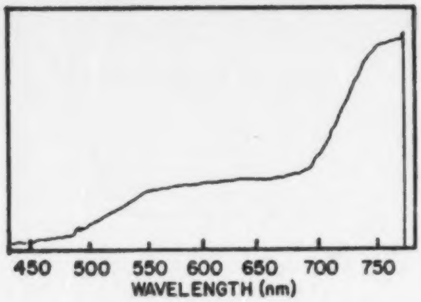

SPECTRUM Soybeans RECORD 14/29
SO_2 CONC 15720 $\mu g/m^3$ .67 h
FOLIAR INJURY: TOTAL 5 %
CHLOROSIS 5 %
NECROSIS ___ %
Y-AXIS COUNTS AT 767nm 283268

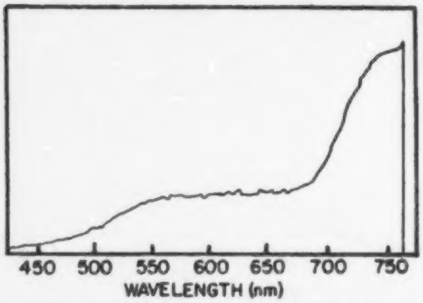

SPECTRUM Soybeans RECORD 14/30
SO_2 CONC 15720 $\mu g/m^3$ .67 h
FOLIAR INJURY: TOTAL 5 %
CHLOROSIS 3 %
NECROSIS ___ %
Y-AXIS COUNTS AT 767nm 316395

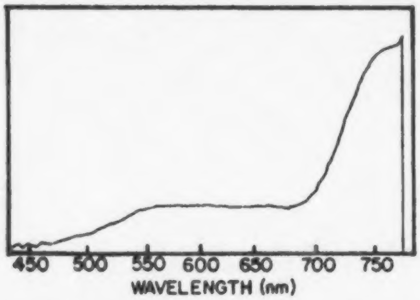

SPECTRUM Soybeans RECORD 14/31
SO_2 CONC 15720 $\mu g/m^3$ .67 h
FOLIAR INJURY: TOTAL 5 %
CHLOROSIS 5 %
NECROSIS ___ %
Y-AXIS COUNTS AT 767nm 295140

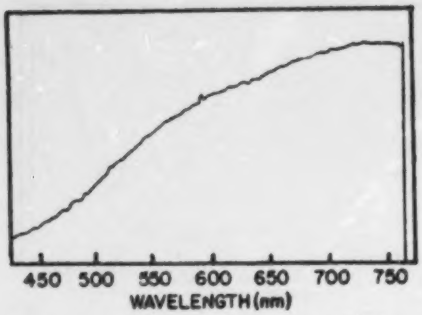

SPECTRUM Gray panel RECORD 14/32

SO2 CONC ______ µg/m³ ______ h

FOLIAR INJURY: TOTAL ______ %

CHLOROSIS ______ %

NECROSIS ______ %

Y-AXIS COUNTS AT 767nm 65916

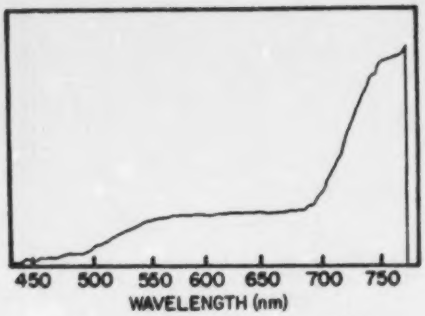

SPECTRUM Soybeans RECORD 14/33

SO2 CONC 10480 µg/m³ .75 h

FOLIAR INJURY: TOTAL 10 %

CHLOROSIS 10 %

NECROSIS ______ %

Y-AXIS COUNTS AT 767nm 293849

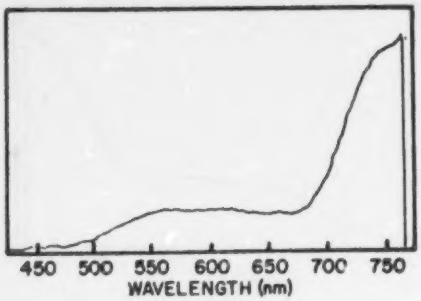

SPECTRUM Soybeans RECORD 14/34

SO2 CONC 10480 µg/m³ .75 h

FOLIAR INJURY: TOTAL 30 %

CHLOROSIS 50 %

NECROSIS ______ %

Y-AXIS COUNTS AT 767nm 276430

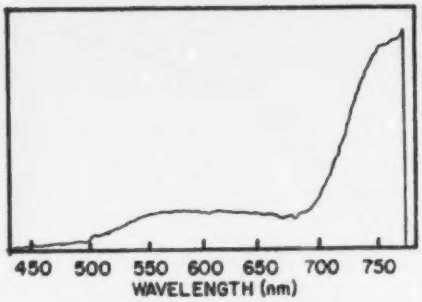

SPECTRUM Soybeans RECORD 14/35

SO2 CONC 10480 µg/m³ .75 h

FOLIAR INJURY: TOTAL 15 %

CHLOROSIS 15 %

NECROSIS ______ %

Y-AXIS COUNTS AT 767nm 269226

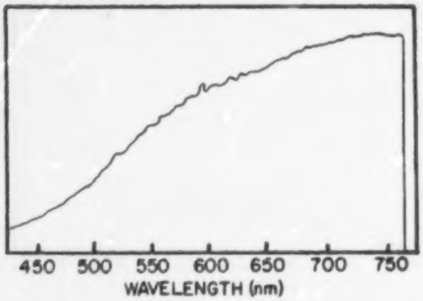

SPECTRUM Gray panel RECORD 14/36

SO2 CONC ______ µg/m³ ______ h

FOLIAR INJURY: TOTAL ______ %

CHLOROSIS ______ %

NECROSIS ______ %

Y-AXIS COUNTS AT 767nm 65747

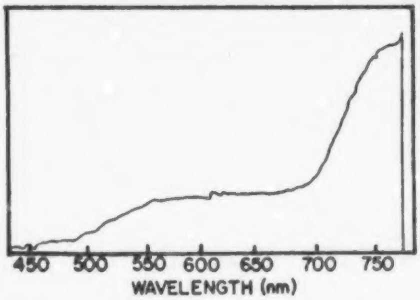

SPECTRUM Soybeans RECORD 14/37

SO2 CONC 10480 µg/m³ .75 h

FOLIAR INJURY: TOTAL 20 %

CHLOROSIS 20 %

NECROSIS ______ %

Y-AXIS COUNTS AT 767nm 282002

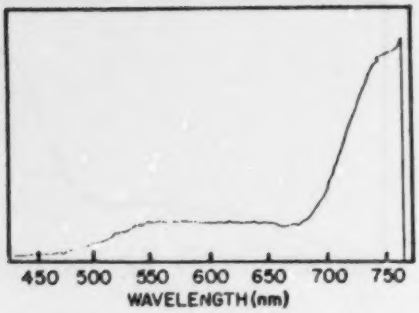

SPECTRUM Soybeans RECORD 14/38

SO_2 CONC 10480 µg/m³ .75 h

FOLIAR INJURY: TOTAL 20 %

CHLOROSIS 20 %

NECROSIS ____ %

Y-AXIS COUNTS AT 767nm 294816

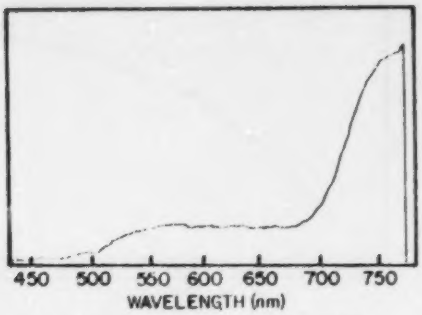

SPECTRUM Soybeans RECORD 14/39

SO_2 CONC 10480 µg/m³ .75 h

FOLIAR INJURY: TOTAL 30 %

CHLOROSIS 30 %

NECROSIS ____ %

Y-AXIS COUNTS AT 767nm 274153

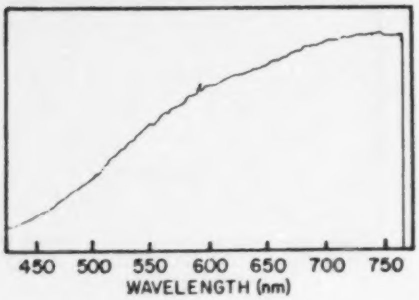

SPECTRUM Gray panel RECORD 14/40

SO_2 CONC ____ µg/m³ ____ h

FOLIAR INJURY: TOTAL ____ %

CHLOROSIS ____ %

NECROSIS ____ %

Y-AXIS COUNTS AT 767nm 65726

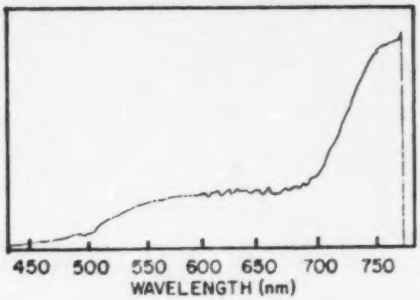

SPECTRUM Soybeans RECORD 14/41

SO_2 CONC 10480 µg/m³ .75 h

FOLIAR INJURY: TOTAL 0 %

CHLOROSIS ____ %

NECROSIS ____ %

Y-AXIS COUNTS AT 767nm 275946

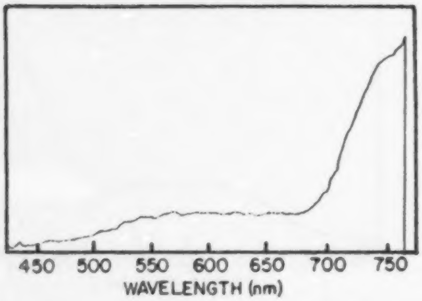

SPECTRUM Soybeans RECORD 14/42

SO_2 CONC 10480 µg/m³ .75 h

FOLIAR INJURY: TOTAL 5 %

CHLOROSIS 5 %

NECROSIS ____ %

Y-AXIS COUNTS AT 767nm 314010

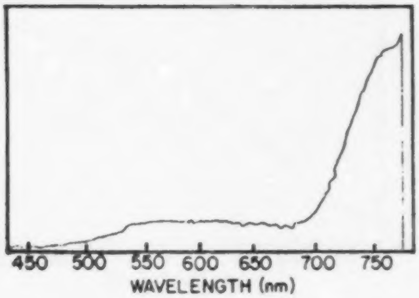

SPECTRUM Soybeans RECORD 14/43

SO_2 CONC 10480 µg/m³ .75 h

FOLIAR INJURY: TOTAL 15 %

CHLOROSIS 15 %

NECROSIS ____ %

Y-AXIS COUNTS AT 767nm 269447

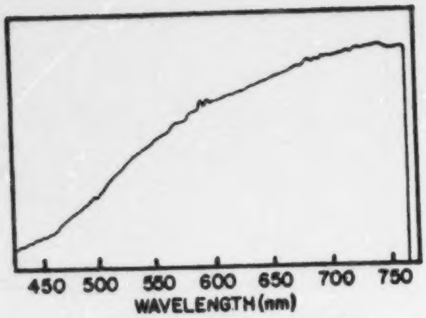

SPECTRUM *Gray panel*
RECORD *14/44*
SO2 CONC ________
μg/m3 ________ h
FOLIAR INJURY:
TOTAL ________ %
CHLOROSIS ____ %
NECROSIS ____ %
Y-AXIS COUNTS AT 767nm *65652*

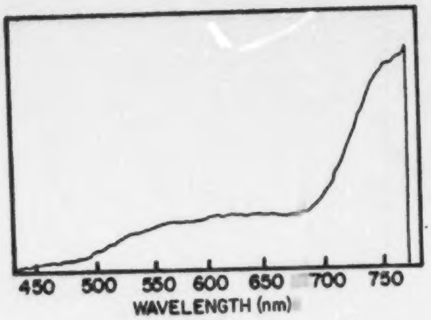

SPECTRUM Soybeans
RECORD *14/45*
SO2 CONC *10480*
μg/m3 *.75* h
FOLIAR INJURY:
TOTAL *40* %
CHLOROSIS *30* %
NECROSIS *10* %
Y-AXIS COUNTS AT 767nm *283309*

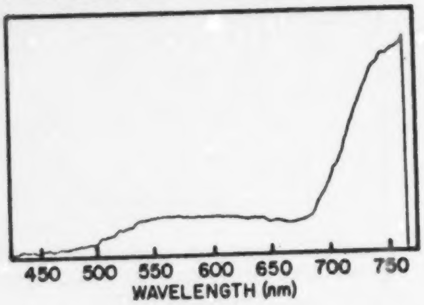

SPECTRUM Soybeans
RECORD *14/46*
SO2 CONC *10480*
μg/m3 *.75* h
FOLIAR INJURY:
TOTAL *65* %
CHLOROSIS *60* %
NECROSIS *5* %
Y-AXIS COUNTS AT 767nm *270538*

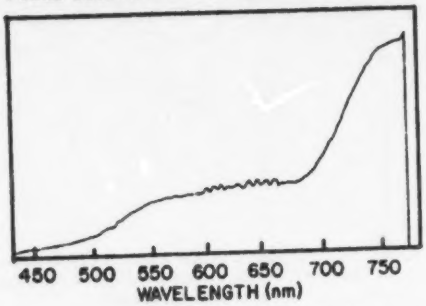

SPECTRUM Soybeans
RECORD *14/47*
SO2 CONC *10480*
μg/m3 *.75* h
FOLIAR INJURY:
TOTAL *85* %
CHLOROSIS *5* %
NECROSIS *80* %
Y-AXIS COUNTS AT 767nm *277695*

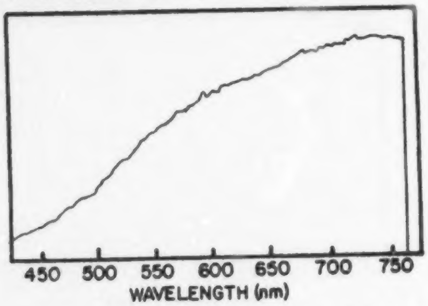

SPECTRUM *Gray panel*
RECORD *14/48*
SO2 CONC ________
μg/m3 ________ h
FOLIAR INJURY:
TOTAL ________ %
CHLOROSIS ____ %
NECROSIS ____ %
Y-AXIS COUNTS AT 767nm *65644*

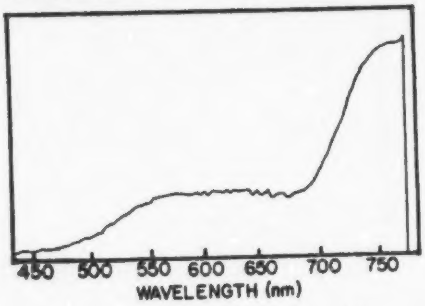

SPECTRUM Soybeans
RECORD *14/49*
SO2 CONC *10480*
μg/m3 *.75* h
FOLIAR INJURY:
TOTAL *90* %
CHLOROSIS *80* %
NECROSIS ____ %
Y-AXIS COUNTS AT 767nm *259301*

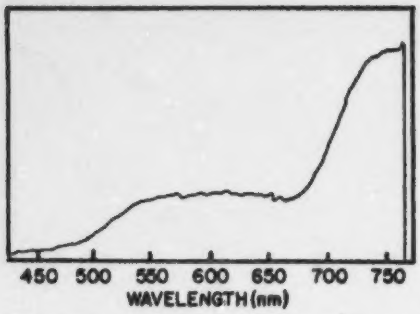

SPECTRUM Soybeans
RECORD 14/50
SO_2 CONC 10480
$\mu g/m^3$ .75 h
FOLIAR INJURY:
TOTAL 70 %
CHLOROSIS 70 %
NECROSIS ___ %
Y-AXIS COUNTS AT 767nm 294594

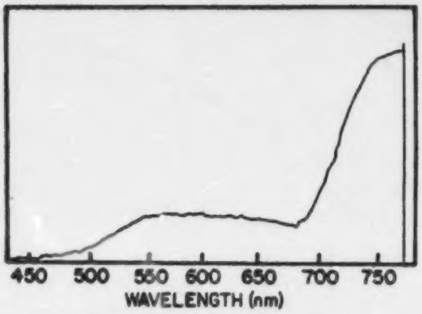

SPECTRUM Soybeans
RECORD 14/51
SO_2 CONC 10480
$\mu g/m^3$ .75 h
FOLIAR INJURY:
TOTAL 70 %
CHLOROSIS 70 %
NECROSIS ___ %
Y-AXIS COUNTS AT 767nm 222435

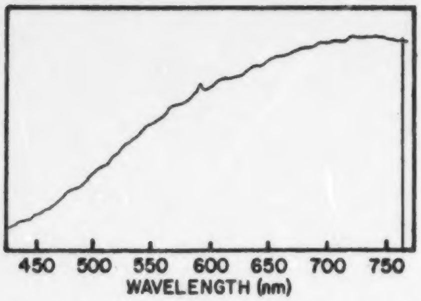

SPECTRUM Gray Panel
RECORD 14/52
SO_2 CONC ___
$\mu g/m^3$ ___ h
FOLIAR INJURY:
TOTAL ___ %
CHLOROSIS ___ %
NECROSIS ___ %
Y-AXIS COUNTS AT 767nm 65583

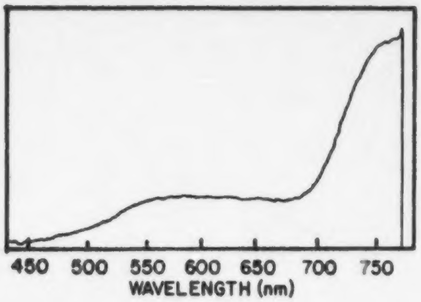

SPECTRUM Soybeans
RECORD 14/53
SO_2 CONC 10480
$\mu g/m^3$ .75 h
FOLIAR INJURY:
TOTAL 60 %
CHLOROSIS 60 %
NECROSIS ___ %
Y-AXIS COUNTS AT 767nm 263316

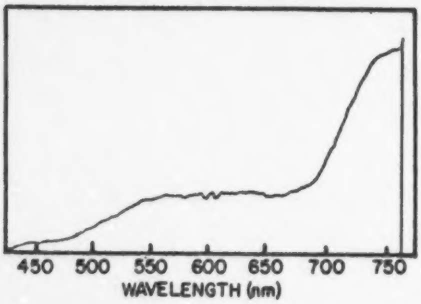

SPECTRUM Soybeans
RECORD 14/54
SO_2 CONC 10480
$\mu g/m^3$ .75 h
FOLIAR INJURY:
TOTAL 10 %
CHLOROSIS 10 %
NECROSIS ___ %
Y-AXIS COUNTS AT 767nm 311764

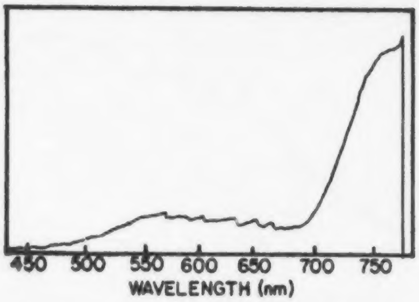

SPECTRUM Soybeans
RECORD 14/55
SO_2 CONC 10480
$\mu g/m^3$ .75 h
FOLIAR INJURY:
TOTAL 30 %
CHLOROSIS 30 %
NECROSIS ___ %
Y-AXIS COUNTS AT 767nm 284581

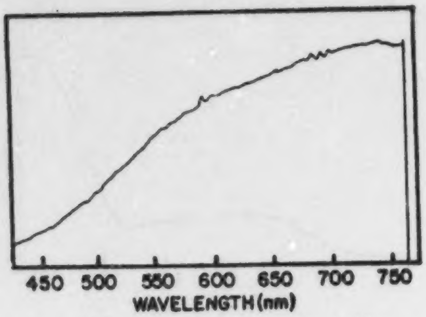

SPECTRUM Gray panel
RECORD 14/56
SO_2 CONC
μg/m^3 h
FOLIAR INJURY:
TOTAL %
CHLOROSIS %
NECROSIS %
Y-AXIS COUNTS AT 767nm 65462

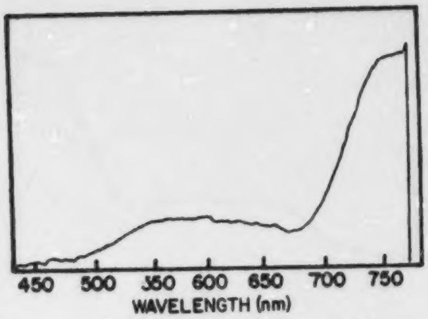

SPECTRUM Soybeans
RECORD 14/57
SO_2 CONC 10480
μg/m^3 .75 h
FOLIAR INJURY:
TOTAL 75 %
CHLOROSIS 70 %
NECROSIS 5 %
Y-AXIS COUNTS AT 767nm 274619

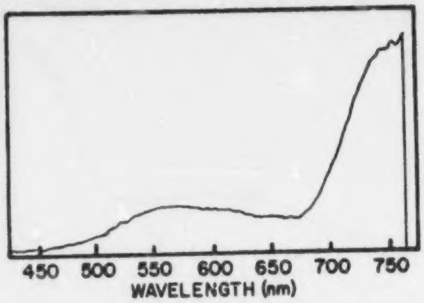

SPECTRUM Soybeans
RECORD 14/58
SO_2 CONC 10480
μg/m^3 .75 h
FOLIAR INJURY:
TOTAL 60 %
CHLOROSIS 60 %
NECROSIS %
Y-AXIS COUNTS AT 767nm 286871

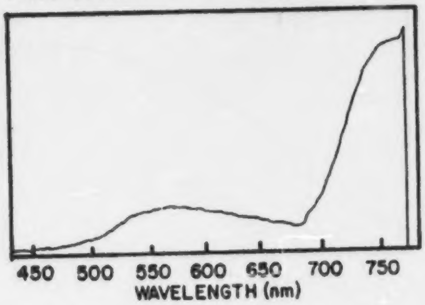

SPECTRUM Soybeans
RECORD 14/59
SO_2 CONC 10480
μg/m^3 .75 h
FOLIAR INJURY:
TOTAL 70 %
CHLOROSIS 70 %
NECROSIS %
Y-AXIS COUNTS AT 767nm 284571

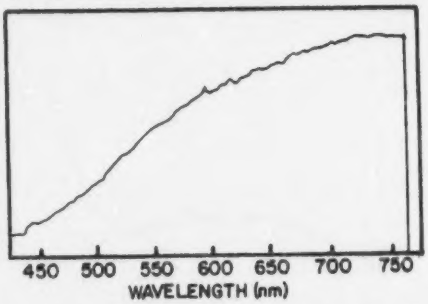

SPECTRUM Gray panel
RECORD 14/60
SO_2 CONC
μg/m^3 h
FOLIAR INJURY:
TOTAL %
CHLOROSIS %
NECROSIS %
Y-AXIS COUNTS AT 767nm 65786

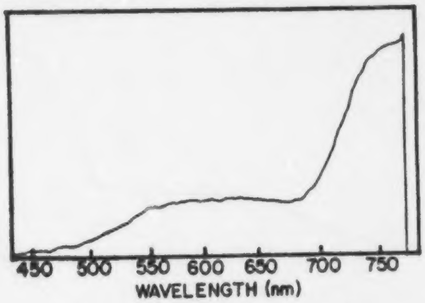

SPECTRUM Soybeans
RECORD 14/61
SO_2 CONC 10480
μg/m^3 .75 h
FOLIAR INJURY:
TOTAL 10 %
CHLOROSIS 10 %
NECROSIS %
Y-AXIS COUNTS AT 767nm 253270

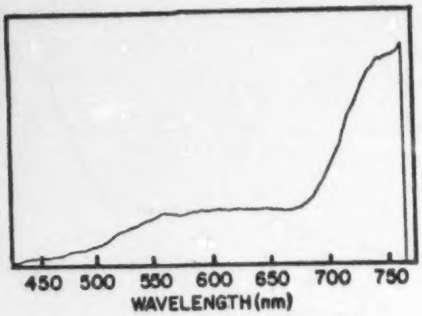

SPECTRUM Soybeans RECORD 14/62
SO_2 CONC 10480 $\mu g/m^3$ .75 h
FOLIAR INJURY: TOTAL 10 %
CHLOROSIS 10 %
NECROSIS ____ %
Y-AXIS COUNTS AT 767nm 289198

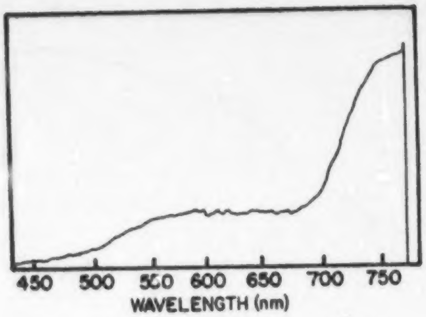

SPECTRUM Soybeans RECORD 14/63
SO_2 CONC 10480 $\mu g/m^3$ .75 h
FOLIAR INJURY: TOTAL 60 %
CHLOROSIS 60 %
NECROSIS ____ %
Y-AXIS COUNTS AT 767nm 283754

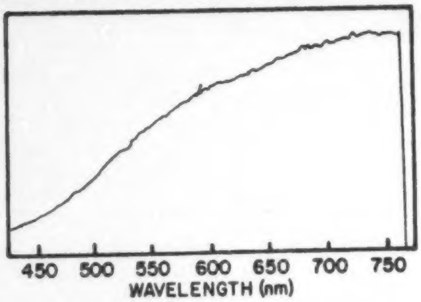

SPECTRUM Gray Panel RECORD 14/64
SO_2 CONC ____ $\mu g/m^3$ ____ h
FOLIAR INJURY: TOTAL ____ %
CHLOROSIS ____ %
NECROSIS ____ %
Y-AXIS COUNTS AT 767nm 65819

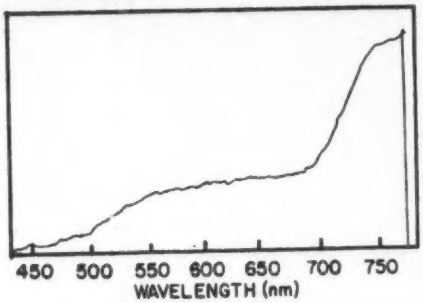

SPECTRUM Soybeans RECORD 14/65
SO_2 CONC 10480 $\mu g/m^3$ .75 h
FOLIAR INJURY: TOTAL 20 %
CHLOROSIS 15 %
NECROSIS 5 %
Y-AXIS COUNTS AT 767nm 270535

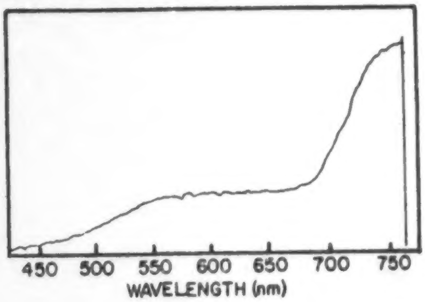

SPECTRUM Soybeans RECORD 14/66
SO_2 CONC 10480 $\mu g/m^3$ .75 h
FOLIAR INJURY: TOTAL 70 %
CHLOROSIS 70 %
NECROSIS ____ %
Y-AXIS COUNTS AT 767nm 296929

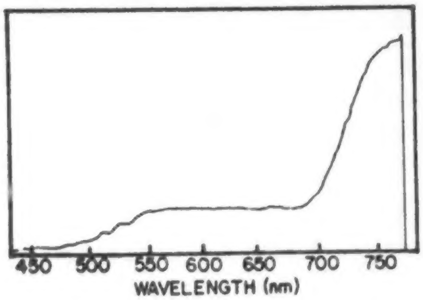

SPECTRUM Soybeans RECORD 14/67
SO_2 CONC 10480 $\mu g/m^3$ .75 h
FOLIAR INJURY: TOTAL 80 %
CHLOROSIS 80 %
NECROSIS ____ %
Y-AXIS COUNTS AT 767nm 289564

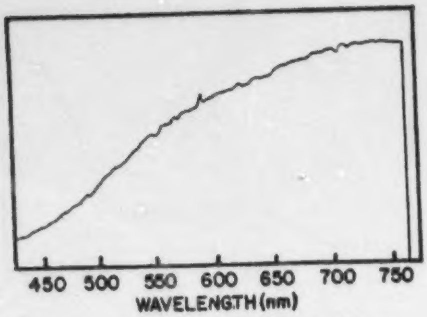

SPECTRUM Gray panel RECORD 14/68

SO_2 CONC ______ $\mu g/m^3$ ______ h

FOLIAR INJURY: TOTAL ______ %

CHLOROSIS ______ %

NECROSIS ______ %

Y-AXIS COUNTS AT 767nm 66019

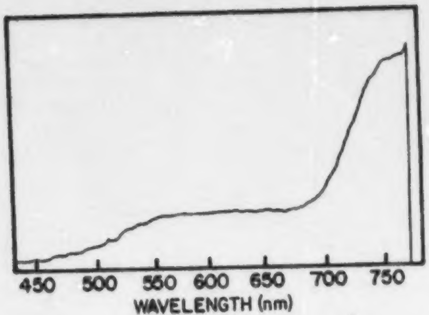

SPECTRUM Soybeans RECORD 14/69

SO_2 CONC 10480 $\mu g/m^3$ .75 h

FOLIAR INJURY: TOTAL 45 %

CHLOROSIS 40 %

NECROSIS 5 %

Y-AXIS COUNTS AT 767nm 293011

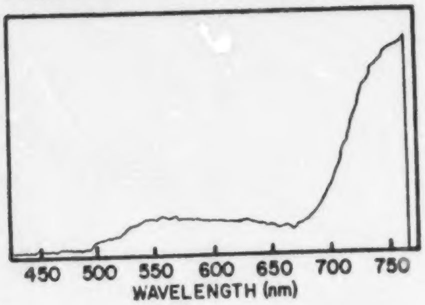

SPECTRUM Soybeans RECORD 14/70

SO_2 CONC 10480 $\mu g/m^3$ .75 h

FOLIAR INJURY: TOTAL 10 %

CHLOROSIS 10 %

NECROSIS ______ %

Y-AXIS COUNTS AT 767nm 263051

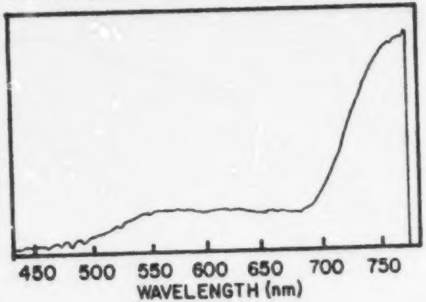

SPECTRUM Soybeans RECORD 14/71

SO_2 CONC 10480 $\mu g/m^3$ .75 h

FOLIAR INJURY: TOTAL 30 %

CHLOROSIS 30 %

NECROSIS ______ %

Y-AXIS COUNTS AT 767nm 362863

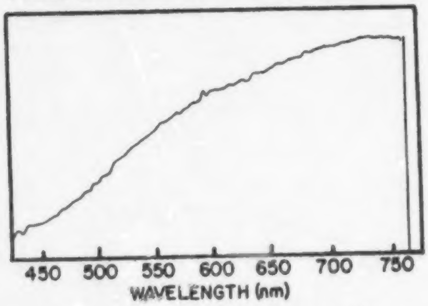

SPECTRUM Gray panel RECORD 14/72

SO_2 CONC ______ $\mu g/m^3$ ______ h

FOLIAR INJURY: TOTAL ______ %

CHLOROSIS ______ %

NECROSIS ______ %

Y-AXIS COUNTS AT 767nm 65899

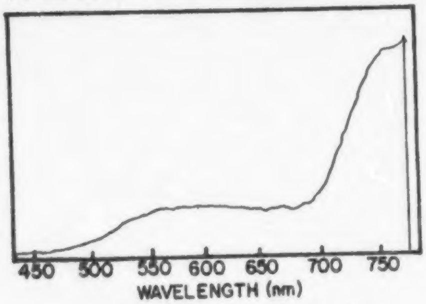

SPECTRUM Soybeans RECORD 14/73

SO_2 CONC 10480 $\mu g/m^3$ .75 h

FOLIAR INJURY: TOTAL 20 %

CHLOROSIS 20 %

NECROSIS ______ %

Y-AXIS COUNTS AT 767nm 287898

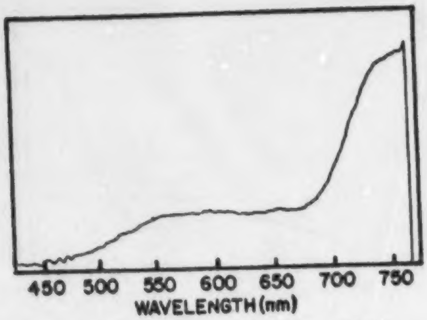

SPECTRUM Soybeans RECORD 14/74

SO$_2$ CONC 10480 µg/m^3 .75 h

FOLIAR INJURY: TOTAL 3 %

CHLOROSIS 5 %

NECROSIS ____ %

Y-AXIS COUNTS AT 767nm 281163

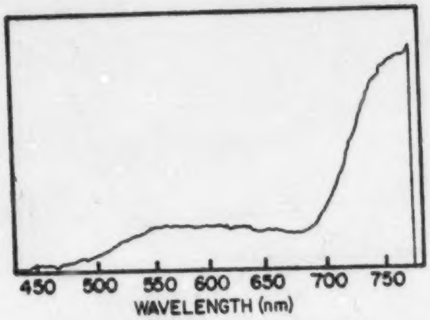

SPECTRUM Soybeans RECORD 14/75

SO$_2$ CONC 10480 µg/m^3 .75 h

FOLIAR INJURY: TOTAL 50 %

CHLOROSIS 50 %

NECROSIS ____ %

Y-AXIS COUNTS AT 767nm 261970

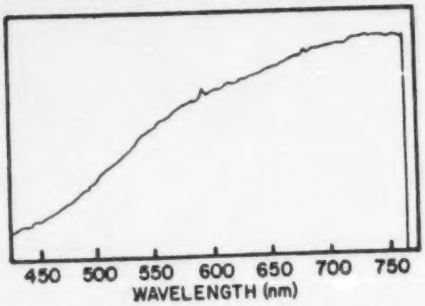

SPECTRUM Gray Panel RECORD 14/76

SO$_2$ CONC ____ µg/m^3 ____ h

FOLIAR INJURY: TOTAL ____ %

CHLOROSIS ____ %

NECROSIS ____ %

Y-AXIS COUNTS AT 767nm 66105

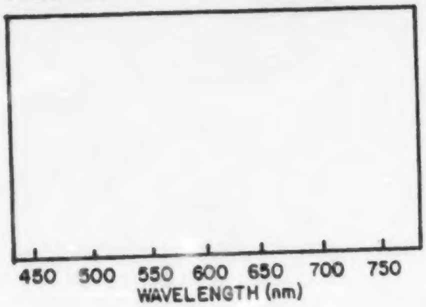

SPECTRUM ____ RECORD ____

SO$_2$ CONC ____ µg/m^3 ____ h

FOLIAR INJURY: TOTAL ____ %

CHLOROSIS ____ %

NECROSIS ____ %

Y-AXIS COUNTS AT 767nm ____

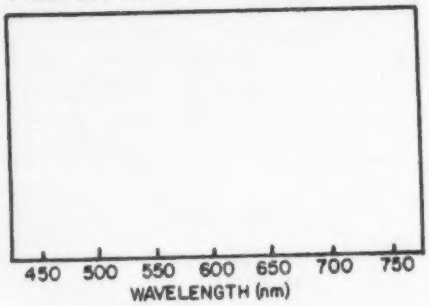

SPECTRUM ____ RECORD ____

SO$_2$ CONC ____ µg/m^3 ____ h

FOLIAR INJURY: TOTAL ____ %

CHLOROSIS ____ %

NECROSIS ____ %

Y-AXIS COUNTS AT 767nm ____

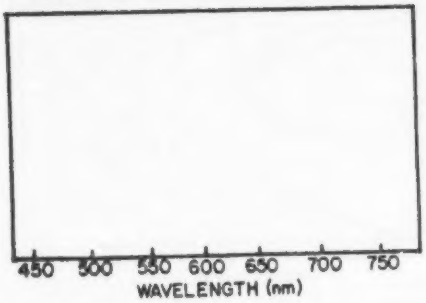

SPECTRUM ____ RECORD ____

SO$_2$ CONC ____ µg/m^3 ____ h

FOLIAR INJURY: TOTAL ____ %

CHLOROSIS ____ %

NECROSIS ____ %

Y-AXIS COUNTS AT 767nm ____

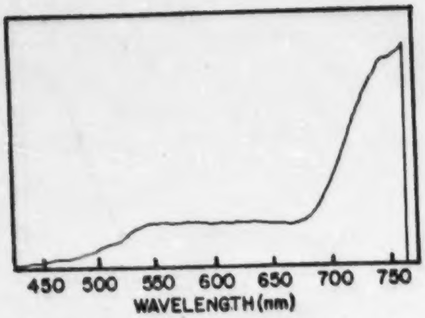

SPECTRUM Soybeans RECORD 15/1
SO_2 CONC 10480 μg/m^3 .75 h
FOLIAR INJURY: TOTAL 15 %
CHLOROSIS 10 %
NECROSIS 5 %
Y-AXIS COUNTS AT 767nm 240672

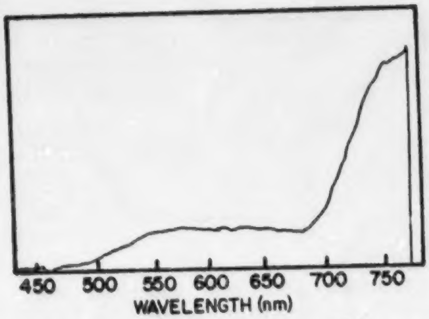

SPECTRUM Soybeans RECORD 15/2
SO_2 CONC 10480 μg/m^3 .75 h
FOLIAR INJURY: TOTAL 55 %
CHLOROSIS 30 %
NECROSIS 25 %
Y-AXIS COUNTS AT 767nm 267417

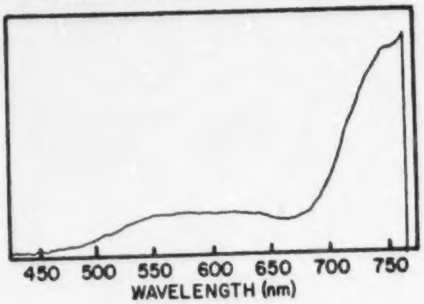

SPECTRUM Soybeans RECORD 15/3
SO_2 CONC 10480 μg/m^3 .75 h
FOLIAR INJURY: TOTAL 25 %
CHLOROSIS 20 %
NECROSIS 5 %
Y-AXIS COUNTS AT 767nm 263083

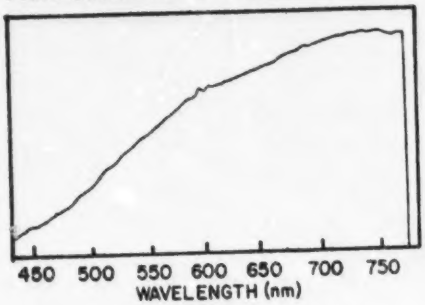

SPECTRUM Gray Panel RECORD 15/4
SO_2 CONC μg/m^3 h
FOLIAR INJURY: TOTAL %
CHLOROSIS %
NECROSIS %
Y-AXIS COUNTS AT 767nm 62844

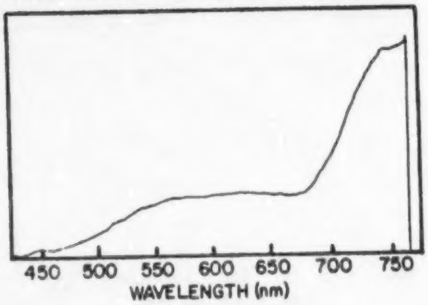

SPECTRUM Soybeans RECORD 15/5
SO_2 CONC 10480 μg/m^3 .75 h
FOLIAR INJURY: TOTAL 80 %
CHLOROSIS 80 %
NECROSIS %
Y-AXIS COUNTS AT 767nm 273276

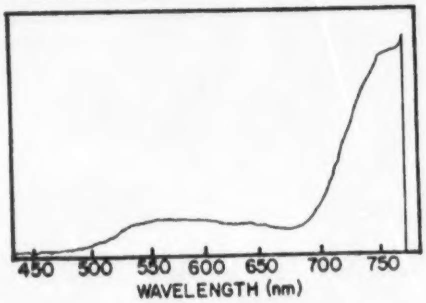

SPECTRUM Soybeans RECORD 15/6
SO_2 CONC 10480 μg/m^3 .75 h
FOLIAR INJURY: TOTAL 80 %
CHLOROSIS 80 %
NECROSIS %
Y-AXIS COUNTS AT 767nm 290579

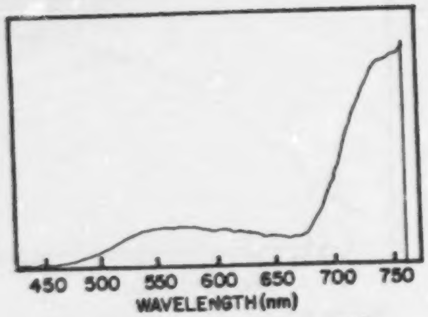

SPECTRUM **Soybeans** RECORD 15/7
SO_2 CONC 10480 $\mu g/m^3$ .75 h
FOLIAR INJURY: TOTAL 90 %
CHLOROSIS 90 %
NECROSIS ____ %
Y-AXIS COUNTS AT 767nm 263886

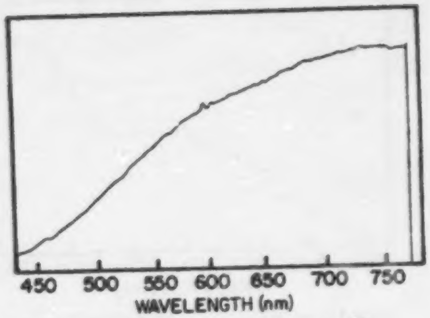

SPECTRUM Gray panel RECORD 15/8
SO_2 CONC ____ $\mu g/m^3$ ____ h
FOLIAR INJURY: TOTAL ____ %
CHLOROSIS ____ %
NECROSIS ____ %
Y-AXIS COUNTS AT 767nm 62737

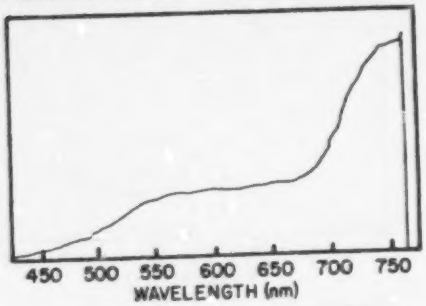

SPECTRUM **Soybeans** RECORD 15/9
SO_2 CONC 10480 $\mu g/m^3$ .75 h
FOLIAR INJURY: TOTAL 10 %
CHLOROSIS 10 %
NECROSIS ____ %
Y-AXIS COUNTS AT 767nm 274181

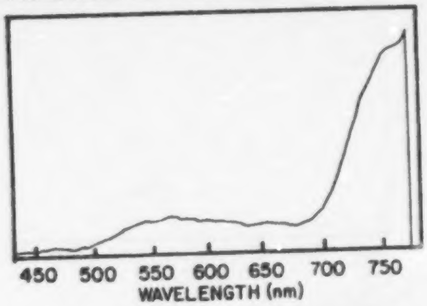

SPECTRUM **Soybeans** RECORD 15/10
SO_2 CONC 10480 $\mu g/m^3$ .75 h
FOLIAR INJURY: TOTAL 10 %
CHLOROSIS 10 %
NECROSIS ____ %
Y-AXIS COUNTS AT 767nm 297049

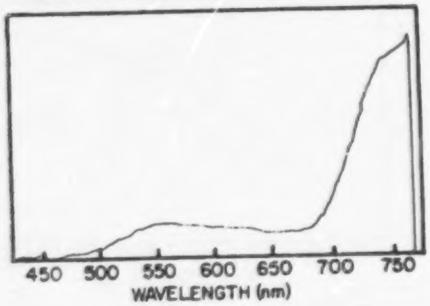

SPECTRUM **Soybeans** RECORD 15/11
SO_2 CONC 10480 $\mu g/m^3$ .75 h
FOLIAR INJURY: TOTAL 10 %
CHLOROSIS 10 %
NECROSIS ____ %
Y-AXIS COUNTS AT 767nm 258282

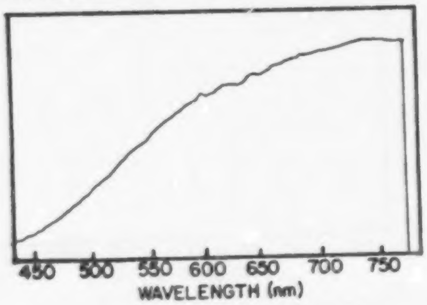

SPECTRUM Gray panel RECORD 15/12
SO_2 CONC ____ $\mu g/m^3$ ____ h
FOLIAR INJURY: TOTAL ____ %
CHLOROSIS ____ %
NECROSIS ____ %
Y-AXIS COUNTS AT 767nm 62983

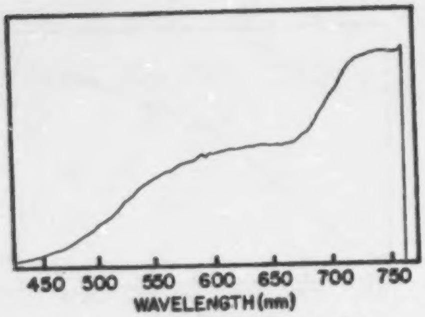

SPECTRUM Soybeans RECORD 15/14
SO_2 CONC 10480 μg/m³ .75 h
FOLIAR INJURY: TOTAL 90 %
CHLOROSIS 80 %
NECROSIS 10 %
Y-AXIS COUNTS AT 767nm 249284

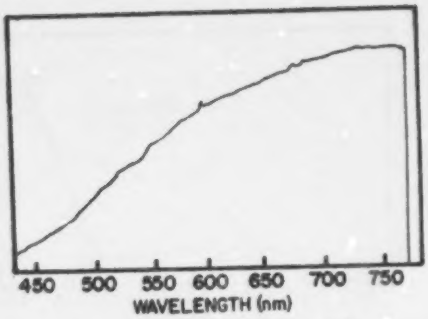

SPECTRUM Gray Panel RECORD 15/16
SO_2 CONC ______ μg/m³ ______ h
FOLIAR INJURY: TOTAL ______ %
CHLOROSIS ______ %
NECROSIS ______ %
Y-AXIS COUNTS AT 767nm 63729

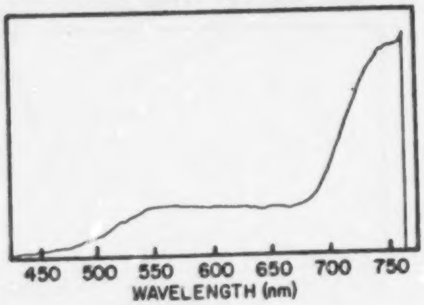

SPECTRUM Soybeans RECORD 15/17
SO_2 CONC 10480 μg/m³ .75 h
FOLIAR INJURY: TOTAL 20 %
CHLOROSIS 20 %
NECROSIS ______ %
Y-AXIS COUNTS AT 767nm 278222

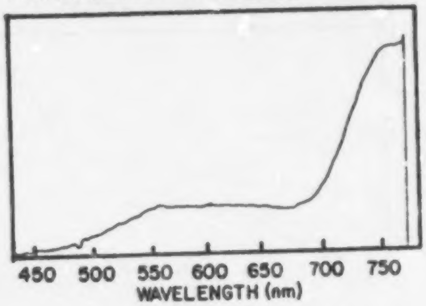

SPECTRUM Soybeans RECORD 15/18
SO_2 CONC 10480 μg/m³ .75 h
FOLIAR INJURY: TOTAL 20 %
CHLOROSIS 20 %
NECROSIS ______ %
Y-AXIS COUNTS AT 767nm 261641

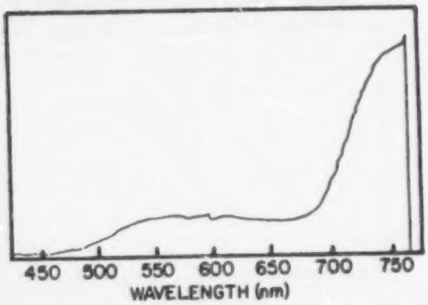

SPECTRUM Soybeans RECORD 15/19
SO_2 CONC 10480 μg/m³ .75 h
FOLIAR INJURY: TOTAL 20 %
CHLOROSIS 20 %
NECROSIS ______ %
Y-AXIS COUNTS AT 767nm 252091

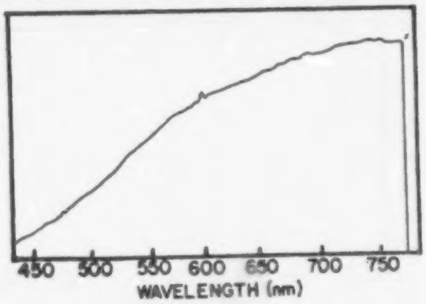

SPECTRUM Gray Panel RECORD 15/20
SO_2 CONC ______ μg/m³ ______ h
FOLIAR INJURY: TOTAL ______ %
CHLOROSIS ______ %
NECROSIS ______ %
Y-AXIS COUNTS AT 767nm 62330

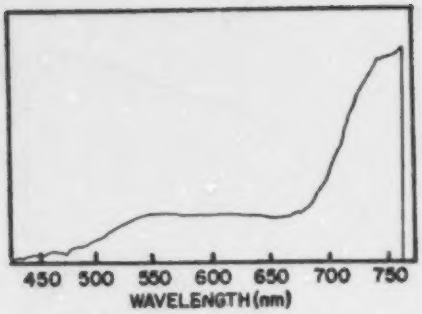

SPECTRUM Soybeans
RECORD 15/21
SO_2 CONC 15720 $\mu g/m^3$ .67 h
FOLIAR INJURY:
TOTAL 5 %
CHLOROSIS 5 %
NECROSIS ____ %
Y-AXIS COUNTS AT 767nm 258424

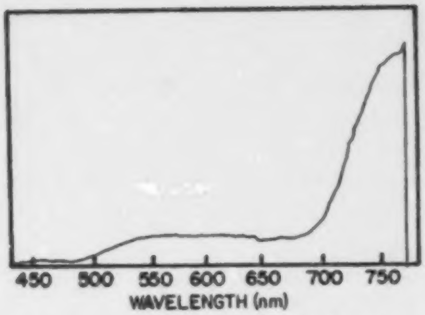

SPECTRUM Soybeans
RECORD 15/22
SO_2 CONC 15720 $\mu g/m^3$ .67 h
FOLIAR INJURY:
TOTAL 5 %
CHLOROSIS 5 %
NECROSIS ____ %
Y-AXIS COUNTS AT 767nm 280000

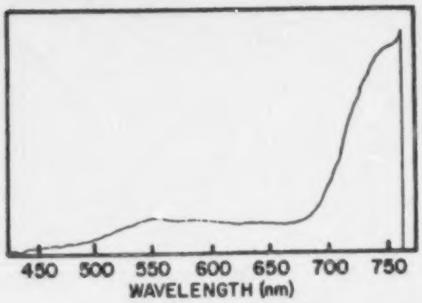

SPECTRUM Soybeans
RECORD 15/23
SO_2 CONC 15720 $\mu g/m^3$ .67 h
FOLIAR INJURY:
TOTAL 5 %
CHLOROSIS 5 %
NECROSIS ____ %
Y-AXIS COUNTS AT 767nm 271231

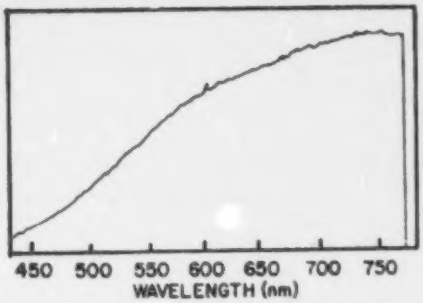

SPECTRUM Gray Panel
RECORD 15/24
SO_2 CONC ____ $\mu g/m^3$ ____ h
FOLIAR INJURY:
TOTAL ____ %
CHLOROSIS ____ %
NECROSIS ____ %
Y-AXIS COUNTS AT 767nm 64071

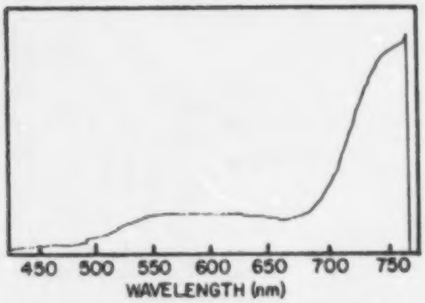

SPECTRUM Soybeans
RECORD 15/25
SO_2 CONC 15720 $\mu g/m^3$ .67 h
FOLIAR INJURY:
TOTAL 10 %
CHLOROSIS 10 %
NECROSIS ____ %
Y-AXIS COUNTS AT 767nm 264944

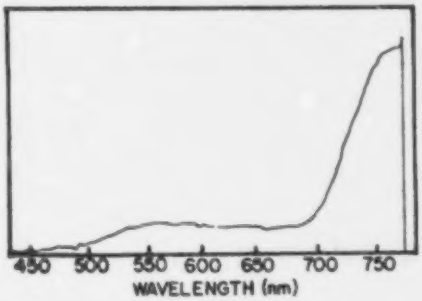

SPECTRUM Soybeans
RECORD 15/26
SO_2 CONC 15720 $\mu g/m^3$ .67 h
FOLIAR INJURY:
TOTAL 5 %
CHLOROSIS 5 %
NECROSIS ____ %
Y-AXIS COUNTS AT 767nm 291950

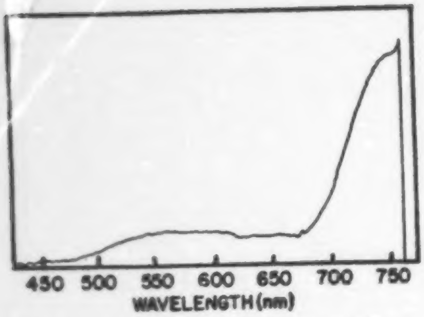

SPECTRUM Soybeans RECORD 15/27
SO_2 CONC 15720 $\mu g/m^3$ .67 h
FOLIAR INJURY: TOTAL 5 %
CHLOROSIS 5 %
NECROSIS ____ %
Y-AXIS COUNTS AT 767nm 281815

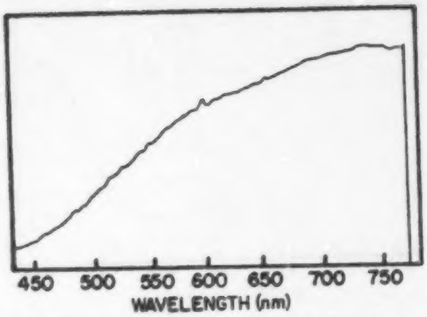

SPECTRUM Gray Panel RECORD 15/28
SO_2 CONC ____ $\mu g/m^3$ ____ h
FOLIAR INJURY: TOTAL ____ %
CHLOROSIS ____ %
NECROSIS ____ %
Y-AXIS COUNTS AT 767nm 63733

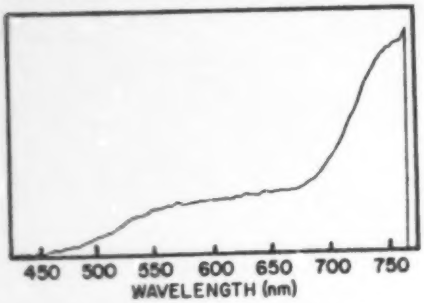

SPECTRUM Soybeans RECORD 15/29
SO_2 CONC 15720 $\mu g/m^3$ .67 h
FOLIAR INJURY: TOTAL 5 %
CHLOROSIS 5 %
NECROSIS ____ %
Y-AXIS COUNTS AT 767nm 299161

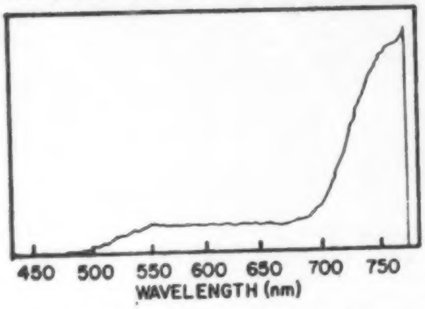

SPECTRUM Soybeans RECORD 15/30
SO_2 CONC 15720 $\mu g/m^3$ .67 h
FOLIAR INJURY: TOTAL 20 %
CHLOROSIS 20 %
NECROSIS ____ %
Y-AXIS COUNTS AT 767nm 274166

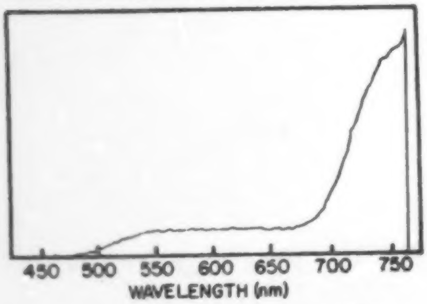

SPECTRUM Soybeans RECORD 15/31
SO_2 CONC 15720 $\mu g/m^3$ .67 h
FOLIAR INJURY: TOTAL 15 %
CHLOROSIS 15 %
NECROSIS ____ %
Y-AXIS COUNTS AT 767nm 277286

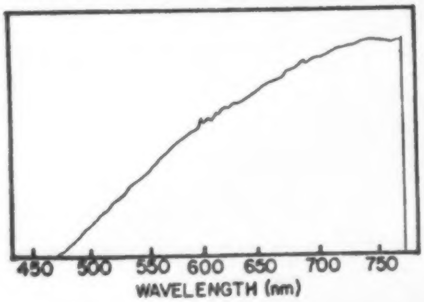

SPECTRUM Gray Panel RECORD 15/32
SO_2 CONC ____ $\mu g/m^3$ ____ h
FOLIAR INJURY: TOTAL ____ %
CHLOROSIS ____ %
NECROSIS ____ %
Y-AXIS COUNTS AT 767nm 56952

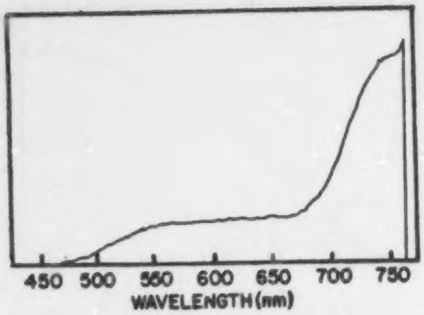

SPECTRUM Soybeans RECORD 15/33

SO$_2$ CONC 15720 μg/m^3 .67 h

FOLIAR INJURY: TOTAL 10 %

CHLOROSIS 10 %

NECROSIS ____ %

Y-AXIS COUNTS AT 767nm 271767

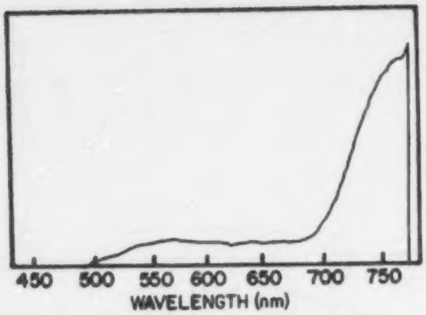

SPECTRUM Soybeans RECORD 15/34

SO$_2$ CONC 15720 μg/m^3 .67 h

FOLIAR INJURY: TOTAL 10 %

CHLOROSIS 10 %

NECROSIS ____ %

Y-AXIS COUNTS AT 767nm 291178

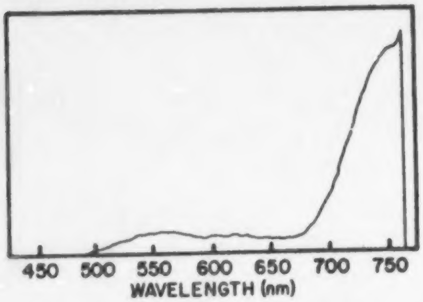

SPECTRUM Soybeans RECORD 15/35

SO$_2$ CONC 15720 μg/m^3 .67 h

FOLIAR INJURY: TOTAL 10 %

CHLOROSIS 10 %

NECROSIS ____ %

Y-AXIS COUNTS AT 767nm 265240

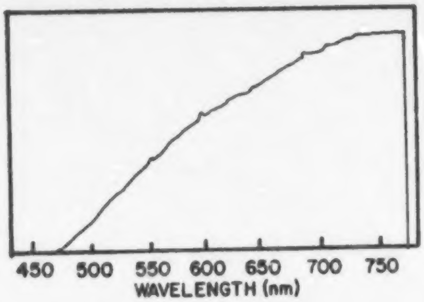

SPECTRUM Gray Panel RECORD 15/36

SO$_2$ CONC ____ μg/m^3 ____ h

FOLIAR INJURY: TOTAL ____ %

CHLOROSIS ____ %

NECROSIS ____ %

Y-AXIS COUNTS AT 767nm 56782

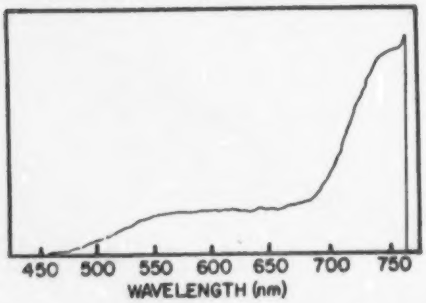

SPECTRUM Soybeans RECORD 15/37

SO$_2$ CONC 15720 μg/m^3 .67 h

FOLIAR INJURY: TOTAL 10 %

CHLOROSIS 10 %

NECROSIS ____ %

Y-AXIS COUNTS AT 767nm 285916

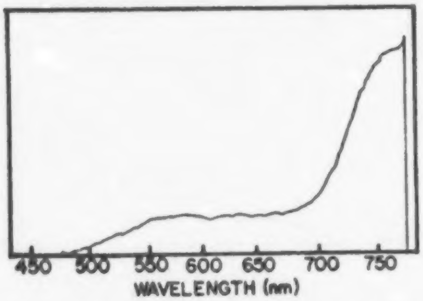

SPECTRUM Soybeans RECORD 15/38

SO$_2$ CONC 15720 μg/m^3 .67 h

FOLIAR INJURY: TOTAL 25 %

CHLOROSIS 25 %

NECROSIS ____ %

Y-AXIS COUNTS AT 767nm 297532

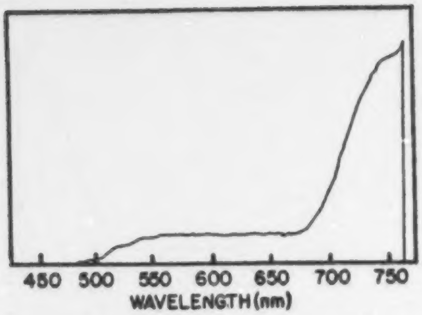

SPECTRUM Soybeans RECORD 15/39
SO_2 CONC 15720 µg/m^3 .67 h
FOLIAR INJURY: TOTAL 25 %
CHLOROSIS 25 %
NECROSIS ____ %
Y-AXIS COUNTS AT 767nm 263121

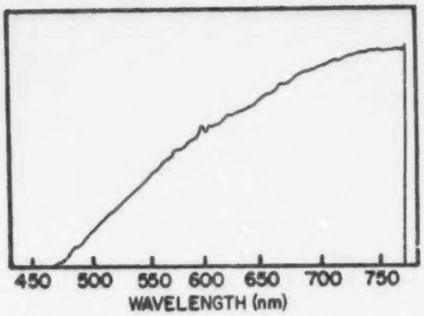

SPECTRUM Gray Panel RECORD 15/40
SO_2 CONC ____ µg/m^3 ____ h
FOLIAR INJURY: TOTAL ____ %
CHLOROSIS ____ %
NECROSIS ____ %
Y-AXIS COUNTS AT 767nm 56931

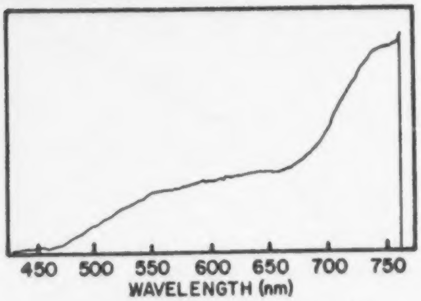

SPECTRUM Soybeans RECORD 15/41
SO_2 CONC 15720 µg/m^3 .67 h
FOLIAR INJURY: TOTAL 10 %
CHLOROSIS 10 %
NECROSIS ____ %
Y-AXIS COUNTS AT 767nm 301793

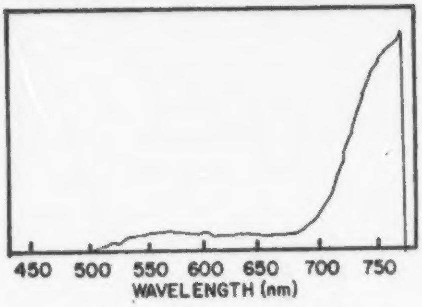

SPECTRUM Soybeans RECORD 15/42
SO_2 CONC 15720 µg/m^3 .67 h
FOLIAR INJURY: TOTAL 10 %
CHLOROSIS 10 %
NECROSIS ____ %
Y-AXIS COUNTS AT 767nm 272673

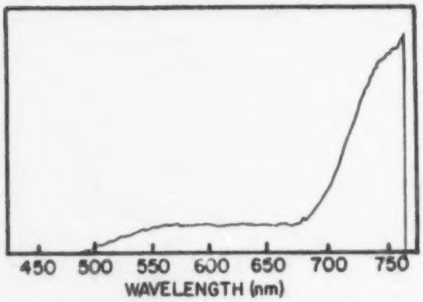

SPECTRUM Soybeans RECORD 15/43
SO_2 CONC 15720 µg/m^3 .67 h
FOLIAR INJURY: TOTAL 10 %
CHLOROSIS 10 %
NECROSIS ____ %
Y-AXIS COUNTS AT 767nm 268257

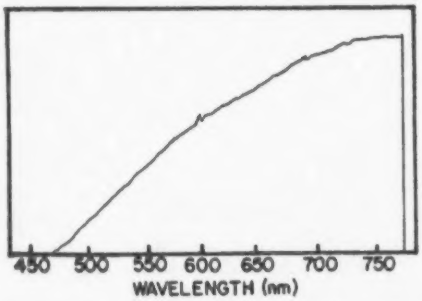

SPECTRUM Gray Panel RECORD 15/44
SO_2 CONC ____ µg/m^3 ____ h
FOLIAR INJURY: TOTAL ____ %
CHLOROSIS ____ %
NECROSIS ____ %
Y-AXIS COUNTS AT 767nm 56822

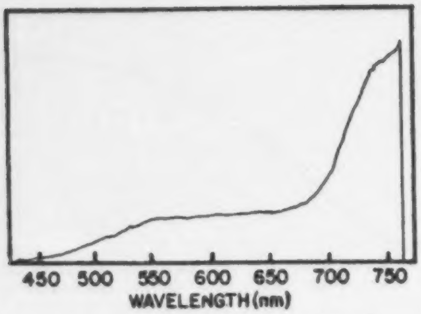

SPECTRUM Soybeans RECORD 15/45
SO_2 CONC 15720 µg/m³ .67 h
FOLIAR INJURY: TOTAL 5 %
CHLOROSIS 5 %
NECROSIS ____ %
Y-AXIS COUNTS AT 767nm 298514

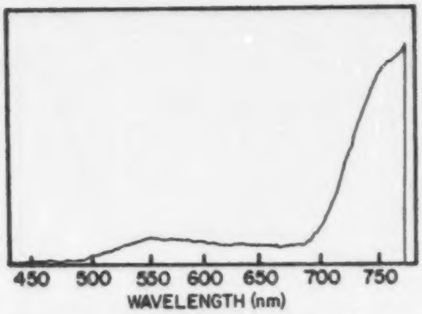

SPECTRUM Soybeans RECORD 15/46
SO_2 CONC 15720 µg/m³ .67 h
FOLIAR INJURY: TOTAL 5 %
CHLOROSIS 5 %
NECROSIS ____ %
Y-AXIS COUNTS AT 767nm ____

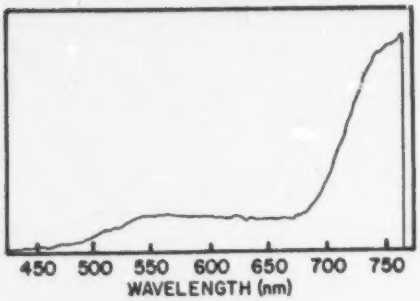

SPECTRUM Soybeans RECORD 15/47
SO_2 CONC 15720 µg/m³ .67 h
FOLIAR INJURY: TOTAL 10 %
CHLOROSIS 10 %
NECROSIS ____ %
Y-AXIS COUNTS AT 767nm 246017

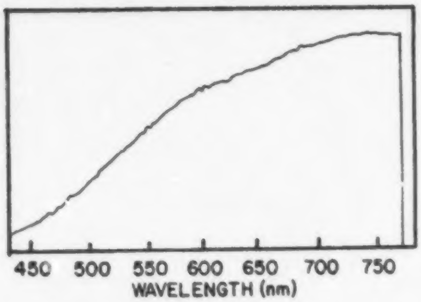

SPECTRUM Gray Panel RECORD 15/48
SO_2 CONC ____ µg/m³ ____ h
FOLIAR INJURY: TOTAL ____ %
CHLOROSIS ____ %
NECROSIS ____ %
Y-AXIS COUNTS AT 767nm 62707

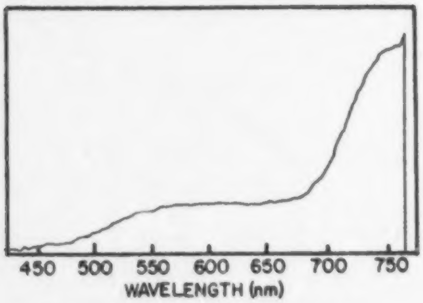

SPECTRUM Soybeans RECORD 15/49
SO_2 CONC 15720 µg/m³ .67 h
FOLIAR INJURY: TOTAL 15 %
CHLOROSIS 15 %
NECROSIS ____ %
Y-AXIS COUNTS AT 767nm 301380

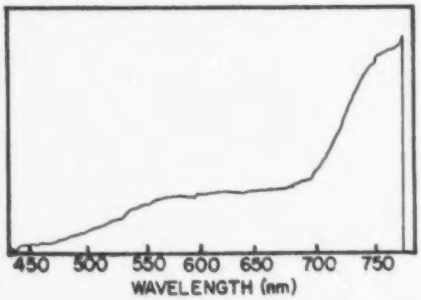

SPECTRUM Soybeans RECORD 15/50
SO_2 CONC 15720 µg/m³ .67 h
FOLIAR INJURY: TOTAL 10 %
CHLOROSIS 10 %
NECROSIS ____ %
Y-AXIS COUNTS AT 767nm 288853

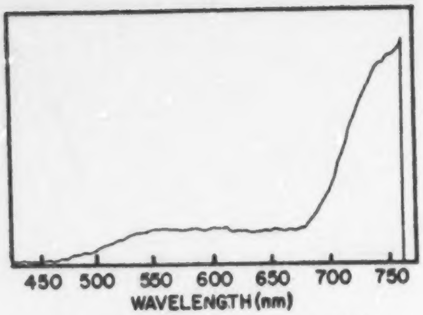

SPECTRUM Soybeans RECORD 15/51
SO$_2$ CONC 15720 μg/m^3 .67 h
FOLIAR INJURY: TOTAL 10 %
CHLOROSIS 10 %
NECROSIS ___ %
Y-AXIS COUNTS AT 767nm 262343

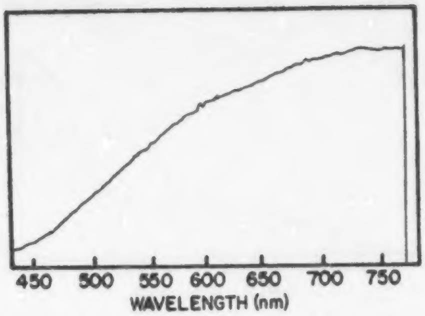

SPECTRUM Gray Panel RECORD 15/52
SO$_2$ CONC ___ μg/m^3 ___ h
FOLIAR INJURY: TOTAL ___ %
CHLOROSIS ___ %
NECROSIS ___ %
Y-AXIS COUNTS AT 767nm 62811

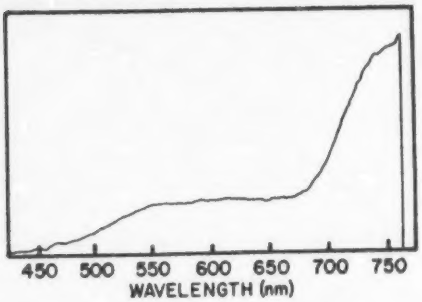

SPECTRUM Soybeans RECORD 15/53
SO$_2$ CONC 10480 μg/m^3 .75 h
FOLIAR INJURY: TOTAL 5 %
CHLOROSIS 5 %
NECROSIS ___ %
Y-AXIS COUNTS AT 767nm 354763

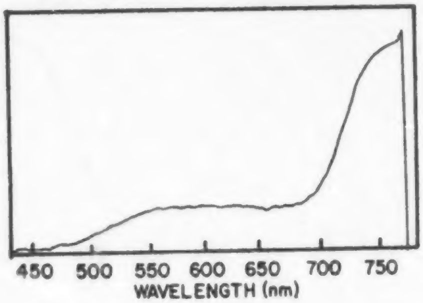

SPECTRUM Soybeans RECORD 15/54
SO$_2$ CONC 10480 μg/m^3 .75 h
FOLIAR INJURY: TOTAL 5 %
CHLOROSIS 5 %
NECROSIS ___ %
Y-AXIS COUNTS AT 767nm 345064

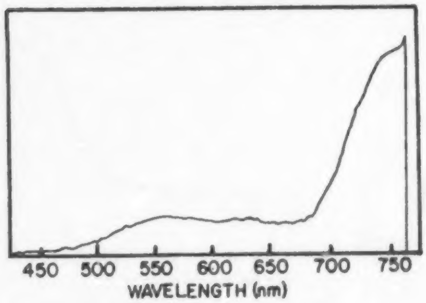

SPECTRUM Soybeans RECORD 15/55
SO$_2$ CONC 10480 μg/m^3 .75 h
FOLIAR INJURY: TOTAL 10 %
CHLOROSIS 10 %
NECROSIS ___ %
Y-AXIS COUNTS AT 767nm 336397

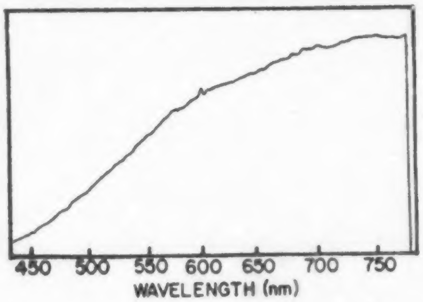

SPECTRUM Gray Panel RECORD 15/56
SO$_2$ CONC ___ μg/m^3 ___ h
FOLIAR INJURY: TOTAL ___ %
CHLOROSIS ___ %
NECROSIS ___ %
Y-AXIS COUNTS AT 767nm 75040

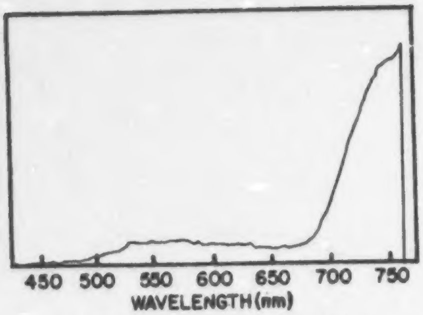

SPECTRUM Soybeans RECORD 15/58

SO_2 CONC 10480 $\mu g/m^3$ .75 h

FOLIAR INJURY: TOTAL 50 %

CHLOROSIS 50 %

NECROSIS ____ %

Y-AXIS COUNTS AT 767nm 344878

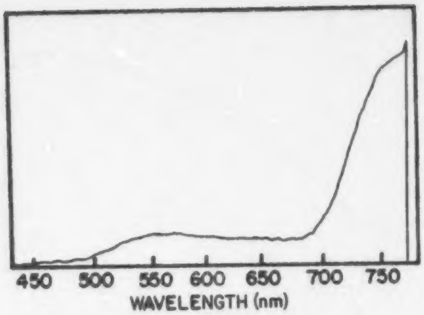

SPECTRUM Soybeans RECORD 15/59

SO_2 CONC 10480 $\mu g/m^3$ .75 h

FOLIAR INJURY: TOTAL 40 %

CHLOROSIS 40 %

NECROSIS ____ %

Y-AXIS COUNTS AT 767nm 300076

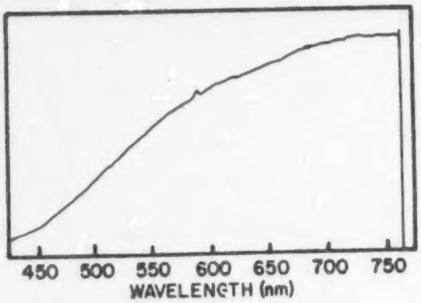

SPECTRUM Gray Panel RECORD 15/60

SO_2 CONC ____ $\mu g/m^3$ ____ h

FOLIAR INJURY: TOTAL ____ %

CHLOROSIS ____ %

NECROSIS ____ %

Y-AXIS COUNTS AT 767nm 74976

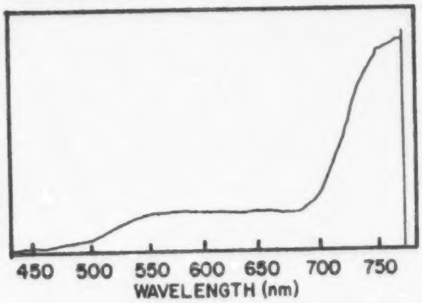

SPECTRUM Soybeans RECORD 15/61

SO_2 CONC 10480 $\mu g/m^3$ .75 h

FOLIAR INJURY: TOTAL 50 %

CHLOROSIS 50 %

NECROSIS ____ %

Y-AXIS COUNTS AT 767nm 372887

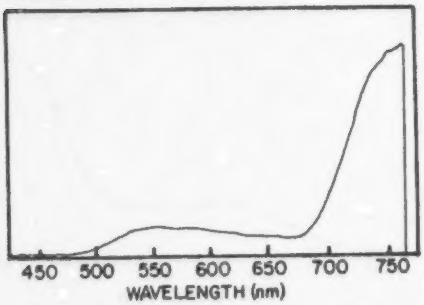

SPECTRUM Soybeans RECORD 15/62

SO_2 CONC 10480 $\mu g/m^3$ .75 h

FOLIAR INJURY: TOTAL 30 %

CHLOROSIS 30 %

NECROSIS ____ %

Y-AXIS COUNTS AT 767nm 342751

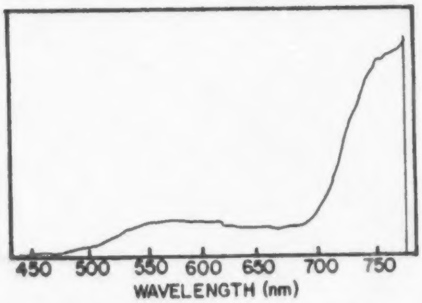

SPECTRUM Soybeans RECORD 15/63

SO_2 CONC 10480 $\mu g/m^3$ .75 h

FOLIAR INJURY: TOTAL 50 %

CHLOROSIS 50 %

NECROSIS ____ %

Y-AXIS COUNTS AT 767nm 342058

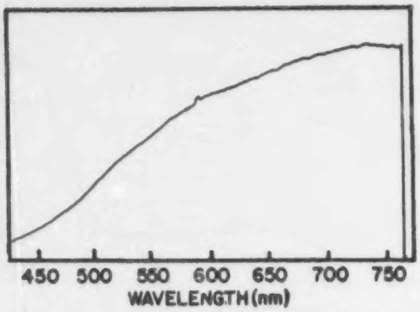

SPECTRUM Gray panel RECORD 15/64

SO$_2$ CONC ______ μg/m^3 ______ h

FOLIAR INJURY: TOTAL ______ %

CHLOROSIS ____ %

NECROSIS ____ %

Y-AXIS COUNTS AT 767nm 75444

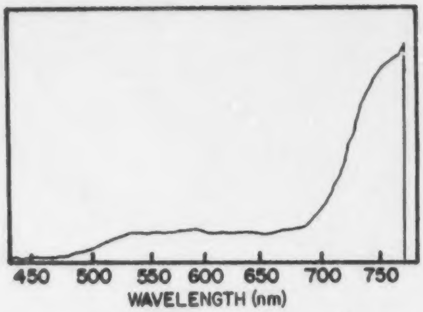

SPECTRUM Soybeans RECORD 15/65

SO$_2$ CONC 10480 μg/m^3 .75 h

FOLIAR INJURY: TOTAL 5 %

CHLOROSIS 5 %

NECROSIS ____ %

Y-AXIS COUNTS AT 767nm 360837

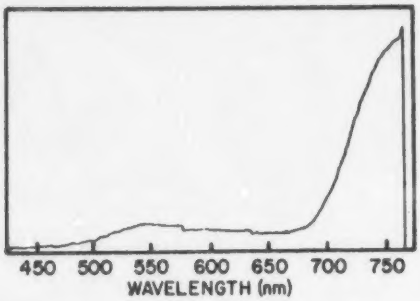

SPECTRUM Soybeans RECORD 15/66

SO$_2$ CONC 10480 μg/m^3 .75 h

FOLIAR INJURY: TOTAL 10 %

CHLOROSIS 10 %

NECROSIS ____ %

Y-AXIS COUNTS AT 767nm 345662

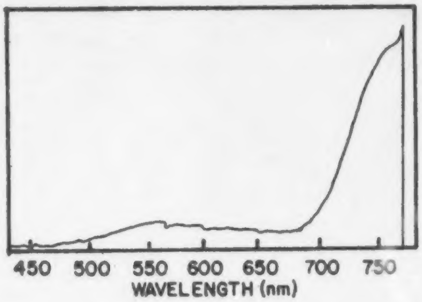

SPECTRUM Soybeans RECORD 15/67

SO$_2$ CONC 10480 μg/m^3 .75 h

FOLIAR INJURY: TOTAL 15 %

CHLOROSIS 15 %

NECROSIS ____ %

Y-AXIS COUNTS AT 767nm 320341

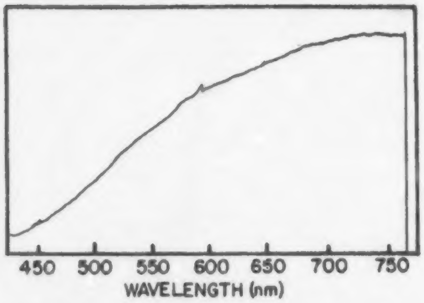

SPECTRUM Gray panel RECORD 15/68

SO$_2$ CONC ______ μg/m^3 ______ h

FOLIAR INJURY: TOTAL ______ %

CHLOROSIS ____ %

NECROSIS ____ %

Y-AXIS COUNTS AT 767nm 75636

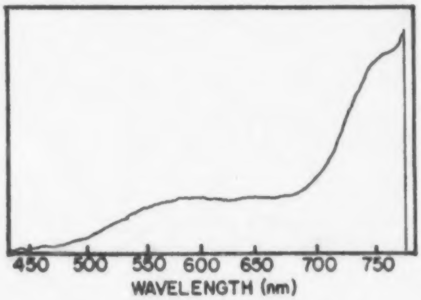

SPECTRUM Soybeans RECORD 15/69

SO$_2$ CONC 10480 μg/m^3 .75 h

FOLIAR INJURY: TOTAL 15 %

CHLOROSIS 15 %

NECROSIS ____ %

Y-AXIS COUNTS AT 767nm 360550

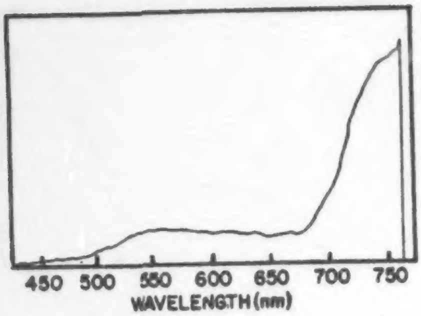

SPECTRUM Soybeans RECORD 15/70
SO_2 CONC 10480 μg/m³ .75 h
FOLIAR INJURY: TOTAL 20 %
CHLOROSIS 20 %
NECROSIS ___ %
Y-AXIS COUNTS AT 767nm 350980

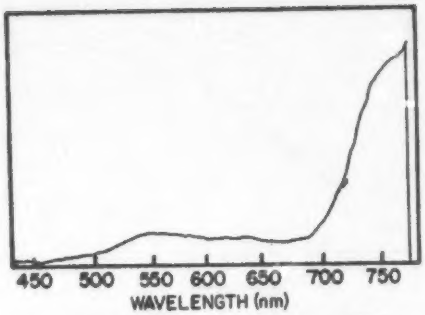

SPECTRUM Soybeans RECORD 15/71
SO_2 CONC 10480 μg/m³ .75 h
FOLIAR INJURY: TOTAL 20 %
CHLOROSIS 20 %
NECROSIS ___ %
Y-AXIS COUNTS AT 767nm 320469

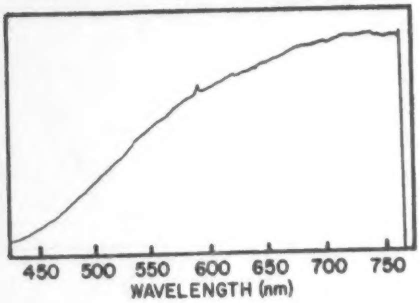

SPECTRUM Gray panel RECORD 15172
SO_2 CONC ___ μg/m³ ___ h
FOLIAR INJURY: TOTAL ___ %
CHLOROSIS ___ %
NECROSIS ___ %
Y-AXIS COUNTS AT 767nm 75817

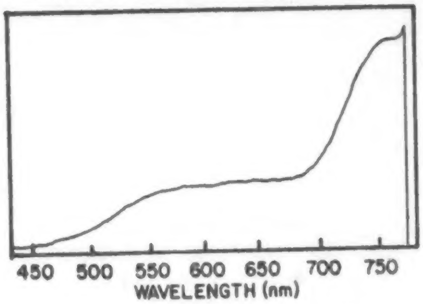

SPECTRUM Soybeans RECORD 15173
SO_2 CONC 10480 μg/m³ .75 h
FOLIAR INJURY: TOTAL 40 %
CHLOROSIS 40 %
NECROSIS ___ %
Y-AXIS COUNTS AT 767nm 341101

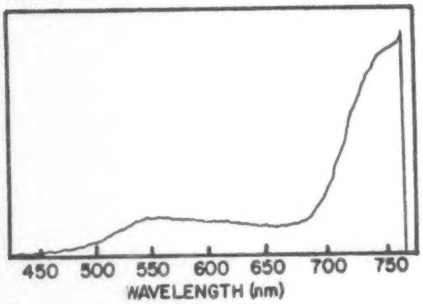

SPECTRUM Soybeans RECORD 15174
SO_2 CONC 10480 μg/m³ .75 h
FOLIAR INJURY: TOTAL 40 %
CHLOROSIS 40 %
NECROSIS ___ %
Y-AXIS COUNTS AT 767nm 335725

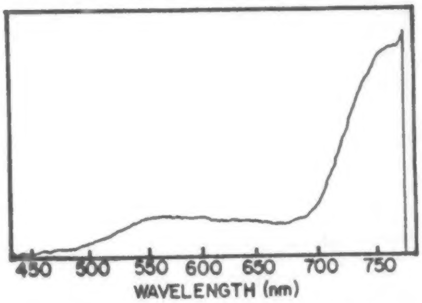

SPECTRUM Soybeans RECORD 15175
SO_2 CONC 10480 μg/m³ .75 h
FOLIAR INJURY: TOTAL 40 %
CHLOROSIS 40 %
NECROSIS ___ %
Y-AXIS COUNTS AT 767nm 296235

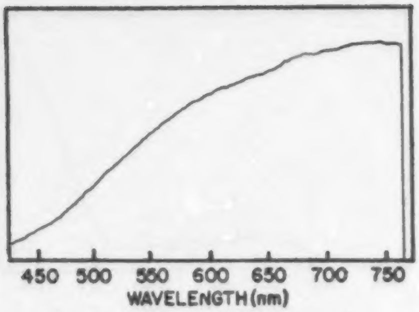

SPECTRUM Gray Panel RECORD 15/76
SO2 CONC ________ µg/m3 ________ h
FOLIAR INJURY: TOTAL ______ %
CHLOROSIS ____ %
NECROSIS _____ %
Y-AXIS COUNTS AT 767nm 75999

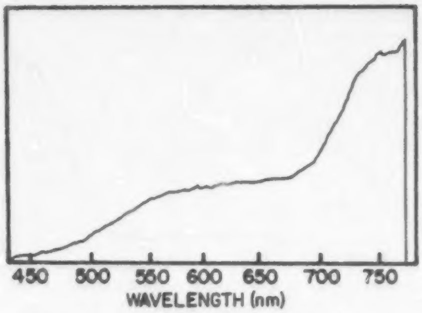

SPECTRUM Soybeans RECORD 16/1
SO2 CONC 10480 µg/m3 1.225 h
FOLIAR INJURY: TOTAL 30 %
CHLOROSIS 10 %
NECROSIS 20 %
Y-AXIS COUNTS AT 767nm 289358

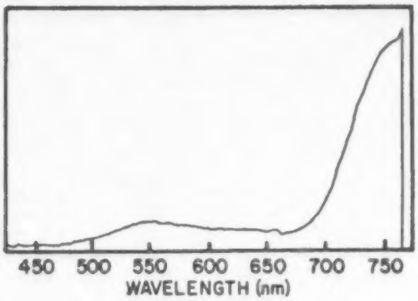

SPECTRUM Soybeans RECORD 16/2
SO2 CONC 10480 µg/m3 1.225 h
FOLIAR INJURY: TOTAL 5 %
CHLOROSIS 5 %
NECROSIS _____ %
Y-AXIS COUNTS AT 767nm 310608

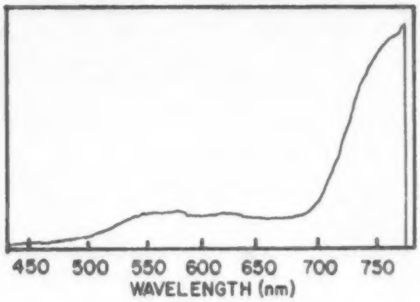

SPECTRUM Soybeans RECORD 16/3
SO2 CONC 10480 µg/m3 1.225 h
FOLIAR INJURY: TOTAL 10 %
CHLOROSIS 5 %
NECROSIS 5 %
Y-AXIS COUNTS AT 767nm 280398

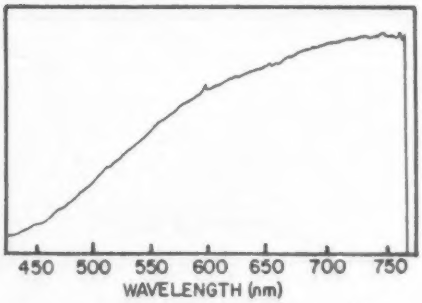

SPECTRUM Gray Panel RECORD 16/4
SO2 CONC ________ µg/m3 ________ h
FOLIAR INJURY: TOTAL ______ %
CHLOROSIS ____ %
NECROSIS _____ %
Y-AXIS COUNTS AT 767nm [illegible]37

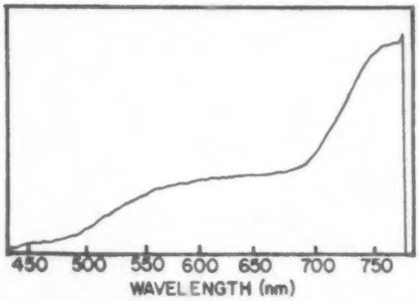

SPECTRUM Soybeans RECORD 16/5
SO2 CONC 10480 µg/m3 1.225 h
FOLIAR INJURY: TOTAL 20 %
CHLOROSIS 20 %
NECROSIS _____ %
Y-AXIS COUNTS AT 767nm 333468

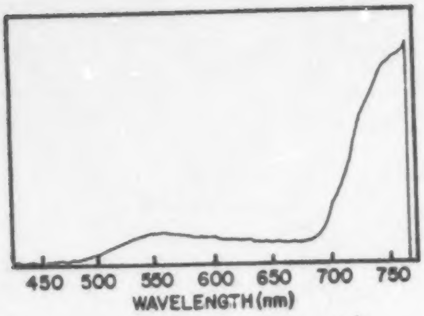

SPECTRUM Soybeans
RECORD 16/4
SO_2 CONC 10480
μg/m³ 1.225 h
FOLIAR INJURY:
TOTAL 26 %
CHLOROSIS 20 %
NECROSIS ___ %
Y-AXIS COUNTS AT 767nm 353057

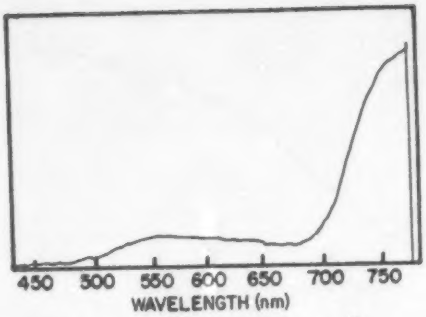

SPECTRUM Soybeans
RECORD 16/7
SO_2 CONC 10480
μg/m³ 1.225 h
FOLIAR INJURY:
TOTAL 30 %
CHLOROSIS 30 %
NECROSIS ___ %
Y-AXIS COUNTS AT 767nm 344922

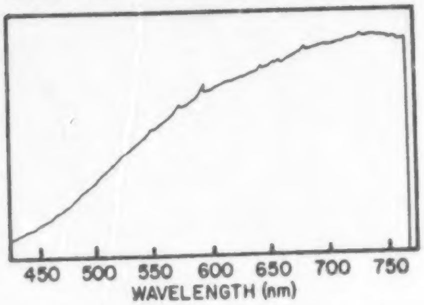

SPECTRUM Gray Panel
RECORD 16/8
SO_2 CONC ___
μg/m³ ___ h
FOLIAR INJURY:
TOTAL ___ %
CHLOROSIS ___ %
NECROSIS ___ %
Y-AXIS COUNTS AT 767nm 74132

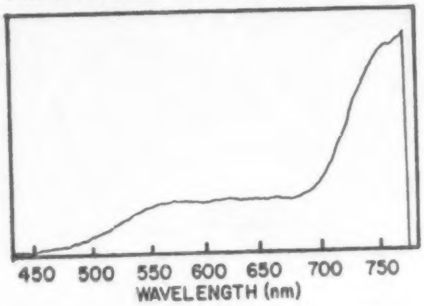

SPECTRUM Soybeans
RECORD 16/9
SO_2 CONC 15720
μg/m³ .50 h
FOLIAR INJURY:
TOTAL 60 %
CHLOROSIS 60 %
NECROSIS ___ %
Y-AXIS COUNTS AT 767nm 269486

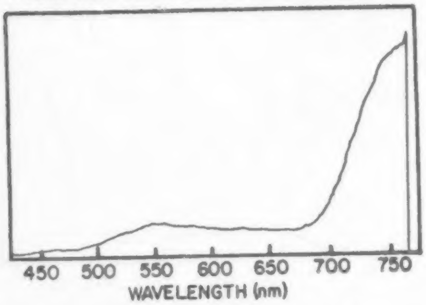

SPECTRUM Soybeans
RECORD 16/10
SO_2 CONC 15720
μg/m³ .50 h
FOLIAR INJURY:
TOTAL 10 %
CHLOROSIS 10 %
NECROSIS ___ %
Y-AXIS COUNTS AT 767nm 288664

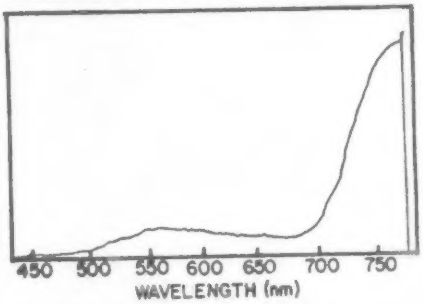

SPECTRUM Soybeans
RECORD 16/11
SO_2 CONC 15720
μg/m³ .50 h
FOLIAR INJURY:
TOTAL 20 %
CHLOROSIS 20 %
NECROSIS ___ %
Y-AXIS COUNTS AT 767nm 282685

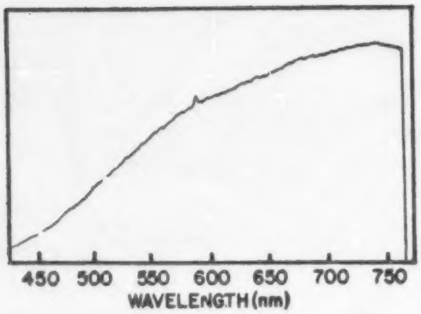

SPECTRUM Gray Panel RECORD 16/12
SO_2 CONC μg/m^3 h
FOLIAR INJURY: TOTAL %
CHLOROSIS %
NECROSIS %
Y-AXIS COUNTS AT 767nm 62261

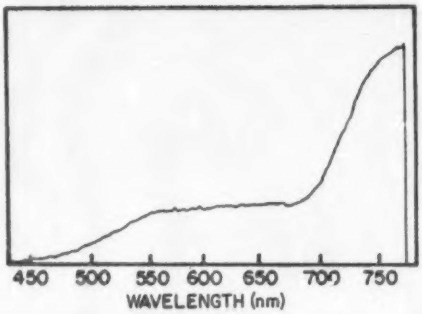

SPECTRUM Soybeans RECORD 16/13
SO_2 CONC 15720 μg/m^3 .50 h
FOLIAR INJURY: TOTAL 5 %
CHLOROSIS 5 %
NECROSIS %
Y-AXIS COUNTS AT 767nm 249354

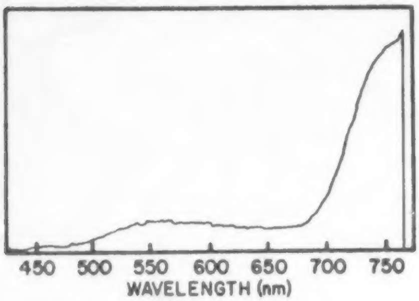

SPECTRUM Soybeans RECORD 16/14
SO_2 CONC 15720 μg/m^3 .50 h
FOLIAR INJURY: TOTAL 40 %
CHLOROSIS 40 %
NECROSIS %
Y-AXIS COUNTS AT 767nm 190742

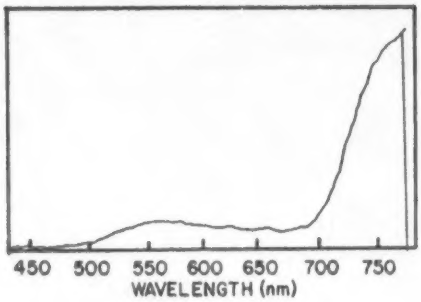

SPECTRUM Soybeans RECORD 16/15
SO_2 CONC 15720 μg/m^3 .50 h
FOLIAR INJURY: TOTAL 50 %
CHLOROSIS 50 %
NECROSIS %
Y-AXIS COUNTS AT 767nm 264825

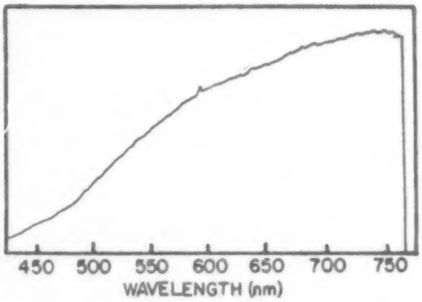

SPECTRUM Gray Panel RECORD 16/16
SO_2 CONC μg/m^3 h
FOLIAR INJURY: TOTAL %
CHLOROSIS %
NECROSIS %
Y-AXIS COUNTS AT 767nm 62828

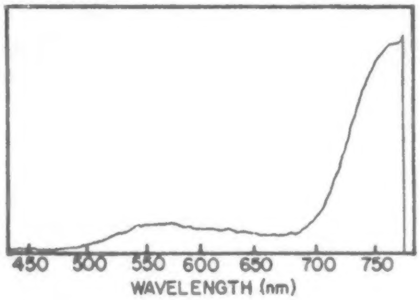

SPECTRUM Soybeans RECORD 16/17
SO_2 CONC 15720 μg/m^3 .50 h
FOLIAR INJURY: TOTAL 50 %
CHLOROSIS 50 %
NECROSIS %
Y-AXIS COUNTS AT 767nm 249005

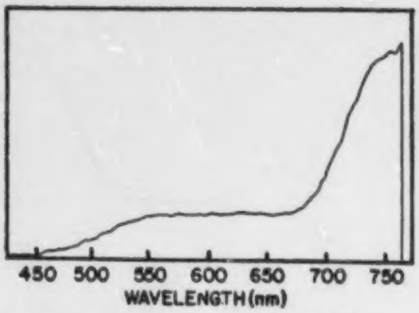

SPECTRUM Soybeans
RECORD 16/18
SO_2 CONC 15720 $\mu g/m^3$ .50 h
FOLIAR INJURY:
TOTAL 10 %
CHLOROSIS 10 %
NECROSIS ____ %
Y-AXIS COUNTS AT 767nm 283671

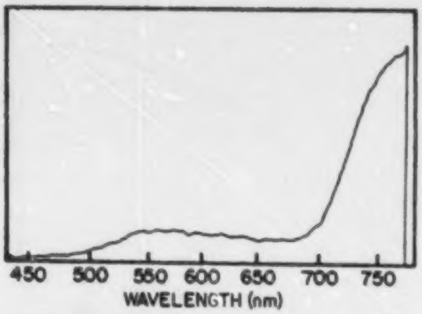

SPECTRUM Soybeans
RECORD 16/19
SO_2 CONC 15720 $\mu g/m^3$ .50 h
FOLIAR INJURY:
TOTAL 5 %
CHLOROSIS 5 %
NECROSIS ____ %
Y-AXIS COUNTS AT 767nm 257906

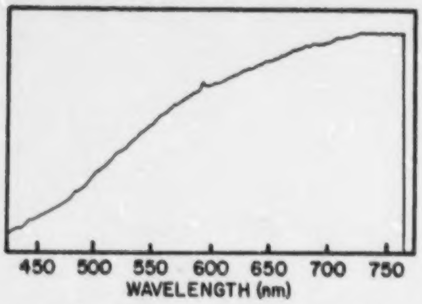

SPECTRUM Grey Panel
RECORD 16/20
SO_2 CONC ____ $\mu g/m^3$ ____ h
FOLIAR INJURY:
TOTAL ____ %
CHLOROSIS ____ %
NECROSIS ____ %
Y-AXIS COUNTS AT 767nm 101739

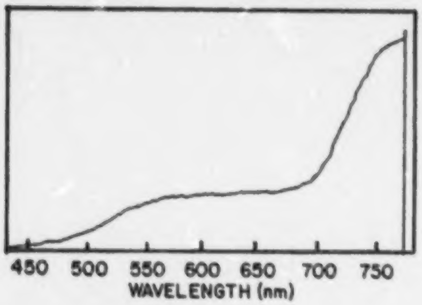

SPECTRUM Soybeans
RECORD 16/21
SO_2 CONC 15720 $\mu g/m^3$ .50 h
FOLIAR INJURY:
TOTAL 0 %
CHLOROSIS ____ %
NECROSIS ____ %
Y-AXIS COUNTS AT 767nm 319408

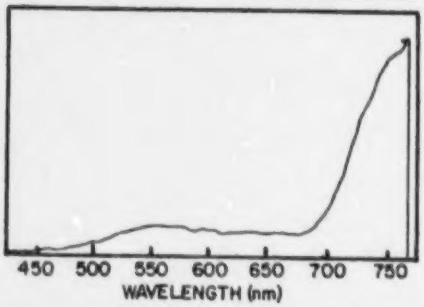

SPECTRUM Soybeans
RECORD 16/22
SO_2 CONC 15720 $\mu g/m^3$ .50 h
FOLIAR INJURY:
TOTAL 0 %
CHLOROSIS ____ %
NECROSIS ____ %
Y-AXIS COUNTS AT 767nm 344819

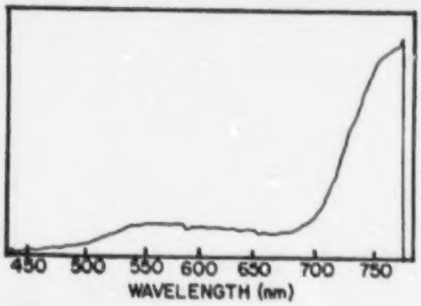

SPECTRUM Soybeans
RECORD 16/23
SO_2 CONC 15720 $\mu g/m^3$ .50 h
FOLIAR INJURY:
TOTAL 5 %
CHLOROSIS 5 %
NECROSIS ____ %
Y-AXIS COUNTS AT 767nm 336853

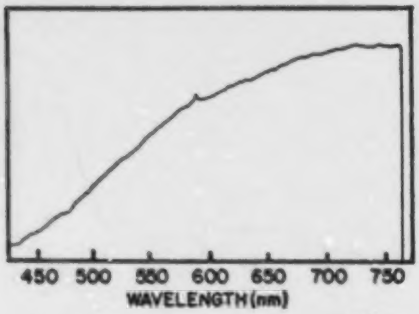

SPECTRUM Gray Panel RECORD 16/24

SO_2 CONC ______ $\mu g/m^3$ ______ h

FOLIAR INJURY: TOTAL ______ %

CHLOROSIS ____ %

NECROSIS ____ %

Y-AXIS COUNTS AT 767nm 73505

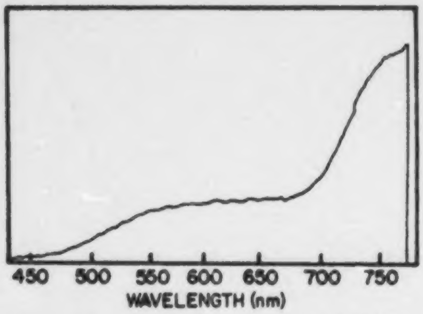

SPECTRUM Soybeans RECORD 16/25

SO_2 CONC 10480 $\mu g/m^3$ 1.225 h

FOLIAR INJURY: TOTAL 10 %

CHLOROSIS 10 %

NECROSIS ____ %

Y-AXIS COUNTS AT 767nm 202159

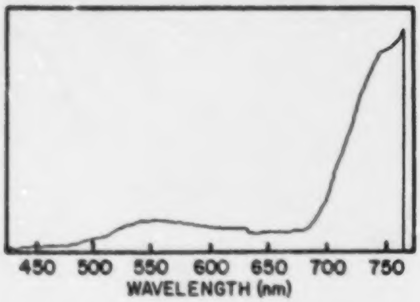

SPECTRUM Soybeans RECORD 16/26

SO_2 CONC 10480 $\mu g/m^3$ 1.225 h

FOLIAR INJURY: TOTAL 5 %

CHLOROSIS 5 %

NECROSIS ____ %

Y-AXIS COUNTS AT 767nm 287086

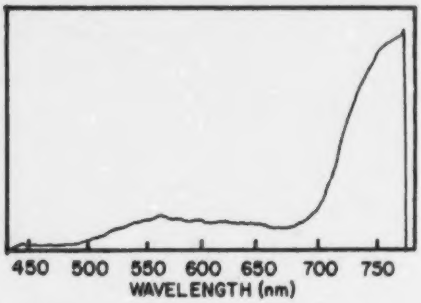

SPECTRUM Soybeans RECORD 16/27

SO_2 CONC 10480 $\mu g/m^3$ 1.225 h

FOLIAR INJURY: TOTAL 10 %

CHLOROSIS 10 %

NECROSIS ____ %

Y-AXIS COUNTS AT 767nm 256314

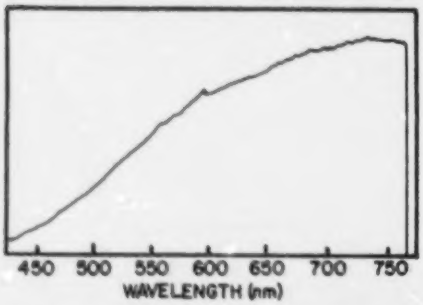

SPECTRUM Gray Panel RECORD 16/28

SO_2 CONC ______ $\mu g/m^3$ ______ h

FOLIAR INJURY: TOTAL ______ %

CHLOROSIS ____ %

NECROSIS ____ %

Y-AXIS COUNTS AT 767nm 61868

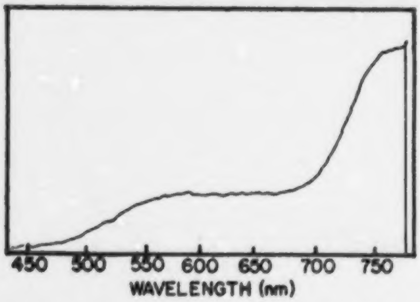

SPECTRUM Soybeans RECORD 16/29

SO_2 CONC 10480 $\mu g/m^3$ 1.225 h

FOLIAR INJURY: TOTAL 40 %

CHLOROSIS 40 %

NECROSIS ____ %

Y-AXIS COUNTS AT 767nm 295487

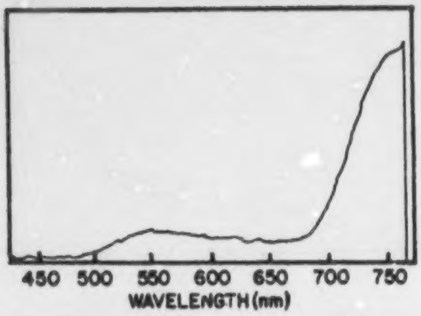

SPECTRUM Soybeans
RECORD 16/30
SO_2 CONC 10480
μg/m^3 1.225 h
FOLIAR INJURY:
TOTAL 10 %
CHLOROSIS 10 %
NECROSIS %
Y-AXIS COUNTS AT 767nm 289169

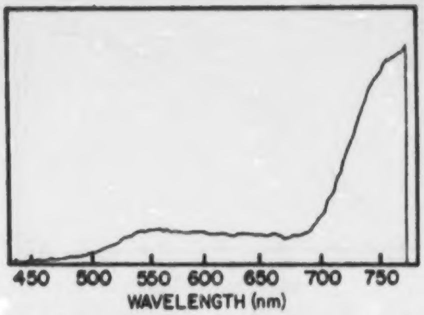

SPECTRUM Soybeans
RECORD 16/31
SO_2 CONC 10480
μg/m^3 1.225 h
FOLIAR INJURY:
TOTAL 20 %
CHLOROSIS 20 %
NECROSIS %
Y-AXIS COUNTS AT 767nm 263240

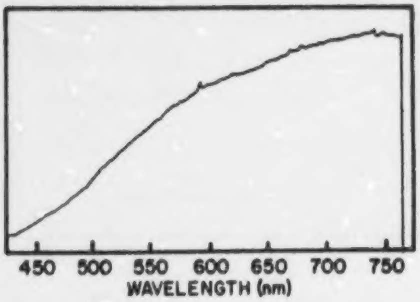

SPECTRUM Gray Panel
RECORD 16/32
SO_2 CONC
μg/m^3 h
FOLIAR INJURY:
TOTAL %
CHLOROSIS %
NECROSIS %
Y-AXIS COUNTS AT 767nm 62081

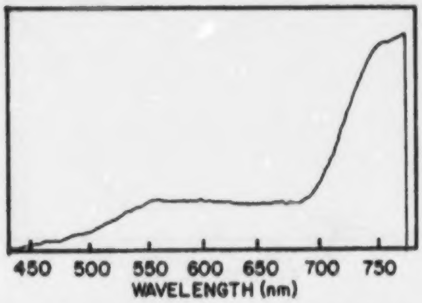

SPECTRUM Soybeans
RECORD 16/33
SO_2 CONC 10480
μg/m^3 1.225 h
FOLIAR INJURY:
TOTAL 70 %
CHLOROSIS 70 %
NECROSIS %
Y-AXIS COUNTS AT 767nm 273993

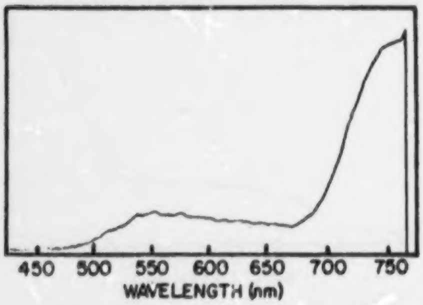

SPECTRUM Soybeans
RECORD 16/34
SO_2 CONC 10480
μg/m^3 1.225 h
FOLIAR INJURY:
TOTAL 60 %
CHLOROSIS 60 %
NECROSIS %
Y-AXIS COUNTS AT 767nm 281202

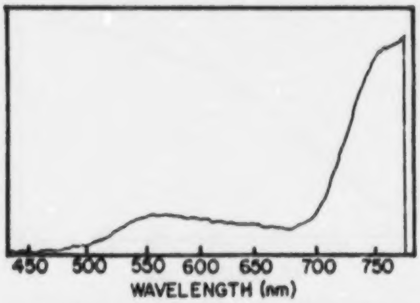

SPECTRUM Soybeans
RECORD 16/35
SO_2 CONC 10480
μg/m^3 1.225 h
FOLIAR INJURY:
TOTAL 50 %
CHLOROSIS 50 %
NECROSIS %
Y-AXIS COUNTS AT 767nm 281202

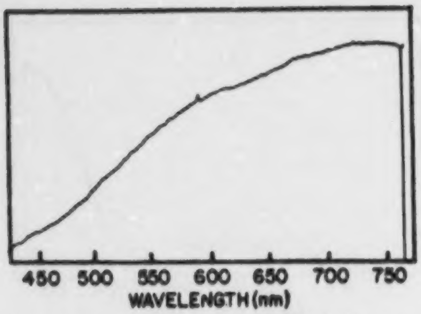

SPECTRUM Gray Panel RECORD 16/36______
SO_2 CONC ______ μg/m³ ______ h
FOLIAR INJURY: TOTAL ______ %
CHLOROSIS ____ %
NECROSIS ____ %
Y-AXIS COUNTS AT 767nm 61893______

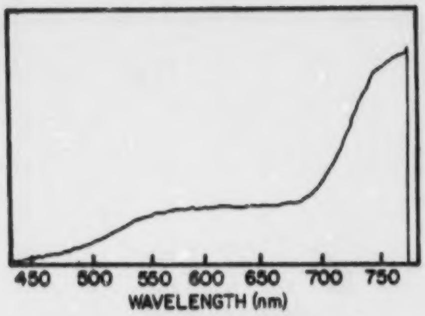

SPECTRUM Soybeans RECORD 16/37______
SO_2 CONC 10480 μg/m³ 1.225 h
FOLIAR INJURY: TOTAL 5 %
CHLOROSIS 5 %
NECROSIS ____ %
Y-AXIS COUNTS AT 767nm 371922______

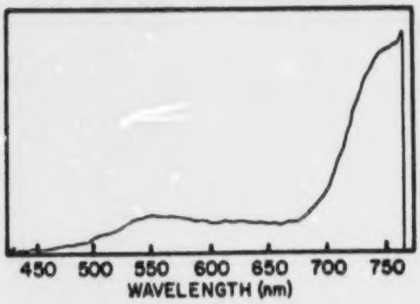

SPECTRUM Soybeans RECORD 16/38______
SO_2 CONC 10480 μg/m³ 1.225 h
FOLIAR INJURY: TOTAL 40 %
CHLOROSIS 40 %
NECROSIS ____ %
Y-AXIS COUNTS AT 767nm 339838______

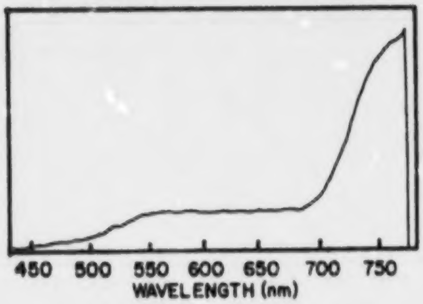

SPECTRUM Soybeans RECORD 16/39______
SO_2 CONC 10480 μg/m³ 1.225 h
FOLIAR INJURY: TOTAL 30 %
CHLOROSIS 30 %
NECROSIS ____ %
Y-AXIS COUNTS AT 767nm 349142______

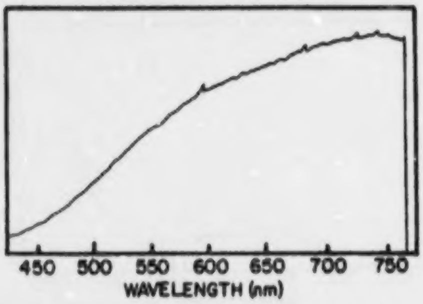

SPECTRUM Gray Panel RECORD 16/40______
SO_2 CONC ______ μg/m³ ______ h
FOLIAR INJURY: TOTAL ______ %
CHLOROSIS ____ %
NECROSIS ____ %
Y-AXIS COUNTS AT 767nm 75186______

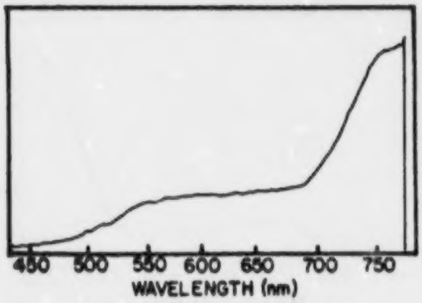

SPECTRUM Soybeans RECORD 16/41______
SO_2 CONC 10480 μg/m³ 1.225 h
FOLIAR INJURY: TOTAL 5 %
CHLOROSIS 5 %
NECROSIS ____ %
Y-AXIS COUNTS AT 767nm 372134______

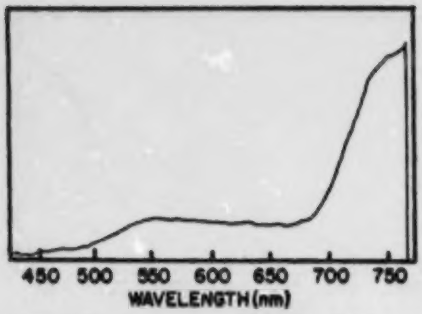

SPECTRUM Soybeans RECORD 16/42
SO$_2$ CONC 10480 μg/m^3 1.225 h
FOLIAR INJURY: TOTAL 10 %
CHLOROSIS 10 %
NECROSIS %
Y-AXIS COUNTS AT 767nm 356491

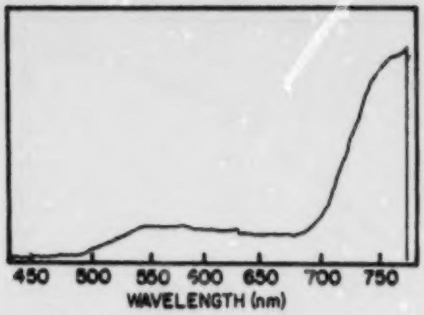

SPECTRUM Soybeans RECORD 16/43
SO$_2$ CONC 10480 μg/m^3 1.225 h
FOLIAR INJURY: TOTAL 10 %
CHLOROSIS 10 %
NECROSIS %
Y-AXIS COUNTS AT 767nm 318079

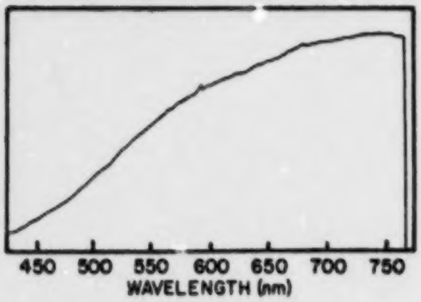

SPECTRUM Gray Panel RECORD 16/44
SO$_2$ CONC μg/m^3 h
FOLIAR INJURY: TOTAL %
CHLOROSIS %
NECROSIS %
Y-AXIS COUNTS AT 767nm 75671

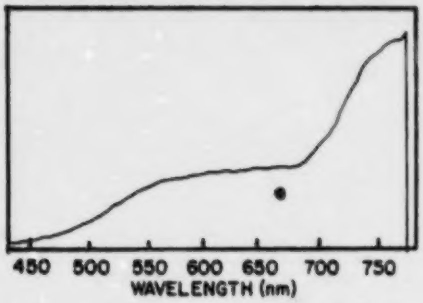

SPECTRUM Soybeans RECORD 16/45
SO$_2$ CONC 10480 μg/m^3 1.225 h
FOLIAR INJURY: TOTAL 10 %
CHLOROSIS 10 %
NECROSIS %
Y-AXIS COUNTS AT 767nm 349469

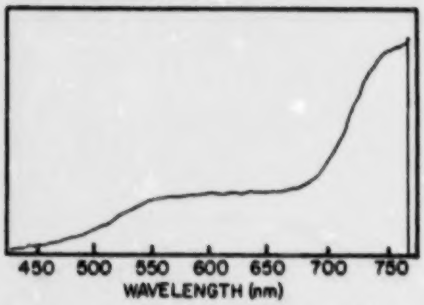

SPECTRUM Soybeans RECORD 16/46
SO$_2$ CONC 10480 μg/m^3 1.225 h
FOLIAR INJURY: TOTAL 40 %
CHLOROSIS 40 %
NECROSIS %
Y-AXIS COUNTS AT 767nm 363707

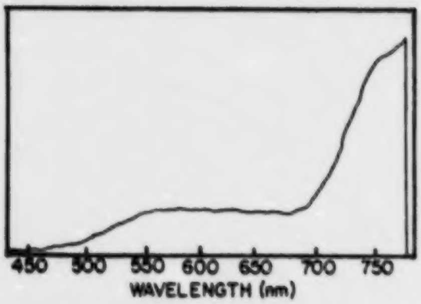

SPECTRUM Soybeans RECORD 16/47
SO$_2$ CONC 10480 μg/m^3 1.225 h
FOLIAR INJURY: TOTAL 30 %
CHLOROSIS 30 %
NECROSIS %
Y-AXIS COUNTS AT 767nm 340792

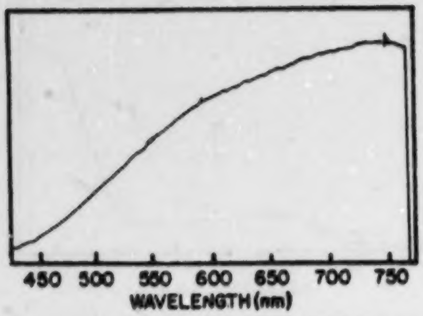

SPECTRUM Gray panel RECORD 16/48

SO_2 CONC ______ μg/m^3 ______ h

FOLIAR INJURY: TOTAL ______ %

CHLOROSIS ____ %

NECROSIS ____ %

Y-AXIS COUNTS AT 767nm 74688

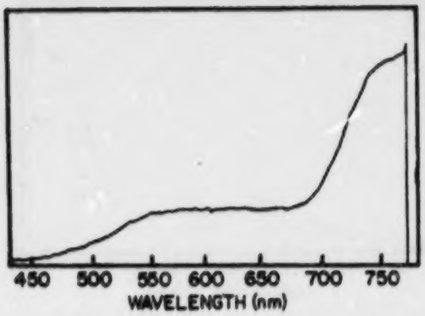

SPECTRUM Soybeans RECORD 16/49

SO_2 CONC 10480 μg/m^3 1.225 h

FOLIAR INJURY: TOTAL 70 %

CHLOROSIS 70 %

NECROSIS ____ %

Y-AXIS COUNTS AT 767nm 360484

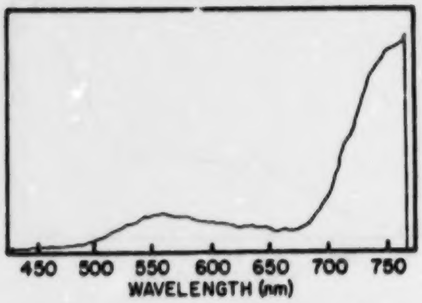

SPECTRUM Soybeans RECORD 16/50

SO_2 CONC 10480 μg/m^3 1.225 h

FOLIAR INJURY: TOTAL 70 %

CHLOROSIS 70 %

NECROSIS ____ %

Y-AXIS COUNTS AT 767nm 350675

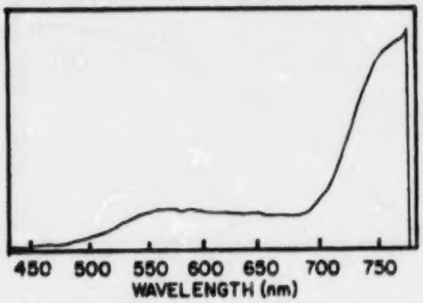

SPECTRUM Soybeans RECORD 16/51

SO_2 CONC 10480 μg/m^3 1.225 h

FOLIAR INJURY: TOTAL 70 %

CHLOROSIS 70 %

NECROSIS ____ %

Y-AXIS COUNTS AT 767nm 336071

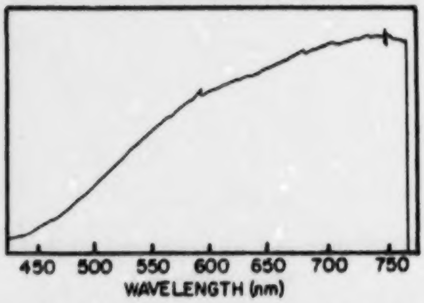

SPECTRUM Gray panel RECORD 16/52

SO_2 CONC ______ μg/m^3 ______ h

FOLIAR INJURY: TOTAL ______ %

CHLOROSIS ____ %

NECROSIS ____ %

Y-AXIS COUNTS AT 767nm 74760

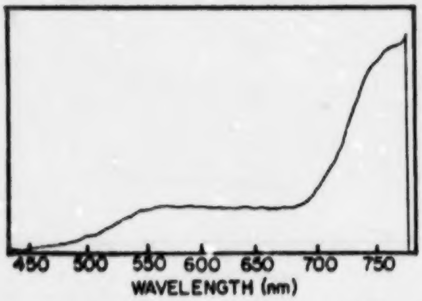

SPECTRUM Soybeans RECORD 16/53

SO_2 CONC 10480 μg/m^3 1.225 h

FOLIAR INJURY: TOTAL 60 %

CHLOROSIS 60 %

NECROSIS ____ %

Y-AXIS COUNTS AT 767nm 339447

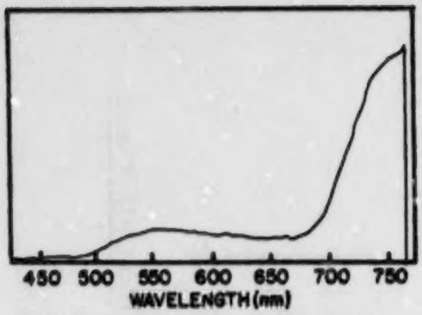

SPECTRUM Soybeans RECORD 16/54

SO_2 CONC 10480 μg/m^3 1.225 h

FOLIAR INJURY: TOTAL 60 %

CHLOROSIS 60 %

NECROSIS ____ %

Y-AXIS COUNTS AT 767nm 353756

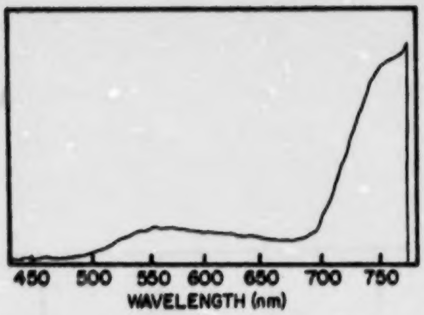

SPECTRUM Soybeans RECORD 16/55

SO_2 CONC 10480 μg/m^3 1.225 h

FOLIAR INJURY: TOTAL 70 %

CHLOROSIS 70 %

NECROSIS ____ %

Y-AXIS COUNTS AT 767nm 326399

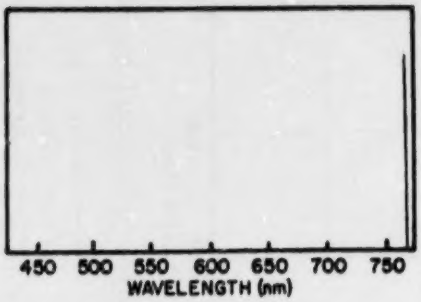

SPECTRUM RECORD

SO_2 CONC ______ μg/m^3 ______ h

FOLIAR INJURY: TOTAL ______ %

CHLOROSIS ____ %

NECROSIS ____ %

Y-AXIS COUNTS AT 767nm 186742

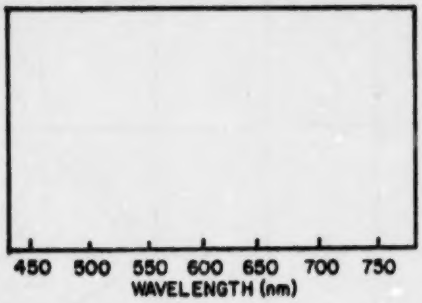

SPECTRUM ______ RECORD ______

SO_2 CONC ______ μg/m^3 ______ h

FOLIAR INJURY: TOTAL ______ %

CHLOROSIS ____ %

NECROSIS ____ %

Y-AXIS COUNTS AT 767nm ______

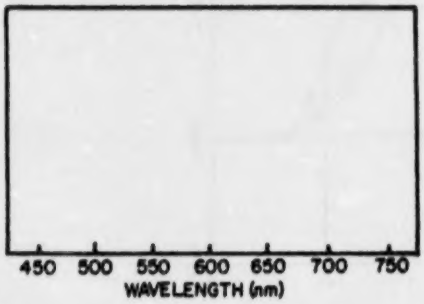

SPECTRUM ______ RECORD ______

SO_2 CONC ______ μg/m^3 ______ h

FOLIAR INJURY: TOTAL ______ %

CHLOROSIS ____ %

NECROSIS ____ %

Y-AXIS COUNTS AT 767nm ______

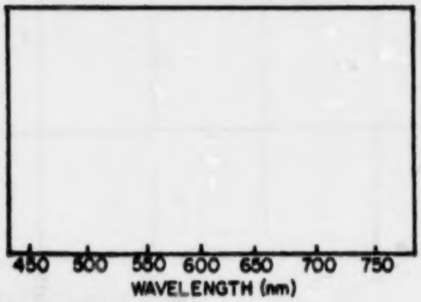

SPECTRUM ______ RECORD ______

SO_2 CONC ______ μg/m^3 ______ h

FOLIAR INJURY: TOTAL ______ %

CHLOROSIS ____ %

NECROSIS ____ %

Y-AXIS COUNTS AT 767nm ______

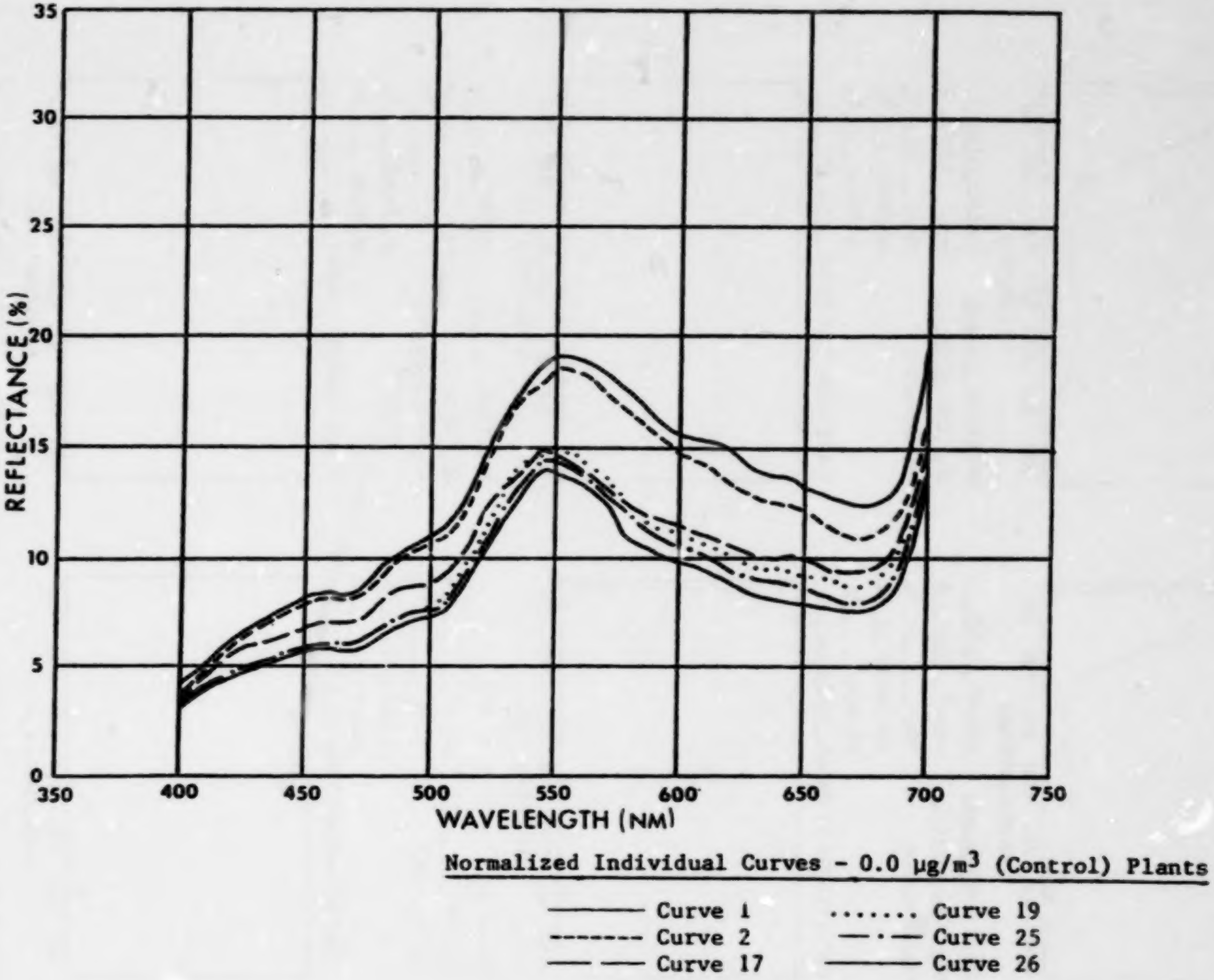

Figure B-2. Normalized Individual Curves of Visible Spectra - Winter Wheat - 0.0 $\mu g/m^3$ (Control)

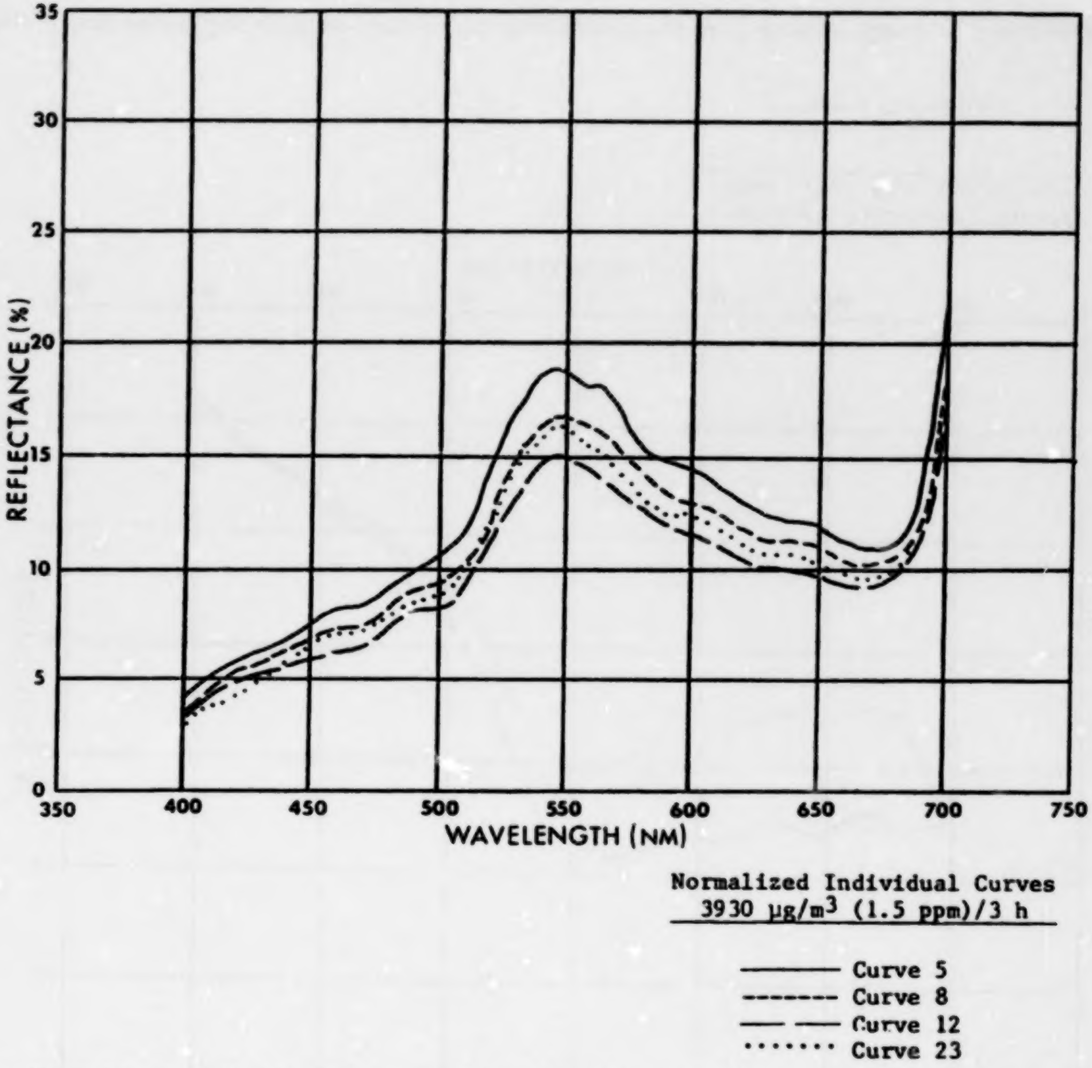

Figure B-3. Normalized Individual Curves of Visible Spectra - Winter Wheat - 3930 $\mu g/m^3$ (1.5 ppm)/3h

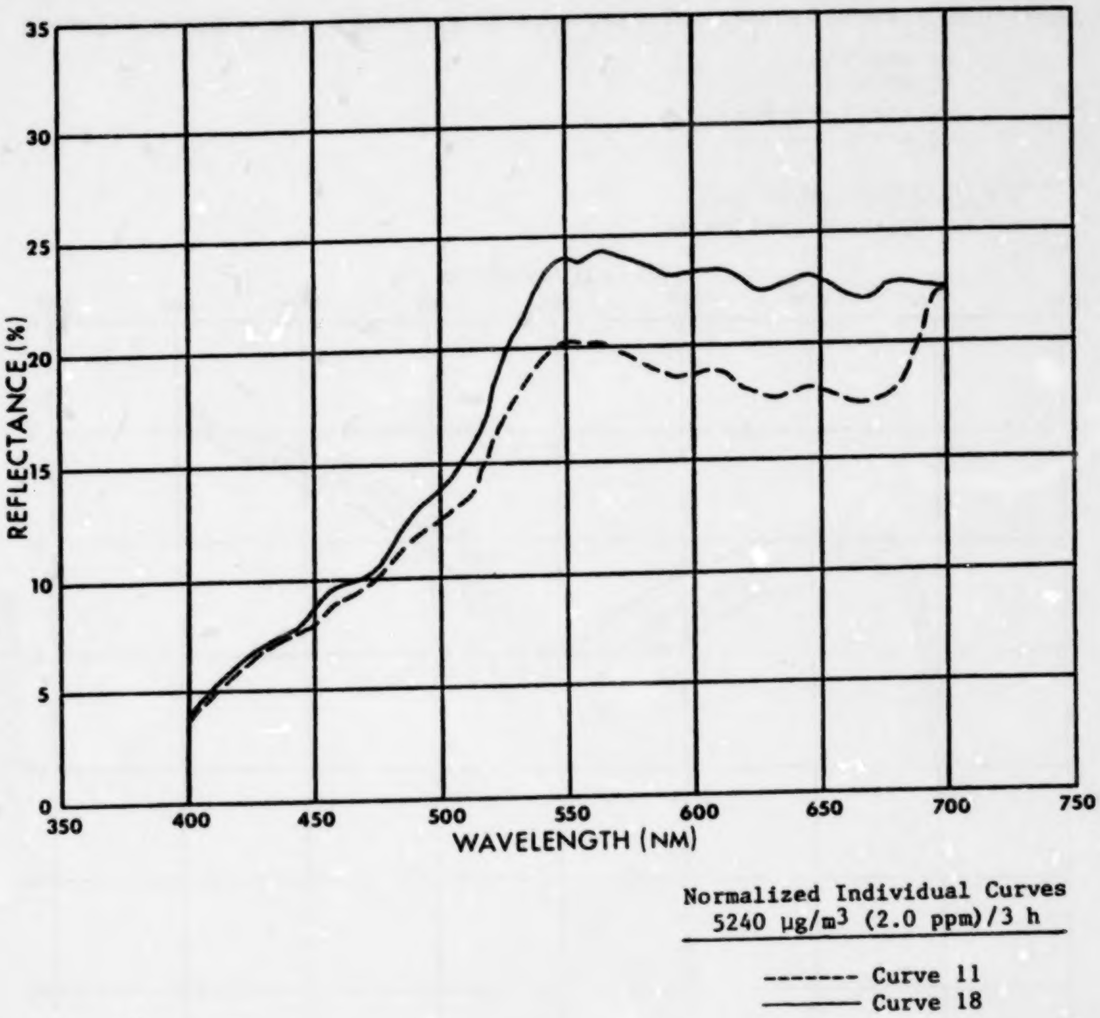

Figure B-4. Normalized Individual Curves of Visible Spectra - Winter Wheat - 5240 $\mu g/m^3$ (2.0 ppm)/3h

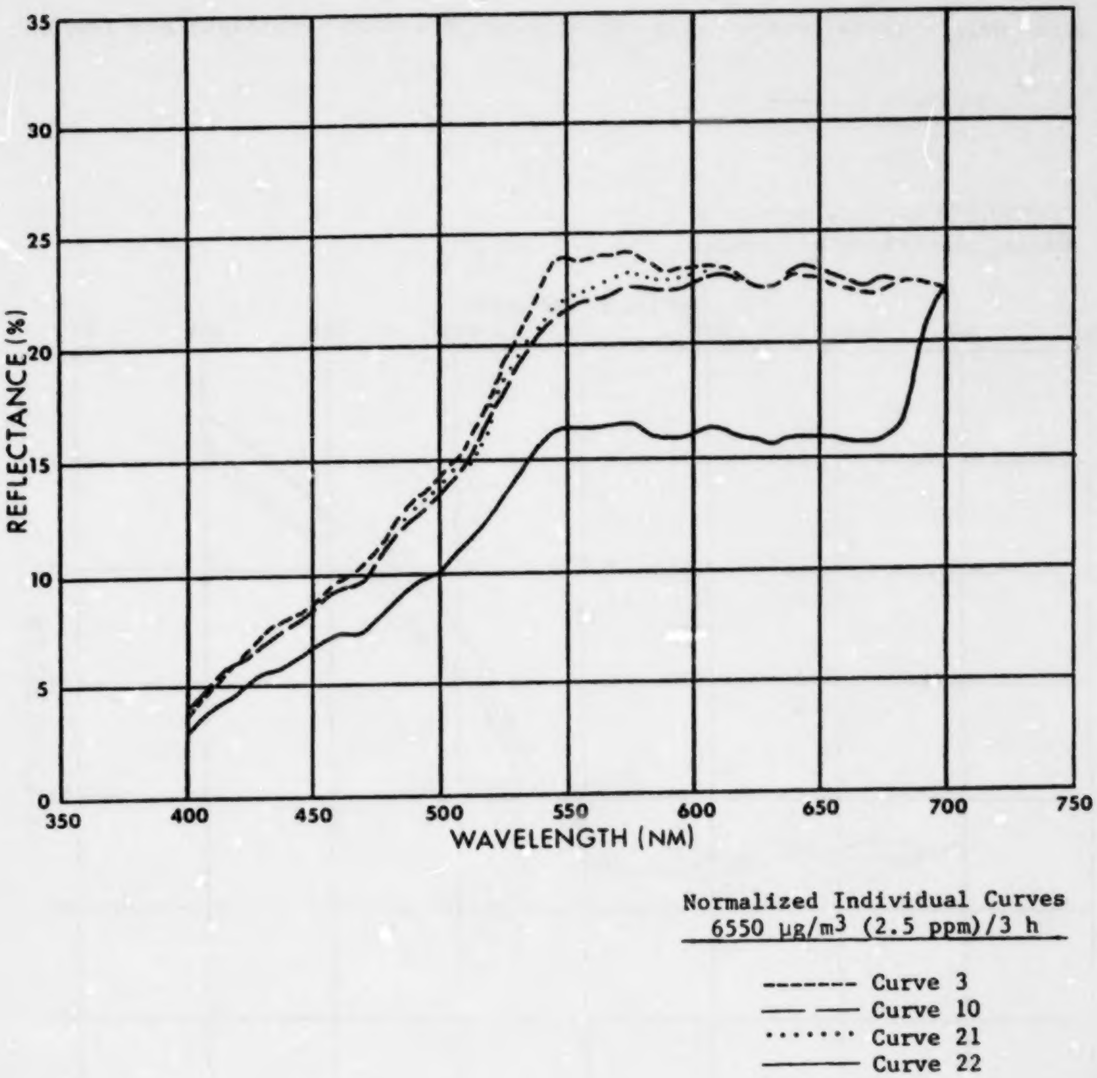

Figure B-5. Normalized Individual Curves of Visible Spectra - Winter Wheat - 6550 $\mu g/m^3$ (2.5 ppm)/3h

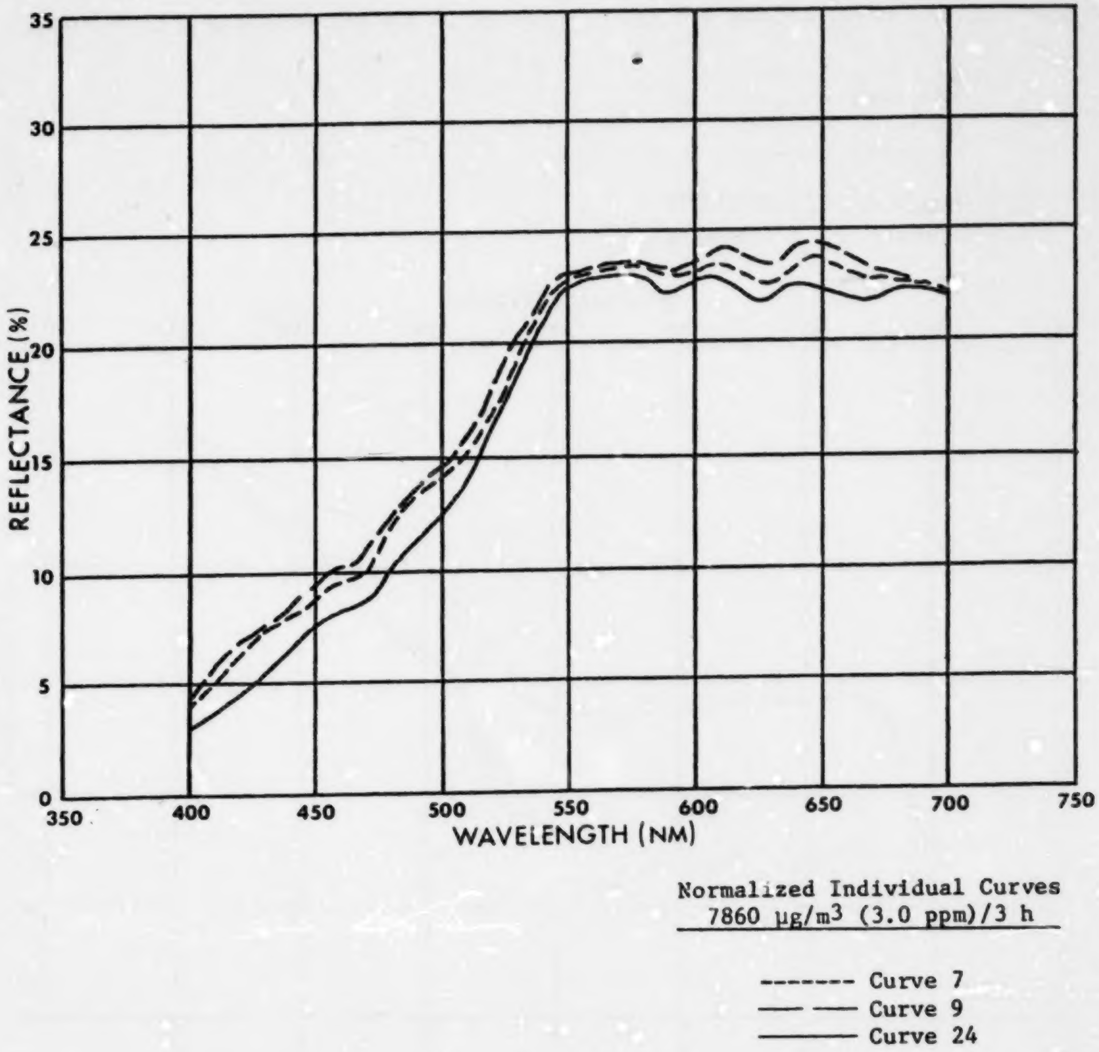

Figure B-6. Normalized Individual Curves of Visible Spectra - Winter Wheat - 7860 $\mu g/m^3$ (3.0 ppm)/3h

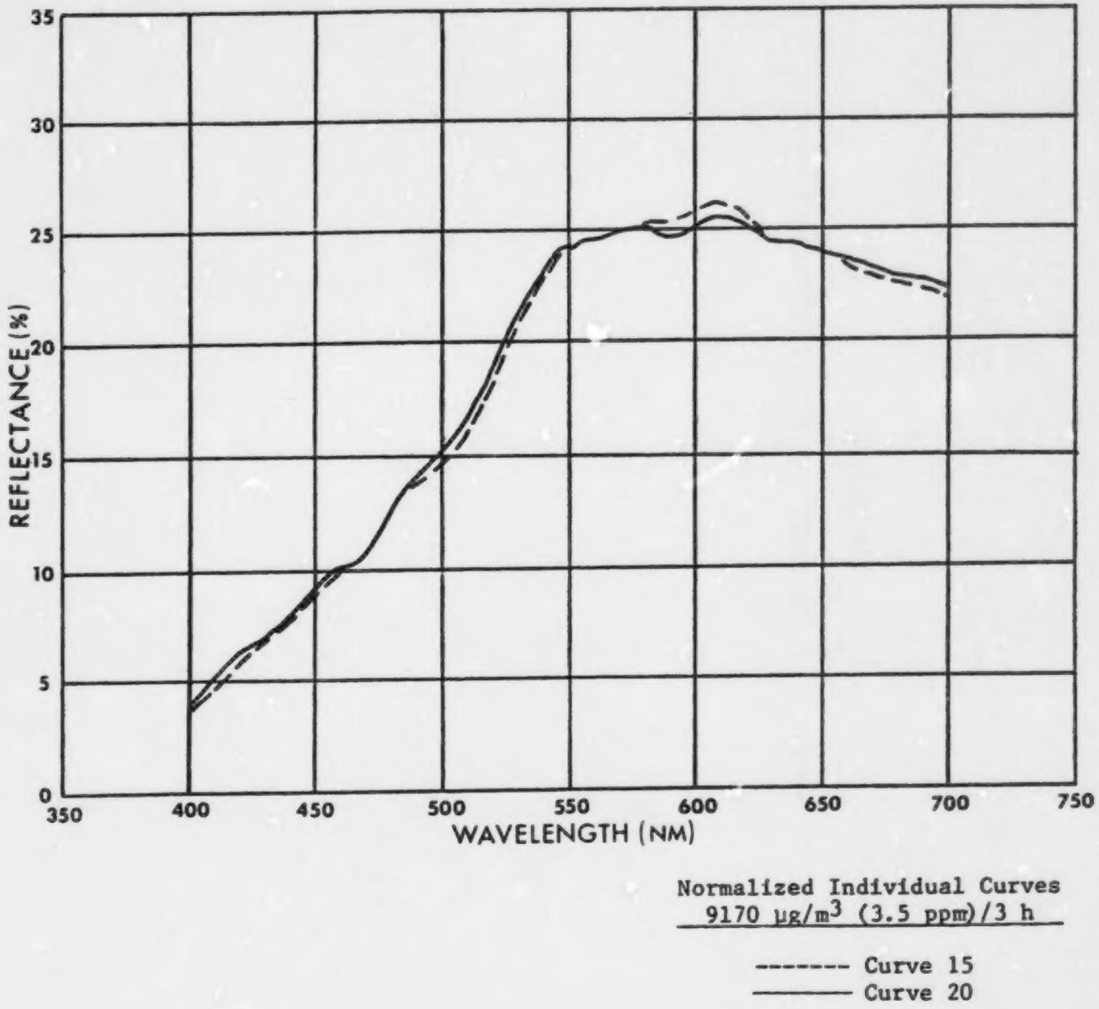

Figure B-7. Normalized Individual Curves of Visible Spectra - Winter Wheat - 9170 μg/m^3 (3.5 ppm)/3h

APPENDIX C

ANALYSIS OF VARIANCE, LABORATORY EXPERIMENT

EXPLANATION OF PROCEDURE FOR ESTIMATING FOLIAR EFFECTS OF SO_2 ON CROP SPECIES

L = Percentage of leaves affected on an average affected plant

A = Percentage of leaf area affected on an average affected leaf

P = Percentage of plants affected in field

L x A = Percentage of total leaf area affected on an average affected plant

L x A x P = T = Average of total leaf area affected in a given field

---

Light foliar injury = up to 10 percent affected.

Moderate = 11-25 percent.

Severe = Greater than 25 percent.

Symptoms of foliar injury:

Chlorosis = visible yellowing of foliage due to bleaching of chlorophyll. Veins on leaves usually remain green if the chlorosis is caused by SO_2.

Necrosis = death of tissue. Appears as ivory, gray, or white interveinal markings which eventually drop out.

TABLE C-1. RESULTS OF ONE-WAY ANALYSIS OF VARIANCE FOR SOYBEANS

Chlorosis

Reflectance Band	Class	$\bar{x}$	s	df	F	Significant ($\alpha = .05$)
Blue	0	7269	1938	4, 135	0.39	No
	1	7660	2709			
	2	7762	2883			
	3	7039	2439			
	4	7691	2215			
Green	0	50966	11029	4, 135	0.04	No
	1	54020	15642			
	2	55141	15936			
	3	53521	15434			
	4	59767	11554			
Red	0	54650	19687	4, 135	0.38	No
	1	58607	26888			
	2	58658	29359			
	3	53267	27498			
	4	61690	26241			
IR	0	272670	23899	4, 135	0.50	No
	1	271735	29836			
	2	276752	27771			
	3	280978	33952			
	4	273767	27122			
IR/R	0	5.48	1.79	4, 135	1.08	No
	1	5.56	2.30			
	2	5.81	2.59			
	3	6.36	2.52			
	4	5.12	1.90			

Measurement for $\bar{x}$ and s in counts, except IR/R ratio.

TABLE C-2. RESULTS OF ONE-WAY ANALYSIS OF VARIANCE FOR SOYBEANS

Necrosis

Reflectance Band	Class	$\bar{x}$	s	df	F	Significant $(\alpha = .05)$
Blue	0	7.269×10^{3}	1.794×10^{3}	1, 25	0.83	No
	1+2+3	8.595×10^{3}	2.141×10^{3}			
Green	0	5.098×10^{4}	1.021×10^{4}	1, 25	1.80	No
	1+2+3					
Green	0	5.098×10^{4}	1.021×10^{4}	1, 10	4.94	Yes
	2+3	6.647×10^{4}	1.173×10^{4}			
Red	0	5.465×10^{4}	1.824×10^{4}	1, 25	1.93	No
	1+2+3	8.554×10^{4}	2.599×10^{4}			
Red	0	5.465×10^{4}	1.824×10^{4}	1, 10	7.34	Yes
	2+3	9.133×10^{4}	2.456×10^{4}			
Infrared (IR)	0	2.727×10^{5}	2.213×10^{4}	1, 25	4.93	Yes
	1+2+3	2.617×10^{5}	8.362×10^{3}			
Infrared (IR)	0	2.727×10^{5}	2.213×10^{4}	1, 10	0.30	No
	2+3	2.661×10^{5}	1.234×10^{4}			
IR/R	0	5.48	1.66	1, 25	0.49	No
	1+2+3	3.66	1.27			
IR/R	0	5.48	1.66	1, 10	5.96	No
	2+3	3.21	1.11			

$\bar{x}$ and s in counts, except IR/R ratio.

TABLE C-3. RESULTS OF ONE-WAY ANALYSIS OF VARIANCE FOR WINTER WHEAT

Reflectance Band	Class	$\bar{x}$	s	df	F	Significant (α = .05)
			Necrosis			
Blue %	1	6.4	.44			
	2	7.3	.17	3, 17	13.92	Yes
	3	7.9	.37			
	4	8.7	.32			
Green %	1	16.2	4.14			
	2	17.6	2.89	3, 17	16.78	Yes
	3	21.1	6.78			
	4	23.7	.25			
Red %	1	10.3	3.86			
	2	12.4	9.62	3, 17	36.44	Yes
	3	21.6	9.68			
	4	24.3	1.84			
			Chlorosis			
Blue %	1	6.4	.44			
	2	7.7	.36	2, 18	10.45	Yes
	3	8.4	.78			
Green %	1	16.2	4.14			
	2	20.2	10.22	2, 18	6.41	Yes
	3	21.9	7.20			
Red %	1	10.3	3.86			
	2	19.0	33.57	2, 18	6.54	Yes
	3	20.3	32.76			

$\bar{x}$ and s data in percent reflectance

APPENDIX D

OBSERVATIONS OF FOLIAR INJURY

TABLE D-1. OBSERVATIONS OF SO_2-EXPOSED SOYBEAN FIELDS NEAR SHAWNEE STEAM PLANT, 1978

Field Designation	Point	LxAxP (%)	Mean Injury (%)
3	1	2.0	0.7
	2	0	
	3	0	
	4	0	
	5	0.4	
	6	1.2	
	7	1.6	
4	1	3.0	2.0
	2	1.2	
	3	1.4	
	4	1.6	
1107	1	14.4	12.6
	2	10.5	
	3	12.6	
1	No point data		
2	1	12.0	13.5
	2	16.2	
	3	13.5	
7	1	9.0	7.5
	2	7.5	
	3	6.0	
1119	1	6.0	6.0
1117	1	0.0	0.0
1122	1	0.0	0.0
1121	1	0.0	0.0
1120	1	3.2	3.2
1118	1	4.0	4.0
13	1	9.0	9.0
15	1	1.8	4.8
	2	4.8	
	3	6.0	
16	1	3.2	6.0
	2	4.0	
	3	6.0	
	4	7.2	
	5	10.0	
17	1	2.4	2.4
	2	2.0	
	3	2.7	

(continued)

TABLE D-1 (continued)

Field Designation	Point	LxAxP (%)	Mean Injury (%)
18	1	1.2	1.8
	2	1.8	
	3	1.8	
19	1	9.6	11.2
	2	2.0	
	3	12.8	
20	1	12.8	12.8
	2	8.4	
	3	12.0	
21	1	9.0	16.0
	2	16.0	
	3	22.5	
22	1	25.0	18.0
	2	24.0	
	3	13.5	
23	1	0.4	0.8
	2	0.8	
	3	0.4	
25	1	0.0	0.0
	2	0.0	
	3	0.0	
	4	0.0	
	5	0.0	
26	1	0.0	0.0
	2	0.0	
	3	0.0	
	4	0.0	
	5	0.0	
14	1	0.6	0.6
8	1	0.0	0.0
1143	1	12.0	19.2
	2	28.0	
	3	21.6	
1145	1	0.0	0.0

(continued)

TABLE D-1 (continued)

Field Designation	Point	LxAxP (%)	Mean Injury (%)
1137	1	35.0	35.0
	2	40.0	
1114	1	3.2	9.0
	2	12.0	
	3	4.8	
	4	8.4	
	5	16.8	
	6	9.0	
	7	19.2	
1113	1	4.8	4.8
	2	1.2	
	3	7.5	
	4	4.8	
	5	4.5	
1112	1	2.4	2.4
	2	4.8	
	3	1.2	
	4	3.2	
1110	1	10.0	12.0
	2	4.8	
	3	18.0	
	4	4.5	
	5	16.2	
1109	1	0.0	4.8
	2	6.0	
	3	6.0	
1108	1	6.0	4.5
	2	3.6	
	3	7.2	

TABLE D-2. COLBERT STEAM PLANT AREA - 1978
SOYBEAN FIELD 1500
INTENSIVE STUDY

OBS	POINT	X	Y	RIR	RR	RG	CHL	PDP	PLANTH	ELEV
1	3	1.5	2.5	0.179	0.033	0.031	0.088	69	9	481
2	4	2.0	2.0	0.144	0.046	0.051	0.060	66	10	480
3	5	3.0	1.5	0.174	0.034	0.032	0.038	66	8	480
4	6	2.5	2.0	0.147	0.037	0.032	0.057	58	8	482
5	7	2.0	2.5	0.144	0.048	0.039	0.088	49	9	483
6	8	2.0	3.0	0.167	0.035	0.029	0.086	60	7	482
7	9	1.5	3.5	0.167	0.036	0.034	0.086	66	7	480
8	10	2.5	3.5	0.176	0.035	0.036	0.038	73	8	482
9	11	2.5	3.0	0.164	0.035	0.031	0.081	63	11	484
10	12	3.0	2.5	.	.	.	.	.	.	.
11	13	3.5	2.0	0.142	0.058	0.044	0.087	64	7	482
12	14	3.5	1.5	0.128	0.049	0.048	0.171	56	7	479
13	15	4.0	2.0	0.144	0.058	0.044	0.076	44	8	483
14	16	4.0	2.5	0.144	0.040	0.038	0.033	62	9	486
15	17	3.5	2.5	0.147	0.041	0.033	0.011	53	9	486
16	18	3.0	3.0	0.180	0.030	0.030	0.033	75	5	483
17	19	3.0	3.5	0.168	0.032	0.029	0.114	67	8	481
18	20	3.5	3.5	0.183	0.036	0.044	0.076	85	6	482
19	21	3.5	3.0	0.173	0.032	0.030	0.028	69	7	484
20	22	4.0	3.0	0.140	0.051	0.039	0.038	47	8	486
21	23	4.5	2.5	0.147	0.071	0.064	0.114	47	7	488
22	24	4.5	2.5	0.148	0.059	0.041	0.043	42	7	484
23	25	.	.	.	.	.	.	.	.	.
24	26	5.0	2.0	0.144	0.060	0.045	0.058	44	7	488
25	27	5.0	2.5	0.153	0.042	0.039	0.029	60	7	488
26	28	4.5	3.0	0.155	0.033	0.032	0.129	67	7	486
27	29	4.5	3.5	0.155	0.033	0.032	0.000	67	7	485
28	30	4.0	4.0	0.173	0.036	0.034	0.029	66	7	486
29	31	3.5	4.5	0.148	0.040	0.034	0.043	57	7	490
30	32	3.5	5.0	0.177	0.051	0.053	0.100	65	6	492
31	33	4.0	5.0	0.180	0.037	0.042	0.058	79	7	494
32	34	4.0	4.5	0.159	0.043	0.039	0.114	60	7	494
33	35	4.5	4.5	0.160	0.037	0.037	0.025	69	8	490
34	36	5.0	4.0	0.185	0.031	0.033	0.025	80	8	486
35	37	5.0	3.5	0.176	0.035	0.040	0.025	80	8	486
36	38	5.5	3.0	0.148	0.040	0.045	0.038	71	8	488
37	39	5.5	2.5	0.140	0.049	0.040	0.201	49	6	488
38	40	6.0	2.0	0.166	0.037	0.038	0.013	70	8	483
39	41	7.0	2.0	0.174	0.033	0.034	0.150	75	8	484
40	42	6.5	2.5	0.148	0.080	0.055	0.088	36	9	487
41	43	6.0	3.0	0.160	0.039	0.032	0.038	56	8	489
42	44	6.0	3.5	0.164	0.034	0.030	0.014	64	1	488
43	45	5.5	4.0	0.166	0.034	0.036	0.033	75	9	487
44	46	5.0	4.5	0.174	0.033	0.032	0.043	71	7	488
45	47	4.5	4.5	0.160	0.040	0.042	0.058	69	7	492
46	48	4.5	5.0	0.163	0.043	0.044	0.038	66	8	496
47	49	4.0	5.5	0.161	0.036	0.033	0.043	64	7	496
48	50	5.0	5.5	0.171	0.034	0.037	0.014	75	7	495
49	51	5.5	5.0	0.201	0.033	0.039	0.029	87	7	491
50	52	5.5	4.5	.	.	.	.	.	.	.
51	53	6.0	4.0	0.182	0.032	0.037	0.025	83	8	488
52	54	6.5	3.5	0.174	0.034	0.038	0.240	79	5	489
53	55	6.5	3.0	0.168	0.036	0.038	0.129	75	7	490
54	56	7.0	2.5	0.166	0.034	0.035	0.171	72	7	489

TABLE D-2 (continued)

OBS	POINT	X	Y	RIR	RR	RG	CHL	PDP	PLANTH	ELEV
55	57	7.5	2.5	0.131	0.047	0.038	0.126	49	8	487
56	58	7.5	2.0	0.176	0.037	0.039	0.043	76	7	484
57	59	8.5	2.0	0.170	0.034	0.034	0.088	72	9	486
58	60	8.0	2.5	0.112	0.041	0.031	0.011	46	9	490
59	61	7.5	3.0	0.115	0.032	0.027	0.013	56	8	491
60	62	7.5	3.5	0.126	0.032	0.030	0.000	63	6	491
61	63	7.0	3.5	0.153	0.028	0.031	0.086	80	7	490
62	64	6.5	4.0	0.148	0.027	0.027	0.000	74	7	489
63	65	6.5	4.5	0.147	0.022	0.026	0.013	91	8	489
64	66	6.0	5.0	0.157	0.025	0.034	0.022	98	9	490
65	67	5.5	5.5	0.139	0.021	0.024	0.043	85	7	496
66	68	5.0	6.0	0.144	0.026	0.028	0.043	79	7	498
67	69	6.0	6.0	0.132	0.029	0.035	0.013	.	8	498
68	70	6.5	5.5	0.153	0.023	0.030	0.025	96	8	496
69	71	6.5	5.0	0.140	0.025	0.032	0.025	92	8	491
70	72	7.0	4.5	0.153	0.023	0.026	0.029	86	7	490
71	73	7.5	4.0	0.139	0.025	0.027	0.014	80	7	490
72	74	7.5	3.5	0.152	0.025	0.028	0.038	81	8	491
73	75	8.0	3.0	0.132	0.034	0.034	0.038	.	8	493
74	76	8.5	3.0	0.131	0.035	0.039	0.000	71	7	492
75	77	9.0	2.5	0.152	0.029	0.033	0.043	79	7	489
76	78	9.5	2.0	0.131	0.034	0.031	0.140	.	7	488
77	79	10.0	2.0	0.105	0.038	0.027	0.030	44	10	489
78	80	.	.	.	.	.	.	.	.	.
79	81	12.0	1.5	0.144	0.035	0.033	0.076	65	8	487
80	82	11.5	1.5	0.104	0.038	0.026	0.076	42	8	490
81	83	11.0	2.0	0.115	0.040	0.028	0.050	44	8	493
82	84	10.5	2.5	0.179	0.023	0.023	0.100	80	8	493
83	85	10.0	2.5	0.143	0.026	0.032	0.038	88	8	492
84	86	9.5	3.0	0.115	0.031	0.028	0.029	60	7	492
85	87	9.0	3.0	0.137	0.038	0.038	0.014	65	7	495
86	88	8.5	3.5	0.155	0.031	0.034	0.022	79	9	493
87	89	8.0	4.0	0.148	0.026	0.028	0.020	79	10	491
88	90	7.5	4.5	0.152	0.024	0.029	0.025	89	8	490
89	91	7.5	5.0	0.145	0.022	0.023	0.013	79	8	490
90	92	7.0	5.5	0.156	0.029	0.034	0.058	81	7	492
91	93	6.5	6.0	0.139	0.030	0.032	0.029	74	7	494
92	94	6.5	6.5	0.140	0.028	0.032	0.000	80	8	498
93	95	7.0	6.5	0.180	0.033	0.024	0.010	76	10	498
94	96	7.0	6.0	0.171	0.031	0.029	0.020	69	10	495
95	97	7.5	5.5	0.166	0.030	0.026	0.011	65	9	492
96	98	8.0	5.5	0.199	0.031	0.033	0.013	79	8	491
97	99	8.0	5.0	0.194	0.033	0.036	0.011	82	9	490
98	100	8.5	4.5	0.196	0.033	0.034	0.014	79	7	491
99	101	9.0	4.0	0.168	0.034	0.036	0.029	75	7	493
100	102	9.5	3.5	0.159	0.033	0.028	0.023	62	8	494
101	103	10.0	3.5	0.176	0.037	0.033	0.076	64	8	493
102	104	10.0	3.0	0.179	0.033	0.032	0.025	70	8	494
103	105	10.5	2.5	0.182	0.037	0.039	0.011	75	9	494
104	106	11.0	2.5	0.180	0.031	0.031	0.013	75	8	495
105	107	11.5	2.0	0.133	0.040	0.028	0.000	46	7	493
106	108	12.0	2.0	0.182	0.042	0.038	0.076	63	8	490
107	109	12.5	1.5	0.188	0.034	0.032	0.058	71	7	488
108	110	.	.	0.173	0.032	0.028	0.000	66	8	487

TABLE D-2 (continued)

OBS	POINT	X	Y	RIR	RR	RG	CHL	PDP	PLANTH	ELEV
109	111	13.5	1.5	0.168	0.034	0.028	0.013	61	8	486
110	112	14.5	1.5	0.159	0.042	0.036	0.038	57	8	486
111	113	15.0	1.0	0.160	0.031	0.027	0.067	65	6	485
112	114	15.0	1.5	0.130	0.033	0.023	0.038	50	9	487
113	115	14.5	1.5	0.134	0.044	0.029	0.071	43	7	489
114	116	14.0	2.0	0.116	0.044	0.030	0.000	42	7	489
115	117	13.5	2.0	0.139	0.038	0.029	0.043	52	7	490
116	118	13.0	2.0	0.102	0.036	0.026	0.014	45	7	492
117	119	12.5	2.5	0.128	0.046	0.029	0.011	40	9	494
118	120	12.0	2.5	0.130	0.043	0.030	0.000	45	9	495
119	121	11.5	3.0	0.166	0.032	0.031	0.013	70	8	494
120	122	11.0	3.0	0.173	0.037	0.043	0.044	79	9	493
121	123	10.5	3.5	0.164	0.037	0.042	0.058	77	7	492
122	124	10.0	4.0	0.167	0.037	0.041	0.038	76	8	492
123	125	9.5	4.0	0.145	0.035	0.033	0.044	64	9	492
124	126	9.0	4.5	0.167	0.033	0.034	0.038	75	8	491
125	127	8.5	5.0	.	.	.	.	.	.	.
126	128	8.5	5.5	0.167	0.032	0.035	0.000	78	8	492
127	129	8.0	6.0	0.176	0.034	0.036	0.000	76	8	495
128	130	7.5	6.5	0.142	0.036	0.035	0.025	.	8	500
129	131	7.5	7.0	0.138	0.034	0.034	0.014	67	7	500
130	132	7.0	7.5	0.149	0.030	0.029	0.114	69	7	500
131	133	7.5	7.5	0.149	0.035	0.035	0.000	69	8	498
132	134	8.0	7.0	0.161	0.032	0.033	0.013	74	8	498
133	135	8.0	6.5	0.137	0.041	0.040	0.025	62	8	498
134	136	8.5	6.5	0.199	0.035	0.035	0.023	73	8	494
135	137	9.0	6.0	0.188	0.032	0.033	0.013	76	8	492
136	138	9.0	5.5	0.155	0.032	0.026	0.000	60	8	492
137	139	9.5	5.0	0.158	0.031	0.030	0.029	72	7	492
138	140	10.0	4.5	0.190	0.032	0.036	0.000	84	8	491
139	141	10.5	4.0	0.185	0.033	0.035	0.013	77	8	491
140	142	11.0	4.0	0.180	0.037	0.034	0.013	66	8	492
141	143	11.5	3.5	0.160	0.036	0.035	0.050	66	8	494
142	144	12.0	3.5	0.174	0.044	0.038	0.014	59	7	495
143	145	12.5	3.0	0.153	0.042	0.037	0.010	58	10	496
144	146	13.0	2.5	0.138	0.052	0.045	0.000	50	7	496
145	147	13.5	2.5	0.138	0.049	0.035	0.022	50	9	494
146	148	14.0	2.5	0.148	0.052	0.038	0.025	46	8	493
147	149	14.5	2.0	0.151	0.053	0.036	0.038	42	8	491
148	150	15.0	2.0	0.137	0.042	0.028	0.013	44	8	490
149	151	15.5	2.0	0.148	0.042	0.038	0.013	50	8	488
150	152	16.0	2.0	0.151	0.034	0.026	0.025	53	8	488
151	153	16.5	2.0	0.152	0.034	0.029	0.033	60	9	487
152	154	17.0	2.0	0.140	0.031	0.024	0.000	56	9	486
153	155	17.5	2.0	0.134	0.031	0.026	0.000	57	9	485
154	156	18.0	2.5	0.111	0.045	0.037	0.013	47	8	486
155	157	17.5	2.5	0.124	0.054	0.046	0.038	47	8	486
156	158	16.5	2.5	0.130	0.041	0.032	0.050	50	8	488
157	159	16.0	2.5	0.140	0.050	0.046	0.038	54	8	489
158	160	15.5	2.5	0.134	0.065	0.051	0.014	42	7	490
159	161	15.0	2.5	0.133	0.051	0.038	0.000	44	6	491
160	162	14.5	2.5	0.138	0.037	0.034	0.017	61	8	492
161	163	14.0	3.0	0.139	0.040	0.033	0.000	54	8	493
162	164	13.5	3.0	0.143	0.034	0.028	0.043	58	7	493

TABLE D-2 (continued)

OBS	POINT	X	Y	RIB	RR	RG	CHL	POP	PLANTH	ELEV
163	165	13.0	3.5	0.121	0.034	0.028	0.000	55	9	493
164	166	12.5	3.5	0.112	0.046	0.029	0.011	38	9	493
165	167	12.0	4.0	0.157	0.038	0.040	0.000	70	8	493
166	168	11.5	4.0	0.159	0.044	0.045	0.000	65	9	492
167	169	11.0	4.5	0.166	0.037	0.037	0.013	70	8	491
168	170	10.5	4.5	0.183	0.032	0.038	0.000	86	10	491
169	171	10.0	5.0	0.142	0.037	0.042	0.013	74	8	494
170	172	9.5	5.5	0.131	0.043	0.041	0.033	57	9	492
171	173	9.5	6.0	0.180	0.031	0.033	0.011	80	9	491
172	174	9.0	6.5	0.171	0.028	0.031	0.000	81	8	492
173	175	8.5	7.0	0.133	0.027	0.028	0.000	72	7	494
174	176	8.5	7.5	0.156	0.029	0.032	0.011	80	9	494
175	177	8.0	8.0	0.133	0.025	0.031	0.000	85	8	496
176	178	8.5	8.5	0.155	0.025	0.029	0.011	87	9	494
177	179	9.0	8.0	0.176	0.028	0.032	0.000	86	3	492
178	180	9.0	7.5	0.168	0.031	0.032	0.013	76	8	492
179	181	9.5	7.0	0.174	0.030	0.034	0.025	82	8	491
180	182	9.5	6.5	0.183	0.032	0.039	0.014	88	7	491
181	183	10.0	6.0	0.183	0.032	0.039	0.013	88	8	490
182	184	10.5	5.5	0.167	0.027	0.029	0.000	82	9	491
183	185	11.0	5.0	0.173	0.030	0.033	0.000	80	8	490
184	186	11.5	5.0	0.182	0.033	0.038	0.000	85	9	490
185	187	12.0	4.5	0.167	0.032	0.030	0.000	69	8	490
186	188	12.5	4.5	0.167	0.032	0.034	0.000	74	9	490
187	189	12.5	4.0	0.149	0.029	0.032	0.000	80	9	490
188	190	13.0	4.0	0.180	0.031	0.034	0.013	79	8	490
189	191	13.5	3.5	0.170	0.031	0.033	0.000	78	9	490
190	192	14.0	3.5	0.142	0.025	0.028	0.013	79	8	490
191	193	15.0	3.0	0.161	0.044	0.046	0.013		8	490
192	194	15.5	3.0	0.148	0.035	0.031	0.000	61	7	489
193	195	16.0	3.0	0.148	0.055	0.043	0.025	46	8	489
194	196	16.5	3.0	0.161	0.044	0.046	0.025	67	8	487

TABLE D-3. OBSERVATIONS OF FOLIAR INJURY TO WINTER WHEAT EXPERIMENTAL PLOT

Subplot	Row	Necrosis (%)	Chlorosis (%)	SO_2 Conc.[a]
C1	1	9	0	0
	2	9	0	0
	3	9	0	0
C2	1	8.5	0	0
	2	8.5	0	0
	3	X[b]	0	0
C3	1	7	0	0
	2	7	0	0
	3	7	0	0
C4	1	8	0	0
	2	8	0	0
	3	8	0	0
C5	1	10.5	0	0
	2	10.5	0	0
	3	10.5	0	0
C6	1	11.5	0	0
	2	11.5	0	0
	3	11.5	0	0
C7	1	11	0	0
	2	11	0	0
	3	11	0	0
C8	1	11.5	0	0
	2	11.5	0	0
	3	11.5	0	0
C9	1	6	0	0
	2	6	0	0
	3	6	0	0
C10	1	6.5	0	0
	2	X	0	0
	3	X	0	0
C11	1	6.5	0	0
	2	6.5	0	0
	3	6.5	0	0
C12	1	6.5	0	0
	2	6.5	0	0
	3	6.5	0	0

(continued)

TABLE D-3 (continued)

Subplot	Row	Necrosis (%)	Chlorosis (%)	SO_2 Conc.[a]
C13	1	8	0	0
	2	8	0	0
	3	8	0	0
C14	1	8.5	0	0
	2	8.5	0	0
	3	8.5	0	0
A1	1	90	0	4
	2	90	0	4
	3	90	0	4
A2	1	10	0	1
	2	10	0	1
	3	10	0	1
A3	1	92.5	0	4
	2	92.5	0	4
	3	92.5	0	4
A4	1	89.5	0	3
	2	89.5	0	3
	3	89.5	0	3
A5	1	52.5	0	2
	2	52.5	0	2
	3	52.5	0	2
A6	1	58	0	3
	2	58	0	3
	3	58	0	3
A7	1	86.5	0	2
	2	86.5	0	2
	3	86.5	0	2
A8	1	29	0	1
	2	29	0	1
	3	29	0	1
A9	1	51.5	0	3
	2	51.5	0	3
	3	51.5	0	3
A10	1	38.5	0	2
	2	38.5	0	2
	3	X	0	2

(continued)

TABLE D-3 (continued)

Subplot	Row	Necrosis (%)	Chlorosis (%)	SO_2 Conc.[a]
A11	1	19.5	0	1
	2	19.5	0	1
	3	19.5	0	1
A12	1	55	0	4
	2	55	0	4
	3	55	0	4
A13	1	55	0	2
	2	55	0	2
	3	55	0	2
A14	1	53.5	0	3
	2	53.5	0	3
	3	53.5	0	3
A15	1	69	0	4
	2	69	0	4
	3	69	0	4
A16	1	19	0	1
	2	19	0	1
	3	19	0	1

[a] Concentration
Number 0 = 0 $\mu g/m^3$ for 2-h avg.
1 = 2620
2 = 5240
3 = 7860
4 = 10480

[b] X = not observed

TABLE D-4. SO_2 EXPOSURE, OBSERVATION, AND SCANNING DATES--WINTER WHEAT EXPERIMENTAL PLOT

SO_2 EXPOSURE DATES

Subplot	Month	Day	Year
A1	5	1	1979
A2	5	1	
A3	5	7	
A4	5	7	
A5	5	1	
A6	5	1	
A7	5	7	
A8	5	7	
A9	4	30	
A10	4	30	
A11	4	30	
A12	4	30	
A13	4	27	
A14	4	27	
A15	4	27	
A16	4	27	

OBSERVATION DATES

All observations done on 5-14-79

SCANNING DATES

Subplots	Month	Day	Year
C1,C2,C3,C4,A1,A2,A3,A4	5	10	1979
All others	5	14	1979

TABLE D-5. REFLECTANCE, FOLIAR INJURY, AND YIELD OF SO$_2$-AFFECTED AND UNAFFECTED SOYBEANS GROWN IN EXPERIMENTAL PLOT

		Reflectance (%)			IR/Red	Injury (%)[a]		Yield
Subplot	Row	Green	Red	IR		Chlorosis	Necrosis	(kg/ha)
					Control			
C1	1	10.25	9.17	53.42	5.82	0	0	3047
	2	10.79	9.71	56.47	5.81	0	0	
	3	10.25	9.35	53.59	5.73	0	0	
C2	1	10.79	9.71	52.88	5.44	0	0	3320
	2	10.61	9.53	51.80	5.43	0	0	
	3	9.89	9.17	49.46	5.39	0	0	
C4	1	9.89	9.17	47.12	5.14	0	0	1824
	2	10.25	9.53	46.58	4.89	0	0	
Mean for Control Subplots		10.34	9.42	51.42	5.46	0	0	2730
					SO$_2$-Affected			
A1	1	10.25	9.35	51.26	5.48	25	0	2596
	2	10.43	9.35	52.34	5.60	25	0	
	3	10.07	9.17	50.72	5.53	25	0	
A2	1	12.05	12.95	41.19	3.18	6	80	2234
	2	10.61	10.97	39.93	3.64	16	54	
	3	10.61	9.71	48.92	5.04	21	1	
A3	1	10.07	9.35	45.32	4.85	25	0	2759
	2	9.89	9.17	44.78	4.88	6	0	
	3	10.97	10.07	48.74	4.84	10	0	
A4	2	10.79	10.79	36.51	3.38	15	30	2352
	3	10.43	10.43	32.55	3.12	8	30	
Mean for Affected Subplots		10.56	10.12	44.75	4.50	16.5	17.7	2485

[a] Injury calculations by LxA method.

TABLE D-6. SO_2 EXPOSURE, OBSERVATION, AND SCANNING DATES--SOYBEAN EXPERIMENTAL PLOT

SO_2 EXPOSURE DATES

Subplot	Month	Day	Year
All	8	16	1979

SCANNING DATES

Subplot	Month	Day	Year
All	8	21	1979

OBSERVATION DATES

Subplot	Month	Day	Year
All	8	21	1979

TABLE D-7. REFLECTANCE, NECROSIS, SO_2 CONCENTRATION, AND YIELD FOR SO_2-EXPOSED AND UNEXPOSED WINTER WHEAT GROWN IN EXPERIMENTAL PLOT

Subplot	SO_2 Conc. (2-h avg)	Mean Reflectance (%)			IR/Red	Mean Necrosis (%)[a]	Yield (kg/ha)
		Green	Red	IR			
C1	0 μg/m³	10.54	9.21	32.55	3.53	9.0	3318
C2	0	9.80	8.65	29.55	3.42	8.5	2661
C3	0	13.83	11.53	43.06	3.73	7.0	2466
C4	0	11.38	10.83	30.23	2.79	8.0	2306
C5	0	10.07	9.12	37.03	4.06	10.5	3297
C6	0	11.90	11.13	40.23	3.61	11.5	2919
C7	0	10.54	9.73	36.22	3.72	11.0	3250
C8	0	10.43	9.96	34.46	3.46	11.5	3357
C9	0	10.97	10.00	34.44	3.44	6.5	3406
C10	0	11.65	12.21	30.97	2.54	6.0	3832
C11	0	9.77	9.93	25.18	2.54	6.5	2482
C12	0	8.71	9.62	21.64	2.25	6.5	3217
C13	0	9.41	10.04	23.88	2.38	8.0	3301
C14	0	12.64	13.45	30.83	2.29	8.5	3499
Mean ± S.D. of Unexposed (control) Subplots		10.83±1.31	10.39±1.26	32.16±5.83	3.13±0.36	8.5±1.9	3094±436

(continued)

TABLE D-7 (continued)

Subplot	SO_2 Conc. (2-h avg)	Mean Reflectance (%)			IR/Red	Mean Necrosis (%)[a]	Yield (kg/ha)
		Green	Red	IR			
A1	10480 μg/m³	10.67	12.09	23.35	1.93	90.0	1512
A2	2620	9.42	8.36	28.02	3.35	10.0	3710
A3	10480	12.90	14.44	32.12	2.22	92.5	948
A4	7860	11.67	14.06	27.75	1.97	89.5	1261
A5	5240	10.29	11.47	29.14	2.54	52.5	2524
A6	7860	10.72	10.77	33.02	3.07	58.0	2670
A7	5240	9.30	12.03	24.06	2.00	86.5	2576
A8	2620	10.59	9.64	36.46	3.78	29.0	3648
A9	7860	10.09	10.61	46.13	4.35	51.5	2562
A10	5240	10.41	11.15	28.02	2.51	38.5	2365
A11	2620	9.78	11.13	23.02	2.07	19.5	2723
A12	10480	8.40	9.62	17.01	1.77	55.0	2105
A13	5240	9.03	10.43	19.41	1.86	55.0	2450
A14	7860	9.93	10.95	21.38	1.95	53.5	2469
A15	10480	11.26	12.43	23.62	1.90	69.0	3010
A16	2620	12.41	13.17	29.26	2.22	19.0	3219
Mean ± S.D. of Exposed Subplots		10.43±1.16	11.40±1.57	27.61±6.90	2.47±0.75	54.3±25.7	2485±739

[a] Injury calculations by LxA method (Appendix D). Light necrosis is classified as ≤10 percent; moderate, 11-25 percent; and severe, >25 percent. Necrosis in control is associated with natural senescence that occurred after scanning but before observations were made.

TABLE D-8. REFLECTANCE, FOLIAR INJURY, SO_2 CONCENTRATION, AND YIELD FOR SO_2-EXPOSED AND UNEXPOSED SOYBEANS GROWN IN EXPERIMENTAL PLOT

Subplot	SO_2 Conc. (2-h avg)	Mean Reflectance (%)			IR/Red	Injury (%)[a]		Yield (kg/ha)
		Green	Red	IR		Chlorosis	Necrosis	
C1	0 μg/m^3	10.43	9.41	54.49	5.79	0	0	3047
C2	0	10.43	9.47	51.38	5.42	0	0	3320
C4	0	10.07	9.35	46.85	5.02	0	0	1824
Mean ± S.D., Control Subplots		10.31±0.17	9.41±0.05	50.91±3.14	5.41±0.31	0	0	2730±650
A1	2620 μg/m^3	10.25	9.29	51.44	5.54	25.00	0	2596
A2	5240	11.09	11.21	43.35	3.95	14.33	45.00	2234
A3	7860	10.31	9.53	46.28	4.86	13.67	0	2759
A4	10480	10.61	10.61	34.53	3.25	11.50	30.00	2352
Mean ± S.D., SO_2-Exposed Subplots		10.57±0.33	10.16±0.78	43.90±6.14	4.40±0.87	16.13±5.23	18.75±19.49	2485±205

[a] Injury calculations by LxA method (Appendix D). Light effects are classified as ≤10 percent; moderate effects, 11-25 percent; and severe effects, >25 percent.

APPENDIX E

SPECTRAL CURVES, EXPERIMENTAL PLOTS

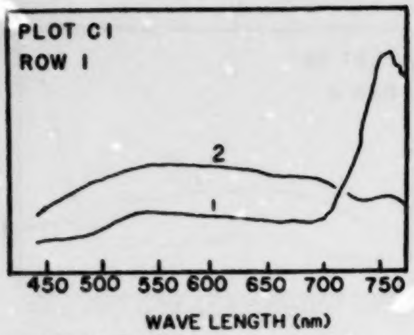

RECORD 7-2

SPECTRUM 1 SOYBEANS; 2 GRAY PANEL

SO$_2$ CONC. 0 μg/m^3 , 2 h

NECROSIS 0 % CHLOROSIS 0 %

Y-AXIS COUNTS, 750 nm: SOYBEANS 2.97

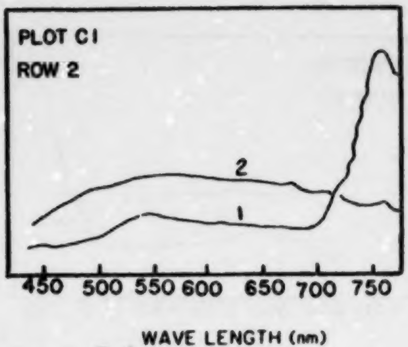

RECORD 7-4

SPECTRUM 1 SOYBEANS; 2 GRAY PANEL

SO$_2$ CONC. 0 μg/m^3 , 2 h

NECROSIS 0 % CHLOROSIS 0 %

Y-AXIS COUNTS, 750 nm: SOYBEANS 3.14

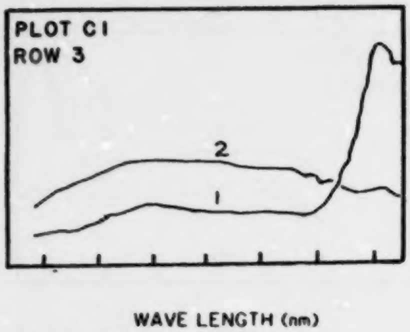

RECORD 7-6

SPECTRUM 1 SOYBEANS; 2 GRAY PANEL

SO$_2$ CONC 0 μg/m^3 , 2 h

NECROSIS 0 % CHLOROSIS 0 %

Y-AXIS COUNTS, 750 nm: SOYBEANS 2.98

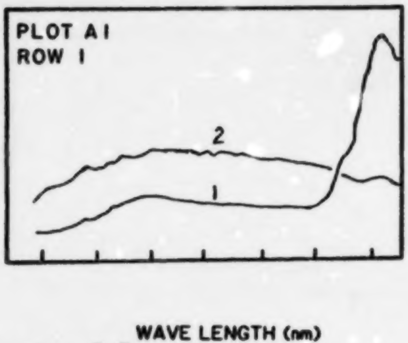

RECORD 7-8

SPECTRUM 1 SOYBEANS; 2 GRAY PANEL

SO$_2$ CONC. 2620 μg/m^3 , 2 h

NECROSIS 0 % CHLOROSIS 25 %

Y-AXIS COUNTS, 750 nm: SOYBEANS 2.85

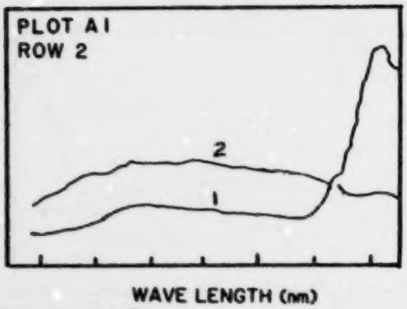

RECORD 7-10

SPECTRUM 1 SOYBEANS; 2 GRAY PANEL

SO$_2$ CONC. 2620 μg/m^3 , 2 h

NECROSIS 0 % CHLOROSIS 25 %

Y-AXIS COUNTS, 750 nm: SOYBEANS 2.91

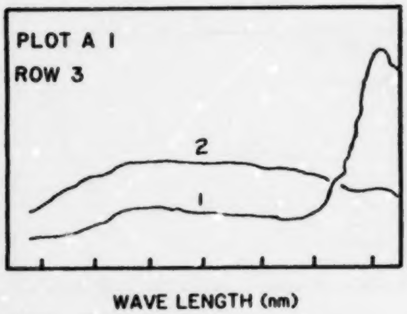

RECORD 7-12

SPECTRUM 1 SOYBEANS; 2 GRAY PANEL

SO$_2$ CONC. 2620 μg/m^3 , 2 h

NECROSIS 0 % CHLOROSIS 25 %

Y-AXIS COUNTS, 750 nm: SOYBEANS 2.82

Figure E-1. Individual Spectral Curves - Soybeans

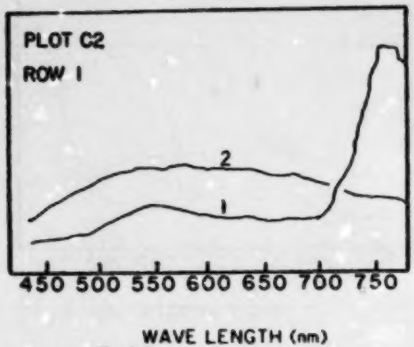

RECORD 7-14

SPECTRUM 1 SOYBEANS; 2 GRAY PANEL

SO_2 CONC 0 $\mu g/m^3$, 2 h

NECROSIS 0 % CHLOROSIS 0 %

Y-AXIS COUNTS, 750 nm: SOYBEANS 2.94

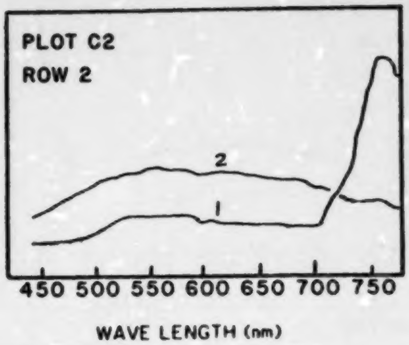

RECORD 7-16

SPECTRUM 1 SOYBEANS; 2 GRAY PANEL

SO_2 CONC 0 $\mu g/m^3$, 2 h

NECROSIS 0 % CHLOROSIS 0 %

Y-AXIS COUNTS, 750 nm: SOYBEANS 2.88

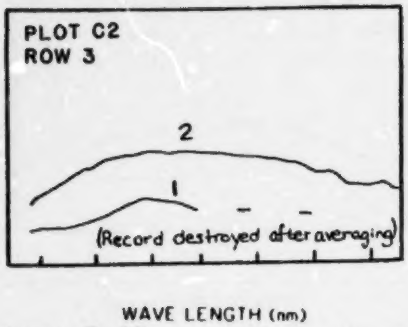

RECORD 7-18

SPECTRUM 1 SOYBEANS; 2 GRAY PANEL

SO_2 CONC 0 $\mu g/m^3$, 2 h

NECROSIS 0 % CHLOROSIS 0 %

Y-AXIS COUNTS, 750 nm: SOYBEANS 2.75

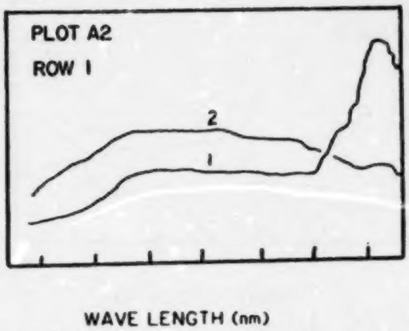

RECORD 7-20

SPECTRUM 1 SOYBEANS; 2 GRAY PANEL

SO_2 CONC 5240 $\mu g/m^3$, 2 h

NECROSIS 80 % CHLOROSIS 6 %

Y-AXIS COUNTS, 750 nm: SOYBEANS 2.29

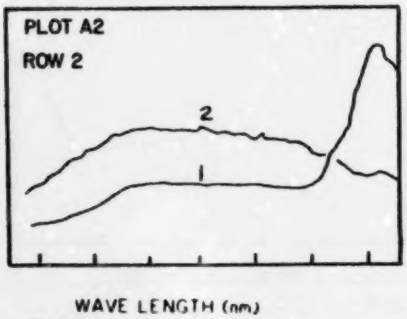

RECORD 7-22

SPECTRUM 1 SOYBEANS; 2 GRAY PANEL

SO_2 CONC 5240 $\mu g/m^3$, 2 h

NECROSIS 54 % CHLOROSIS 16 %

Y-AXIS COUNTS, 750 nm: SOYBEANS 2.22

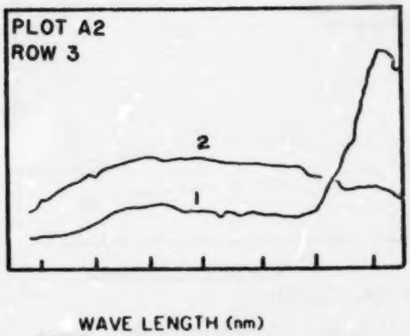

RECORD 7-24

SPECTRUM 1 SOYBEANS; 2 GRAY PANEL

SO_2 CONC 5240 $\mu g/m^3$, 2 h

NECROSIS 1 % CHLOROSIS 21 %

Y-AXIS COUNTS, 750 nm: SOYBEANS 2.72

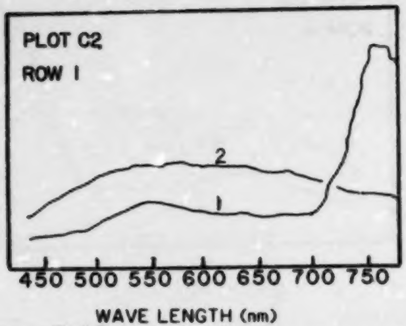

RECORD 7-14

SPECTRUM 1 SOYBEANS; 2 GRAY PANEL

SO$_2$ CONC. 0 $\mu g/m^3$, 2 h

NECROSIS 0 % CHLOROSIS 0 %

Y-AXIS COUNTS, 750 nm: SOYBEANS 2.94

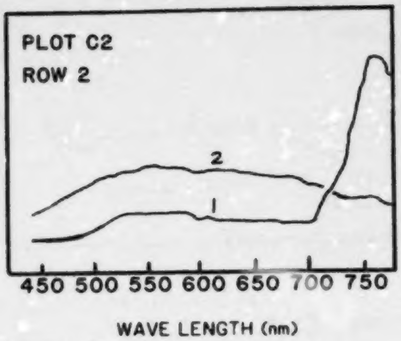

RECORD 7-16

SPECTRUM 1 SOYBEANS; 2 GRAY PANEL

SO$_2$ CONC. 0 $\mu g/m^3$, 2 h

NECROSIS 0 % CHLOROSIS 0 %

Y-AXIS COUNTS, 750 nm: SOYBEANS 2.88

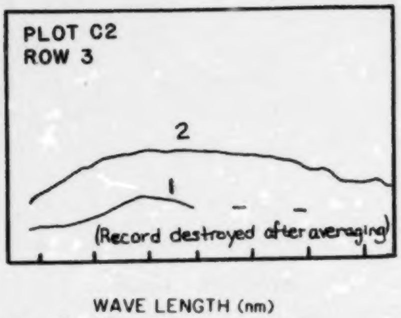

RECORD 7-18

SPECTRUM 1 SOYBEANS; 2 GRAY PANEL

SO$_2$ CONC. 0 $\mu g/m^3$, 2 h

NECROSIS 0 % CHLOROSIS 0 %

Y-AXIS COUNTS, 750 nm: SOYBEANS 2.75

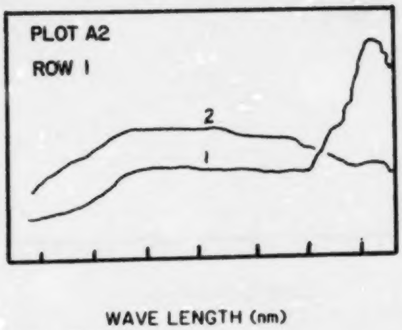

RECORD 7-20

SPECTRUM 1 SOYBEANS; 2 GRAY PANEL

SO$_2$ CONC. 5240 $\mu g/m^3$, 2 h

NECROSIS 80 % CHLOROSIS 6 %

Y-AXIS COUNTS, 750 nm: SOYBEANS 2.29

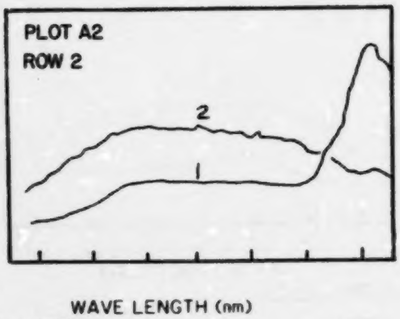

RECORD 7-22

SPECTRUM 1 SOYBEANS; 2 GRAY PANEL

SO$_2$ CONC. 5240 $\mu g/m^3$, 2 h

NECROSIS 54 % CHLOROSIS 16 %

Y-AXIS COUNTS, 750 nm: SOYBEANS 2.22

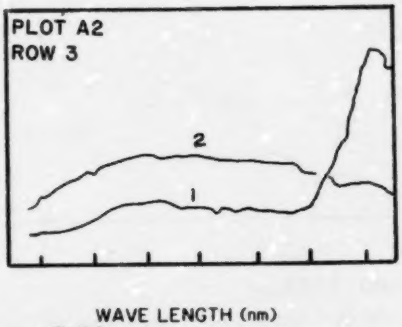

RECORD 7-24

SPECTRUM 1 SOYBEANS; 2 GRAY PANEL

SO$_2$ CONC. 5240 $\mu g/m^3$, 2 h

NECROSIS 1 % CHLOROSIS 21 %

Y-AXIS COUNTS, 750 nm: SOYBEANS 2.72

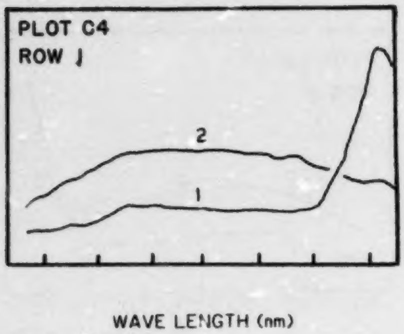

RECORD 7-26

SPECTRUM 1 SOYBEANS; 2 GRAY PANEL

SO_2 CONC. 0 μg/m³ , 2 h

NECROSIS 0 % CHLOROSIS 0 %

Y-AXIS COUNTS, 750 nm: SOYBEANS 2.62

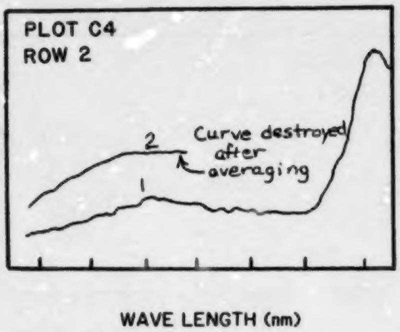

RECORD 7-28

SPECTRUM 1 SOYBEANS; 2 GRAY PANEL

SO_2 CONC. 0 μg/m³ , 2 h

NECROSIS 0 % CHLOROSIS 0 %

Y-AXIS COUNTS, 750 nm: SOYBEANS 2.59

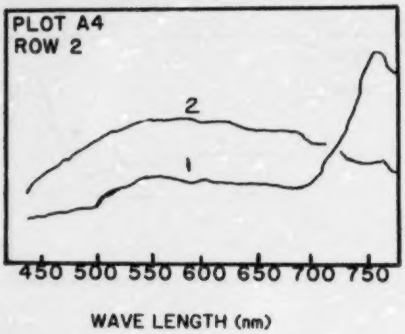

RECORD 7-40

SPECTRUM 1 SOYBEANS; 2 GRAY PANEL

SO_2 CONC. 10480 μg/m³ , 2 h

NECROSIS 30 % CHLOROSIS 15 %

Y-AXIS COUNTS, 750 nm: SOYBEANS 2.03

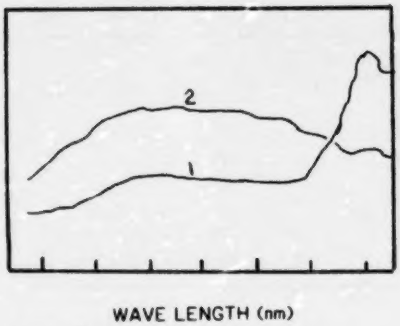

RECORD 7-42

SPECTRUM 1 SOYBEANS; 2 GRAY PANEL

SO_2 CONC. 10480 μg/m³ , 2 h

NECROSIS 30 % CHLOROSIS 8 %

Y-AXIS COUNTS, 750 nm: SOYBEANS 1.81

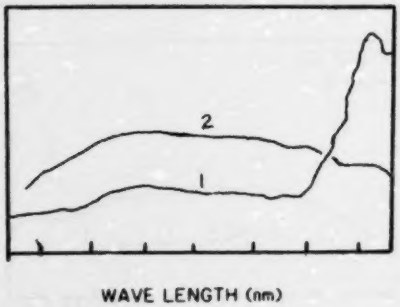

RECORD 7-32

SPECTRUM 1 SOYBEANS; 2 GRAY PANEL

SO_2 CONC. 7860 μg/m³ , 2 h

NECROSIS 0 % CHLOROSIS 25 %

Y-AXIS COUNTS, 750 nm: SOYBEANS 2.52

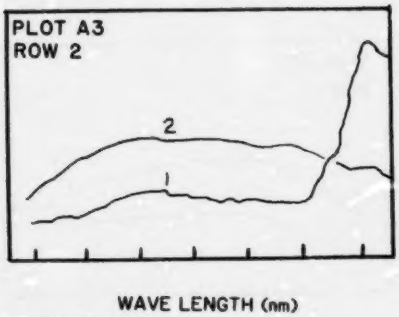

RECORD 7-34

SPECTRUM 1 SOYBEANS; 2 GRAY PANEL

SO_2 CONC. 7860 μg/m³ , 2 h

NECROSIS 0 % CHLOROSIS 6 %

Y-AXIS COUNTS, 750 nm: SOYBEANS 2.49

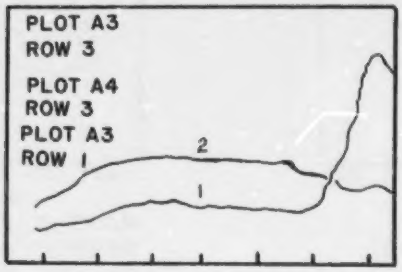

WAVE LENGTH (nm)

RECORD 7-36

SPECTRUM 1 SOYBEANS; 2 GRAY PANEL

SO_2 CONC. 7860 $\mu g/m^3$, 2 h

NECROSIS 0 % CHLOROSIS 10 %

Y-AXIS COUNTS, 750 nm: SOYBEANS 2.71

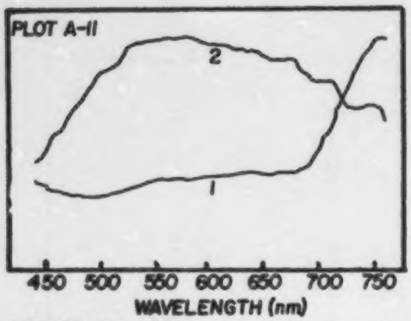

RECORD 26-83
SPECTRUM 1 WHEAT; 2 GRAY PANEL
SO_2 CONC. 2620 mg/m^3 2 h
FOLIAR NECROSIS 19.5 %
Y-AXIS COUNTS 750nm: WHEAT 1.280401
: GRAY PANEL 672168

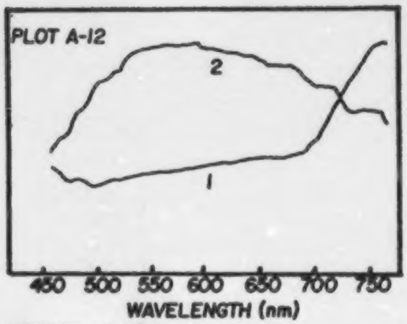

RECORD 18-84
SPECTRUM 1 WHEAT; 2 GRAY PANEL
SO_2 CONC. 10480 mg/m^3 2 h
FOLIAR NECROSIS 55.0 %
Y-AXIS COUNTS 750nm: WHEAT 0.945315
: GRAY PANEL 640975

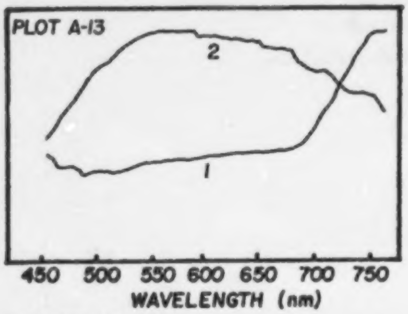

RECORD 19-85
SPECTRUM 1 WHEAT; 2 GRAY PANEL
SO_2 CONC. 5240 mg/m^3 2 h
FOLIAR NECROSIS 55.0 %
Y-AXIS COUNTS 750nm: WHEAT 1.077337
: GRAY PANEL 752645

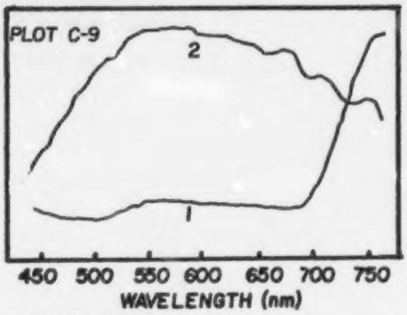

RECORD 38-86
SPECTRUM 1 WHEAT; 2 GRAY PANEL
SO_2 CONC. 0 mg/m^3 h
FOLIAR NECROSIS 6.5 %
Y-AXIS COUNTS 750nm: WHEAT 1.915188
: GRAY PANEL 553822

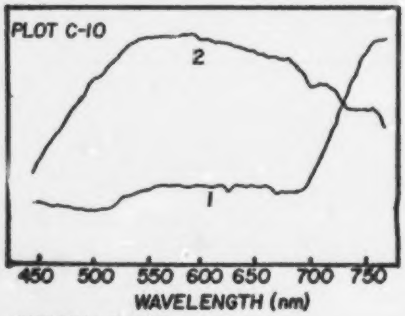

RECORD 39-87
SPECTRUM 1 WHEAT; 2 GRAY PANEL
SO_2 CONC. 0 mg/m^3 h
FOLIAR NECROSIS 6.0 %
Y-AXIS COUNTS 750nm: WHEAT 1.722374
: GRAY PANEL 245727

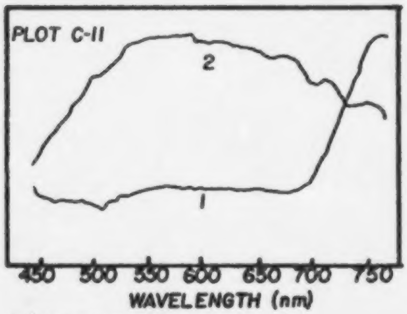

RECORD 40-88
SPECTRUM 1 WHEAT; 2 GRAY PANEL
SO_2 CONC. 0 mg/m^3 h
FOLIAR NECROSIS 6.5 %
Y-AXIS COUNTS 750nm: WHEAT 1.400387
: GRAY PANEL 649670

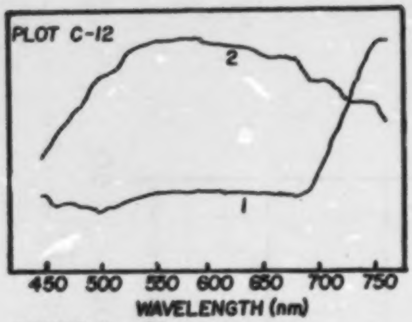

RECORD 41 - 89
SPECTRUM I WHEAT; 2 GRAY PANEL
SO_2 CONC. 0 mg/m^3 ______ h
FOLIAR NECROSIS 6.5 %
Y-AXIS COUNTS 750nm: WHEAT 1,400387
: GRAY PANEL 163210

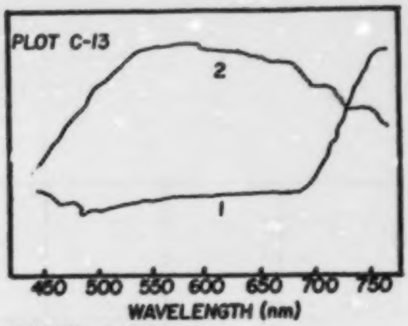

RECORD 42-90
SPECTRUM I WHEAT; 2 GRAY PANEL
SO_2 CONC. 0 mg/m^3 ______ h
FOLIAR NECROSIS 8.0 %
Y-AXIS COUNTS 750nm: WHEAT 1.327795
: GRAY PANEL 780158

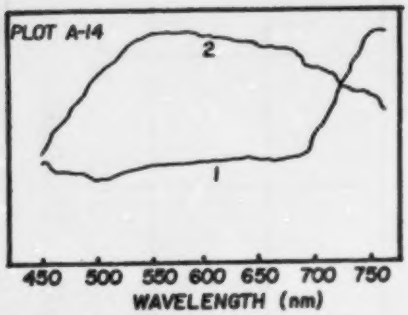

RECORD 20-91
SPECTRUM I WHEAT; 2 GRAY PANEL
SO_2 CONC. 7860 mg/m^3 2 h
FOLIAR NECROSIS 53.5 %
Y-AXIS COUNTS 750nm: WHEAT 1.189157
: GRAY PANEL 807624

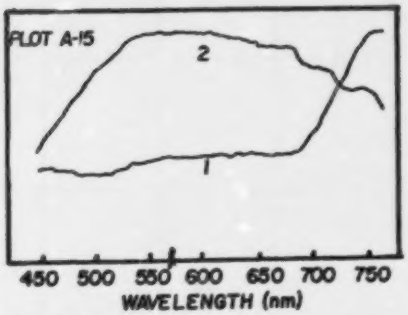

RECORD 21-92
SPECTRUM I WHEAT; 2 GRAY PANEL
SO_2 CONC. 10480 mg/m^3 2 h
FOLIAR NECROSIS 69.0 %
Y-AXIS COUNTS 750nm: WHEAT 1.313454
: GRAY PANEL 818176

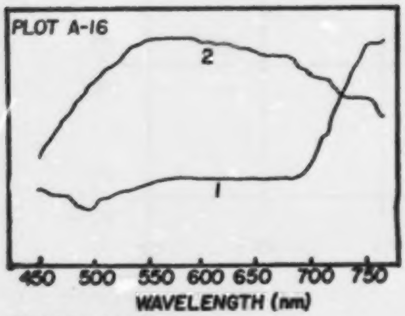

RECORD 27-93
SPECTRUM I WHEAT; 2 GRAY PANEL
SO_2 CONC. 2620 mg/m^3 2 h
FOLIAR NECROSIS 19.0 %
Y-AXIS COUNTS 750nm: WHEAT 1.626688
: GRAY PANEL 817713

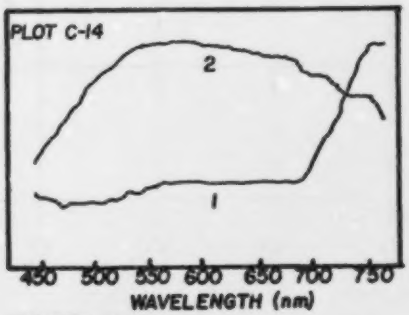

RECORD 43-94
SPECTRUM I WHEAT; 2 GRAY PANEL
SO_2 CONC. 0 mg/m^3 ______ h
FOLIAR NECROSIS 8.5 %
Y-AXIS COUNTS 750nm: WHEAT 1.714491
: GRAY PANEL 789600

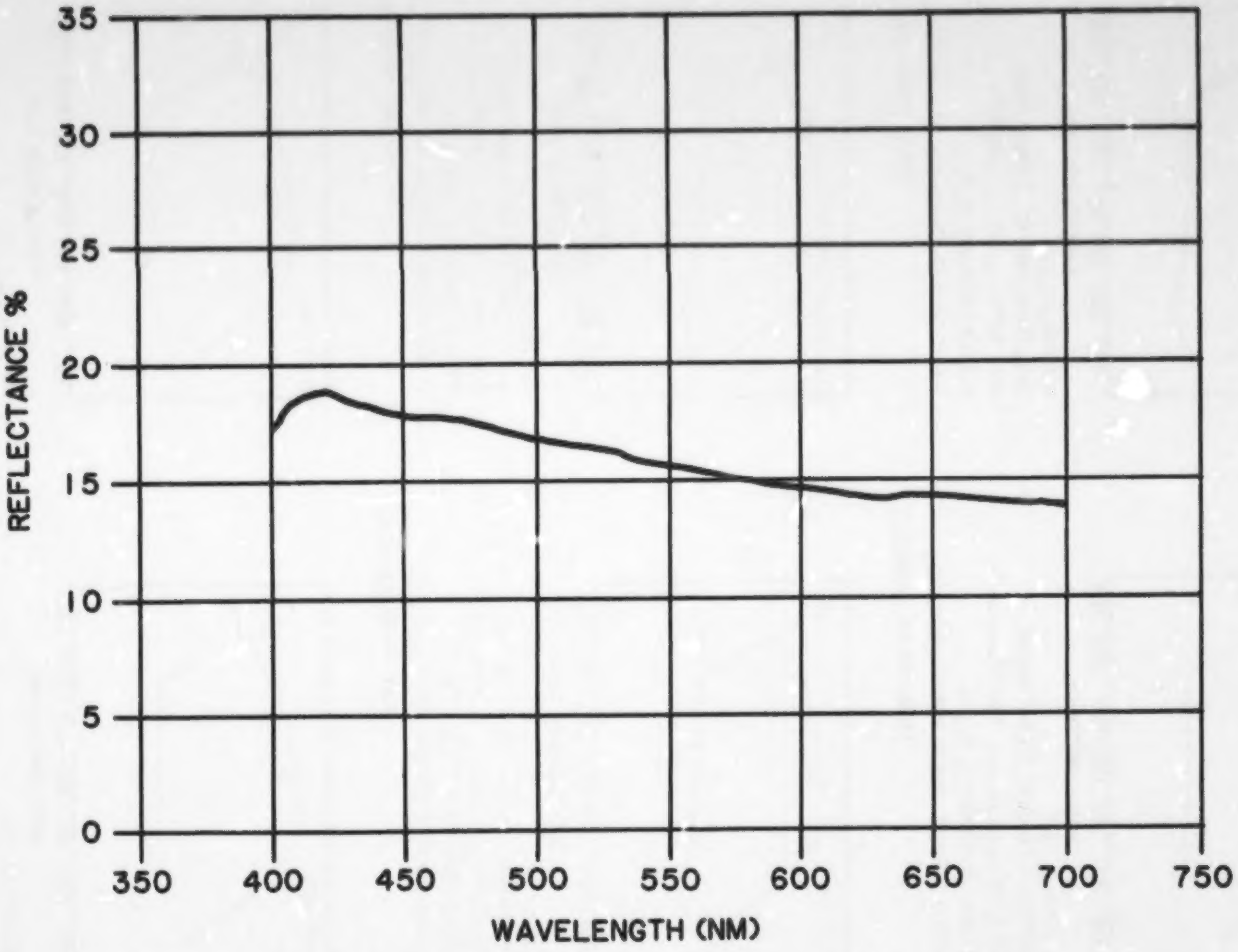

Figure 3. NASA GRAY TARGET NO. 4 SPECTRAL REFLECTANCE

APPENDIX F

ANALYSIS OF VARIANCE, EXPERIMENTAL PLOT

TABLE F-1. ANALYSIS OF VARIANCE FOR GREEN BAND BY DOSE SET - SOYBEANS

Dose Set	Conc. ($\mu g/m^3$)	No. Obs.	$\overline{X}$ (counts)	S (counts)	Sum (counts)
1	Control	8	0.58	0.02	4.60
2	2620 5240 7860 10480 — combined	11	0.59	0.03	6.46

ANOVA Data

	SS	df	MS	F
Treatments	6.98×10^{-4}	1	6.98×10^{-4}	0.87
Error	0.01	17	8.01×10^{-4}	
Total	0.01	18		

F = 0.87 does not exceed $F_{.05,1,17} = 4.45$.

Null hypothesis is not rejected.

Means of green reflectance of the two dose sets are not significantly different.

TABLE F-2. ANALYSIS OF VARIANCE FOR RED BAND BY DOSE SET - SOYBEANS

Dose Set	Conc. ($\mu g/m^3$)	No. Obs.	$\bar{X}$ (counts)	S (counts)	Sum (counts)
1	Control	8	0.52	0.01	4.18
2	2620 5240 7860 10480 — combined	11	0.56	0.06	6.19

ANOVA Data

	SS	df	MS	F
Treatments	0.01	1	0.01	3.07
Error	0.04	17	2.45×10^{-3}	
Total	0.05	18		

F = 3.07 does not exceed $F_{.05,1,17} = 4.45$.

Null hypothesis is not rejected.

Means of red reflectance of the two dose sets are not significantly different.

TABLE F-3. ANALYSIS OF VARIANCE FOR IR BAND BY DOSE SET - SOYBEANS

Dose Set	Conc. ($\mu g/m^3$)	No. Obs.	$\bar{X}$ (counts)	S (counts)	Sum (counts)
1	Control	8	2.86	0.19	22.87
2	2620 5240 7860 10480 — combined	11	7.55	0.38	28.01

ANOVA Data

	SS	df	MS	F
Treatments	0.45	1	0.45	4.58
Error	1.68	17	0.10	
Total	2.13	18		

F = 4.58 does exceed $F_{.05,1,17}$ = 4.45.

Null hypothesis is rejected.

Means of IR reflectance of the two dose sets are significantly different.

TABLE F-4. ANALYSIS OF VARIANCE FOR IR/RED RATIO BY DOSE SET - SOYBEANS

Dose Set	Conc. ($\mu g/m^3$)	No. Obs.	$\bar{X}$ (counts)	S (counts)	Sum (counts)
1	Control	8	5.46	0.33	43.69
2	2620 5240 7860 10480 — combined	11	4.51	0.98	49.56

ANOVA Data

	SS	df	MS	F
Treatments	4.23	1	4.23	6.95
Error	10.35	17	0.61	
Total	14.58	18		

F = 6.95 does exceed $F_{.05,1,17}$ = 4.45.

Null hypothesis is rejected.

Means of IR/red ratios of the two dose sets are significantly different.

NOTE: STATISTICS FOR CHLOROTIC VERSUS UNAFFECTED (CONTROL) SOYBEANS ARE IDENTICAL TO THE PRECEDING STATISTICS FOR DOSE SETS 1 AND 2.

TABLE F-5. ANALYSIS OF VARIANCE FOR GREEN BAND BY NECROSIS SET - SOYBEANS

Necrosis Set	No. Obs.	$\bar{X}$ (counts)	S (counts)	Sum (counts)
Unaffected	5	0.58	0.02	4.60
Necrotic	8	0.60	0.04	3.02

ANOVA Data

	SS	df	MS	F
Treatments	2.59×10^{-3}	1	2.59×10^{-3}	3.42
Error	0.01	11	7.56×10^{-4}	
Total	0.01	12		

$F = 3.42$ does not exceed $F_{.05,1,17} = 4.45$.

Null hypothesis is not rejected.

Means of green reflectance of the two necrosis sets are not significantly different.

TABLE F-6. ANALYSIS OF VARIANCE FOR RED BAND BY NECROSIS SET - SOYBEANS

Necrosis Set	No. Obs.	$\bar{X}$ (counts)	S (counts)	Sum (counts)
Unaffected	5	0.52	0.01	4.19
Necrotic	8	0.61	0.07	3.05

ANOVA Data

	SS	df	MS	F
Treatments	0.02	1	0.02	13.12
Error	0.02	11	1.74×10^{-3}	
Total	0.04	12		

$F = 13.12$ does exceed $F_{.05,1,11} = 4.84$.

Null hypothesis is rejected.

Means of red reflectance of the two necrosis sets are significantly different.

TABLE F-7. ANALYSIS OF VARIANCE FOR IR BAND BY NECROSIS SET - SOYBEANS

Necrosis Set	No. Obs.	$\bar{X}$ (counts)	S (counts)	Sum (counts)
Unaffected	8	2.86	0.19	22.87
Necrotic	5	2.21	0.34	11.07

ANOVA Data

	SS	df	MS	F
Treatments	1.28	1	1.28	19.73
Error	0.71	11	0.06	
Total	1.99	12		

$F = 19.73$ does exceed $F_{.05,1,11} = 4.84$.

Null hypothesis is rejected.

Means of IR reflectance of the two necrosis sets are significantly different.

TABLE F-8. ANALYSIS OF VARIANCE FOR IR/RED RATIO BY NECROSIS SET - SOYBEANS

Necrosis Set	No. Obs.	$\bar{X}$	S	Sum
Unaffected	8	5.46	0.33	43.65
Necrotic	5	3.67	0.79	18.36

ANOVA Data

	SS	df	MS	F
Treatments	9.80	1	9.80	33.02
Error	3.26	11	0.30	
Total	13.06	12		

F = 33.02 does exceed $F_{.05,1,11} = 4.84$.

Null hypothesis is rejected.

Means of IR/red ratio of the two necrosis sets are significantly different.

TABLE F-9. ANALYSIS OF VARIANCE FOR CROP YIELD BY CHLOROSIS SET - SOYBEANS

Chlorosis Set	No. Obs.	$\bar{X}$ (kg/ha)	S (kg/ha)	Sum (kg/ha)
Unaffected	8	2844	642	22749
Chlorotic	5	2497	220	27471

ANOVA Data

	SS	df	MS	F
Treatments	555312	1	555312	2.80
Error	3369044	17	198179	
Total	3924356	18		

F = 2.80 does not exceed $F_{.05,1,17} = 4.45$.

Null hypothesis is not rejected.

Means of yield of the two chlorosis sets are not significantly different.

TABLE F-10. ANALYSIS OF VARIANCE FOR CROP YIELD BY NECROSIS SET - SOYBEANS

Necrosis Set	No. Obs.	$\bar{X}$ (kg/ha)	S (kg/ha)	Sum (kg/ha)
Unaffected	8	2844	642	22749
Necrosis	5	2281	65	11406

ANOVA Data

	SS	df	MS	F
Treatments	973298	1	973298	3.69
Error	2900863	11	263715	
Total	2844	12		

$F = 3.69$ does not exceed $F_{.05,1,11} = 4.84$.

Null hypothesis is not rejected.

Means of yield of the two necrosis sets are not significantly different.

TABLE F-11. ANALYSIS OF VARIANCE FOR RED BAND BY DOSE SET - WINTER WHEAT

Dose Set	Conc. ($\mu g/m^3$)	No. Obs.	$\bar{X}$ (counts)	S (counts)	Sum (counts)
1	Control	37	0.57	0.08	21.21
2	2620	12	0.59	0.11	7.05
3	5240	11	0.63	0.05	6.91
4	7860	12	0.64	0.10	7.73
5	10480	11	0.68	0.13	7.51

ANOVA Data

	SS	df	MS	F
Treatments	0.13	4	0.03	3.82
Error	0.67	78	0.01	
Total	0.80	82		

$F = 3.82$ does exceed $F_{.05,4,78} = 2.50$.

Null hypothesis is rejected.

Means of red reflectance of the five dose sets are significantly different.

TABLE F-12. ANALYSIS OF VARIANCE FOR GREEN BAND BY DOSE SET - WINTER WHEAT

Dose Set	Conc. ($\mu g/m^3$)	No. Obs.	$\overline{X}$ (counts)	S (counts)	Sum (counts)
1	Control	37	0.60	0.08	22.33
2	2620	12	0.58	0.06	6.34
3	5240	11	0.54	0.04	5.95
4	7860	12	0.59	0.07	7.07
5	10480	11	0.59	0.09	6.49

ANOVA Data

	SS	df	MS	F
Treatments	0.04	4	0.01	1.37
Error	0.46	78	0.01	
Total	0.49	82		

F = 1.37 does not exceed $F_{.05,4,78}$ = 2.50.

Null hypothesis is not rejected.

Means of green reflectance of the five dose sets are not significantly different.

TABLE F-13. ANALYSIS OF VARIANCE FOR IR BAND BY DOSE SET - WINTER WHEAT

Dose Set	Conc. ($\mu g/m^3$)	No. Obs.	$\bar{X}$ (counts)	S (counts)	Sum (counts)
1	Control	37	1.81	0.35	66.98
2	2620	12	1.62	0.29	19.48
3	5240	11	1.38	0.25	15.22
4	7860	12	1.52	0.28	18.24
5	10480	11	1.26	0.23	13.83

ANOVA Data

	SS	df	MS	F
Treatments	3.52	4	0.88	9.25
Error	7.41	78	0.10	
Total	10.93	82		

$F = 9.25$ does exceed $F_{.05,4,78} = 2.50$.

Null hypothesis _is_ rejected.

Means of IR reflectance of the five dose sets _are_ significantly different.

TABLE F-14. ANALYSIS OF VARIANCE FOR IR/RED RATIO BY DOSE SET - WINTER WHEAT

Dose Set	Conc. (μg/m³)	No. Obs.	$\bar{X}$	S	Sum
1	Control	37	3.21	0.70	118.59
2	2620	12	2.86	0.77	34.31
3	5240	11	2.21	0.35	24.26
4	7860	12	2.39	0.53	28.70
5	10480	11	1.85	0.14	20.34

ANOVA Data

	SS	df	MS	F
Treatments	21.49	4	5.37	14.71
Error	28.48	78	0.37	
Total	49.97	82		

F = 14.71 does exceed $F_{.05,4,78}$ = 2.50.

Null hypothesis _is_ rejected.

Means of the IR/red ratio for the five dose sets _are_ significantly different.

TABLE F-15. ANALYSIS OF VARIANCE FOR GREEN BAND BY NECROSIS SET - WINTER WHEAT

Necrosis Set	Range of injury (%)	No. Obs.	$\bar{X}$ (counts)	S (counts)	Sum (counts)
1	0-10	28	0.60	0.09	16.73
2	11-25	18	0.60	0.07	10.88
3	26-50	5	0.59	0.01	2.94
4	51-100	32	0.57	0.07	18.35

ANOVA Data

	SS	df	MS	F
Treatments	.01	3	4.71×10^{-3}	0.80
Error	.47	79	0.01	
Total	.48	82		

F = 0.80 does not exceed $F_{.05,3,79} = 2.73$.

Null hypothesis is not rejected.

Means of green reflectance for the four necrosis sets are not significantly different.

TABLE F-16. ANALYSIS OF VARIANCE FOR RED BAND BY NECROSIS SET - WINTER WHEAT

Necrosis Set	Range of injury (%)	No. Obs.	$\bar{X}$ (counts)	S (counts)	Sum (counts)
1	0-10	28	0.57	0.09	15.93
2	11-25	18	0.60	0.09	10.72
3	26-50	5	0.57	0.05	2.85
4	51-100	32	0.65	0.10	20.91

ANOVA Data

	SS	df	MS	F
Treatments	0.12	3	0.04	4.58
Error	0.68	79	0.01	
Total	0.80	82		

F = 4.58 does exceed $F_{.05,3,79}$ = 2.73.

Null hypothesis is rejected.

Means of red reflectance for the four necrosis sets are significantly different.

TABLE F-17. ANALYSIS OF VARIANCE FOR IR BAND BY NECROSIS SET - WINTER WHEAT

Necrosis Set	Range of injury (%)	No. Obs.	$\bar{X}$ (counts)	S (counts)	Sum (counts)
1	0-10	28	1.68	0.34	46.97
2	11-25	18	1.74	0.53	31.40
3	26-50	5	1.84	0.27	9.21
4	51-100	32	1.37	0.27	43.83

ANOVA Data

	SS	df	MS	F
Treatments	2.51	3	0.84	6.37
Error	10.38	79	0.13	
Total	12.89	82		

$F = 6.37$ does exceed $F_{.05,3,79} = 2.73$.

Null hypothesis is rejected.

Means of IR reflectance for the four necrosis sets are significantly different.

TABLE F-18. ANALYSIS OF VARIANCE FOR IR/RED RATIO BY NECROSIS SET - WINTER WHEAT

Necrosis Set	Range of injury (%)	No. Obs.	$\bar{X}$	S	Sum
1	0-10	28	2.99	0.61	83.63
2	11-25	18	3.17	0.88	53.93
3	26-50	5	3.28	0.73	16.42
4	51-100	32	2.11	0.46	67.43

ANOVA Data

	SS	df	MS	F
Treatments	19.05	3	6.35	15.92
Error	31.11	79	0.40	
Total	50.16	82		

F = 15.92 does exceed $F_{.05,3,79} = 2.73$.

Null hypothesis is rejected.

Means of the ratios for the four necrosis sets are significantly different.

TABLE F-19. ANALYSIS OF VARIANCE FOR CROP YIELD BY NECROSIS SET - WINTER WHEAT

Necrosis Set	Range of injury (%)	No. Obs.	$\overline{X}$ (kg/ha)	S (kg/ha)	Sum (kg/ha)
1	0-10	28	3044	498	85220
2	11-25	18	3128	235	56295
3	26-50	5	3135	703	15674
4	51-100	32	2229	606	71313

ANOVA Data

	SS	df	MS	F
Treatments	14419609	3	4806536	18.09
Error	20985118	79	265634	
Total	35404727	82		

$F = 18.09$ does exceed $F_{.05,3,79} = 2.73$.

Null hypothesis is rejected.

Means of crop yield for the four necrosis sets are significantly different.

APPENDIX G

PHOTOMETRIC CALIBRATION

Photometric Analyses Related to Soy Bean Crop Yield and SO_2 Stress

Final Report Calspan Number 6258-M-1
Contract No. TV-48080A
30 May 1978

Prepared For:

The Tennessee Valley Authority
Division of Environmental Planning
Muscle Shoals, Alabama 37401
Mr. C. Daniel Sapp

Prepared By:

John E. Walker
Calspan Corporation
Advanced Technology Center
Post Office Box 400
Buffalo, New York 14225

PHOTOMETRIC CALIBRATION

The atmospheric and illumination contributions to the total exposure of an image on film are, by definition,[1]

(1) a multiplicative attenuation of the energy for every object in the scene (α) and

(2) an additive contribution of energy from the optical path between the objects and the sensor (β).

To measure these two parameters (α and β), one must first derive the relationship between image density (D), which is measured from the images, and the exposing energy (E) that caused the image density. This is accomplished by using a step wedge (series of known exposures) that has been imaged on the film before it is processed. TVA furnished one set of EPA aerial photographs with a step wedge (Colbert) and two sets of TVA photographs without wedges (Johnsonville). The densities of the steps in the Colbert wedge were measured and plotted against their known relative log exposure values. The resultant curves are shown in Figures G-1, G-2, and G-3 for the infrared energy (red filter), red energy (green filter), and green energy (blue filter). The Eastman Kodak Handbook curve for CIR film was also plotted. The comparison of these curves showed a significant difference in the low-exposure end, with severe density compression present in the EPA film. Examination of both the wedge and scenes under 30X magnification revealed a microscopic pattern generally related to processing to correct for underexposure during data collection. This processing problem could manifest itself in several ways in photometric analyses if the analyst were not aware of its presence.

The first manifestation could be in the photometric calibration process to derive the additive contribution to image exposure (β). This task is accomplished by performing a regression analysis of the exposures of dark and light objects in the scene illuminated by skylight (shadow) and also by sunlight plus skylight. Because of density compression due to processing, the exposure range between objects illuminated by skylight and those illuminated by skylight plus sunlight is reduced. Thus, the plotting scale used in the computerized regression program to derive β must be expanded to obtain meaningful values for β. This actually occurred in the first attempt to derive β for the Colbert data, with negative β's being output by the regression program. Expanding the plotting scale, however, did allow the derivation of meaningful β's. The expanded scale and plot allowed the operator to recognize erroneous data points and eliminate them from the analysis, an important interactive step in calibration.

Another manifestation that could occur is that the density of healthy soybean fields located in the extreme corners of the film format, especially in the red information band (green filter-chlorophyll absorption band), could reach the maximum density limit imposed by the processing problem;

---

[1] Piech, R., and J. R. Schott. Atmospheric Corrections for Satellite Water Quality Studies. Proceedings of the SPIE, 51:84-89, 1974.

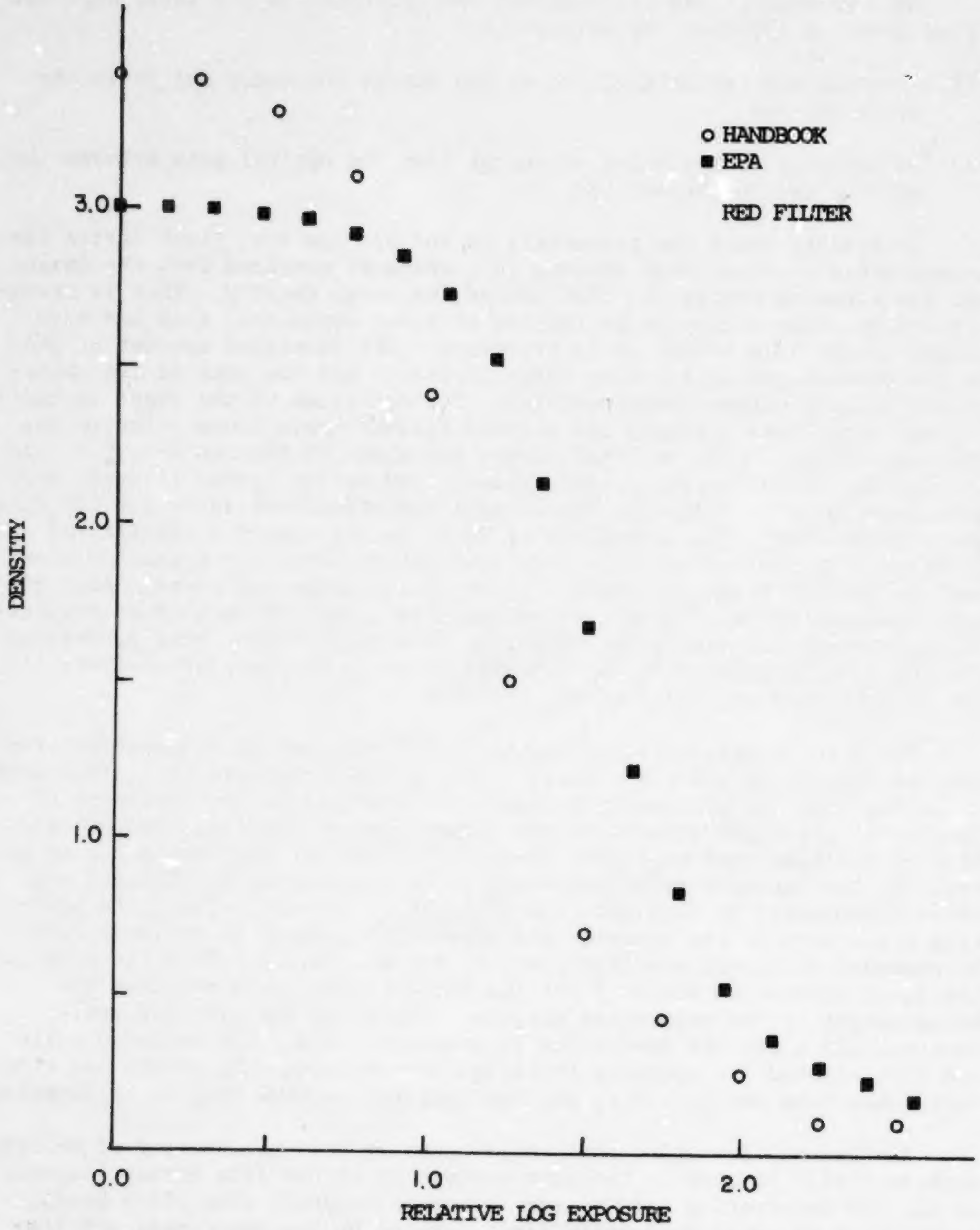

Figure G-1. Comparison of D-log E curves--red filter.

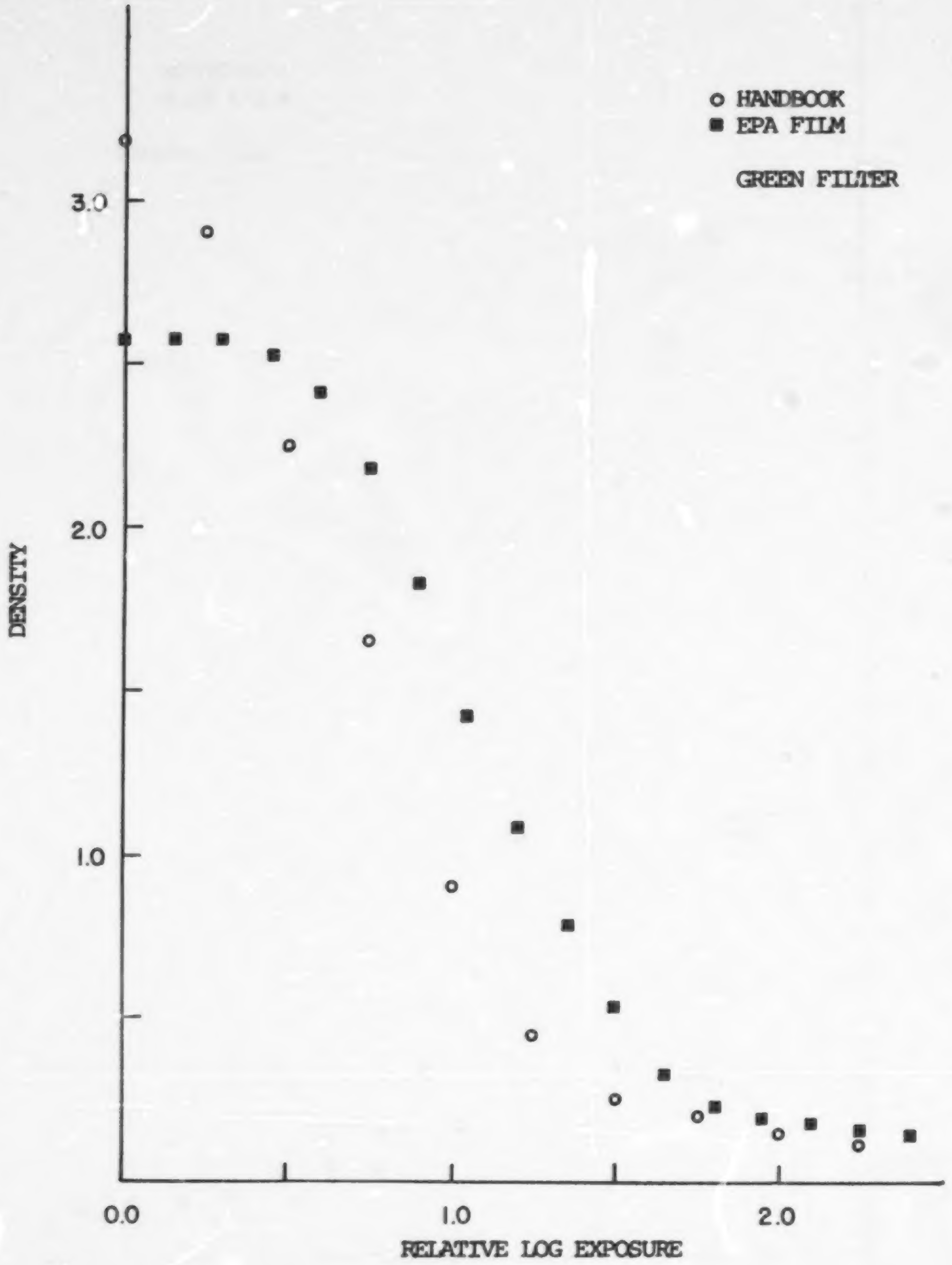

Figure G-2. Comparison of D-log E curves--green filter.

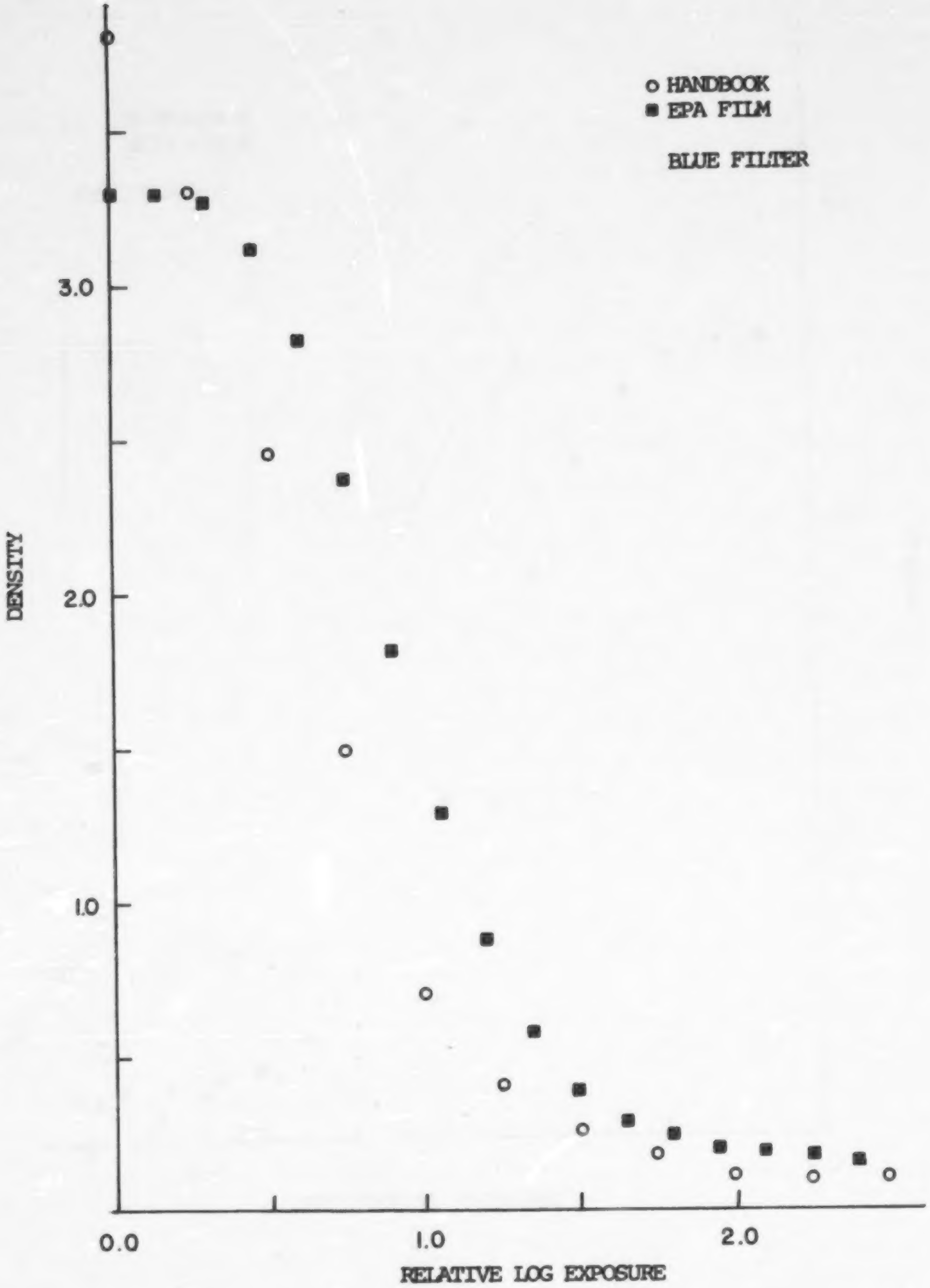

Figure G-3. Comparison of D-log E curves--blue filter.

even with the correction for lens fall off, an incorrect value of red reflectance could result. This did not occur in the case of Colbert data, but the analyst should be aware that processing problems can result in maximum density compression.

A third manifestation to be aware of, because of this type of processing problem, is the effect of the microscopic pattern on densitometry. If a large-aperture (1 mm) densitometer is used, it integrates the variations in density within the microscopic pattern anomaly with little or no effect on the densitometry. However, if a densitometer with a small sample aperture (50 μm) is used, the placement of the aperture is critical. The processing pattern consists of circular areas, under 100 μm in diameter, over the entire film format. In the center of each circular area of normal dye concentration is an abnormal "snowflake" pattern that is generally of higher density than the normal dye concentration surrounding the "snowflake." Therefore, the analyst must be sure he places the small aperture in the normal dye area and not on a "snowflake" when making an image density measurement.

Fortunately, the Colbert photographs were acquired in late August, when most soybean crops had reached full cover condition. Therefore, it was possible to use the 1-mm aperture and have the effect of the processing problem averaged into the noise of the overall measurement process.

The α's and β's derived for the Colbert photographs are shown in Table G-1.

TABLE G-1. α'S AND β'S FOR COLBERT PHOTOGRAPHS OF AUGUST 29, 1977

Parameter	Infrared band	Red band	Green band
α	206.92	157.14	174.70
β	6.72	3.45	10.37

For the Johnsonville photographs it was necessary to assume characteristic curves to obtain α's and β's. The Johnsonville films were examined under 30X magnification to determine whether the microscopic pattern present in the Colbert wedge and scenes was still present. The pattern was not present in either the July 13, 1977, films furnished by EPA to TVA or in the August 2, 1977, TVA films. The maximum densities of these films were checked (i.e., zero exposure in borders), with the expectation that they would be significantly higher. However, because the maximum densities were not found to be significantly higher, we decided to use the original wedge data for the Colbert scene to derive α's and β's for Johnsonville. The α's and β's for the two sets of Johnsonville films are given in Table G-2.

TABLE G-2. α'S AND β'S FOR JOHNSONVILLE PHOTOGRAPHS

Parameter	Infrared band	Red band	Green band
	July 13, 1977		
α	322.588	130.486	138.611
β	13.39	3.21	4.27
	August 2, 1977		
α	329.139	214.169	219.411
β	7.15	3.28	3.45

The assumptions necessary to obtain a photometric calibration of these films were pointed out to the TVA representative. The necessity for the exposure of a 21-step wedge on the original aerial films and a duplicate of this wedge for subsequent duplicates of scenes to be analyzed in any future field experiment was also emphasized. This requirement was the first experimental design criterion resulting from this effort.

Because of the problems of sensitometric and densitometric control for the aerial photographs, absolute spectral reflectances and reflectance ratios could not be obtained from photometric interpretation; however, important relative reflectance information within any one scene could still be obtained, depending on the level of reflectance. The film covering the Colbert site (frames 5353 through 5355, August 29, 1977) was selected for analysis because it did have a wedge. Thus, these reflectances would be closest to absolute values.

The TVA representative measured the spectral reflectance and reflectance ratio properties of soybean plants in five fields at the Colbert site (fields A through E). The number of measurements per field was limited by the field of view of the densitometer used. This was a 1-mm-diam aperture, representing a 12-m-diam area on the ground. A 0.6-m-diam area could have been used, but this was not considered necessary for these fields because they were mature fields with very full cover. The 12-m-diam area still allowed about 50 samples to be measured per field in less than 15 min.

This is considered a very important point relative to the comparison of any potential aerial photometric method of soybean stress measurement to a ground survey method. It would be very difficult to obtain a sample rate of 200 samples/h per field when using a ground survey method, whether they are spectral reflectances from a ground-based TSR or L x A x P (see Appendix D) estimates. This is a very practical advantage of an aerial photographic approach. Furthermore, the photograph would provide a valuable permanent record of the crop condition.

The TVA representative compared the mean IR/R reflectance ratios for these fields and found the most injured (4 percent by the L x A x P method) plants had a ratio of 3.0±0.49, whereas the lease injured (0 percent) plants had a ratio of 5.7±0.34. In previous photometric interpretation analyses of vegetation stress (chlorosis-necrosis) by Calspan, the mean IR/R reflectance ratio has always been high when stress was low and low when stress was high. Thus, even with known processing problems, the reflectance and ratio results obtained were consistent with previous studies.

However, one inconsistency was noted. The standard deviation in the red (chlorophyll absorption) band is usually extremely large in comparison with that in the infrared band. These data showed the infrared band to have the larger standard deviation. The presence of a sunspot image in the Colbert scene could have caused these inconsistencies.

Field B, having 2 percent injury by the L x A x P method, appeared on three frames (nos. 5353, 5354, and 5355) at different format positions relative to the sunspot and center of the format. Spectral reflectance gradient functions from the center of the sunspot image through the center of each format to the edge of the film away from the sunspot were derived from regressions of soybean reflectances against distance from the center format. Deciduous tree reflectance was also regressed relative to distance with almost identical results. This result would be expected since both canopies are highly textured and contain multiple reflectances.

A second-order regression resulted in a functional relation with high correlation coefficients (r^2):

$$F_\lambda = B_2X^2 + B_1X + B_0,$$

where X = the distance of an image from the center of the film format (0) to (+) the sunspot and away from (-) the sunspot, in inches along the sunspot, center format line.

The constants B_0, B_1, and B_2 are shown in Table G-3, with the correlation coefficients for each spectral band.

TABLE G-3. SPECTRAL REFLECTANCE GRADIENT CONSTANTS

Constants	R_{IR}	R_R	R_G
B_0	0.0248	0.0575	0.0539
B_1	0.0139961	0.008437	0.0076
B_2	0.001159	0.0007353	0.0008
r^2	0.728	0.879	0.865

Eight to nine spectral reflectance measurements were made in field B on each of the three frames on which the field was imaged. The results of the measurements are shown in Table G-4.

TABLE G-4. MEASUREMENTS OF REFLECTANCE--FIELD B

Frame no.	R_{IR}	$\sigma(\%)^a$	R_R	$\sigma(\%)^a$	R_G	$\sigma(\%)^a$	R_{IR}/R_R	$\sigma(\%)^a$
5353	29.26	±7.5	05.65	±3.4	06.14	±4.1	5.2	±8
5354	28.89	±3.0	05.76	±6.0	05.83	±7.0	5.4	±4
5355	24.88	±5.0	04.51	±4.0	04.38	±5.0	5.5	±2
All data	27.5	±9	05.14	±5.3	05.38	±15.8	5.4	±6

[a] Standard deviation, as percentage of mean reflectance.

Next a preliminary gradient correction method under development at Calspan was applied to the spectral measurements. The corrected reflectance data for the field are shown in Table G-5.

TABLE G-5. REFLECTANCES CORRECTED FOR ILLUMINATION GRADIENT

Frame no.	R_{IR}	$\sigma(\%)^a$	R_R	$\sigma(\%)^a$	R_G	$\sigma(\%)^a$	R_{IR}/R_R	$\sigma(\%)^a$
5353	31.96	±7.6	07.01	±3.3	07.39	±4.1	4.5	±8
5354	32.60	±3.3	07.10	±6.0	07.44	±7.4	4.6	±4
5355	31.67	±4.7	08.04	±4.1	06.94	±5.2	3.0	±2
All data	32.06	±5.2	07.37	±7.9	07.24	±6.4	4.3	±9

[a] Standard deviation, as percentage of mean reflectance.

The preliminary correction for illumination gradient normalizes all reflectances to a common point in the scene--in this case, the sunspot location. Theoretically, the mean values of reflectance for field B should be identified on all three frames. Therefore, we can compare the difference of the mean reflectance values for any single frame with the mean reflectance for all frames, as a measure of the accuracy of the photometric interpretation method with and without the correction for illumination gradient. The results of such a comparison are shown in Table G-6. There can be no doubt from these results that a correction provides a major improvement.

TABLE G-6. COMPARISON OF PHOTOMETRIC INTERPRETATION ACCURACY WITH AND WITHOUT PRELIMINARY ILLUMINATION GRADIENT CORRECTION

Frame no.	R_{IR}(%)		R_R(%)		R_G(%)	
	With	Without	With	Without	With	Without
5353	0.3	6	5	10	2	12
5354	2	5	4	12	3	8
5355	1	10	9	12	4	18

$$\text{Accuracy in \%} = \frac{\bar{R}\lambda \text{ (all data)} - \bar{R}\lambda \text{ (field)}}{\bar{R}\lambda \text{ (all data)}} \times 100$$

SPECTRAL REFLECTANCES OF SOYBEAN FIELD COMPONENTS

Being acquired about four weeks earlier than the Colbert (8/29/77) films, the Johnsonville (7/13/77) films had many immature, partially covered fields and few mature, full cover fields. This necessitated the use of the 0.6-m diam ground sample size densitometer because too much soil and herbaceous cover were integrated into the 12-m diam samples. Reflectance measurements of tilled soils, untilled soils, and weeds were made as well as measurements of soybeans per se. These are other major components of a less than full cover (immature) soybean field.

Table G-7 shows the reflectance and reflectance ratio data for five tilled fields (visually white), as well as data for six untilled fields, (visually cyan).

TABLE G-7. JOHNSONVILLE FIELD REFLECTANCE RESULTS

Field No.	R_{IR}	R_R	R_G	R_{IR}/R_R	R_R/R_G	R_{IR}/R_G	$\bar{\bar{R}}$
Visually White Fields (Tilled)							
106.10+	36.3	30.9	20.9	1.18	1.47	1.74	29.4**
110.02	42.7	37.1	24.7	1.52	1.50	1.73	34.8*
201.08	36.7	23.7	18.6	1.55	1.27	1.97	26.3**
115.08	32.2	25.7	14.5	1.25	1.78	2.22	24.1**
110.01	38.8	33.0	22.5	1.18	1.47	1.72	31.4
Mean/	37.3	30.1	20.2	1.3	1.5	1.9	
Std.Dev.	±3.8	±5.4	±3.9	±0.2	±0.2	±0.2	
Visually Cyan Fields (Untilled)							
100.07+	21.1	16.8	13.5	1.26	1.25	1.57	17.1**
105.09+	18.8	18.3	14.1	1.03	1.30	1.34	17.1
107.01	19.7	15.5	12.8	1.27	1.21	1.54	16**
107.02	18.5	14.7	12.6	1.26	1.17	1.47	15.3
108.01	22.7	17.1	14.1	1.33	1.21	1.61	18**
108.02	22.8	20.3	15.3	1.12	1.33	1.49	19.5*
Mean/	20.6	17.1	13.7	1.2	1.3	1.5	
Std. Dev.	±1.9	±2.0	±1.0	±0.1	±0.1	±0.1	

+All more than 5" from sunspot, all others less than 5" from sunspot.
*Brightest overall.
**Darker but with higher long to short wavelength ratio.

It is quite apparent that tilled and untilled soils are as easily separable on the basis of these spectral reflectance properties, as they are by visual color discrimination. Applying the illumination gradient correction will only result in a slight increase in reflectances of fields marked with the symbol (+) and slight decreases for those not so marked.

This should not have a significant effect upon the differences between the mean values shown in Table G-7.

These data all exhibit the normal characteristics of soil reflectance ratios, i.e., long to short wavelengths, are greater than 1.0. It is possible to demonstrate a photometric method to assess moisture variations in the fields based upon average brightness $\bar{R}$ and the R_{IR}/R_G ratio of these data. Field 110.02 is the brightest of the tilled fields. If moisture is present it will cause a lower overall brightness, and an increase in the infrared to green ratio. If the soil brightness decreases and the ratio does also, then it is some other parameter that is causing the difference. From the data of Table G-7 it appears that practically all of the variation in tilled soil areas (3 out of 4 fields) is due to moisture whereas in the untilled fields only 3 out of 5 appear to vary due to moisture. The soybeans in tilled fields are visually red whereas those in untilled fields are visually pink. This alone suggests that tilling which reduces moisture retention in fields may also reduce stress on soybean plants, or cause stress if not practiced. The soil results suggest that in future TVA efforts to assess injury to soybeans, an experiment should be conducted to assess the effects of soil moisture levels in tilled and untilled fields upon the soybean growth rate, reflectance properties, and yield. This is the second experimental design criterion to be derived from this brief photometric analysis of TVA's CIR films.

Seven fields (100, 101, 102, 103, 104, 105, and 106) were selected for analysis at the Johnsonville site. These fields are all in close proximity to each other and therefore relative reflectance data would be valid without correction for the sunspot illumination gradient effect. Data was acquired by the TVA representative from 11 other fields as well, but most were located such that the gradient correction would have to be applied for a comparison to the results from these fields. Field 100 and 101 are "double planted" fields. Field 106 is also about 12 weeks old compared to 5 weeks for the other fields. Field 106 is a tilled field whereas the rest are not tilled.

In reviewing the reflectance measurements acquired by the TVA representative for Field 101, it was noted that five sets of readings were identified as "weeds" and had been included in the computations for the mean values of soybean reflectances and reflectance ratios in the field. There were sufficient samples of both weeds and soybeans to derive a mean value and standard deviation of reflectance and reflectance ratios for each. These values are shown in Table G-8 along with the original values for weeds plus soybeans and the values for the 11-week old Field 106.

TABLE G-8. SOYBEANS AND WEEDS IN FIELD 101

Vegetation	R_{IR}	R_R	R_G	R_{IR}/R_R
Soybeans	23.2±4.5	6.5±0.9	7.5±1.3	3.6±0.73
Weeds	19.0±1.0	3.2±0.8	4.0±0.7	6.3±1.6
Weeds + Soybeans	22.2±4.3	5.44±1.82	6.68±1.55	4.555±1.787
Mature Soybeans (106)	22.7±1.0	4.6±0.8	4.7±0.6	5.6±.95

The data of Table G-8 is interesting in several respects. First, a visual check on the image of Field 101 by three interpreters results in 100 percent agreement that visually it was impossible to separate weeds from soybeans by the visual assessment of color in this image. Therefore, we suspect the representative "identified" weeds from *a priori* knowledge of their location and presence from his field observations. However, there is a definite signature for weeds if all facts are considered.

First, this is an untilled field, i.e., cyan-colored soil image. Second, it is a field with immature soybean growth, i.e., row effects are clearly defined in most of the field. Third, it is unlikely that under these conditions, mature soybeans will be present anywhere in the field, although the spectral properties of mature soybeans (106) are very similar to the spectral properties of areas identified as weeds by the representative. Fourth, in view of the surficial drainage pattern of this field and the lack of tilling, it would be feasible for weeds having a preference for high moisture to develop to maturity long before soybeans which prefer lower moisture levels. Fifth, weeds would not develop the stacked leaf canopy of soybeans and would therefore have lower infrared reflectance than soybeans at maturity although their visible light reflectance properties would be nearly identical. Sixth, the very high mean infrared-to-red reflectance ratio of the identified weed areas (6.3±1.6) indicates a significantly higher vegetal biomass is present at these locations that at the identified soybean location where the mean ratio is 3.6±0.7.

Applying these facts to Field 101, and generating an infrared-to-red ratio mask or sampling the reflectance properties of the vegetation in the field on a grid basis, the weed areas can be mapped from the growing soybean areas. This analysis illustrates the need for ancillary data to develop an effective photometric measure of SO_2 stress on soybeans. Specifically, for every field to be assessed, a preplanting, postpreparation-for-planting photograph should be acquired after a period of rainfall to assess the moisture pattern distribution. In view of the apparent importance of soil moisture retention related to soybean and weed conditions it is recommended that an experimental effort be undertaken by TVA to assess the full significance of moisture retention.

APPENDIX H

NASA/ERL LETTER REPORT

Lyndon B. Johnson Space Center
Earth Resources Laboratory
1010 Gause Boulevard
Slidell, Louisiana 70458

NASA
National
Aeronautics and
Space
Administration

REPLY TO
ATTN OF: GC

May 10, 1976

Mr. Herbert C. Jones
Supervisor, Air Quality Research
Tennessee Valley Authority
Muscle Shoals, Alabama 35660

Dear Mr. Jones:

We have analyzed the multispectral data taken in the vicinity of the Joppa and Shawnee power plants near Paducah, Kentucky. The results of this analysis indicate that spectral differences due to vegetation stress associated with SO_2 plumes from power plants to be too subtle to be resolved.

Examination of the excellent ground truth information supplied by your organization revealed that the estimate of total leaf area affected in a given field was low--usually less than five percent. When this is considered, together with the percentage of ground cover usually around 75 percent, the percent of affected leaves in the field of view of the scanner is very small. Thus, it is not surprising that areas of affected leaves were not identifiable from the scanner data.

I do not believe that it would be accurate to extrapolate from this particular set of data that the problem of detecting stressed vegetation due to SO_2 from multispectral scanner data is generally untenable; however, for this specific set of data this appears to be the case. For instance, it would seem much more likely that stressed vegetation might be detected in an area comprised of one crop and cultivated using similar farming practices. This situation is quite different than existed here where there were several crop types cultivated using diverse farming practices and at different stages of growth. With this situation, there is much variability in the scene causing the slight change in spectral quality of the data due to SO_2 vegetation stress to essentially be in the "noise level" of the data.

If you have any questions in regard to the analysis of the data, please contact me and we will be happy to furnish you with additional information.

Sincerely,

E. L. Tilton

E. L. TILTON, III
Assistant Director

APPENDIX I

SUPERVISED CLASSIFICATION PROCEDURE

SUPERVISED CLASSIFICATION OF MSS DATA

When preprocessing of the digital tapes is complete, the analyst may implement the supervised classification procedure. The first step is training sample selection and statistics calculation, second is divergence analysis, and the third is the classification of the scene.

Training sample selection begins with an examination of ground truth and collateral sources such as photography and maps to obtain information on candidate sites for training samples. These samples are areas having apparently homogeneous physical characteristics. They are outlined as polygons on the display monitor using a trackball and cursor. Training samples may be grouped as land cover classes. At least three training samples per class are normally obtained. Statistics are computed to determine the homogeneity of the training samples. Histograms are plotted (Figure I-1) to ascertain that the samples are normally distributed with no biomodal tendencies or skips in the data. Coefficients of variation are also checked.

Since the selection task is interactive, unacceptable samples may be replaced with new ones and the appropriate data stored upon completion.

The divergence analysis step examines spectral separability between classes. Inseparable classes may be grouped if this is considered advantageous. When this step is completed, we are ready to classify the scene.

Supervised classification involves computation of n-dimensional (n = number of channels) decision boundaries and assignment of pixels to classes or categories. Hyperellipsoidal decision boundaries are computed from the class statistics with a program called ELLIPSE. A second program, ASSIGN, assigns pixels to classes or an unclassified category. The assigning process is iterated for each pixel and scan line until the entire scene has been classified. A classified data tape is the product. This tape can serve as input to the display monitor for viewing and film recorder for hard copy.

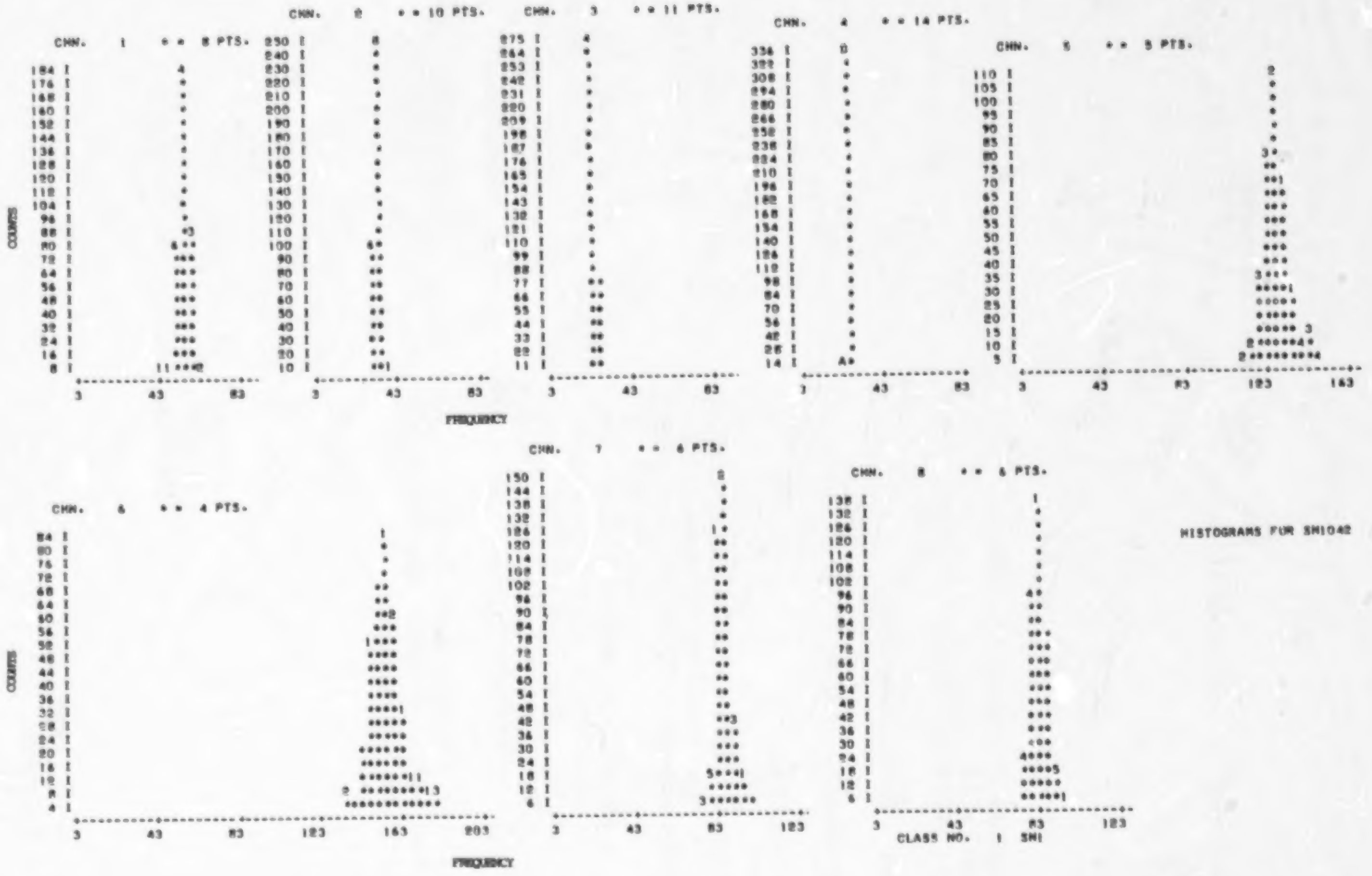

Figure I-1. Selected histograms describing homogeneity of a training sample used in supervised classification of MSS data. This is unaffected soybeans.

LEC

LOCKHEED ELECTRONICS COMPANY, INC.

SYSTEMS AND SERVICES DIVISION

P. O. BOX 15027 ◻ LAS VEGAS, NEVADA 89114 ◻ TELEPHONE (AREA CODE 702) 736-2969, EXT. 271

April 25, 1978

Environmental Protection Agency
P. O. Box 15027
Las Vegas, Nevada 89114

Attention: G. A. Shelton

Subject: Supervised Classification of TVA Scenes, Project 7736

Dear Mr. Shelton:

This letter is in response to Dan Sapp's request. The paragraph below is an explanation of the inability to perform supervised classifications on TVA Tapes 319 and 320.

Training fields were selected when Mr. Sapp was here at EMSL-LV. By error, interactive stats were run on the wrong data file and output indicated that all classes were separable. This error was discovered after Mr. Sapp's visit and stats were run on the correct file. Results indicated that the classes were not separable.

Other training fields were selected by myself and again by Chuck Tanner. However, in both cases, the stats run indicated non-separability of classes.

Very truly yours,

David R. Williams
Environmental Analyst, Sr.
Remote Sensing Laboratory

DRW:mb

cc: J. R. Donaldson
H. V. Johnson
J. O. 11.01

A SUBSIDIARY OF LOCKHEED AIRCRAFT CORPORATION

APPENDIX J

PSEUDOSUPERVISED CLASSIFICATION OF MSS DATA

PSEUDOSUPERVISED CLASSIFICATION OF MSS DATA

GENERAL

The pseudosupervised classifier is an alternative to the time-consuming supervised classifier. The pseudosupervised classifier implemented at EMSL-LV is entitled MAXL4. It uses a fast clustering program in combination with a limited amount of manual selection of training samples. The basis of the procedure is a trainer called SEARCH.[58]

SEARCH

This program is an unsupervised trainer for a maximum likelihood classifier that is unlike conventional cluster analysis. SEARCH evaluates contiguous 6-scan line by 6-element blocks of 4-channel input data through use of a covariance matrix that permits comparison of relative variability about a different sized mean. Alternatively, a 3-scan line by 3-element block may be evaluated. The output of SEARCH is means, standard deviations, and covariances for the 4-channel data for each training sample. These statistics are stored and the pair of statistics with the smallest pairwise divergence is determined and merged reiteratively until the minimum divergence exceeds a specified value.

SEARCH can be run from either the background or foreground (interactive) mode. The interactive mode permits the analyst to change program parameters in real time. The interactive SEARCH program requires a statistics (STAT) file and a 4-channel data tape.

Classification Processor

A maximum likelihood scheme is used to classify the data with MAXL4. This scheme assumes the samples within a given class (e.g., soybeans) are distributed according to a normal multivariate probability density function.

The MAXL4 classifier begins with statistics obtained from the program SEARCH. The mean vector $\underline{M}$ and the covariance matrix $\underline{C}$ are estimated. MAXL4 classified each vector $\underline{X}$, where $\underline{X}^t = (X_1, X_2, X_3, X_4)$ as belonging to one of NCL classes (NCL $\leq$ 63) or, under certain conditions, as "other."

Since MAXL4 can process only 4 channels of MSS data, the mathematics involved is not complex. Baye's Rule is used to assign pixels to classes.

Baye's Rule as used by Pearson of NASA/ERL is as follows:

$$P(i\ \underline{X}) = \frac{P(\underline{X}\ i) \cdot APR_i}{P(\underline{X})} \qquad (1)$$

where

$P(i\ \underline{X})$ = probability of class i given the occurrence of $\underline{X}$.

$P(\underline{X}\ i)$ = probability of $\underline{X}$ given the occurrence of class i.

APR_i = *a priori* probability of class i.

$P(\underline{X})$ = Probability of $\underline{X}$.

For the 4-channel case:

$$P(\underline{X}\ i) = \frac{1}{(2\pi)^2\ D_i^{\frac{1}{2}}} \cdot e^{-\frac{1}{2}(\underline{X} - \underline{M}i)^t\ \underline{C}i^{-1}(\underline{X} - \underline{M}i)} \qquad (2)$$

where

D_i = determinant of matrix $\underline{C}_i$

$\underline{C}_i^{-1}$ = inverse of $\underline{C}_i$

For a given vector $\underline{X}$ ($P(\underline{X}) = 1$):

$$P(i\ \underline{X}) = \frac{APR_i}{(2\pi)^2 \cdot D_i^{\frac{1}{2}}}\ \pi\ e^{-\frac{1}{2}(\underline{X} - \underline{M}i)^t\ \underline{C}i^{-1}(\underline{X} - \underline{M}i)} \qquad (3)$$

MAXL4 assigns vector $\underline{X}$ to class j if:

$$P(j\ \underline{X}) \geq (P(i\ \underline{X}) \qquad (4)$$

where

$1 \leq i \leq NCL$, $1 \leq j \leq NCL$, and $i \neq j$

Considerable time is required to process a typical MSS scene, which consists of up to 714 pixels by 512 scan lines, so the MAXL4 classification is run in the background (batch) mode. If the output shows that less than 90 percent of the data has been classified, the results are considered unsuccessful and the analyst proceeds with the pseudosupervised mode. In this mode, the analyst selects training samples from the unclassified areas and programs the computer to recognize the signatures during upcoming classification runs. The analyst delineates training fields as rectangles (boxes) or polygons on the CRT using a cursor and trackball. Then the statistics are computed. An interactive color-coding operation follows, and then the classifier is run to generate an entire color-coded scene. This output is then compared to ground truth to evaluate classification accuracy.

APPENDIX K

UNSUPERVISED CLASSIFICATION PROCEDURE

UNSUPERVISED CLASSIFICATION PROCEDURE

PROGRAM PURPOSE

This program was developed by NASA/ERL to afford users the capability to peruse training field areas as subsets of larger areas.[59] The user selects a general region of interest of which his training field is a subset and the program classifies this region and determines homogeneity of the training field.

DETAILED PROGRAM DESCRIPTION

Technique

The existing programs that produce channel composite images are restricted by the arbitrariness in selection of bin edges in the grey scale, the compression factor that results in a 36 to 1 count resolution reduction for 255 count range aircraft data for a 2-channel gray scale, and the loss of coherence information between channels. The unsupervised sequential clustering technique program (UNSUP) was developed to alleviate some of these restrictions and to facilitate users in selecting homogeneous training fields. The major assumption in this program is that the data has some homogeneous patterns. The data flow consists of the following: (1) establishing the initial population, (2) developing tables for classes, (3) determining if the sample belongs to established populations, and (4) establishing additional populations.

Mathematics

The initial population is established in the following manner:

$$\bar{X}(j,k) = \mathrm{NVARBS} \sum_{i=1}^{\mathrm{NVARBS}} 1/\mathrm{XDATA}(i,j) \tag{1}$$

where

$1 \leq j \leq \mathrm{NCHAN}$;NCHAN number channels

$1 \leq i \leq \mathrm{NVARBS}$;NVARBS number samples

$1 \leq K \leq \mathrm{MAXPOP}$;MAXPOP maximum number populations

Then the individual samples are compared to this mean ($\bar{X}$) as follows:

$$\mathrm{THRESH} * \bar{X}(j,k_1) < \bar{X}(j,K_1) - \mathrm{XDATA}(i,j) \tag{2}$$

where

$1 \leq j \leq \mathrm{NCHAN}$

$1 \leq i \leq \mathrm{NVARBS}$

If this test holds for all channels (NCHAN) and variables (NVARBS), it is accepted for k_1 initial population.

The program then generates tables for the NCHAN channels of the k_1 population as follows:

$$\mathrm{LSTART} = \mathrm{XBAR}(j_1,K_1) - (\sigma(j_1k_1)\mathrm{xPRBLTY}) \quad 1 < \mathrm{LSTART} < 256$$

$$\mathrm{LEND} = \mathrm{XBAR}(j_1,k_1) - (\sigma(j_1,k_1(\mathrm{XPRBLTY}) \quad 1 < \mathrm{LEND} < 256$$

$$\mathrm{PTABLE}\ (i,j_1) = k_1 \qquad (3)$$

$$\text{for } \mathrm{LSTART} \leq i \leq \mathrm{LEND}$$

where

σ ( ) is standard deviation

$1 \leq i \leq 256$ count range of data

PTABLE( ) specifies k_1 class for 1 count range

PRBLTY is fractional value of one standard deviation as specified by confidence interval selected.

This procedure is repeated for NCHAN channels of the k_1 population.

The next pixel is compared to the existing table to determine which population it best fits as follows:

$$\mathrm{LPOS} = \mathrm{ZDATA}\ (j_1,m,n)$$

;m, specifies element and n, specifies scanline

where

LPOS specifies count value to peruse in tables as:

$$k = \mathrm{PTABLE}(\mathrm{LPOS},j_1) \qquad (4)$$

where

k = the population that the pixel fits.

If k equals zero no established population corresponds to the count value of pixel. The following procedure is repeated for all NCHAN channels. If the pixel fits more than one population, the most likely population is determined as follows:

$$\mathrm{SCMAX}\ (k) = \sum_{j=1}^{\mathrm{NCHAN}} \mathrm{XBAR}(j,k) - \mathrm{ZDATA}(j,m,n) \qquad (5)$$

The kth population with the lowest SCMAX(k) values is selected as the most likely population. The mean and sum of the square are updated accordingly as:

$$\mathrm{XBAR}(j_1,k)_{\mathrm{NPOPL}+1} = \left(\mathrm{NPOPL} \Big/ \mathrm{NPOPL}+1\right) \mathrm{XBAR}(j_1,k)_{\mathrm{NPOPL}} + \left(1 \Big/ \mathrm{NPOPL}+1\right) \mathrm{ZDATA}(j_1,m,n) \qquad (6)$$

where

NPOPL = the number of pixels in existing population statistics.

The PTABLE( ) describing population count ranges is updated as described in eq. 3.

If the pixel does not fit any of the established populations since the k of equation 4 equals zero, then this pixel is stored in XDATA(i,j) array until i reaches the value of NVARBS. At this time it is evaluated the same as the initial population was in equations 1 and 2 to test its validity in establishing a new population.

UPGRADING AND ENHANCEMENT OF UNSUP PROGRAM SOFTWARE FOR VARIAN V-75 COMPUTER

Purpose

Enhancements to UNSUP establish the relationship between classes, select the optimal four channels for subsequent supervised data classification, and reassign classes based upon a selected channel queueing. The enhancements provided include: (1) feature selections, (2) class separability determination, and (3) reassignment of classes to match the standardized color table (chip).

General Description of Upgrading and Enhancements

The existing UNSUP program is a multichannel sequential clustering program. The channels 1 through 12 designate the channel bandwidth of the Daedulus 1260 scanner. The UNSUP program determines the validity of an initial population by the coefficient of variation. Upon establishing the initial population, proceeding data elements are tested against a specified Chi-Squared confidence. Any samples that satisfy this Chi-Squared confidence interval are designated to be in that class. The elements that exceed this confidence interval are stored in a buffer until the designated number elements are accumulated for testing by coefficient of variation. After complete processing of the input data set, an output is generated consisting of the program-determined classes. These class statistics are processed by a similarity criterion technique for selecting the four optimum channels.

Average normalized distance separations for all four channel subsets of the channels are computed. The four-channel subset with the largest numerical average normalized distance separation is optimum. This procedure compares each class with the other classes and also compares all class combinations.

The upgrading also includes an automated color chip generation feature for displaying classified outputs.

Processing

The upgrade to the UNSUP program is implemented through the following equations:

$$D(i,j) = \Sigma \frac{(XBARi(K) - XBARj(K)}{\{STUDEVi(K)\}\{STUDEVj(K)\}}$$

where

i and j represent the classes being compared for similarity.